UNIVERSIDADE ESTADUAL DE CAMPINAS

INSTITUTO DE BIOLOGIA

VERÔNICA APARECIDA MONTEIRO SAIA CEREDA

Células tronco pluripotentes na compreensão dos aspectos do neurodesenvolvimento na esquizofrenia

Pluripotent stem cells in understanding neurodevelopmental aspects in schizophrenia

CAMPINAS

2021

VERÔNICA APARECIDA MONTEIRO SAIA CEREDA

Células tronco pluripotentes na compreensão dos aspectos do neurodesenvolvimento na esquizofrenia

Pluripotent stem cells in understanding neurodevelopmental aspects in schizophrenia

Tese apresentada ao Instituto de Biologia da Universidade Estadual de Campinas como parte dos requisitos exigidos para a obtenção do Título de Doutora em Biologia Funcional e Molecular na Área de Bioquímica.

Thesis presented to the Institute of Biology of the University of Campinas in partial fulfillment of the requirements for the degree of Doctor's degree in Functional and Molecular Biology in the area of Biochemistry.

Orientador: Daniel Martins de Souza

Co-Orientador: Juliana Minardi Nascimento

ESTE ARQUIVO DIGITAL CORRESPONDE À VERSÃO FINAL DA TESE PELA ALUNA VERÔNICA APARECIDA MONTEIRO SAIA CEREDA E ORIENTADA PELO PROF. DR. DANIEL MARTINS DE SOUZA.

CAMPINAS

2021

Ficha catalográfica
Universidade Estadual de Campinas
Biblioteca do Instituto de Biologia
Mara Janaina de Oliveira - CRB 8/6972

Sa21c

Saia-Cereda, Veronica Aparecida Monteiro, 1988-
Células tronco pluripotentes na compreensão dos aspectos do neurodesenvolvimento da esquizofrenia / Veronica Aparecida Monteiro Saia Cereda. – Campinas, SP : [s.n.], 2021.

Orientador: Daniel Martins de Souza.
Coorientador: Juliana Minardi Nascimento.
Tese (doutorado) – Universidade Estadual de Campinas, Instituto de Biologia.

1. Esquizofrenia - Fisiopatologia. 2. Células tronco pluripotentes. I. Martins-de-Souza, Daniel, 1979-. II. Nascimento, Juliana Minardi. III. Universidade Estadual de Campinas. Instituto de Biologia. IV. Título.

Informações para Biblioteca Digital

Título em outro idioma: Pluripotent stem cells in understanding neurodevelopmental aspects in schizophrenia
Palavras-chave em inglês:
Schizophrenia - Physiopathology
Pluripotent stem cells
Área de concentração: Bioquímica
Titulação: Doutora em Biologia Funcional e Molecular
Banca examinadora:
Daniel Martins de Souza [Orientador]
Adriana Franco Paes Leme
Carolina Demarchi Munhoz
Karina Diniz Oliveira
Karina Griesi Oliveira
Data de defesa: 23-10-2021
Programa de Pós-Graduação: Biologia Funcional e Molecular

Identificação e informações acadêmicas do(a) aluno(a)
- ORCID do autor: https://orcid.org/0000-0002-6285-1201
- Currículo Lattes do autor: http://lattes.cnpq.br/9934032655071945

Campinas, 23 de outubro de 2021.

COMISSÃO EXAMINADORA

Prof.(a) Dr.(a). Daniel Martins de Souza

Prof.(a). Dr.(a) Adriana Franco Paes Leme

Prof.(a) Dr(a). Carolina Demarchi Munhoz

Prof.(a) Dr(a). Karina Diniz Oliveira

Prof.(a) Dr(a). Karina Griesi Oliveira

Os membros da Comissão Examinadora acima assinaram a Ata de Defesa, que se encontra no processo de vida acadêmica do aluno.

A Ata da defesa com as respectivas assinaturas dos membros encontra-se no SIGA/Sistema de Fluxo de Tese e na Secretaria do Programa de Biologia Funcional e Molecular da Unidade do Instituto de Biologia.

DEDICATÓRIA

Este trabalho é dedicado às crianças adultas que,

quando pequenas, sonharam em se tornar cientistas.

AGRADECIMENTOS

À Fundação de Amparo à Pesquisa do Estado de São Paulo – FAPESP pelo apoio financeiro (Processo 2016/07332-7) e pela bolsa de estágio de pesquisa no exterior (Processo 2018/07034-1).

"Por vezes sentimos que aquilo que fazemos não é senão uma gota de água no mar.

Mas o mar seria menor se lhe faltasse uma gota."

Madre Teresa de Calcutá

RESUMO

Atualmente, a compreensão das bases moleculares de doenças complexas que, mesmo com todos os avanços tecnológicos, possuem ainda processos a serem elucidados, tem sido um grande desafio para a ciência. Um exemplo dessas doenças a ser destacado é a esquizofrenia. A esquizofrenia é um transtorno mental incurável que afeta cerca de 1% da população mundial e pode ser causada tanto por componentes genéticos, quanto por fatores ambientais. Assim, compreender essa doença de um ponto de vista mais abrangente, considerando a ação conjunta de diversas vias e tipos celulares, pode favorecer e viabilizar o desenvolvimento de novos caminhos para tratamentos. Em concordância com o elucidado, esta tese conjugou proteômica shotgun e células tronco pluripotentes, com o intuito de investigar os mecanismos biológicos moleculares da esquizofrenia, utilizando modelos celulares. Estudando células neurais derivadas de células de pacientes com esquizofrenia, comparadas a células de indivíduos saudáveis, observou-se que várias vias essenciais para o neurodesenvolvimento são impactadas, como a orientação do axônio e a sinaptogênese, com diversas proteínas com a expressão reduzida. Uma delas é a proteína PHGDH, que é fundamental na via de produção da molécula D-Serina, um neuromodulador do receptor de NMDA, que tem papel na maturação neuronal durante o neurodesenvolvimento. Devido a isso, viu-se a necessidade da investigação dessa proteína alvo na comunicação celular durante o neurodesenvolvimento, visando a compreensão do papel de desregulação na fisiopatologia do transtorno psiquiátrico. Ademais, foi observado também que a inibição da proteína PHGDH, que altera a produção de serina, não altera a expressão direta de marcadores de maturação neural, porém afeta processos básicos de diferenciação neuronal, como metabolismo energético e migração axonal. Os dados obtidos neste estudo foram bastante abrangentes e podem revelar mecanismos subjacentes da origem do desenvolvimento da esquizofrenia. Mas, por se tratar de uma doença complexa, muito ainda há que se desvendar sobre o papel do neurodesenvolvimento na fisiopatologia desse transtorno.

Palavras-chave: Esquizofrenia, Neurodesenvolvimento, Células tronco pluripotentes.

ABSTRACT

Understanding the molecular basis of complex diseases has been a major challenge for science. An example of these diseases to be highlighted is schizophrenia. Schizophrenia is an incurable mental disorder that affects about 1% of the world population and can be caused by both genetic components and environmental factors. Thus, understanding this disease from a broader point of view, considering action of different pathways and cell types, can favor and enable the development of new paths for treatments. Thus, this thesis combined shotgun proteomics and pluripotent stem cells, with the aim of investigating the biological mechanisms of schizophrenia using cell models. Looking at neural cells derived from patients with schizophrenia, compared to cells from healthy individuals, showed that several essential pathways for neurodevelopment are disturbed, such as axon orientation and synaptogenesis, with several proteins with reduced expression. One of them is the PHGDH protein, which is fundamental in the production pathway of D-Serine, a neuromodulator of the NMDA receptor, which plays a role in neuronal maturation during neurodevelopment. Because of this, there was a need to investigate this target protein in cell communication during neurodevelopment, aiming to understand the role of its dysregulation in the pathophysiology of this psychiatric disorder. Furthermore, it was also observed that the inhibition of PHGDH protein does not alter the direct expression of markers of neural maturation, but affects basic processes of neuronal differentiation, such as energy metabolism and axonal migration. The data obtained in this study were quite comprehensive and may reveal underlying mechanisms behind the development of schizophrenia. However, being such a complex disease, much remains to be unraveled about the role of neurodevelopment in the pathophysiology of schizophrenia.

Keywords: Schizophrenia, Neurodevelopment, Pluripotent Stem Cells.

Lista de ilustrações

Lista de abreviaturas e siglas

UNICAMP	Universidade Estadual de Campinas
IB	Instituto de Biologia
2DE	Eletroforese bidimensional
CC	Corpo caloso
CHAPS	3- [3-colamidopropildimetilamônio] -1-propanossulfonato
CSF	Líquido cefalorraquidiano
DTT	Ditiotreitol
hESCs	Células embrionárias pluripotentes humanas
ESI	Ionização por *electrospray*
GAPDH	Gliceraldeído-3-fosfato desidrogenase
GFAP	Proteína Glial Fibrilar Ácida
IAA	Iodoacetamida
IM	Mobilidade iônica
MCI	Massa celular interna
IPA	*Ingenuity* - Análise de *Pathways*
iPSCs	Células tronco pluripotentes induzidas
KEGG	Genes e genomas da Enciclopédia de Kyoto
LSD	Ácido D-lisérgico
MRM	Monitoramento de múltiplas reações
MS	Espectrometria de massas
MS / MS	Espectrometria de massas sequencial
nano LC-MS / MS	Nanocromatografia acoplada à espectrometria de massas sequencial
NMDA	Receptor N-metil-D-aspartato

NSC	Células-tronco neurais
OXPHOS	Fosforilação oxidativa
PRM	Monitoramento de reação paralela
PTMs	Modificações pós-traducionais
ROS	Espécies que reagem ao oxigênio
SCZ	Esquizofrenia
SNC	Sistema Nervoso Central
SOD1	Superóxido dismutase [Cu-Zn]
SRM	Monitoramento de reação seletiva
STRING	Ferramenta de Pesquisa para a Recuperação de Genes / Interação de proteínas
TOF	Tempo de vôo
TQ ou QqQ	Espectrômetros de massa triplo quadrupolo
YWHAE	14-3-3 proteína epsilon
YWHAG	14-3-3 proteína gama
YWHAZ	14-3-3 proteína zeta / delta
MAM	Modelo de acetato de metilazoximetanol
NMDA	N-metil-D-aspartato
AMPA	Ácido a-amino-3-hidroxi-5-metil-4-isoxazolpropiônico
CNS	Sistema nervoso central
mGluR	Receptores de glutamato acoplados à proteína G
PCP	Fenciclidina
MK801	Dizocilpina
EAAT	Transportador de aminoácido excitatório
PSD95	Proteína de densidade pós-sináptica 95
CaMKII	Proteína quinase dependente de cálcio / calmodulina

NPCs	Células progenitoras neurais
GMS	Sítio modulador de glicina
PHGDH	3-fosfoglicerato desidrogenase
DAPI	4 ', 6-diamidino-2-fenilindol
TUBB3	β 3-tubulina
DAPI	4 ', 6-diamidino-2-fenilindol
MAP2	Proteína 2 associada a microtúbulos
TH	Tirosina 3-monooxigenase
NeuN	Proteína de ligação de RNA fox-1 homólogo 3
21 DIV	21 dias *in vitro*
CBR5884	5- (furano-2-carboxamido) -3-metil-4-tiocianatotiofeno-2-carboxilato de etil

Sumário

1 Introdução

1.1 Esquizofrenia

Inicialmente, a esquizofrenia foi denominada como demência precoce pelo psiquiatra francês Benedict Morel, já que esse transtorno psiquiátrico normalmente se manifestava no início da adolescência (SADOCK; SADOCK; LEVIN, 2007). Em 1911, o psiquiatra Eugen Bleuler propôs o termo esquizofrenia (do grego esquizo – "dividido", frenia – "estado da mente") e descreveu esse transtorno como sendo a dissociação das funções psíquicas, caracterizado pela perturbação das associações de pensamento e afetividade (FUSAR-POLI; POLITI, 2008). A etiologia da esquizofrenia (SCZ) envolve fatores exógenos (ou ambientais) e fatores endógenos (pré-disposição genética), e muitos dos seus aspectos moleculares ainda não foram completamente compreendidos, embora seja evidente o caráter genético da esquizofrenia, como demonstrado em estudos com gêmeos idênticos (GEJMAN; SANDERS; DUAN, 2010). Os fatores ambientais são o abuso de álcool e drogas, a vida conturbada de centros urbanos, além dos fatores ligados ao neurodesenvolvimento, como complicações obstétricas e infecções virais severas (BROWN, 2011).
A esquizofrenia tende a se desenvolver na adolescencia ou no início da vida adulta e persiste durante toda a vida do paciente, e seus sintomas são divididos em três categorias: i) sintomas positivos, como delírios (crenças falsas), alucinações (percepções falsas) e desorganização do pensamento; ii) sintomas negativos, que incluem isolamento social, inabilidade de sentir prazer e iniciativa e energia diminuídas e iii) sintomas cognitivos, como distúrbios de atenção, funções executoras e memória de trabalho (LEWIS; LIEBERMAN, 2000). Ainda, como em todos os transtornos psiquiátricos, o diagnóstico da esquizofrenia é estritamente clínico, baseado apenas na entrevista paciente-médico (TANDON; NASRALLAH; KESHAVAN, 2010).

1.2 Tratamentos atuais e suas limitações

O tratamento atual para a SCZ se baseia principalmente no uso de fármacos antipsicóticos, que podem ser classificados em típicos e atípicos (TANDON; NASRALLAH; KESHAVAN, 2010). Os antipsicóticos típicos atuam principalmente como antagonistas dopaminérgicos, e agem de forma eficaz no controle dos sintomas positivos, porém podem causar efeitos colaterais extrapiramidais, discinesia tardia, sedação, rigidez muscular e cãibras (TANDON; NASRALLAH; KESHAVAN, 2010). Já os antipsicóticos atípicos promovem menor ocupação e se dissociam rapidamente dos receptores de dopamina, atuando

também em receptores de glutamato e serotonina. Assim, a ocorrência dos efeitos colaterais se dá numa menor extensão, podendo, no entanto, causar outra gama de sintomas, como é o caso da síndrome metabólica (LIEBERMAN et al., 2005), que é capaz de acarretar distúrbios cardiovasculares (DIESET et al., 2012). Devido a esses efeitos colaterais, cerca de 60% dos pacientes abandonam o tratamento, além dos 10% de pacientes que são refratários ao tratamento (TANDON; NASRALLAH; KESHAVAN, 2010). Pacientes sem tratamento adequado têm prejuízos na qualidade de vida, não conseguindo trabalhar ou estudar, sendo que 40% desses pacientes tentam o suicídio, chegando a óbito em 4,9% dos casos (HOR; TAYLOR, 2010).

O emprego de intervenções não farmacológicas, como o aconselhamento individual e/ou em grupo, a terapia cognitivo-comportamental, a psicoeducação, as intervenções dietéticas e os exercícios, é comumente associado aos tratamentos farmacológicos, para proporcionar melhor qualidade de vida aos pacientes com esquizofrenia (VANCAMPFORT et al., 2019). Dessa forma, é possível que os pacientes tenham uma vida mais satisfatória e independente (GANGULY; SOLIMAN; MOUSTAFA, 2018). As intervenções não farmacológicas mais disseminadas são intervenções dietéticas e terapia cognitivo comportamental (TCC).

Estudos indicam que pacientes com esquizofrenia consomem mais gordura total, além de menos fibra total e vitaminas se comparados com indivíduos saudáveis (BROWN; ROFFMAN, 2014; KALAYDJIAN et al., 2006). Ademais, a administração das vitaminas C, E, B e D por indivíduos com esquizofrenia mostrou melhora geral nos sintomas (GRAHAM et al., 2015; BROWN; ROFFMAN, 2014). Porém, a comunidade cientifica afirma que estudos complementares precisam ainda ser realizados a fim de atestar a eficiência dessas intervenções dietéticas nos pacientes com esquizofrenia.

Diversos grupos de estudo vêm ressaltando a importância de TCC em combinação a intervenções farmacológicas no manejo de sintomas da esquizofrenia, e principalmente na melhora da qualidade de vida desses pacientes (MORRISON, 2009; TAI; TURKINGTON, 2009; SUBRAMANIAM et al., 2012). Além disso, esses estudos indicaram que a TCC pode melhorar déficits cognitivos apresentados pelos pacientes, uma gama de sintomas que tem baixa remissão apenas com o uso de antipsicóticos (EACK et al., 2011; SUBRAMANIAM et al., 2012). Existem diversas técnicas aplicadas na TCC e elas vão desde reestruturação cognitiva, onde o paciente é desafiado a apresentar provas de que suas crenças são reais, até técnicas ligadas ao relacionamento social do paciente (GANGULY; SOLIMAN; MOUSTAFA, 2018). A eficiência do TCC foi comprovada em diversos âmbitos: ela pode causar reduções significativas em sintomas positivos e negativos, no comportamento violento, além de diminuir a ideação suicida e, portanto, o risco de suicídio (SENSKY et al., 2000; GANGULY; SOLIMAN; MOUSTAFA, 2018).

1.3 Hipóteses associadas à patofisiologia da esquizofrenia

As diversas teorias sobre a patofisiologia da esquizofrenia estão centradas em desregulações nos neurotransmissores. A hipótese dopaminérgica foi proposta depois de observações que indicaram que drogas usadas recreativamente como anfetamina e cocaína, que são agonistas de receptores dopaminérgicos, causam psicoses semelhantes às que os pacientes com esquizofrenia vivenciam (MELTZER; STAHL, 1976). A teoria serotoninérgica também foi formulada a partir de sintomas psicóticos causados pelo LSD (ácido D-lisérgico), também uma droga recreativa. Essa substância possui a ação agonista em receptores de serotonina, ou seja, o mal funcionamento desse receptor, induzido pela droga, pode causar sintomas parecidos com os da esquizofrenia (FELDSTEIN; HOAGLAND; FREEMAN, 1958). A hipótese glutamatérgica foi baseada na capacidade de antagonistas dos receptores de glutamato do tipo N-metil D-Aspartato (NMDA) induzirem psicose semelhante à que ocorre em pacientes com SCZ (JAVITT; ZUKIN, 1991). Além disso, estudos farmacológicos e de imagem reforçam que a disfunção glutamatérgica também se encontra associada aos déficits cognitivos observados nesses pacientes (BARCH; CEASER, 2012; KANTROWITZ; JAVITT, 2010; MOGHADDAM; JAVITT, 2012).

Já a hipótese sináptica, por sua vez, está baseada principalmente em estudos de cérebros *post-mortem*, que indicam um déficit nas interações sinápticas (JAARO-PELED et al., 2010; MAYNARD et al., 2001). Essa hipótese é um concatenado das hipóteses da desregulação dos neurotransmissores, nas quais os sintomas que estão relacionados com a esquizofrenia são resultado da convergência de pequenos fatores associados à deficiência sináptica. Essa hipótese abrange também a idade de desenvolvimento do transtorno, pois a conectividade sináptica anormal no período da infância é modesta, passando despercebida em muitos casos, devido à redundância dos contatos sinápticos dessa época. Porém, no período de maturação do sistema nervoso, que ocorre na pré-puberdade (idade em que normalmente se iniciam os sintomas), essas disfunções sinápticas se tornam aparentes (FRANKLE; LERMA; LARUELLE, 2003).

As hipóteses que explicam o desenvolvimento da esquizofrenia, principalmente a sináptica, são centradas em desregulações observadas nos neurônios. Atualmente, no entanto, vêm crescendo em número estudos que indicam um possível papel das células da glia na patofisiologia do transtorno, já que essas células têm um papel importante na regulação da neurotransmissão (SAIA-CEREDA et al., 2016; ZUCCOLI et al., 2021). As células da glia, também chamadas de neuroglia, podem ser classificadas de acordo com a sua origem embrionária em dois grupos distintos, morfológica e funcionalmente: o primeiro é a microglia, que tem origem mesodermal; e o segundo, a macroglia de origem ectodermal (KETTENMANN, 1990). A microglia é responsável pela defesa imune primária do sistema nervoso central (SNC). Suas células possuem similaridades com os macrófagos, e recentemente foram associadas ao processo de eliminação e estabilização das sinapses (SCHAFER; LEHRMAN; STEVENS, 2013). Já a macroglia possui dois tipos celulares principais: os

astrócitos, que são as células gliais mais abundantes do SNC, e os oligodendrócitos (GOMES; TORTELLI; DINIZ, 2013). Os oligodendrócitos correspondem à 51% das células que envolvem os neurônios (POLAK et al., 1982), e realizam funções como sinalização trófica, síntese de fatores de crescimento e mielinização de axônios de neurônios (DU; DREYFUS, 2002). Já os astrócitos desempenham uma série de funções essenciais para a homeostase do SNC, incluindo: manutenção dos níveis iônicos do meio extracelular, captação e liberação de diversos neurotransmissores, participação na formação da barreira hematoencefálica, secreção de fatores tróficos essenciais para a sobrevivência e diferenciação dos neurônios, direcionamento de axônios e formação e funcionamento das sinapses (MELDOLESI, 2011; STIPURSKY et al., 2012). Além disso, essas células têm grande impacto no controle energético cerebral, em razão do fornecimento de energia e metabólitos (ROUACH et al., 2008).

A teoria do neurodesenvolvimento como causa da esquizofrenia infere que fatores genéticos e ambientais podem influenciar no desenvolvimento cerebral do indivíduo, que se estende do período pré-natal até o pós-natal, finalizando na adolescência, que é a fase em que o indivíduo apresenta seus primeiros sintomas psicóticos (mais detalhes sobre essa teoria se encontram no capítulo 3). A teoria é fundamentada em três pilares: i) anormalidades estruturais cerebrais, ii) anormalidades cognitivas e motoras em jovens, seguidas de desenvolvimento da doença em adultos, e iii) lesões em primatas durante o desenvolvimento e alterações cognitivas futuras (OWEN et al., 2011). Porém, essa teoria considera que a esquizofrenia vem se desenvolvendo ao longo do tempo, e que, por isso, há um quadro de sintomas prodrômicos, ou seja, um conjunto de sintomas que antecedem aos surtos psicóticos, momento em que normalmente o paciente é diagnosticado (LEWIS; LIEBERMAN, 2000; OWEN; O'DONOVAN, 2017).

Devido à impossibilidade de se estudar desregulações genéticas e efeitos de fatores ambientais no neurodesenvolvimento humano, principalmente no período embrionário, a maioria dos estudos que confirmam a hipótese do neurodesenvolvimento ainda são realizados em modelos animais. Porém, o neurodesenvolvimento humano e de camundongos possuem diferenças relevantes, principalmente no âmbito molecular. Nesse contexto, o desenvolvimento das células tronco humanas de pluripotência induzida (hiPSC), e modelos de culturas de células e tridimensionais (como organoides e esferoides), possibilitaram a aplicação de modelos mais semelhantes à condição patológica humana, tornando-se uma alternativa para o estudo de patologias complexas como a esquizofrenia. Uma das grandes vantagens das hiPSC é a possibilidade de se entender alterações decorrentes do estado de pluripotência celular e estados subsequentes à formação de uma célula madura, refletindo, por exemplo, os estágios do neurodesenvolvimento. Por este motivo, utilizaremos esse modelo para analisar organoides, neurônios e células progenitoras neurais de hiPSC de pacientes com esquizofrenia, além de analisar se a alteração da produção de D-serina por neurônios e astrócitos, modulando-se a enzima PHGDH, causa a hipofunção glutama-

térgica, e assim leva à desregulações no desenvolvimento de circuitos neuronais, funções conhecidamente alteradas em pacientes com esquizofrenia (GLAUSIER; LEWIS, 2013; RUIZ; BIRBAUMER; SITARAM, 2013).

1.4 Células tronco pluripotentes

As células tronco pluripotentes são células capazes de se diferenciar possivelmente em todos os tipos celulares de um organismo adulto. Por essa possibilidade, são uma promessa em estudos de patofisiologia de doenças, além de poder ajudar na descoberta de novos biomarcadores, assim como na triagem para o desenvolvimento de novas drogas (COLMAN; DREESEN, 2009). Existem dois tipos de células tronco pluripotentes: as células embrionárias pluripotentes (ESCs) e as células pluripotentes induzidas (iPSCs). Thomson et al (THOMSON et al., 1998) desenvolveram, a partir de embriões produzidos *in vitro* com finalidade clínica, o primeiro modelo de cultura com células tronco embrionárias de humanos (hESC). As hESC são derivadas do estágio inicial da diferenciação embrionária, quando são coletadas da massa celular interna (MCI) do blastocisto humano no dia 5 da fertilização *in vitro* do ovócito (figura 1), podendo ser propagadas indefinidamente nesse estágio indiferenciado, e têm capacidade de se diferenciar em células dos três diferentes folhetos embrionários (endoderme, mesoderme e ectoderme) (PERA; REUBINOFF; TROUNSON, 2000). Inicialmente, o propósito do cultivo de hESC era restrito à função de reposição de células em tecido adulto lesionado, porém, com o avanço das tecnologias, esse tipo celular se transformou em uma promessa no estudo das bases moleculares da diferenciação celular (BOPPART; LISIO; WITKOWSKI, 2015).

Outra técnica que revolucionou o âmbito da pesquisa em neurodesenvolvimento foi desenvolvida por Yamanaka et al. (YAMANAKA, 2010). Nela, há a reprogramação de células somáticas adultas, utilizando-se quatro fatores de transcrição ligados ao estado de plenipotência (oct-4, sox-2, Klf-4 e c-Myc). Nesse estudo, foi desenvolvido o modelo celular que chamamos hoje de células tronco de pluripotência induzida humanas (hiPSC, da sigla em inglês: *induced pluripotent stem cells*)(figura 1). Como a ESC, essas células podem gerar diversos tipos celulares dos três folhetos embrionários (YU; THOMSON, 2008). Esse modelo se tornou uma promessa nos estudos de doenças, já que as hiPSC carregam o padrão genético do doador. Tanto as hESCs, quanto as hiPSCs, têm a capacidade de recapitular as etapas do neurodesenvolvimento, já que, quando tratadas com específicos fatores de crescimento, expressam genes e ativam vias moleculares mimetizando o que ocorre *in vivo* (DVASH; BEN-YOSEF; EIGES, 2006).

Atualmente, o estudo do cérebro em desenvolvimento pré-natal pode ser feito de três formas: a investigação do cérebro fetal *ex vivo*, o estudo de prematuro, e o estudo de fetos no útero. No entanto, cada umas dessas abordagens possui grandes limitações (THOMASON et al.,

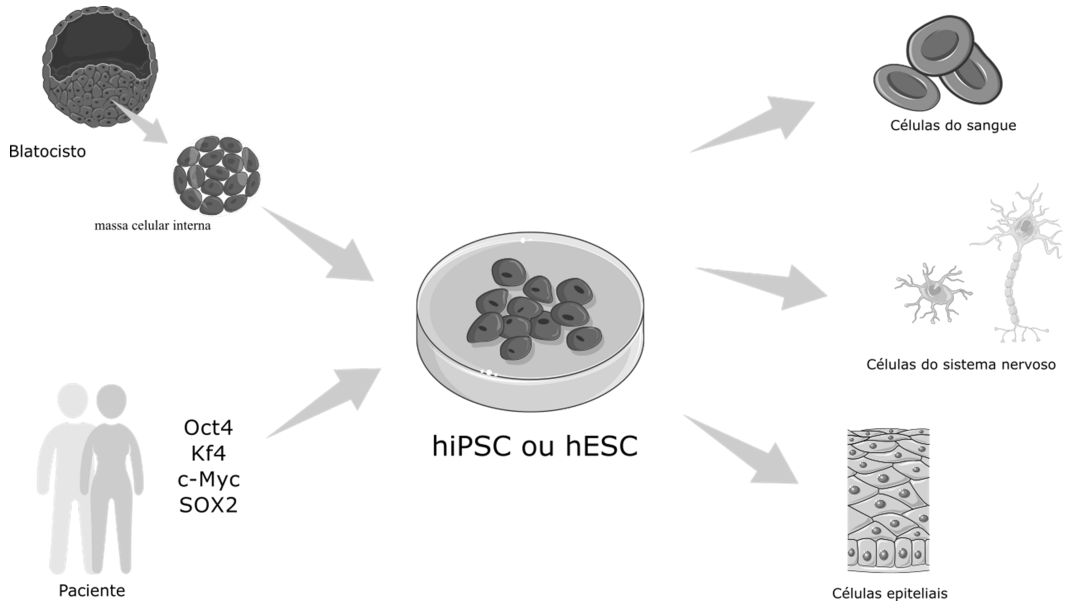

Figura 1 – Esquema da formação dos modelos de cultura de células tronco embrionárias e células tronco pluripotentes induzidas

2021). Devido a isso, os estudos com células tronco se transformaram em uma promessa no entendimento do neurodesenvolvimento humano, principalmente no âmbito molecular, já que embriões humanos são inacessíveis para pesquisa.

1.5 Neuroproteômica

O proteoma é definido como o conjunto de proteínas expressas por uma célula, tecido ou organismo em um determinado tempo sob uma dada condição; e o estudo do proteoma é denominado proteômica (WILKINS et al., 1996). Proteômica é uma ferramenta pertinente para estudos de distúrbios multifatoriais, como é o caso da esquizofrenia, já que possibilita a compreensão da patofisiologia molecular de maneira integrada. Como as proteínas são as bases dos processos metabólicos celulares e, consequentemente, do organismo como um todo, qualquer alteração no equilíbrio proteico pode acarretar mudanças fisiológicas que muitas vezes são associadas à alguma doença.

Atualmente, a principal ferramenta usada em estudos proteômicos é a espectrometria de massas (MS), e o esquema de um fluxograma de trabalho para estudos proteômicos está representado na figura 2. Em princípio, essa técnica permite a caracterização de moléculas com base na medida de sua razão massa/carga (m/z), ou seja, para que uma molécula seja caracterizada por MS, ela precisa ser ionizada. A ionização é a conversão de um átomo ou molécula em um íon pela adição ou remoção de partículas carregadas, ocorrendo através da permuta de elétrons ou outros íons. Há diversas técnicas de ionização usadas em MS, sendo a atualmente a mais aplicada a ionização por *electrospray* (ESI).

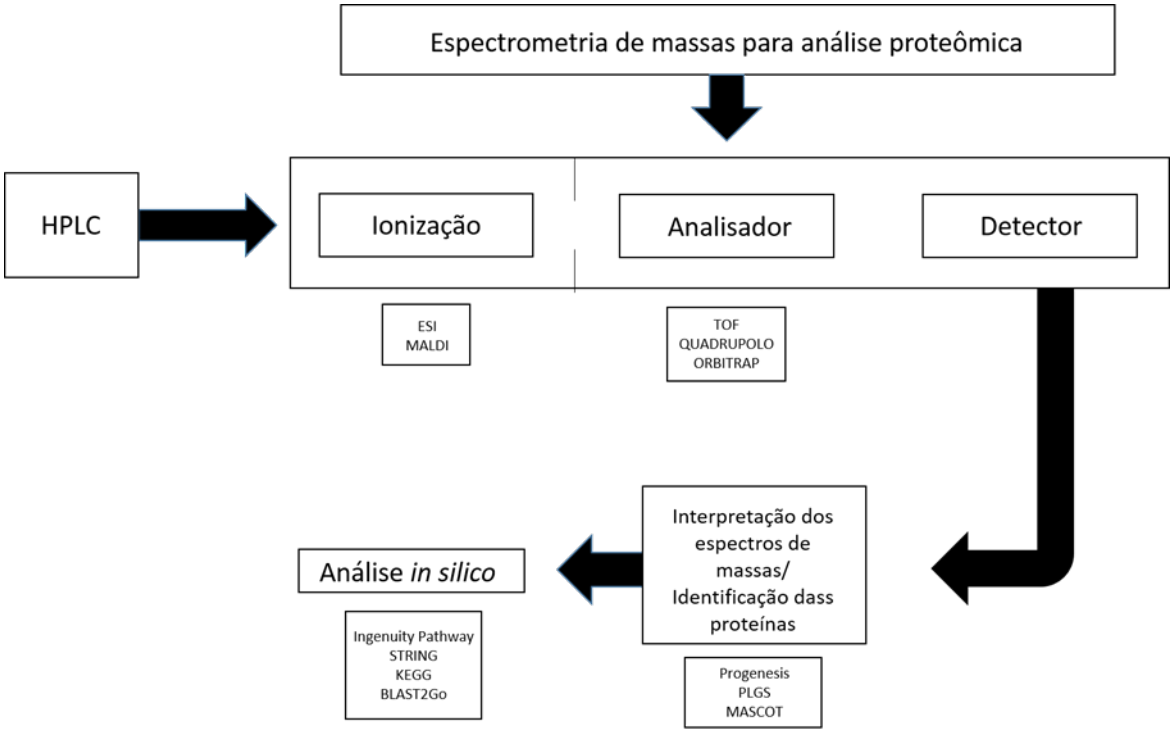

Figura 2 – Esquema de uma plataforma usada em análises proteômicas

Nessa técnica de ionização, as moléculas a serem analisadas são solubilizadas em um solvente aquoso que irá conferir carga à molécula, como, por exemplo, uma solução com ácido fórmico ou formiato de amônio. Em seguida, a solução é submetida à altas voltagens através de um forte campo elétrico, e assim a amostra é dispersa em aerossol. Esse procedimento faz com que haja a evaporação do excesso de solventes, processo que é auxiliado por um gás inerte a temperaturas elevadas que envolve o aerossol. As moléculas previamente carregadas repelem umas às outras até que ocorre um colapso na gota e as moléculas são expelidas em forma de íons (HO, 2003).

Além da fonte de ionização, um espectrômetro de massas tipicamente contém outras duas partes: o analisador de massas, onde a massa/carga (m/z) do íon é medida, e o detector, onde é captada e amplificada a informação do analisador. Há vários tipos de analisadores, e cada um tem uma maior aplicabilidade dependendo do tipo de análise feita. Um dos analisadores usados em estudos proteômicos é o *time-of-flight* (TOF), que estima a m/z de um composto a partir do tempo em que moléculas ionizadas percorrem uma trajetória de comprimento conhecido. Já o quadrupólo, que é formado por quatro barras metálicas, utiliza campos elétricos oscilantes para selecionar íons, o que possibilita a separação desses compostos de acordo com os seus valores de m/z (HOFFMANN; STROOBANT, 2007).

O espectrômetro de massas (MS) utilizado nessa pesquisa é o *Synapt G2 Si (Waters Corp., Milford, EUA)*, com a proteômica do tipo *shotgun*. Essa técnica tem sido um método amplamente utilizado para a identificação e quantificação de proteínas provenientes de misturas complexas, como lisado de tecido e células, além de urina e sérum. Nessa aborda-

gem, os peptídeos são separados de acordo com suas características físico-químicas por cromatografia líquida de alta performance (HPLC), e subsequentemente são analisados pelo espectrômetro de massas.

O *Synapt* possui uma fonte de ionização do tipo *electrospray* (ESI). Esse equipamento é um equipamento do tipo Q-TOF, ou seja, é um espectrômetro de massas híbrido que possui dois tipos de analisadores: um quadrupólo (Q) seguido de um analisador do tipo *time of flight* (TOF), conectados por uma câmara de colisão. Esse MS possui, ainda, uma cela de mobilidade iônica (IM), que permite a separação de íons precursores ou de íons de transição.

Em termos de análise de massas, um equipamento híbrido permite a realização de um experimento de espectrometria de massas sequencial (MSe, ou tandem MS, MS/MS), que envolve a fragmentação de precursores seguida da aquisição de suas transições. O processo de fragmentação mais utilizado em MS/MS é a técnica de dissociação induzida por colisão (*Collision Induced Dissociation-CID*); nela, os íons precursores são acelerados em uma câmara contendo gás inerte (hélio, argônio ou nitrogênio) e a energia gerada a partir dessa colisão é transferida para as ligações presentes nos íons, fragmentando-os (LEVIN; HRADETZKY; BAHN, 2011). Com esse equipamento, é possível fazer experimentos do tipo análise independente de dados (*data-independent analysis - DIA*).

Uma característica própria do *Synapt G2-Si* é a possibilidade de se analisar a seção de choque de uma molécula devido à presença da câmara de mobilidade iônica. Nesse experimento, um íon submetido a um campo elétrico é transportado ao longo de uma câmara contendo gás inerte, tendo sua velocidade (*drift time*) mensurada ao longo do processo. Uma vez que íons de maior seção de choque levarão maior tempo para atravessar a câmara, temos acesso a mais um nível de informação acerca dos peptídeos que estão em análise (LALLI et al., 2010).

Para a identificação e quantificação das proteínas foi utilizado o *software Progenesis QI for proteomics (Waters Corp., Milford, EUA)*. Esse *software* utiliza a dimensão adicional da separação de mobilidade iônica para melhorar a precisão de identificação das proteínas. Para a quantificação dessas proteínas, foram utilizadas abordagens quantitativas independentemente de marcação isotópica (*label-free*). No *Progenesis QI*, o método de quantificação utilizado é a técnica de Hi-N ou Hi-All, que foi descrita por Silva et al. 2006 (SILVA et al., 2006). Nesse método, após a identificação dos peptídeos e proteínas, há a realização da quantificação de cada peptídeo a partir de todos os seus íons peptídicos constituintes. Assim, para a quantificação de cada proteína, é considerada a média dos N peptídeos mais abundantes. Os peptídeos usados nessas quantificações devem seguir o critério de serem peptídeo único, ou seja, eles têm de ser peptídeos que são constituintes apenas da proteína em questão e não fazer parte de outra proteína. A utilização de peptídeos únicos pode diminuir o número de proteínas quantificadas, porém, é a forma mais segura e eficiente na identificação de proteínas.

Análises proteômicas geram uma quantidade maciça de dados, principalmente quando se trata de misturas biológicas complexas. Em consequência disso, visualizar, analisar e categorizar esses dados têm sido um grande desafio (CAGNEY et al., 2003). Além do dado propriamente dito, advindo da proteômica, também é possível realizar análises de interação proteína-proteína e vislumbrar vias envolvidas em fenótipos celulares. Assim, diversas ferramentas de análise *in silico* vêm sendo desenvolvidas e aprimoradas, facilitando os estudos proteômicos.

Uma dessas ferramentas é o programa *Ingenuity Pathways Analysis* (IPA, QIAGEN) que, além das características citadas acima, ainda promove *insights* sobre interações químicas, fenótipos celulares e doenças que estão relacionadas às proteínas de estudo. Esse programa é baseado em algoritmos que usam informações da literatura, previamente descritas, para determinar essas redes de interação e, por isso, possui uma maior confiabilidade em seus resultados comparados com outras ferramentas de bioinformática (CALVANO et al., 2005).

Outra ferramenta muito usada é a *Search Tool for the Retrieval of Interacting Genes/-Proteins* (STRING, http://string-db.org/), que consiste em um banco de dados dedicado à interação proteína-proteína, tanto no âmbito físico quanto no funcional, levando em consideração informações de várias fontes, incluindo repositórios experimentais, métodos de previsão computacional e artigos publicados. STRING abrange cerca de 2,5 milhões de proteínas de 630 organismos, o que proporciona uma visão abrangente das interações entre as proteínas de um conjunto de resultados (JENSEN et al., 2009).

O *Kyoto Encyclopedia Genes e Genomes* (KEGG, http://www.genome.ad.jp/kegg/) é uma ferramenta que visa a compreensão e simulação do fenótipo de células e organismos a partir de um banco de dados de informações do genoma. Para isso, i) ele integra dados e conhecimentos sobre as interações proteína-proteína e possíveis reações químicas ligadas a processos celulares específicos; ii) reconstrói redes de interação de organismos que têm seu genoma completamente sequenciado; e, por fim, iii) pode ser utilizado para estudos proteômicos, principalmente os de integração de mapas metabólicos, representando-os em forma de gráficos (KANEHISA; GOTO, 2000). Outro *software* amplamente utilizado é o *Blast2Go* (http://www.blast2go.de), que é uma ferramenta de anotação, visualização e análises, na qual é possível realizar a investigação em base de dados via *Gene Ontology*, sendo adequado para análises de investigação tanto de genes quanto de proteínas (CONESA et al., 2005). As três últimas ferramentas (STRING, KEGG, BLAST2Go) estão disponíveis online sem custo; já o programa IPA, que é um programa pago por possuir um banco de dados curado manualmente, tem uma maior confiabilidade nos dados gerados.

2 Objetivo geral

O objetivo dessa tese foi entender o papel de moléculas presentes em vias constituintes do neurodesenvolvimento e sua contribuição para a patofisiologia da esquizofrenia, pretendendo uma melhor compreensão desse transtorno psiquiátrico em nível molecular, atualmente pouco conhecida inerente aos aspectos ligados ao desenvolvimento.

2.1 Objetivos específicos

2.1.1 Capítulo 4

Entender os mecanismos moleculares da disfunção glutamatérgica na esquizofrenia e sua relação com o neurodesenvolvimento utilizando dados de proteômica.

2.1.2 Capítulo 5

Analisar alterações em células tronco pluripotentes de pacientes com esquizofrenia, com o intuito de entender como linhagens neurais mimetizam aspectos do transtorno psiquiátrico *in vitro* .

2.1.3 Capítulo 6

Analisar se a inibição da proteína PHGDH em neurônios e astrócitos causa problemas no neurodesenvolvimento, mais especificamente na diferenciação neural, e se os fenótipos observados são semelhantes aos encontrados em pacientes com doenças psiquiátricas como a esquizofrenia.

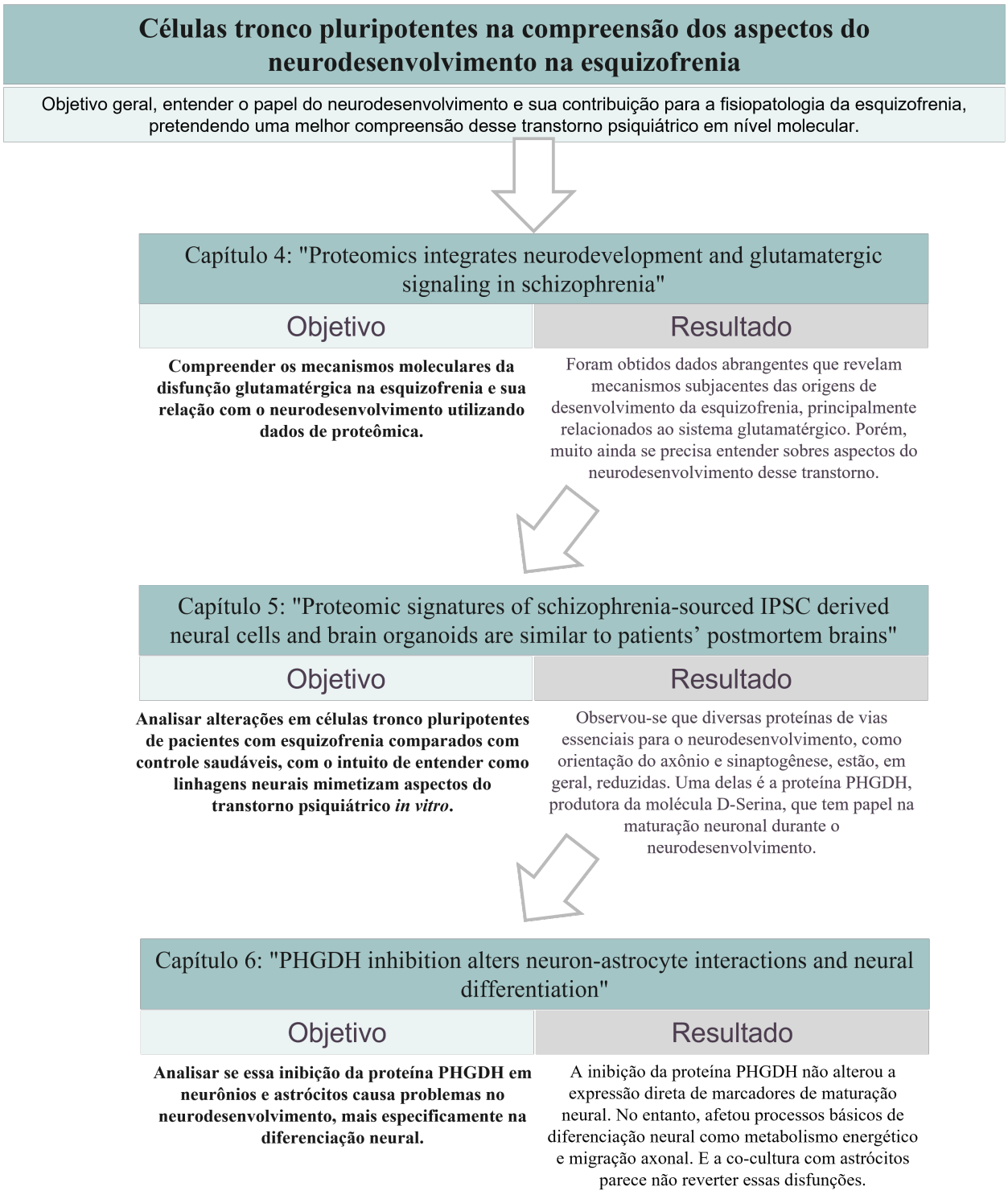

Figura 3 – Fluxograma do racional dos artigos presentes nesta tese

3 Proteomics integrates neurodevelopment and glutamatergic signaling in schizophrenia

Verônica M. Saia-Cereda[1], Guilherme Reis-de-Oliveira[1], Bradley J. Smith[1], Fernanda Crunfli[1], André S. L. M. Antunes[1], Daniel Martins-de-Souza[1,2,3]

1 Laboratory of Neuroproteomics, Department of Biochemistry and Tissue Biology, Institute of Biology, University of Campinas, Campinas, Brazil.

2 Experimental Medicine Research Cluster (EMRC), University of Campinas, Campinas 13083-862, SP, Brazil.

3 Instituto Nacional de Biomarcadores em Neuropsiquiatria, Conselho Nacional de Desenvolvimento Científico e Tecnológico, São Paulo, Brazil.

3.1 Abstract

Schizophrenia is a mental disorder that results from a combination of endogenous (both genetic and biochemical) and environmental factors. Its molecular bases still need better understanding, and currently there are several theories for its development and the onset of the symptoms, which include the dopaminergic, glutamatergic, and neurodevelopmental hypotheses. Over the last decade, although scientific advances have uncovered possible connections among the various hypotheses, a deeper discussion about how they are linked is still lacking. Therefore, this review intends to evaluate the molecular bases of the glutamatergic hypothesis and its connection with the neurodevelopmental hypothesis. To achieve this, we cross-checked differentially expressed proteins from the *postmortem* brains of schizophrenia patients with the proteome of human fetal brain tissue at 16-36 weeks of gestation. In addition, the relationship between the deregulated molecular pathways affected in patients and their role in neurodevelopment was evaluated. In this review, we provide extensive analyses that reveal underlying mechanisms during the development of schizophrenia. It was observed that the dysregulated proteins in patients were mainly related to the glutamatergic system but have links with other neurotransmitter systems such as the GABAergic and dopaminergic systems.

3.2 Introduction

3.2.1 Schizophrenia: Clinical features, risk factors, and pathology

In 1911, psychiatrist Eugen Bleuler coined the term schizophrenia from the Greek schizo - "divided", phrenia - "state of mind", describing this disease as the dissociation of psychic functions, characterized by the disturbance of associations of thought and affectivity (ASHOK; BAUGH; YERAGANI, 2012). Schizophrenia is now recognized to be a neurodevelopmental disorder (MURRAY et al., 2017) whose symptoms are classified into three categories: positive symptoms, such as hallucinations, delusions, and thinking disorders; negative symptoms, such as losses in social interaction, lack of motivation, and anhedonia; and cognitive deficits, such as decreased executive functions, selective attention, diminished working memory, and reduced mental flexibility (WEICKERT et al., 2000).
As there is no cure, symptom management is the main line of treatment, which relies primarily on antipsychotics, which are effective nearly exclusively in the reduction of positive symptoms. In addition to this limitation, these drugs can cause several side effects that significantly impair the quality of life of patients (DIESET et al., 2012; LIEBERMAN et al., 2005; TANDON; KESHAVAN; NASRALLAH, 2008). Poor treatment efficacy and serious side effects lead to treatment dropout in up to 70% of cases (TORREY, 1999). Further worsening a patient's prognosis, 40% of schizophrenia patients attempt suicide at some point in their lives, and nearly 1 in 20 succeed (HOR; TAYLOR, 2010). Compounded by inadequate treatment, the disorder places an enormous burden on patients and their families, as well as public coffers, totaling an annual cost of over US$ 60 billion in the United States (MARCUS; OLFSON, 2008) with some estimates surpassing US$ 280 billion and representing a considerable fraction of healthcare costs in emerging economies, such as Brazil (MATOS et al., 2015).
Schizophrenia has a heritability of 64 - 85% (LICHTENSTEIN et al., 2009; SULLIVAN; KENDLER; NEALE, 2003) and a study involving monozygotic twins indicated that environmental factors also play a role in its development (CARDNO; GOTTESMAN, 2000). In fact, this disorder has non-Mendelian characteristics, as its development stems from several mutations in different genes with small effects, which together lead to the pathophysiology of the disease (KIROV et al., 2005). Studies have shown arrays of gene mutations and protein expression levels that are related to the pathophysiology of schizophrenia (MOGHADDAM; JAVITT, 2012); however, there is still no consensus as to the etiology of the disease. It is currently accepted that the etiology of schizophrenia has a neurodevelopmental component (RAPOPORT; GIEDD; GOGTAY, 2012) and that imbalances in the dopaminergic and glutamatergic neurotransmitter systems are among its pathophysiological hallmarks (HOWES; MCCUTCHEON; STONE, 2015).
In this review, we discuss proteins and pathways associated with the neurodevelopmental aspects of schizophrenia. To achieve this, we analyzed the currently available proteomic

data of *postmortem* brain tissue from patients with schizophrenia and cross-referenced these data with proteins that are expressed during neurodevelopment. This approach allowed us to unveil potential targets that may be associated with glutamatergic impairments throughout the development of schizophrenia.

3.2.2 The Neurodevelopmental Hypothesis

The idea that neurodevelopmental impairments are etiological factors in schizophrenia was proposed in the 19th century by Thomas Clouston; at the time, he referred to schizophrenia as 'adolescent insanity' (O'CONNELL et al., 1997). This idea was generally dismissed until 100 years later when a study group carried out a large follow-up study with children who showed cognitive difficulties during childhood and later developed schizophrenia (BERARDIS et al., 2021; O'CONNELL et al., 1997). Neurodevelopmental diseases are now defined as heterogeneous conditions involving a series of different impairments, including delays or disturbances in social, motor, cognitive, and language skills (JESTE, 2015), many of which are dysfunctions that are pillars of the neurodevelopmental hypothesis of schizophrenia.

The foundations of the neurodevelopmental hypothesis of schizophrenia are built upon three main pieces of evidence: i) structural abnormalities are seen in the brains of individuals affected by schizophrenia (ANDREASEN et al., 1986; ERP et al., 2018; PERI et al., 2012), ii) despite the onset of psychotic symptoms starts in final of adolescence, the negative and cognitive symptoms are present even in the childhood of patients (prodromal symptoms) (WALKER; SAVOIE; DAVIS, 1994), and iii) brain lesions in a primate development study led to delayed cognitive and behavioral changes similar to observed in schizophrenia patients (OWEN et al., 2011). Gupta and Kulhara (GUPTA; KULHARA, 2010) extensively reviewed numerous studies that support this hypothesis and compiled a list of the main neurodevelopmental cues that are associated with the onset of the disease in adult individuals, including obstetric complications, social and intellectual deficits, variations in brain neuroimaging as a child (first episode psychosis), and alterations in several proteins and genes involved in development.

Schizophrenia has also been linked to environmental insults during neurodevelopment such as influenza infection, hypoxia, rubella, retroviruses, toxoplasmosis, respiratory infections, herpes simplex virus, and famine (BALLON; DEAN; CADENHEAD, 2008; BROWN, 2006; CLAIR et al., 2005; FATEMI; FOLSOM, 2009; JAARO-PELED; SAWA, 2020; KARLSSON et al., 2001). These insults can affect the developing embryo in two ways: first, a pathological agent can cross the placenta and directly affect the developing embryo; second, exposure to a pathogen may induce an immune response in the mother, whereupon cytokines are transmitted to the fetus, indirectly affecting the developing embryo (reviewed by (FATEMI; FOLSOM, 2009)).

As neurodevelopment progress is tightly regulated in spatiotemporal terms, fetal exposure to environmental factors can be a crucial turning point in the development of diseases. As processes are interconnected, even small abnormalities during the initial developmental stages can greatly affect the steps that follow. Molecular signaling is crucial at each stage of development, and different molecules act at different stages, requiring precise coordination for each molecule to be expressed at the right time (reviewed in (GUPTA; KULHARA, 2010)). Most of the cerebral architecture is defined before birth and in mammalian neurodevelopment, the first cells to be established from neuronal progenitor cells are neurons, after basic morphological boundaries of the developing brain are established (MOLYNEAUX et al., 2007). Following the extensive proliferation of neural progenitor cells between 28-140 days after conception, these cells migrate to their final positions within the brain (THOMASON et al., 2021).

Neuronal differentiation relies on complex machinery for regulation and is largely controlled by cell-cell interactions and careful regulation of gene transcription. The Schizophrenia Working Group of the Psychiatric Genomics Consortium found 108 independent loci significantly associated with schizophrenia patients (RIPKE et al., 2014); and 7 genes within these loci were already known to play an important role in neurodevelopment (FXR1, SATB2, PODXL, BCL11B, TLE1, TLE3, and FAM5B). When neural progenitor cells reach their destinations in the developing brain, synaptic connections are formed during a process called synaptogenesis. During this phase, an excess of synaptic connections is formed before being refined throughout development until late adolescence, the point at which neurodevelopment is normally considered to end, resulting in a fully developed brain (reviewed by (THOMASON et al., 2021))). It is hypothesized that the completion of synaptic pruning during adolescence coincides with the point time that is related to the point at which affected individuals present their first psychotic symptoms in schizoprenia (JAARO-PELED; SAWA, 2020).

Throughout neurodevelopment and adult life, neurotransmitter receptors function to receive signals at synapses. In addition to the neurodevelopment-associated gene loci found by the Schizophrenia Working Group of the Psychiatric Genomics Consortium, other loci covered several genes that function at glutamatergic synapses, especially NMDA receptor function (GRIA1, GRM3, GRIN2A, and SRR) (RIPKE et al., 2014), tying this hypothesis in with other theories for the development, such as the glutamate hypothesis.

3.2.3 The Glutamate Hypothesis

The first model that proposed a relationship between neurodevelopment and the glutamatergic system in schizophrenia was the methylazoxymethanol acetate model (MAM), in which pregnant rats undergo treatment with anti-mitotic methylazoxymethanol acetate, a selective antiproliferative agent for neuroepithelial cells (JONGEN-RÊLO et al.,

2004). When female rats undergo treatment during the period from E9 to E16, marking the peak of neocortex neurogenesis, several morphological changes such as disorganised cortical layering and abnormal temporal asymmetries are observed in the cortical structures of the brain (TALAMINI et al., 1998). These morphological impairments were then found to be similar to those seen in patients with schizophrenia (JONGEN-RÊLO et al., 2004). These changes are the result of NMDA receptor hypofunction, though the exact mechanisms are not fully understood (SNYDER; ADELMAN; GAO, 2013). Gulchina et al (GULCHINA et al., 2017), were the first to confirm that the hypofunction of NMDA receptors can cause problems in postnatal development and to associate the cognitive impairments observed in schizophrenia models and patients with synaptic dysfunction during neurodevelopment.
Glutamate is the main excitatory neurotransmitter in the nervous system and is the most abundant amino acid in the brain, playing a fundamental role in the regulation of the glutamatergic system, which is important for neural plasticity (ZHOU; DANBOLT, 2014). The glutamatergic system is composed of two types of receptors: ionotropic receptors, which can bind to N-methyl-D-aspartate (NMDA), α-amino-3-hydroxy-5-methyl-4-isoxazolepropionic acid (AMPA), and kainate; and metabotropic receptors, which are G protein-coupled glutamate receptors (mGluR), subdivided into groups I, II, and III (reviewed in (MELDRUM, 2000)).
The glutamate neurotransmission hypothesis of schizophrenia was originally based on the evidence that NMDA-type glutamate receptor antagonists such as phencyclidine (PCP), dizocilpine (MK-801), and ketamine induce psychosis, negative symptoms, and cognitive dysfunction in normal subjects, similarly to what occurs in patients with schizophrenia (KRYSTAL et al., 2003; LEWIS; GONZÁLEZ-BURGOS, 2008; GONZALEZ-PINTO et al., 1998; NEWCOMER et al., 1999). NMDAR hypofunction, however, does not appear to be a direct consequence of low glutamate availability, but rather a signaling deficit in postsynaptic receptors (LEWIS; GONZÁLEZ-BURGOS, 2008).
The impairment of this system has been proposed to lead to the neural disconnection seen in schizophrenia. The hypofunction of NMDA receptors also affects parvalbumin-positive interneurons in the hippocampus and cerebral cortex, leading to a hyperfunction of the mesolimbic pathway and a hypofunction of the mesocortical pathway (EGERTON et al., 2020; FRANKLE; LERMA; LARUELLE, 2003). Both of these pathways are part of the dopaminergic system and are associated with positive and negative symptoms, respectively. Therefore, NMDA receptor dysregulation covers several hypotheses, such as dopaminergic and gabaergic, and impairments already discussed for schizophrenia symptoms and treatment (EGERTON et al., 2020).
In addition to glutamate, several endogenous and exogenous molecules, including D-serine and glycine, can modulate the activity of the NMDA receptor (Figure 4), making it a key player in the regulation of the glutamatergic system. In the adult brain, D-serine plays a role in the regulation of synaptic plasticity (ROSENBERG et al., 2013); however, during

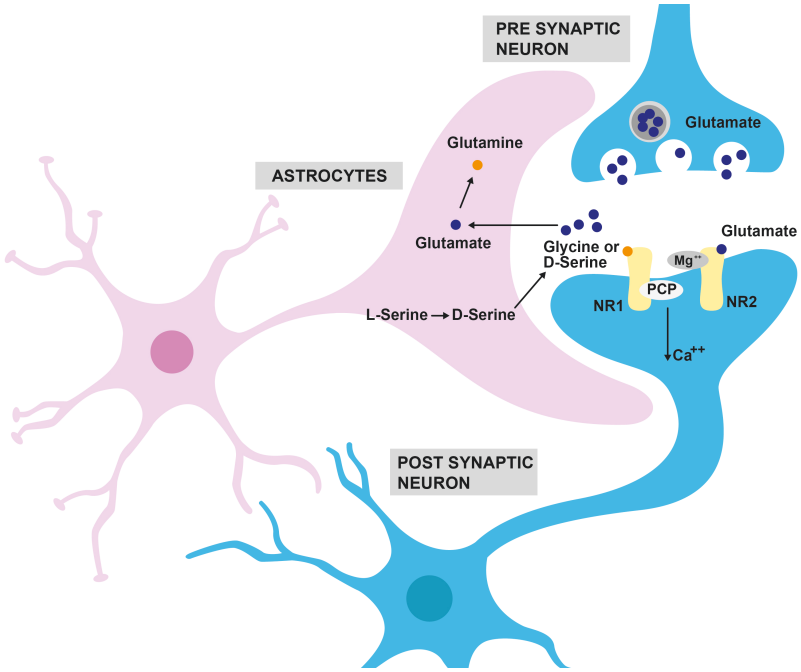

Figura 4 – N-methyl-D-aspartate (NMDA) receptor activation: Representation of the tripartite synapse and NMDA receptor modulator molecules. NR1 and NR2 - NMDA receptor subunits1 and 2, magnesium (Mg++), phencyclidine (PCP). For an NMDA receptor to be activated, 3 events must occur simultaneously: i) binding of glutamate to AMPA or kainate receptors, which leads to the depolarization of the membrane of postsynaptic neurons; ii) binding of glutamate to its NMDA site; and iii) binding of glycine or D-serine to the co-agonist binding site. After these steps, a magnesium ion that blocks the receptor channel is displaced, allowing a cation influx (mainly sodium and calcium) into the postsynaptic neuron, thereupon generating a series of cellular responses (BERGER; DIEUDONNÉ; ASCHER, 1998; HONG et al., 2004)

.

neurodevelopment, D-serine is found in relative abundance and co-localizes with NMDA receptors, suggesting a greater importance than glycine, even though both molecules similarly activate NMDA receptors (HASHIMOTO et al., 1993a; HORN; SILD; RUTHAZER, 2013). The glutamatergic system participates in important canonical functions such as synaptic transmission, neuronal migration, learning and memory, synaptic plasticity, and long-term potentiation and depression (PITTENGER; BLOCH; WILLIAMS, 2011; WILLARD; KOOCHEKPOUR, 2013). A decrease in D-serine concentration can lead to NMDAR hypofunction, a phenotype seen in patients with schizophrenia (HASHIMOTO et al., 2003).

Despite advances in the D-serine and MAM models, the precise role of the glutamatergic system during neurodevelopment still must be better understood. Preclinical studies indicate that inadequate glutamatergic signaling at this stage may have long-lasting effects and possibly contribute to the development of schizophrenia (EGERTON et al., 2020). These complex characteristics regarding the pathophysiology of schizophrenia require

equally complex tools. One promising methodology to understand these dysfunctions is the investigation of proteomic differences between individuals with schizophrenia and healthy controls. Protein expression reflects not only any downstream effects of genetic dysregulations but can also depict changes that occur in response to environmental stimuli, providing a viewpoint closer to the phenotype of schizophrenia than genetics alone can provide.

With this in consideration, to understand what the dysregulations found in the adult individual can tell us about the neurodevelopmental component of schizophrenia, we performed a comparative analysis of the proteins dysregulated in schizophrenia against those that are highlighted during neurodevelopment.

3.3 Methods

3.3.1 PubMed-Sourced Data

We previously compiled several proteomic studies in schizophrenia in a review article (SAIA-CEREDA et al., 2017a) involving the corpus callosum, anterior temporal lobe, anterior cingulate cortex, dorsolateral prefrontal cortex, mediodorsal thalamus, insular cortex, frontal cortex, and Wernicke's area. Together, the differentially regulated proteins revealed consistent alterations in signaling pathways, axon maturation, myelination, and metabolic processes, thus underpinning the multifaceted nature of schizophrenia. Here, we updated that list of differentially regulated proteins in schizophrenia with recent publications involving the cerebellum, posterior cingulate cortex, caudate nucleus, and the hippocampus (OLIVEIRA et al., 2020; ZUCCOLI et al., 2021)(Supplementary table 1). Articles included in this review were selected by searching the Pubmed database (https://pubmed.ncbi.nlm.nih.gov) using the following keywords: proteomics, schizophrenia and *postmortem* brain. A further selection criterion was the requirement for analysis methods to be based on mass spectrometry, such as *shotgun* proteomics (using labeling methods or label-free techniques) or two-dimensional gel analysis.

3.3.2 *in silico* analyses

The complete set of proteins found to be differentially regulated in patients with schizophrenia compared to controls were compiled into a single table and used for subsequent *in silico* analyses (Supplementary table 1). For over-representation and canonical pathway analyses, we used clusterProfiler (WU et al., 2021) and ReactomePA (YU; HE, 2016) in an R environment (v. 4.0), searched against the Kyoto Encyclopedia Genes and Genomes database (KEGG, http://www.genome.ad.jp/kegg/) (KANEHISA;

GOTO, 2000) and Reactome pathway database (http://reactome.org/) (JASSAL et al., 2020), respectively. Visualization was carried out, in addition to Cytoscape, with Omics Visualizer App (LEGEAY et al., 2020).

3.3.3 Molecular links between schizophrenia and neurodevelopment

To assess possible molecular links between schizophrenia and neurodevelopment, the resulting list of proteins that were identified to be dysregulated in postmortem schizophrenia brains was cross-checked with the proteins that were identified in human fetal brain tissue from 16-36 weeks of gestation (DJURIC et al., 2017) (Figure 5A). We compiled a list of commonly differentially regulated proteins in the *postmortem* brains of patients with schizophrenia (modified from (SAIA-CEREDA et al., 2017a), Supplementary table 1), henceforth called schizophrenia proteome. In a second list, we compiled the proteins found in different brain regions (cortex, subplate, intermediary zone, and ventricular zone) during neurodevelopment (16-36 gestational weeks) (DJURIC et al., 2017), hereby called the neurodevelopmental proteome. Proteins that were found in common were used as the input list for all following *in silico* analyses. The aim was to find which differentially expressed proteins in schizophrenia are also key proteins in the developing brain, uncovering what modulations may be occuring in schizophrenia during neurodevelopment. The analysis revealed that, out of 1209 differentially regulated proteins found in the postmortem brains of schizophrenia patients, 910 (approximately 75%) are expressed during neurodevelopment. An upset plot (Figure 5B) indicates that most of the proteins in common between schizophrenia and neurodevelopment are expressed in multiple brain regions during the period of cortical development (16-36 gestational weeks).

Previously published and discussed processes were highlighted in the schizophrenia proteome (Figure 5D), such as the citric acid (TCA) cycle and respiratory electron transport (p-adjusted = 4.55e-24) and pyruvate metabolism (p-adjusted = 4.87e-5), both of which are fundamental in cellular energy metabolism. Dysfunctions in energy metabolism pathways negatively impact development in a schizophrenia patient-sourced iPSC model (BRENNAND et al., 2011; KATHURIA et al., 2020), reinforcing its role not only in adults but also throughout neurodevelopment.

The major processes that appeared in both the schizophrenia proteome and neurodevelopmental proteome when searched against the Reactome database were neuronal system (p-adjusted = 1.64e-11), transmission across chemical synapses (p-adjusted = 3.73e-18), and neurotransmitter receptor and postsynaptic signal transmission (p-adjusted = 1.34e-12). Studies using neural progenitor cells (NPCs) and iPSC-derived neurons from patients have indicated reduced neural connectivity, also associating these dysfunctions with Wnt/cAMP signaling pathways and NCAM expression (BRENNAND et al., 2011; TOPOL et al., 2015).

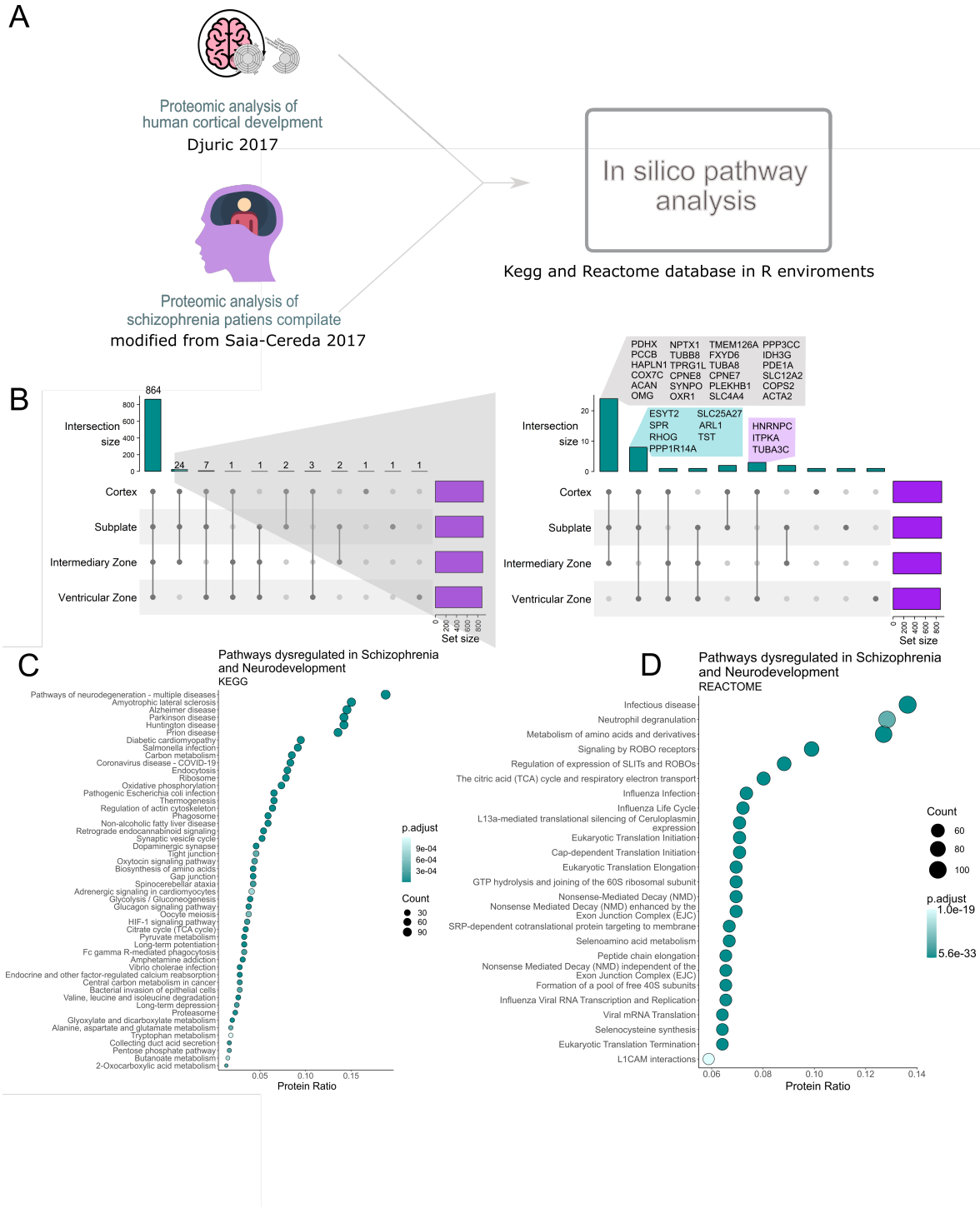

Figura 5 – Comparison between proteins found differentially regulated in schizophrenia and proteins identified throughout neurodevelopment. A) Workflow of the comparison between *postmortem* brain-related proteins from patients with schizophrenia versus human fetal brain tissue-related proteins from different regions (16-36 gestational weeks). B) Upset plots highlighting the different brain regions that may be affected in schizophrenia throughout neurodevelopment. C-D) Over-representation analysis of pathways against the KEGG and Reactome databases. The enriched pathways were considered significant if they obtained an adjusted p-value below 0.05. Proteins that were found in common between schizophrenia proteome and neurodevelopmental proteome were used as the input list for *in silico* analyses

Other overlapping processes between the schizophrenia and neurodevelopmental proteomes include several signaling pathways that are related to axon guidance, such as L1CAM interaction (p-adjusted= 1.22e-19) and signaling by ROBO receptor (p-adjusted = 4.97e-30). Axon guidance processes are regulated by a series of protein families, such as ephrins, semaphorins, and L1CAM, many of which are known to be deregulated in patients with schizophrenia ((CHÉDOTAL, 2019; SAIA-CEREDA et al., 2016). Furthermore, impaired cell migration has been observed in NPCs derived from patients with schizophrenia (TOPOL et al., 2015). All the processes mentioned above are central to dynamic brain development, and small disruptions in any of those pathways can later result in diseases. The glutamatergic system was another synaptic process that was found in common between the two proteomes (Figure 6A), encompassing activation of NMDA receptors and postsynaptic events (p-adjusted = 4.82e-15), and post NMDA receptor activation events (p-adjusted = 3.25e-16). The subunits of the NMDA receptor can vary, thereby regulating its function at different stages of development. As such, mutations in subunits of this receptor can lead to future cognitive deficits and intellectual disabilities (ENDELE et al., 2010; MIELNIK et al., 2020). *De novo* mutations have also been found in the GluN2A and B subunits of patients with schizophrenia (ENDELE et al., 2010; TARABEUX et al., 2011). As such, by broadening the perspective of glutamate dysregulation, changes in the arrangement of NMDA receptor subunits should be studied during early development to determine if they are causative of the cognitive deficits observed in adults with schizophrenia.

Other signaling pathways that regulate the function of this receptor were also found dysregulated in schizophrenia (Figure 6A), such as assembly and cell surface presentation of NMDA receptor (p-adjusted = 7.36e-13) and negative regulation of NMDA-mediated neuronal transmission (p-value = 7.16e-5). This suggests that there may be not only a structural problem in this receptor but also dysregulations in the signaling mechanisms that regulate its activity and/or expression. Supporting this hypothesis, mRNA levels of NMDAR regulatory proteins, as well as the density of proteins accessory to the NMDA receptor, have also been found to be decreased in schizophrenia patients (LIN; LANE, 2019).

NMDA receptor hypofunction is a known feature of schizophrenia, suggested to be due to a lack of D-serine, which has been found in lower concentrations in the cerebrospinal fluid of schizophrenia patients (HASHIMOTO et al., 2005; STEVENS et al., 2003). Moreover, administering D-serine together with antipsychotics helps reduce negative and positive symptoms and improves cognitive function (HERESCO-LEVY et al., 2002; TSAI et al., 1998). In a murine model, D-serine supplementation during youth and adolescence was seen to prevent psychosis and cognitive deficits in adult mice that had undergone maternal immune activation (MIA) (FUJITA; ISHIMA; HASHIMOTO, 2016). The main functions

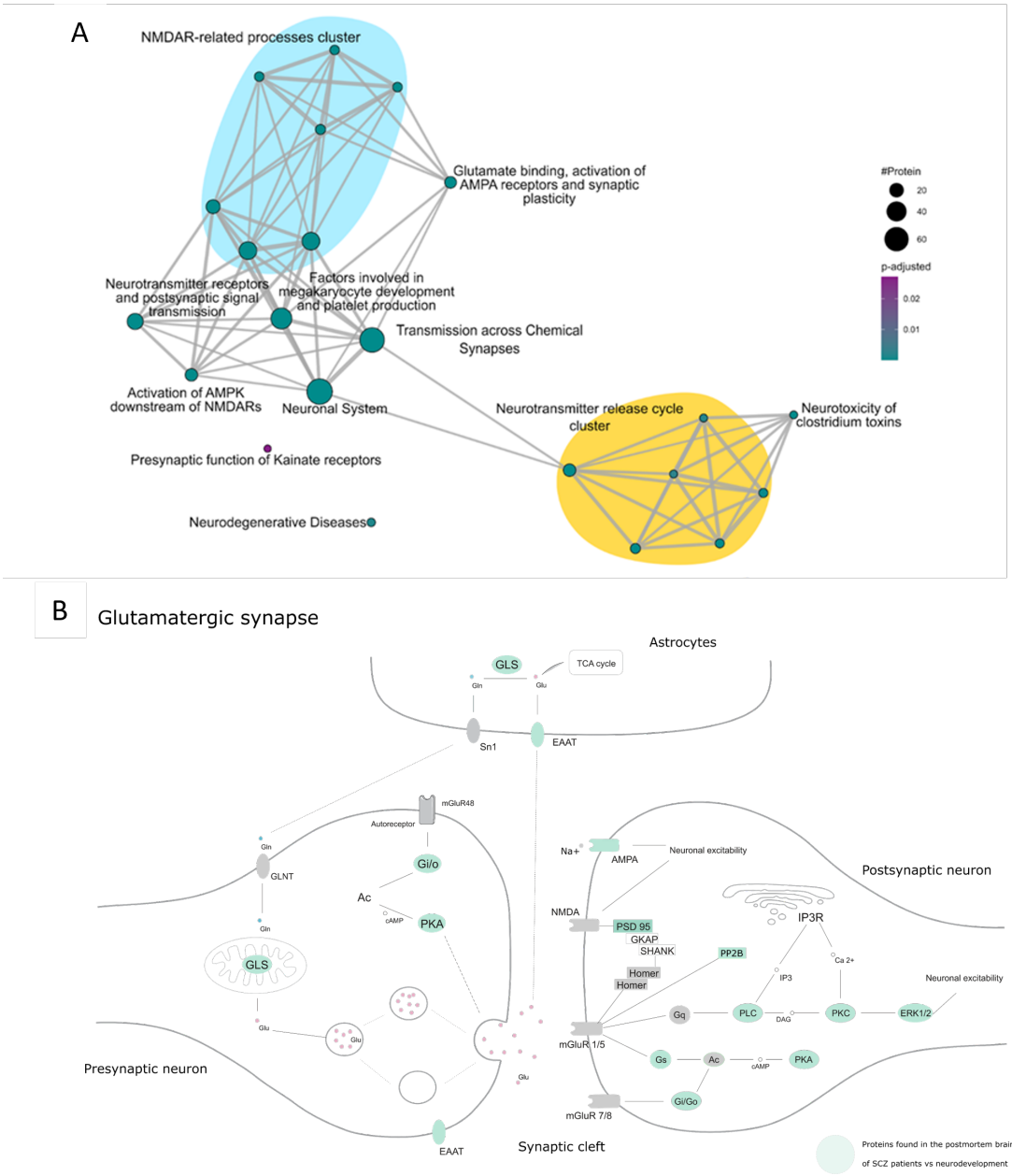

Figura 6 – The role of glutamate signaling in neurodevelopment and its relationship to the pathophysiology of schizophrenia. A) Enrichment map of pathways associated with glutamatergic synapses, generated with the list of differentially regulated proteins in schizophrenia that are also found throughout neurodevelopment. Each pathway is represented by a circle, and size corresponds to the number of proteins present. B) Glutamatergic synapse proteins (represented in green) are found in the schizophrenia and neurodevelopmental proteomes. Enriched pathways were considered significant if they obtained an adjusted p-value below 0.05. Proteins that were found in common between schizophrenia proteome and neurodevelopmental proteome were used as the input list for *in silico* analyses.

associated with D-serine in neurodevelopment are synaptic plasticity, maturation of glutamatergic synapses, dendritic formation, and neuronal migration (BROADBELT; BYNE; JONES, 2002; GAREY et al., 1998; GLANTZ; LEWIS, 2000; HASHIMOTO et al., 1993b; KALUS et al., 2000). Many proteins involved in these processes were found in both the schizophrenia and neurodevelopmental proteomes. In addition, a dysregulation in proteins of amino acid metabolism (p-adjusted = 3.21e-28) was seen (Figure 5 D).

Using the proteins found in common between the schizophrenia and the neurodevelopmental proteomes, we performed an enrichment analysis using DAVID and filtered for proteins related to the glutamatergic synapse (Figure 6B). This indicated the presence of proteins such as the excitatory amino acid transporter (EAAT) and postsynaptic density protein 95 (PSD-95). EAAT2 is responsible for the reuptake of glutamate in the synaptic cleft and is mostly expressed in astrocytes (ZHANG et al., 2015). This is a reminder that, despite the significant focus placed on neuronal dysregulation to explain the pathophysiology of schizophrenia, other cell types play an important role (SAIA-CEREDA et al., 2015). PSD-95 is a postsynaptic density protein that plays a role in maintaining synaptic dynamics, especially at glutamatergic synapses (BALAN et al., 2013). This protein participates directly in synaptic maturation, being therefore essential for synaptogenesis, and regulates glutamatergic receptor function (both NMDARs and AMPARs - amino-3-hydroxy-5-methyl-4-isox-azoleproprionic acid receptors) (reviewed in (COLEY; GAO, 2019)).

Digging deeper into the protein regulation throughout the pathways found dysregulated in schizophrenia and present in neurodevelopment, we performed a pathway-protein network analysis, highlighting the z-scored abundance of proteins between 16 and 36 gestational weeks of brain development (Figure 7). Cytoskeletal proteins of the cytoskeleton were found in both the schizophrenia and neurodevelopmental proteomes (Figure 7A), including several isoforms of tubulin, neurofilaments, and microfilament-associated proteins. These proteins play a fundamental role in neural differentiation and regulate organization, maintenance, and axon guidance. Genetic studies show the role of cytoskeleton dysregulation in the development of schizophrenia (ROMANIELLO et al., 2012). Since brain development relies on proper cytoskeletal organization for cell maintenance and differentiation of several cell types, these proteins are found throughout the developmental period in all regions of the developing brain (Figure 7 A).

Another protein family, related to the NMDAR/axon maturation system, is the calcium/calmodulin-dependent protein kinase (CAMKII) family. In neurodevelopment, CAMKII regulates synaptogenesis and synaptic plasticity (VIBERG, 2009). This family of proteins is essential for NMDAR regulation, thereby controlling excitatory synapse transmission (INCONTRO et al., 2018). In addition, this group of proteins was defined as a marker of neurotoxicity during neurodevelopment (VIBERG, 2009) and is related

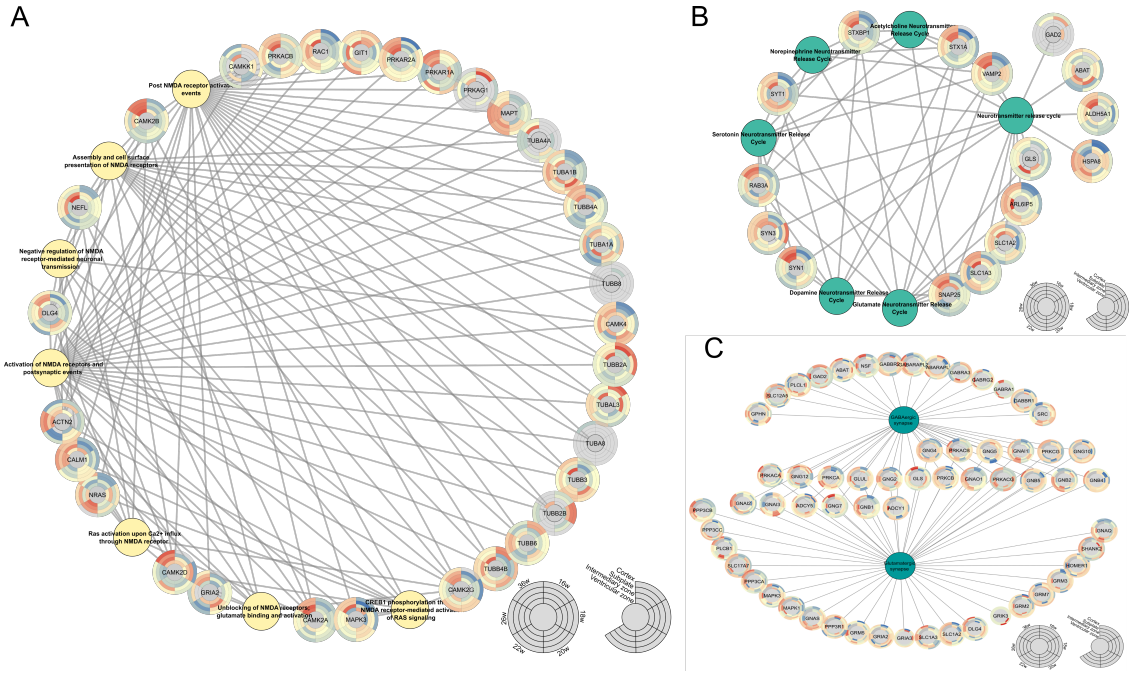

Figura 7 – Glutamatergic system and its relationship with other hypotheses of schizophrenia. A) Pathway-protein network of pathways associated with schizophrenia and synaptic processes. B) Pathway-protein network of the neurotransmitter release cycle clusters, highlighting the regulation of these proteins throughout neurodevelopment periods (16-36 gestational weeks) and regions (cortex, subplate, intermediary zone and ventricular zone). C) Proteins related to schizophrenia that participate in the glutamatergic and GABAergic transmission systems and their regulation throughout development. Networks were generated using the Reactome database. The enriched pathways were considered significant if they obtained an adjusted p-value below 0.05. Proteins that were found in common between schizophrenia proteome and neurodevelopmental proteome were used as the input list for *in silico* analyses.

to several neuropsychiatric disorders (AKITA et al., 2018). These proteins were found predominantly between weeks 26-36 of development (Figure 7A). This suggests that these proteins play an important role in neural maturation, which occurs around gestational week 27, when cortical neogenesis ends and the maturation phase intensifies (CLANCY; DARLINGTON; FINLAY, 2001).

The proteins in common between schizophrenia and neurodevelopment did not present exclusive functions in the glutamatergic system, rather also acting in the GABAergic, dopaminergic, and serotonergic systems (Figure 7A-C). Studies in *postmortem* brain and animal models have suggested that the reduced activation of the GABAergic system and the hyperfunction of the dopaminergic system may be a consequence of the hypofunction of the glutamatergic system (LI et al., 2002; PAULSON et al., 2003; WOO; WALSH; BENES, 2004). In this hypothesis, the hypofunction of cortical NMDA receptors would cause a reduction in parvalbumin-positive GABAergic interneurons and thus the loss of their inhibitory brake, consequently leading to a decrease in dopaminergic neurotransmission in

the mesocortical pathway in addition to an increase in the mesolimbic pathway (STAHL, 2018). In neurodevelopment, both the glutamatergic and GABAergic systems develop early. In the rat cortex, for example, these receptors begin to develop at E12 (BYSTRON; BLAKEMORE; RAKIC, 2008). The balance between these two neurotransmitters plays a role in signaling cascades that regulate, among other pathways, neuron proliferation, migration, differentiation, and survival, all functions that are fundamental for the correct development of the fetal brain (LUJÁN; SHIGEMOTO; LÓPEZ-BENDITO, 2005).

3.3.4 Conclusions and Future Direction

Conclusions and Future Directions As Lewis et al. (LEWIS; GONZÁLEZ-BURGOS, 2008) wrote, dissecting the cause, the consequence, the compensation (the organism's response to the disease in an attempt to restore homeostasis), and the disease confound (factor associated with the disease that is not part of its process) is a challenging process. Schizophrenia is a disorder that spans a spectrum, classified by the predominance of different symptoms, making each patient a unique case. Further confounding research, diagnosis, and treatment, this disease has a silent prodrome, wherein the first clinical signs appear only when the disease has already reached an advanced stage. This in turn has often led to an erroneous conclusion that several effects resulting from the progression of the disease are instead causative. The unique nature of each patient makes the task of finding the best antipsychotic for that specific patient and their symptoms exceptionally difficult, which is also a consequence of the great plurality of the pathophysiology of the disease. Moreover, a lack of prompt and effective treatment compounded by late-onset symptoms drastically increases the severity and impact of the disease.

Due to the spectral nature of schizophrenia, there is no current consensus as to whether a given dysregulation, for example NMDAR hypofunction, occurs universally, nor is there a comprehensive list of which molecules are involved in the dysregulation of this process. Several hypotheses exist that implicate environmental factors, such as obstetric complications, that can directly interfere with this receptor; that question the existence of a genetic factor so that individuals, when exposed to environmental factors, develop the disease; and that suggest the possibility that each patient may possess different combinations of deregulations that collectively generate the spectrum of symptoms that we call schizophrenia, instead of the existence of a common dysregulation present in every patient.

Despite extensive analysis, there is still little evidence of the nuances of schizophrenia at a systemic level, particularly regarding development in the fetal period. Although the onset of schizophrenia occurs in late adolescence to early adulthood, the disease appears to begin to develop long before the first symptoms emerge. The administration of D-serine in an animal model holds potential to prevent the development of the disease (FUJITA; ISHIMA; HASHIMOTO, 2016), raising the possibility but also ethicality of using this

compound as a preventative treatment with individuals that are presumed to develop the disease as adults.

With many questions still unanswered, we emphasize the importance of studies that investigate the role of neurodevelopmental processes and the glutamatergic system in the pathophysiology of schizophrenia. We hope that, with continued integration of hypotheses and research methods, it will be possible to develop novel medications with a greater range of action, ameliorating not only positive symptoms, but also the elusive negative and cognitive symptoms, thus obtaining greater treatment efficacy, reducing treatment dropout, and improving the quality of life of patients.

4 Proteomic signatures of schizophrenia-sourced iPSC-derived neural cells and brain organoids are similar to patients' *postmortem* brains

Juliana M. Nascimento[1,2,@], Verônica M. Saia-Cereda[1,@], Giuliana S. Zuccoli[1], Guilherme Reis-de-Oliveira[1], Bradley J. Smith[1], Stevens K. Rehen[2,3*], Daniel Martins-de-Souza[1,4,5*]

1 Laboratory of Neuroproteomics, Department of Biochemistry and Tissue Biology, Institute of Biology, University of Campinas (UNICAMP), Campinas, Brazil.

2 D'Or Institute for Research and Education (IDOR), Rio de Janeiro, Brazil.

3 Institute of Biomedical Sciences, Federal University of Rio de Janeiro (UFRJ), Rio de Janeiro, Brazil.

4 Instituto Nacional de Biomarcadores em Neuropsiquiatria (INBION), Conselho Nacional de Desenvolvimento Científico e Tecnológico (CNPq), São Paulo Brazil

5Experimental Medicine Research Cluster (EMRC), University of Campinas, Campinas, São Paulo Braz.

@ Contributed Equally

*Corresponding authors

4.1 Abstract

Schizophrenia is a complex and severe neuropsychiatric disorder, with a wide range of debilitating symptoms. Several aspects of its multifactorial complexity are still unknown, and some are accepted to be an early developmental deficiency with a more specifically neurodevelopmental origin. Understanding timepoints of disturbances during neural cell differentiation processes could lead to an insight into the development of the disorder. In this context, human brain organoids and neural cells differentiated from patient-derived induced pluripotent stem cells are of great interest as a model to study the developmental origins of the disease. Here we evaluated the differential expression of proteins of schizophrenia patient-derived neural progenitors, early neurons, and brain organoids compared to healthy subjects. Using bottom-up *shotgun* proteomics with a label-free approach for quantitative analysis, 535 proteins were found differentially expressed in

organoids, 364 in neural progenitor cells (NPCs), and 264 in immature neurons compared to control. Multiple dysregulated proteins were found in pathways related to synapses, in line with *postmortem* tissue studies of schizophrenia patients. Furthermore, it was observed that organoids and immature neurons exhibit deficiencies in pathways never before found in studies with patient-derived induced pluripotent stem cells, such as spliceosomes and amino acid metabolism. In conclusion, here we provide comprehensive, large-scale, protein-level data that may uncover underlying mechanisms of the developmental origins of schizophrenia. Data are available via ProteomeXchange with identifier PXD026381 (organoids) and PXD026593 (NPC and neurons).

4.2 Introduction

Schizophrenia is one the most prevalent neuropsychiatric disorders, though poorly understood regarding its molecular mechanisms. In general, initial symptoms are present at the beginning of adulthood; however, molecular roots of the disease have been linked to neurodevelopmental dysfunctions (SCHMIDT; MIRNICS, 2015). Several symptoms overlap with other disorders, such as major depression and bipolar disorders, making an early diagnosis and treatment strategies more difficult (GONZALEZ-PINTO et al., 1998). Both genetics and the environmental course on neurodevelopment have been associated with the disease onset. Thus, continued discoveries and characterization of new factors that contribute to disease onset and progression are key to understanding the complexity of the disorder (KOHANE; MASYS; ALTMAN, 2006).

Advances over the past few years are a result of employing a broader spectrum of tools to research *postmortem* brains and animal models, from brain imaging to cell-based studies, including induced pluripotent stem cells (iPSCs) (TOPOL et al., 2015; BRENNAND, 2017). Furthermore, human iPSCs (hiPSCs) overcome the unpracticality and poor accessibility of human brain cell types (PEDROSA et al., 2011) and are providing the possibility to challenge and question neural cell fates, prior to or during the onset of a disease in question. Considerable progress has been made regarding the neural differentiation of human pluripotent stem cells into mature neurons and cerebral organoids (KELAVA; LANCASTER, 2016). Human neural progenitor cells (hNPC) form a useful cell system for high-throughput screening due to their homogeneity, along with low complexity and limited differentiation potential. In comparison, cerebral organoids are complex, three-dimensional (3D) culture systems composed of multiple cell types that self-organize into various brain regions similar to those *in vivo* , including the cerebral cortex, ventral forebrain, midbrain-hindbrain boundary, and hippocampus (LANCASTER; KNOBLICH, 2014; QIAN et al., 2016; CAMP et al., 2015). The combination of different cell types in a complex 3D configuration can better simulate brain biology and function, allowing cerebral organoids to reproduce the function and architecture of the brain, especially regarding

development and neuronal plasticity.

Through the combination of hiPSCs with neural organoid differentiation and label-free *shotgun* proteomics, we can expand our knowledge of expression dynamics, providing a deeper understanding of biological processes along the course of development, simulating *in vivo* conditions (TOPOL et al., 2015; NASCIMENTO et al., 2019). Therefore, here we evaluate schizophrenia using neural progenitor cells (NPCs), immature neurons, and brain organoids derived from schizophrenia patients and compared them to control subject-derived neural cells using *shotgun* label-free proteomics. Cells derived directly from schizophrenia patients offered an integrated view of protein expression during neurodevelopment, depicting compromised biochemical pathways. In addition, it established an *in vitro* schizophrenia platform with the potential to modify and manipulate compromised pathways using a plethora of chemical compounds. This global proteome analysis during cell development may contribute to the search for new therapies with a focus on the personalized treatment of the disease.

4.3 Materials and methods

4.3.1 Pluripotent stem cell culture

Human induced pluripotent stem cells (hiPSCs) were reprogrammed from three subjects diagnosed with the schizophrenia spectrum, GM23760B (male, 26y), GM23761B (female, 27y), and GM23762B (male, 23y) 12, available at Coriell. Three control hiPSC cell lines were used, GM23279A (female, 36y, available at Coriell), and CF1 (male, 37y) and CF2 (male, 31y), reprogrammed at the D'Or Institute for Research and Education (SOCHACKI et al., 2016). Organoids were derived from human embryonic stem cell lines BR1 - Laboratory for Embryonic Stem Cell Research (LaNCE), University of São Paulo (FRAGA et al., 2011) and H9 (WiCell). Cells were cultured in mTeSR1 (Stemcell Technologies) or E8 medium (Thermo Scientific), on a Matrigel (BD Biosciences)-coated surface. Colonies were manually passaged at 70% confluence and maintained at 37°C in humidified air with 5% CO2. The establishment of hiPSCs and the derivation of NPCs, neurons, and organoids were carried out following international standards and with the approval of the local research ethics council (CAAE: 32385314.9.0000.5249).

4.3.2 Human neural progenitor cells and neuronal differentiation

To induce the differentiation of hiPSCs into neural progenitors, we used a previously described protocol (BAHARVAND et al., 2003). In brief, the hiPSC cultures from six individuals (three control and three schizophrenia patients), at 70% confluence were induced into a neural lineage in a defined adherent culture by retinoic acid and

basic fibroblast growth factor (bFGF). After 18 days, neural tube-like structures can be collected and plated on dishes coated with 10 μg/mL of poly-L-ornithine and 2.5 μg/mL of laminin (Thermo Fisher Scientific), in N2B27 medium (DMEM-F12 with 1x N2 and 1x B27 supplements, 1% penicillin/streptomycin) supplemented with 25 ng/mL bFGF and 20 ng/mL EGF (Thermo Fisher Scientific). Human neural progenitor cells (hNPCs) then migrate from the neural tube-like structures and were thereupon tested for the expression of neural markers before expansion. Cell expansion was done in N2B27 medium supplemented with EGF and bFGF and replaced every other day. hNPCs were expanded for no more than 5 passages. Basic characterization of this culture has been previously published in (DAKIC et al., 2017). For neuronal differentiation, hNPCs of each lineage were plated on poly-L-ornithine- and laminin-coated dishes, and 24h after plating, bFGF and EGF were removed from the N2B27 medium to trigger differentiation. Neuronal cultures were differentiated for 21 days *in vitro* . The medium was replaced every 5 days. Both hNPCs and neuronal cells were incubated at 37ºC and 5% CO2. After the period described, cells were collected for proteomics or immunocytochemistry.

4.3.3 Differentiation into brain organoids

For differentiation of schizophrenia and control human iPSCs and ESCs, cells were cultured in mTeSR1 medium (Stemcell Technologies) on Matrigel (BD Biosciences)-coated cell culture dishes. Differentiation of pluripotent stem cells into cerebral organoids was based on a previously described protocol (SARTORE et al., 2017; LANCASTER et al., 2013). In summary, hPSCs were passaged into single-cells with Accutase (Merck Millipore) and inoculated in a spinner flask containing mTeSR1 medium supplemented with 10 μM Y-27632 (Rho-associated protein kinases inhibitor, iRock) (Merck Millipore) under constant rotation (40 rpm). The following day, the medium was replaced to initiate embryoid body formation. One week later, neural induction medium [DMEM/F12 1:1 supplemented with N2 (1x) supplement, 2 mM glutamax, 1% MEM-NEAA (Thermo Scientific), and heparin (1 μg/mL, Sigma)] was added. After 4 days, cellular aggregates were covered in Matrigel and cultured in differentiation medium [DMEM/F12:Neurobasal (1:1), supplemented with N2 (0.5x) and B27 minus vitamin A (1x) supplements, 2 mM glutamax, 0.5% MEM-NEAA, 0.2 μM 2-mercaptoethanol (Thermo Scientific), and 2.5 μg/mL insulin (Sigma)] for another 4 additional days. Subsequently, the medium was replaced with a neuronal differentiation medium, which comprises the same formulation, except for the use of 1x B27 containing vitamin A (Thermo Scientific). This final medium was then changed every week for the complete differentiation of cerebral organoids, grown for up to 45 days.

4.3.4 Immunohistochemistry

Cells were grown on coverslips for 5 days (for NPCs) or directly differentiated into neurons (for 21 DIV), washed with PBS to remove medium, and fixed in 4% paraformaldehyde (PFA). Cerebral organoids were collected after 45 days of differentiation and immediately fixed in 4% PFA, followed by incubation in sucrose solutions over an increasing gradient (10, 20, and 30%) in phosphate-buffered saline (PBS). Subsequently, the organoids were embedded in an optimal cutting temperature compound (OCT) and frozen in liquid nitrogen. The organoids were sectioned with a cryostat (Leica) into 20 μm-thick sections. After being fixed, cells and organoids were washed with PBS, permeabilized in a 0.3% Triton-X solution, and blocked in a 3% bovine serum albumin (BSA) solution before immunolabeling. Immunofluorescence was performed using the primary antibodies: anti-MAP2 (M1406, Sigma-Aldrich), anti-class III β-tubulin (MAB1637, Millipore), anti-nestin (MAB5326, Chemicon), anti-PAX6 (sc11357, Santa Cruz), anti-SOX1 (AB15766, Chemicon), and anti-SOX2 (AB5603, Millipore); secondary antibodies used were as follows: AlexaFluor 488 goat anti-rabbit (A11008) and goat anti-mouse (A11001); and AlexaFluor 594 goat anti-mouse (A11032, Invitrogen). DAPI was used for nucleus staining. Images were acquired using a Leica TCS SP8 confocal microscope.

4.3.5 Sample preparation and processing

From each schizophrenia patient or control cell line, NPCs (5 DIV) and neurons (21 DIV), were harvested and pelleted in PBS. After 45 days in culture, five to six cerebral organoids were pooled from the spinner flask and pelleted in PBS to provide population variability within each experiment. Cell lines were independently sampled and analyzed. Pellets of cells or organoids were removed from PBS and homogenized in lysis buffer [7 M urea, 2 M thiourea, 1% CHAPS, 70 mM DTT, and EDTA-free complete protease inhibitor cocktail (Roche)]. Sample lysates were kept on ice for approximately 20 min and centrifuged at 10,000 x g for 10 min at 4°C; supernatants were collected, and protein content was quantified using a Qubit® 3.0 Fluorometer (Thermo Fisher Scientific). Each sample (100 μg) was subjected to a short SDS-PAGE run and a sequence of reduction, alkylation, and overnight trypsin digestion (1:50 w/w trypsin:total protein) at 37°C. Peptides collected from this digestion were dried in a SpeedVac (Thermo Fisher Scientific) and stored at -80°C until quantitative and qualitative *shotgun* mass spectrometry analyses.

4.3.6 Liquid chromatography-mass spectrometry

Peptides were separated by a two-dimensional nanoAcquity UPLC M-Class System (Waters Corporation, Milford, MA) liquid chromatographer coupled to a Synapt G2-Si mass spectrometer (Waters Corporation). For first-dimension reverse-phase chromatography, peptides (5 μg) were loaded onto an M-Class BEH C18 Column (130 Å, 5

μm, 300 μm X 50 mm, Waters Corporation). Fractionation was performed in samples of organoids using increasing steps of acetonitrile concentration (13%, 18%, and 50% ACN); while for NPC and neurons there was no fractionation, and samples were directed to the second-dimension column. Peptide loads were directed to a second-dimensional separation on an HSS T3 Column (100Å, 1.8 μm, 75 μm X 150mm, Waters Corporation, Milford, MA), with a binary gradient of 7% to 40% ACN (v/v) over 54 min at a flow rate of 0.4 μL/min. Peptides entered the mass spectrometer using nano-electrospray ionization in positive ion mode, nanoESI (+). The MS analyses were performed using data-independent acquisition (DIA) enhanced with ion mobility separation (HDMSE). [Glu1]-Fibrinopeptide B human was used as the lock mass compound, which was sampled every 30 s. Each biological sample was run in technical duplicate. The LC-MS/MS method used was based on a previously described protocol (CASSOLI et al., 2017).The mass spectrometer measured in MSE mode, performing an acquisition switching low and high energy, with no selection window and a continuum ion current. The mass spectrometer operated in resolution mode with an m/z resolving power of at least 25,000 FWHM, using ion mobility with a cross-section resolving power of at least 40 $\Omega/\Delta\Omega$. The effective resolution obtained with the conjoined ion mobility was 1,800,000 FWHM. MS/MS analyses were performed by nano-electrospray ionization in positive ion mode nanoESI (+) using a NanoLock Spray (Waters, Manchester, UK)

4.3.7 Database search and quantitation

Raw data were aligned and processed in Progenesis® QI for proteomics version 3.0 (Waters). Protein identification and quantification were performed using the ion accounting algorithm with default parameters and searching against the Homo sapiens database – revised (Uniprot, version 2017/10). For protein identification, the following parameters were set: up to two missed cleavages for trypsin digestion; variable modification by oxidation (M) and fixed modification by carbamidomethyl (C), False Discovery Rate (FDR) less than 1%. The quantitative analysis was carried out on the log2-values of the intensities after normalization by a software-calculated global scaling factor, and only proteins present in at least two out of three biological samples were selected for further analysis.Proteins with ANOVA (p) $\leqslant 0.05$ between groups were considered differentially expressed. Raw data have been deposited in PRIDE (Proteomics Identifications Database) - Project accession: PXD026381 (organoids) and PXD026593 (NPC/immature neurons).

4.3.8 *In silico* analysis

Gene ontology and pathway enrichment were analyzed with DAVID (the Database for Annotation, Visualization and Integrated Discovery) (HUANG; SHERMAN; LEMPICKI, 2009a; HUANG; SHERMAN; LEMPICKI, 2009b) and Metascape (ZHOU et

al., 2019), using default settings and the following databases: KEGG Pathway, GO Biological Processes, Reactome and CORUM. Protein networks and canonical pathways associated with differentially expressed proteins were identified using Ingenuity Pathway Analysis software (IPA, Ingenuity Systems, Qiagen, Redwood, CA, USA; www.ingenuity.com). The significance of biological functions was calculated using Fisher's exact test. Multiple correlation hypotheses were calculated with the Benjamini-Hochberg (B-H) approach using a 1% FDR threshold; the significance levels of the IPA tests were expressed as p-values. Gene ontology was also analyzed using DAVID and Panther databases. The manipulation of data and comparative analyses of our proteomic data and differentially regulated proteins in schizophrenia *postmortem* brain tissue was performed in the Python programming language (v. 3.7.3). The overlap between proteins identified in our data and previous *postmortem* studies was visualized with a Circos plot (KRZYWINSKI et al., 2009). The over-representation analysis of brain regions and KEGG pathways was carried out using ClusterProfiler (YU et al., 2012) in the R programming environment (v. 4.0).

4.4 Results

hiPSC from three schizophrenia patients and three paired controls were differentiated into neural cells and submitted to proteomic analysis, as presented in the workflow (Figure 8). Each of the hiPSC samples from patients and controls (Figure 8A) were differentiated into neural progenitor cells (NPCs) (Figure 8B), young neurons with 21 days *in vitro* (21 DIV) (Figure 8C), and brain organoids (cultured for 45 days) (Figure 8D). Whole-cell proteomic profiles were generated using label-free quantitative proteomics (Figure 8E) to uncover some of the molecular mechanisms of schizophrenia during neurodevelopment. Data generated from a schizophrenia-related regulation of organoids (Supplementary Table 2) were further compared to publicly available proteomics datasets (Supplementary Table 1) from *postmortem* brain tissue of schizophrenia patients (Figure 8F).

4.4.1 Establishing hiPSC derived models

We first established cultures with progenitors and neurons differentiated from hiPSC cells of schizophrenia patients and controls. While NPCs were kept under proliferative medium, neuronal differentiation was performed by removing FGF and EGF from the growth medium, switching the proliferation program to a neuronal one. At the end of each culture period, NPCs in both control and schizophrenia-derived cells stained positive for neural progenitor markers such as nestin and SOX2 (SRY-Box 2) (Figure 9 A. Differentiation progenitors into young neurons was also induced in both schizophrenia and control cells. After 21 days of differentiation *in vitro* (21 DIV), morphological changes were observed in both control and schizophrenia cells, showing small cell bodies and a large

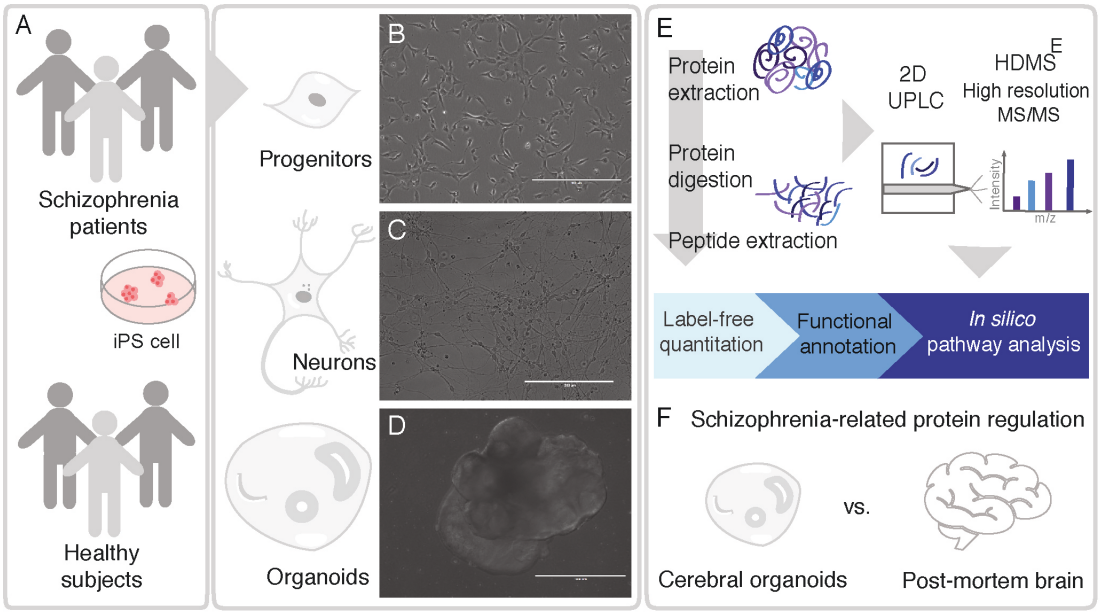

Figura 8 – Schematic organization of the experimental design and analysis workflow. (A) Human iPSCs from schizophrenia patients and controls were differentiated into neural cell types: progenitors, neurons and organoids. Representative photomicrographs of (B) neural progenitor cells (NPC), (C) neurons at 21 days *in vitro* and (D) 45-day cerebral organoids. (E) Proteomics workflow processing. Label-free sample preparation (protein extraction and peptide digestion) followed by 2D-UPLC fractionation and on-line detection using HDMSE high resolution MS/MS acquisition. Peptides and proteins were identified and quantified before functional annotation and other *in silico* analyses. (F) Differentially regulated proteins in cerebral organoids of schizophrenia patients were compared to available proteomics data from *postmortem* brains of schizophrenia patients. Scale bars shown are (B) 400 μm (C) 200 μm and (D) 1000 μm.

number of cells with neurite elongation (Figure 9A). Neurons at 21 DIV continued to stain for nestin and SOX2, with few cells staining for PAX6 (paired box 6), while several stained for β3-tubulin (TUBB3) (Figure 9A). Proteomic analysis also indicated the expression of nestin and TUBB3; in progenitors, the transcription factor PAX6 was observed, though it was not detected in neurons (Supplementary Table 2).

To evaluate a more complex model of cellular organization *in vitro* , we generated cerebral organoids at 45 days, a point at which a neuronal network has already been initially formed (NASCIMENTO et al., 2019; SARTORE et al., 2017). The whole-cerebral organoid protocol used has no cues for inducing a specific region, and the self-organized cytoarchitecture in both controls and schizophrenia-derived organoids were similar. The organoids from control and schizophrenia showed no major morphological differences, and 45-day-old cerebral organoids developed one to several putative ventricles, with young neurons identified by TUBB3-positive cells found at the subventricular zone in both control- and schizophrenia-derived organoids (Figure 9B). Control organoids showed organized

ventricle zones with SOX2-expressing progenitor cells and MAP2-expressing neuronal cells at the cortical layer, while schizophrenia patients had a larger area covered by SOX2 progenitors, also showing MAP2 distribution throughout the organoid (Figure 9C). In summary, these morphological aspects and protein markers confirm the models as suitable for comparison of schizophrenia and control differences during neurodevelopment.

4.4.2 Proteomic analysis of iPSC derived models

Proteomic analyses were performed at three different developmental stages of hiPSC-derived neural cells: neural progenitor cells (NPCs), neurons at 21 days *in vitro* (21 DIV), and cerebral organoids at 45 days (Supplementary Table 2). The NPC dataset yielded a total of 1949 quantified proteins, of which 364 proteins were found to be deregulated ($p < 0.05$) between schizophrenia-patients NPCs and controls. Of those proteins, 84% (306) were downregulated (Supplementary Table 2). At the second stage of differentiation, 1833 proteins were quantified in young neurons, 264 of which were considered dysregulated ANOVA, ($p < 0.05$) between schizophrenia and controls. Of these proteins, 70% (185) were downregulated. A slightly larger number of proteins was quantified from the 45-day cerebral organoids, which yielded 2177 quantified proteins. Between schizophrenia and control groups, 535 proteins were considered dysregulated (ANOVA, $p < 0.05$), 59% (317) of which were downregulated.

When comparing between the three cellular models, we found dysregulated proteins in common among NPC, neurons, and cerebral organoids (Figure 10A, represented by purple lines), along with several disrupted pathways at all developmental stages (Figure 10A, represented by blue lines).

Combining these observations of dysregulated proteins, their constituent pathways can be observed in more detail (Figure 10B). Organoids and neurons have deregulation in mRNA processing, including splicing. This is followed by disruptions in protein synthesis and folding at all cell stages analyzed, which are presumed to have downstream consequences and on axon guidance, exocytosis, cell-cell adhesion, and cytoskeleton organization, disrupting hemostasis, and cell maintenance.

Ephrin B and ephrin receptor signaling canonical pathways were dysregulated in schizophrenia-derived cerebral organoids, NPCs, and neurons in comparison with controls. Our data indicate a major downregulation of proteins involved in Ephrin signaling (-Log10 p-value– organoids: 6.53; NPCs: 2.60; neurons: 1.24) and further prediction analysis using Ingenuity Pathway Analysis offered some possible outcomes (Figure 10C). Another family of proteins found enriched in all analyses was 14-3-3 signaling (-Log10 p-value– organoids: 4.96; NPCs: 2.97; neurons: 2.44), indicating inhibition of this pathway. Axon guidance (-Log10 p-value – organoids: 7.68; NPCs: 2.63; neurons: 1.25) and synaptogenesis (-Log10 p-value – organoids: 3.74; NPCs: 3.77; neurons: 3.54) were also found dysregulated in all schizophrenia neural

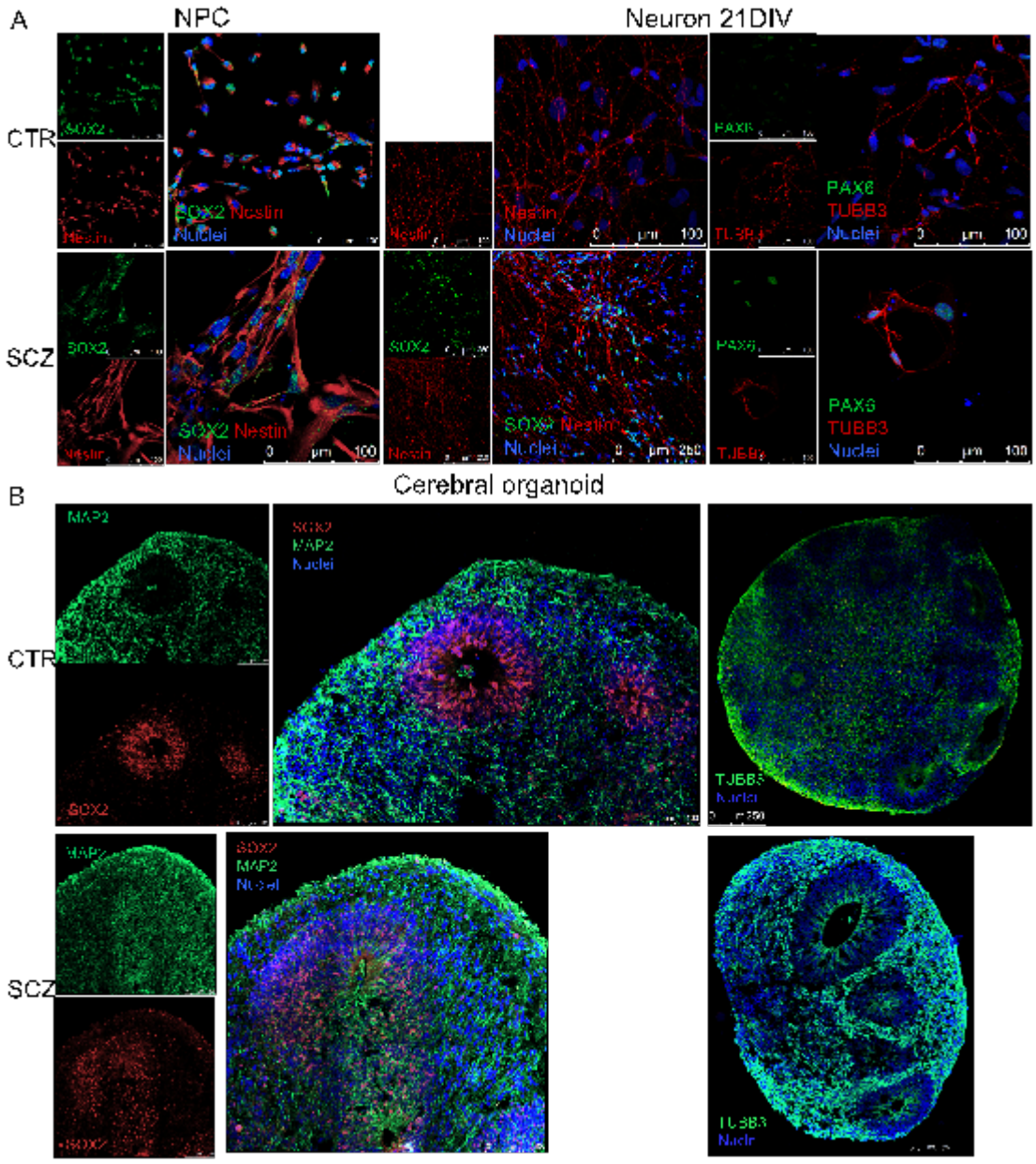

Figura 9 – NPCs, neurons and cerebral organoids show similar morphological characteristics between controls and SCZ patients. (A) Immunocytochemistry characterization of NPCs and 21 DIV neurons. Representative micrographs of control NPCs and neurons in upper panels (CTR), and SCZ NPC and neurons in the lower panels (SCZ). Showing SOX2 and nestin (NPC scale bars = 100 μm; neuron scale bars: CTR = 100 μm; SCZ = 250 μm); and PAX6 and TUBB3 (bars = 100 μm). (B) Immunocytochemistry of controls and SCZ-derived cerebral organoids showing ventricle-like morphology and SOX2 and MAP2 staining (bar = 100 μm), as well as TUBB3 (Bar = 250 μm).

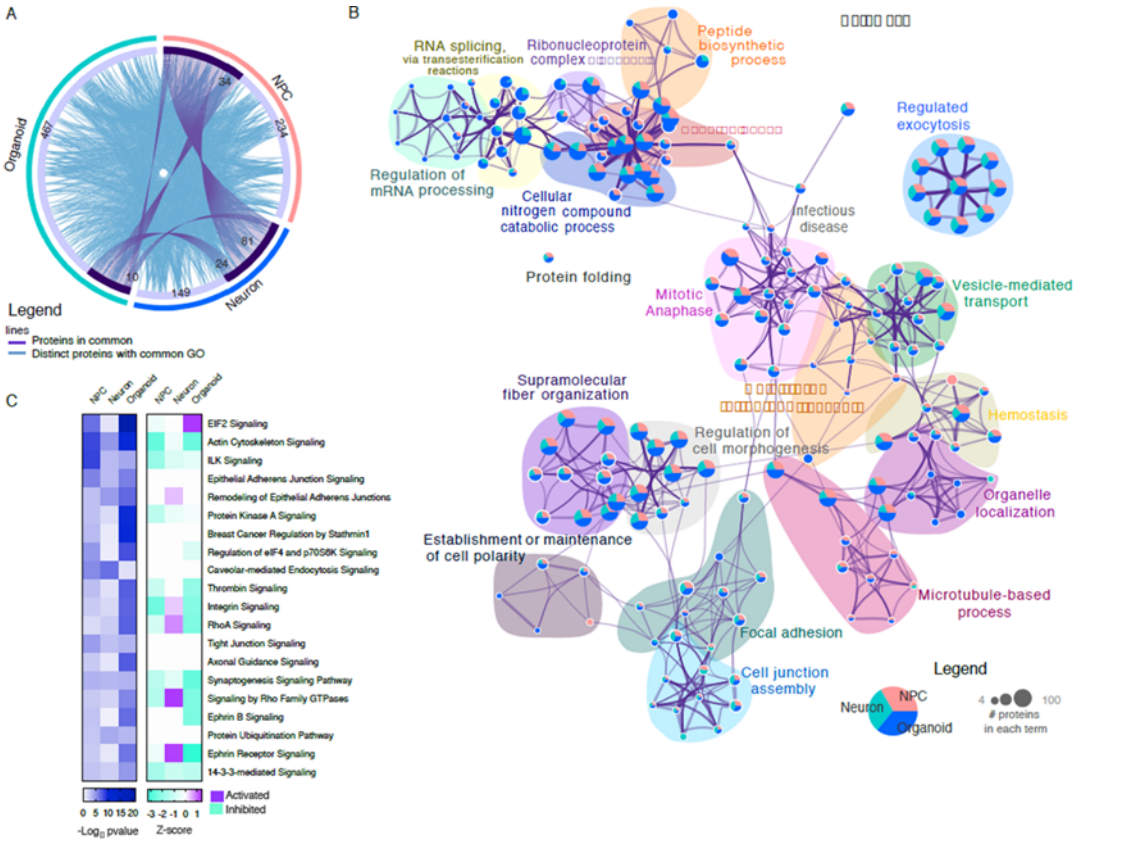

Figura 10 – Network representation of enriched pathways and processes. Terms were grouped by similarity metric (kappa scores) and the most statistically significant term within a cluster was set to represent the cluster. As provided by Metascape: (A) Circos overlap, (B) GO terms and pathway tree and (C) Canonical pathway IPA analysis.

cells (Figure 10). All these pathways have been previously associated with schizophrenia, and they perform essential roles in brain development.

Proteins with differential expression of neural progenitors, immature neurons, and brain organoids from derived patients with schizophrenia compared to healthy individuals were subjected to protein-protein interaction (PPI) analyses separately. Individual analyses of organoids, NPCs, and neurons derived from patients with schizophrenia are represented in Figure 11 (A, C, and E). Furthermore, the protein-protein interaction (PPI) analyses performed by Metascape show that schizophrenia-derived cerebral organoid presented dysregulated proteins that are involved in mRNA splicing and RNA metabolism (Figure 11B). Schizophrenia-derived NPCs presented proteins related to translation and oxidative phosphorylation (Figure 11D). Lastly, proteins seen in schizophrenia-derived neurons (21 DIV) are associated with amino acid metabolic processes and cytosolic tRNA aminoacylation (Figure 11F).

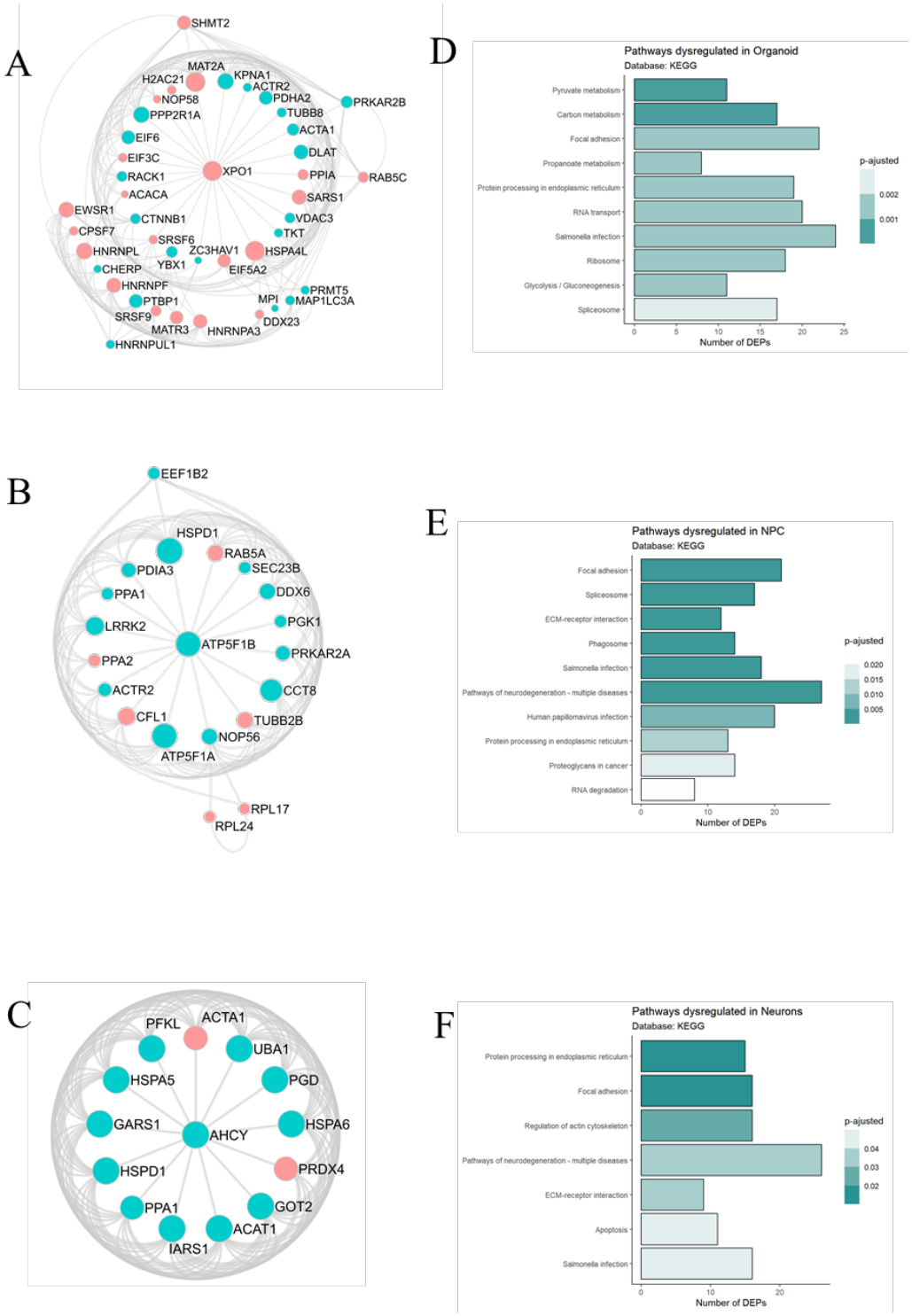

Figura 11 – Protein-protein interaction (PPI) visualization by Metascape for 21 DIV neurons for (A) mRNA Splicing/Metabolism of RNA for cerebral organoid, (B) Translation/Axon Guidance/Oxidative phosphorylation for neural progenitor cells (NPCs) and (C) Cellular amino acid metabolic process/Cytosolic tRNA aminoacylation. Red indicates upregulation of proteins and green indicates downregulation of proteins

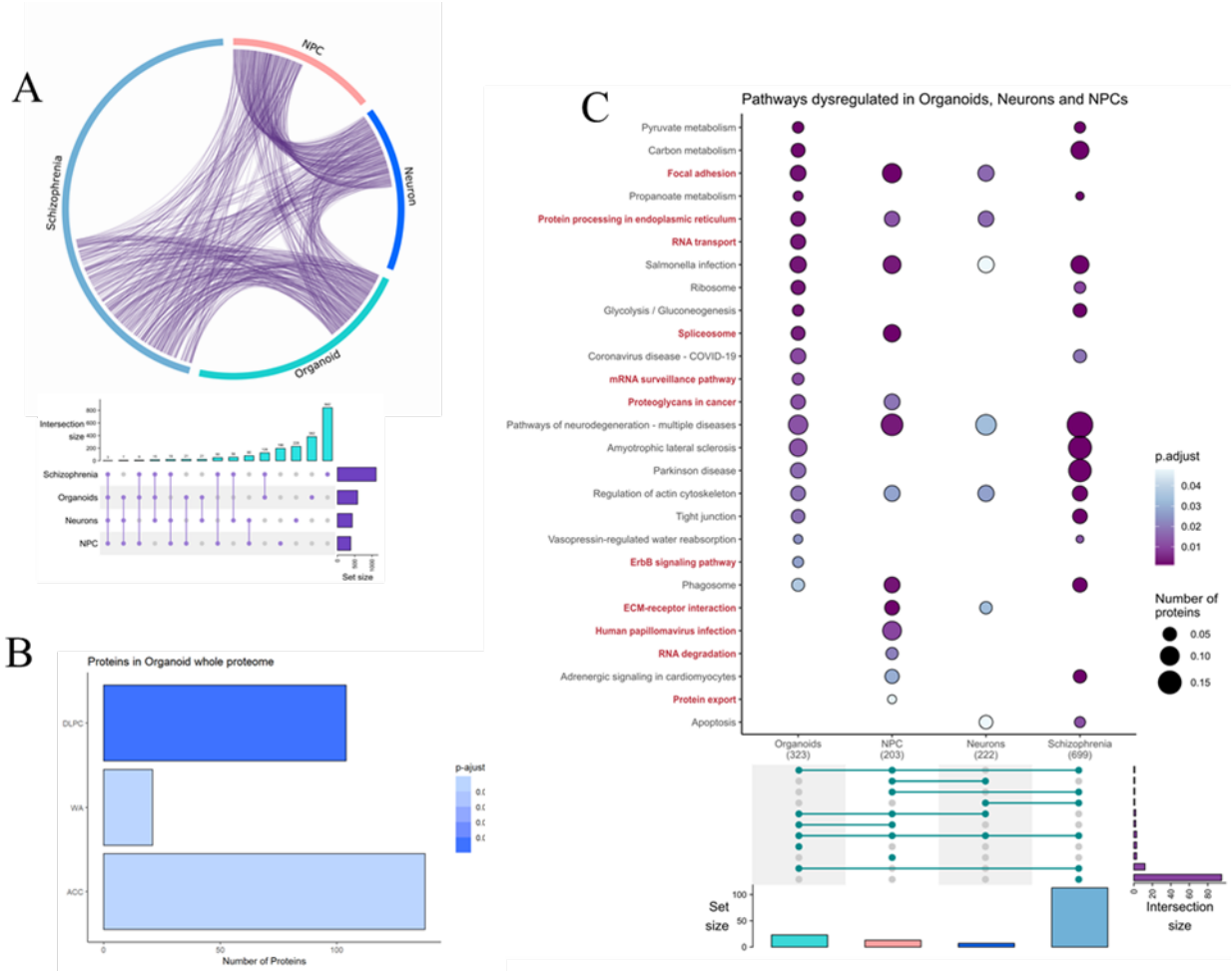

Figura 12 – Visualization of the proteomic dysregulations found in post-mortem brains of patients with schizophrenia compared to iPSC-derived neural cells/organoids. (A) Circos overlap, (B) Enrichment of organoids with specific brain regions and (C) Canonical pathway KEGG analysis. DLPC - dorsolateral prefrontal cortex, WA – Wernicke's area, ACC - anterior cingulate cortex.

4.4.3 Similarities among hiPSC-derived neural cells, brain organoids and schizophrenia *postmortem* brains

We also compared the dysregulated proteins highlighted by the analyses of these three sample types derived from schizophrenia patients (organoids, NPCs, and 21 DIV neurons) with a compilation of the proteomic studies carried out so far in different regions of the *postmortem* brain (Supplementary Table 1). The signaling pathways and proteins that were found in common between hiPSC-derived neural cells/organoids and brain tissue are shown in Figure 12. A total of 126 proteins were found in common between organoids and *postmortem* brain tissue, whereas 50 were found in common between NPCs and brain tissue and 56 in common between neurons and brain tissue (Figure 12A).

Due to the high similarity between organoids and *postmortem* brain analyses of patients with schizophrenia, both in terms of proteins (Figure 12A) and in terms of canonical

pathways (Figure 12B), we performed a comparative analysis using proteins identified in the organoids and in different brain regions to identify which *postmortem* brain region shows the greatest similarity to organoid data. The region with the highest similarity to the organoid was the dorsolateral prefrontal cortex (DLPC), followed by Wernicke's area (WA) and the anterior cingulate cortex (ACC) (Figure 12B).

4.5 Discussion

hiPSC cultures, especially 3D models such as organoids, hold great promise for the study of neurodevelopment and complex, multifactorial diseases since these cells preserve the genetic background of patients (QUADRATO; BROWN; ARLOTTA, 2016). The neurodevelopmental hypothesis of schizophrenia is largely accepted and is based on structural, cognitive, and motor abnormalities that are identified in childhood and coincide with the development of the disease as adults (reviewed in (FATEMI; FOLSOM, 2009; OWEN et al., 2011). Furthermore, environmental factors such as hypoxia, viral infections, perinatal injury, and maternal drug abuse have been considered major risk factors for the development of this disease (ABDOLMALEKY et al., 2004; BROWN, 2011; SINGH; MURPHY; O'REILLY, 2003; SØRENSEN et al., 2010; CLAIR et al., 2005). It is for this reason that this study investigated the proteins expressed in brain organoids (45 days), neural progenitor cells, and immature neurons (21 DIV) to understand the neurodevelopmental machinery at work in the cells of patients with schizophrenia.

4.5.1 The synaptic system is dysregulated in schizophrenia at the protein level, in line with previous hiPSC and *postmortem* tissue studies

The ephrin receptor signaling pathway (Figure 9C) was found dysregulated at all the stages studied of neural cells. Studies using genetic approaches, both *in vivo* and *in vitro* , have shown the role of this pathway in important processes of neural development such as axon guidance and dendritic spine formation (TAKEUCHI; KATOH; NEGISHI, 2015; HENKEMEYER et al., 2003; LAI; IP, 2009; KAO; KANIA, 2011; KLEIN, 2009). This canonical pathway was also found to be dysregulated in the *postmortem* brains of patients with schizophrenia (SAIA-CEREDA et al., 2017a).

The decrease of constituent proteins of the ephrin pathway impairs the formation of dendritic spines (HENKEMEYER et al., 2003; KAYSER et al., 2006) and *postmortem* tissue studies show that patients with schizophrenia have a reduced number of dendritic spines (MOYER; SHELTON; SWEET, 2015). Both in organoids and NPCs, this pathway was predicted to be inhibited (according to Ingenuity Pathway analyses (IPA) – Figure10C). In

contrast, this pathway was predicted to be more active in neurons (Figure 10C), suggesting that regulatory mechanisms are being triggered in this cell type to reverse the dysregulation in synaptic formation observed in neural progenitor cells (NPCs). The ephrin pathway is known to regulate NMDA receptor activity (KAYSER et al., 2006), which has already been widely associated with the pathophysiology of schizophrenia, and glutamatergic dysfunction is another hypothesis for the etiology of the disease (JAVITT; ZUKIN, 1991). NMDA hypofunction in neurodevelopment causes changes in the number of dendritic spines and the development of the neural circuit (HORN; SILD; RUTHAZER, 2013).

Another signaling pathway found dysregulated in all three analyses was 14-3-3 (Figure 9C). These proteins are abundant in the mammalian brain and comprise 1% of the cerebral proteome (CORNELL; TOYO-OKA, 2017), playing roles in cell cycle regulation, apoptosis, differentiation, and migration, as well as more complex processes such as neurotransmission, neuroplasticity, and synaptogenesis (reviewed in (ZHANG; ZHOU, 2018)). 14-3-3 pathway proteins have also been specifically associated with the pathophysiology of schizophrenia (SAIA-CEREDA et al., 2017a; FÖCKING et al., 2011). Functional knockout of 14-3-3 family proteins lead to deficits in neuronal migration and structural organization of cells of the cortex and hippocampus (XU et al., 2016; TOYOOKA et al., 2002), as well as behavioral changes and cognitive deficits (CLAPCOTE et al., 2007; STARK et al., 2008). 14-3-3 eta (YWHAH) was found downregulated in NPCs, neurons, and organoids. This protein is located in a chromosomal region (22q12) that is considered a risk region for developing schizophrenia; and RNA levels of this protein have been found downregulated in *postmortem* cerebellum (VAWTER et al., 2001; BELL et al., 2000; MURATAKE et al., 1996). In addition, this protein has been found altered in 4 separate *postmortem* brain regions of patients with schizophrenia (SAIA-CEREDA et al., 2015; SOUZA et al., 2009; MIDDLETON et al., 2005).

The actin cytoskeleton signaling pathway which was found to be dysregulated in NPCs, neurons, and organoids (Figure10C) plays a role in the movement of growth cones, maintenance of neural polarization, formation of dendritic spines, and formation/stabilization of the synapse, functions that are known to be affected in patients with schizophrenia (reviewed in (KONIETZNY; BÄR; MIKHAYLOVA, 2017)). The regulation of actin in neuronal morphology is performed by the Rho GTPase family (KUHN et al., 2000). In NPCs and organoids, this pathway was predicted by IPA to be inhibited; and both transforming protein RhoA (RHOA) and actin-related protein 2 (ACRT2) were found downregulated in the schizophrenia-patients' cells. However, in neurons, this pathway was predicted by IPA to be more active, with Rho guanine nucleotide exchange factor 4 (ARHGEF4) and Rho GTPase-activating protein 45 (ARHGAP45) upregulated in these cells. As the Rho GTPase family plays a role in the regulation of axon guidance and synaptogenesis, the activation of these proteins in neurons is probably a cellular response to restore actin signaling and consequently proper synaptic formation, which is impaired in NPCs derivate

of patients with schizophrenia (IRIE; YAMAGUCHI, 2002). Synaptic impairment was also observed in a transcriptome study of brain organoids (KATHURIA et al., 2020) and an *in vivo* proteomic study of neural progenitor cells from schizophrenia patients (TOPOL et al., 2015), a decrease of synaptic proteins and a neural connection was seen. Overall, these results indicate a possible dysregulation in the formation and maturation of synapses during development, especially regarding axon guidance and synaptogenesis and it is in line with previous hiPSC and *postmortem* tissue studies.

The spliceosomal pathway was enriched in protein-protein interaction (PPI) analyzes using proteins differentially expressed between organoids derived from patients compared with organoids derived from healthy individuals. This PPI analysis was performed using String databases in the Cytoescape APP environment, each edge representing protein-protein interaction (Figure 11B). This process is coordinated by five multi-megadalton ribonucleoproteins (snRNPs), and defects in this process can lead to several diseases, many in the nervous system (WARD; COOPER, 2010). Malfunctions in the splicing complex leads to neurotransmission dysregulation, especially within the GABAergic, dopaminergic, and glutamatergic systems (HUNTSMAN et al., 1998; PARK et al., 2011). Moreover, genes related to brain development and maturation demonstrate abnormal regulation of alternative splicing in schizophrenia (MORIKAWA; MANABE, 2010).

Some proteins of the snRNP complex, the core component of the splicing operation, such as heterogeneous nuclear ribonucleoproteins L (HNRNPL), F (HNRNPF), and A2/B1 (HNRNPA2), along with heat shock 70 kDa protein 4L (HSPA4L), were found upregulated in the schizophrenia-derived organoids (Figure 11B). These proteins have been highlighted in previous studies involving *postmortem* brains and *in vitro* techniques to investigate the pathophysiology of schizophrenia (SAIA-CEREDA et al., 2017b; CASSOLI et al., 2016; IWATA et al., 2011). No previous study with hiPSCs from schizophrenia patients had indicated dysregulations in this pathway, placing focus on this target for future hiPSC studies.

The proteins highlighted in the PPI analyses of patient-derived neural progenitor cells (NPCs) are related to oxidative phosphorylation (Figure 11D). Defects in this pathway during neurodevelopment are associated with several psychiatric diseases (FALK, 2010). OXPHOS is especially important in neural development, a process that requires high energy demand, though it also supports signaling processes, calcium homeostasis, and reactive oxygen species (ROS) production (reviewed in (BERGMAN; BEN-SHACHAR, 2016)). Proteins of the oxidative phosphorylation complex (OXPHOS) have been found dysregulated in four *postmortem* brain regions of patients (MAURER; ZIERZ; MÖLLER, 2001). hiPSC-derived NPCs from schizophrenia patients have morphological differences in mitochondria, suggesting functional impairment in this organelle 74. Several genes related to mitochondrial function have also been found to be differentially expressed in patient cells (KATHURIA et al., 2020). Lastly, neuroimaging and *postmortem* brain studies have shown

that patients with schizophrenia have deregulation in energy metabolism (MAURER; ZIERZ; MÖLLER, 2001; RICE et al., 2014), and a study that integrated proteomics, metabolomics, and genomics, performed using prefrontal cortexes, demonstrated that oxidative phosphorylation is reduced in patients with schizophrenia (PRABAKARAN et al., 2004).

The proteins found in the PPI network of neurons derived from patients with schizophrenia fall under cellular amino acid metabolic processes and cytosolic tRNA aminoacylation (Figure 11E). Several studies have shown that differences in the level of amino acids are associated with schizophrenia patients (reviewed in (SALEEM et al., 2017)). However, no hiPSC study has identified this deregulation in schizophrenia, indicating new targets for future hiPSC studies. Amino acids that play an important role in the neurotransmission system, such as glycine and serine, should be investigated further. Defects in glycine binding to this receptor have been linked to cognitive and negative symptoms of schizophrenia (LABRIE; LIPINA; RODER, 2008) and a decrease in D-serine has been observed in different brain regions, the blood, and the cerebral spinal fluid of patients (reviewed in (MACKAY et al., 2019)). In the context of NMDA receptor activation, both glycine and D-serine have the same function; however, it has been hypothesized that in neurodevelopment, D-serine may have greater importance than glycine, since it is found in abundance during this period, as well as being co-located with NMDA receptors (HORN; SILD; RUTHAZER, 2013). Knockout mice for serine racemase are also used as an established model of schizophrenia because they satisfactorily mimic NMDA receptor hypofunction (BALU et al., 2013).

4.5.2 The prefrontal cortex stands out in schizophrenia development when comparing brain organoids and regions of *postmortem* tissue

The dorsolateral prefrontal cortex (DLPC) is located in the prefrontal cortex and is involved in working memory and attention, both of which are known to be altered in patients with schizophrenia (GOLD et al., 2018; BENNETT, 2009; WIBLE et al., 2001; ABBRUZZESE et al., 1995). There is an excess of synapse pruning in the DLPC that can reach up to 30% more than what occurs in a healthy individual (reviewed in (BENNETT, 2009)). This loss of synaptic connections in patients with schizophrenia usually occurs in late adolescence or early adulthood, a period marking the end of neurodevelopment and the point at which the onset of the disease usually occurs. In addition, this increase in synaptic pruning is related to the previous appearance of prodromal symptoms; that is, this dysregulation begins before the noticeable onset of the disease and is linked to synaptic formation (BENNETT, 2009). Gulsuner el al. (GULSUNER et al., 2013) mapped *de novo* mutations in fetal DLPC, taking into consideration those who were later diagnosed with schizophrenia; genes for proteins that play a role in axon guidance, synaptic trans-

mission, and transcriptional regulation were all highlighted. These results are consistent with those obtained in this study, reinforcing the role of the synaptic system, especially in the prefrontal cortex, in brain development and the emergence of schizophrenia from a pathophysiological point of view. The results presented here have shown that several essential pathways for neurodevelopment, such as axon guidance and synaptogenesis, have constituent proteins with reduced abundance. In our models of hiPSCs from patients with schizophrenia, 89% of dysregulated proteins were found to be downregulated, which we hypothesize to be a delay or slowing in brain development, thus reinforcing the hypothesis of schizophrenia as a neurodevelopmental disease. Our findings show similarities to the dysregulations found in *postmortem* brains of patients with schizophrenia, which indicates that, in addition to causing problems during neurodevelopment, these deregulations persist in the adult individual and thus contribute to the multifactorial nature of the pathophysiology of schizophrenia. However, we were also found new targets of study such as amino acid metabolism and spliceosomes. Despite the reduced number of subjects whose cells were hiPSCs sources, these data confirm the viability of *postmortem* tissue in proteomic studies, and further support patient-derived cell cultures as a valid technique to study schizophrenia.

5 PHGDH inhibition alters neuron-astrocyte interactions and neural differentiation

Verônica M Saia-Cereda[1], Fernanda Crunfli[1], Guilherme Reis-de-Oliveira[1], Aline Gazzola Fragnani Valença[1], Victor Corasolla Carregari[1], Pedro Henrique Vendramini[1], Bradley J. Smith[1], Juliana Minardi Nascimento[1], Daniel Martins-de-Souza[1,2,3*]
1 Laboratory of Neuroproteomics, Department of Biochemistry and Tissue Biology, Institute of Biology, University of Campinas (UNICAMP), Campinas, Brazil.
2 Instituto Nacional de Biomarcadores em Neuropsiquiatria (INBION), Conselho Nacional de Desenvolvimento Científico e Tecnológico (CNPq), São Paulo,Brasil.
3 Experimental Medicine Research Cluster (EMRC), University of Campinas, Campinas 13083-970, SP, Brazil.

5.1 Abstract

Neurodevelopmental disorders stem from multiple synergistic deficiencies within connected biological networks and biochemical pathways. Neuronal differentiation has complex regulatory machinery and neuron-astrocyte interactions play a crucial role in neural development. In astrocyte-neuron complexes, D-serine, a neuromodulatory amino acid, is produced through a series of reactions, making communication between these cells important for the regulation of its production. Glucose is the initial precursor for D-serine production, and one of the downstream enzymes of this pathway, 3-phosphoglycerate dehydrogenase (PHGDH), showed differential expression in postmortem brain tissue and neuronal cells derived from patients with schizophrenia. In this study, we integrated neuroproteomics, pluripotent stem cells, and PHGDH inhibition to further investigate the biological mechanisms involved in synaptic dysfunction at early stages of neurodevelopment. The results obtained showed that neurons and astrocytes exhibited phenotypic alterations after exposure to a PHGDH inhibitor, though neurons were more sensitive to this exposure. The main dysfunctions observed in neurons treated with this inhibitor during their differentiation were related to cell death and axonal migration, possibly caused by the dysregulations in the energy metabolism of these cells and the co-culture of neurons and astrocytes did not reverse these alterations. Data are available via ProteomeXchange with identifier PXD029731

5.2 Introduction

In mammalian neurodevelopment *in vivo* , the first cells to be established from neural progenitor cells are neurons (MOLYNEAUX et al., 2007). These cell types usually develop at embryonic day 42 (E42; 42 days post-conception) (BYSTRON; BLAKEMORE; RAKIC, 2008) and perform an important function in the brain: information processing. Neuronal differentiation has complex regulatory machinery and is strongly rooted in cell-cell interactions. These interactions are important in the genesis of glial cell types, such as astrocytes, and play a crucial role in neural development (FREEMAN, 2010). The glutamatergic neural system is known to develop early in the neurodevelopmental process; in the rat cortex, this receptor begins to develop at day E12 and regulates functions such as neuronal proliferation, migration, differentiation, and survival (LUJÁN; SHIGEMOTO; LÓPEZ-BENDITO, 2005). Due to the lack of *in vitro* models to mimic neural development, hypotheses involving neurodevelopment have thus far not been satisfactorily evaluated using human cells. The glutamatergic system has been proposed as a cause of dysregulation in several psychiatric diseases, one which is schizophrenia. In the glutamatergic theory for the development of this mental disorder, a wide range of symptoms can be explained and other theories such as the GABAergic and dopaminergic hypotheses are integrated (reviewed in (MOGHADDAM; JAVITT, 2012)). This hypothesis originally stemmed from the evidence that antagonists of N-methyl-D-aspartate (NMDA)-type glutamate receptors, such as phencyclidine (PCP), dizocilpine (MK-801), and ketamine can induce positive symptoms as well as negative symptoms and cognitive dysfunction, covering all symptom classes that occur in patients with schizophrenia (JAVITT; ZUKIN, 1991). The focus of most past studies has been on the role of this receptor in the adult individual, with little being known during the period of neurodevelopment. NMDA receptor requires the binding of a co-agonist, D-serine, or glycine, at the glycine modulatory site (GMS). Studies have shown that D-serine is found in abundance during neurodevelopment when compared to glycine, suggesting an important role for this molecule during this period (HORN; SILD; RUTHAZER, 2013; HASHIMOTO et al., 1993a). D-serine is produced through a series of reactions in astrocyte-neuron complexes, making communication between these cells important for the regulation of molecule production. Glucose is the initial precursor for D-serine production, and one of the downstream enzymes of this pathway, 3-phosphoglycerate dehydrogenase (PHGDH), showed differential expression in postmortem brain (OLIVEIRA et al., 2020) and neuron progenitor cells (NPCs) and immature neurons of pluripotent stem cells derived from patients with schizophrenia (unpublished data). Stem cells are cells capable of differentiating into all cell types of an adult organism. They hold promise to study disease pathophysiology and can help in the discovery of new biomarkers as well as screening for the development of new drugs (COLMAN; DREESEN, 2009). Possibilities for *in vitro* neurodevelopmental studies have emerged together with the development of induced pluripotent cell techniques. Considering the neurodevelopmental

applications of pluripotent cells, we used this model to analyze whether the inhibition of 3-phosphoglycerate dehydrogenase (PHGDH) affects neuronal differentiation. Serine production in neural stem cells (NSC) and neurons was decreased after treatment with a PHGDH protein inhibitor (CBR5884). However, astrocytes did not show significant changes in the production of serine though their ability to support neurons was nonetheless impaired. Cell death and axonal migration were the most affected neuronal differentiation pathways by PHGDH inhibition.

5.3 Materials and methods

5.3.1 Generation of hESC-derived neural stem cells

Neural stem cells were differentiated from human pluripotent human embryonic stem cells (hESC, cell line BR-1 (FRAGA et al., 2011)), according to Yan et al, (YAN et al., 2013), ., hESCs were cultured in E8 media on Geltrex-coated plates until 60% of confluence before exchanging the medium with PSC neural induction medium (Thermo Fisher Scientific, MA, USA) containing neurobasal medium and PSC supplement, according to the manufacturer's protocol (Yan et al., 2017). The medium was changed every other day until day 7, whereupon the neural stem cells (NSCs) were collected and expanded in the neural induction medium (advanced DMEM/F-12 (Dulbecco's Modified Eagle Medium/Nutrient Mixture F-12): Neurobasal medium (1:1) with neural induction supplement; Thermo Fisher Scientific, MA, USA). Cells were passed weekly and kept at 37ºC and 5

5.3.2 Generation of hESC-derived immature neurons

For neuronal differentiation, hNSCs of each lineage were plated on Geltrex-coated (Thermo Fisher Scientific, MA, USA) plates in B27 medium (DMEM/F-12 (Dulbecco's Modified Eagle Medium/Nutrient Mixture F-12): Neurobasal media (1:1) + 1x B27 + 1% penicillin/streptomycin). Neuronal cultures were differentiated for 21 days *in vitro* at 37ºC and 5

5.3.3 Generation of hESC-derived astrocytes

Astrocytes were obtained by differentiating neural stem cells (NSCs) (TRINDADE et al., 2020) that were obtained from pluripotent human embryonic stem cells (cell line BR-1; as described above). NSCs were cultured on Geltrex-coated plates (Thermo Fisher Scientific, MA, USA) using NSC growth medium. The next day, the medium was changed to DMEM/F-12 (Dulbecco's Modified Eagle Medium/Nutrient Mixture F-12) with 1% N2 supplement, 1% fetal bovine serum (FBS), and 1% penicillin-streptomycin. Cells were maintained at 37°C in humidified air with 5% CO2 for 21 days, resulting in

glial progenitor cells (GPCs). GPCs were then plated at low density (20-30% confluence) on Geltrex-coated plates and and cultivated in DMEM/F-12 medium with 1% GlutaMAX Supplement, 10% FBS and 1% penicillin-streptomycin for 30 days. The differentiation medium was replaced every 2-3 days.

5.3.4 Generation of neurospheres

NSCs were dissociated with Accutase™ (Thermo Fisher Scientific, MA, USA) and then cultured for 72 hours on plates shaken with an orbital shaker at 90 rpm in NSC medium to generate neurospheres. Next, the medium was exchanged with B27 medium (neurobasal medium:DMEM/F-12 (Dulbecco's Modified Eagle Medium/Nutrient Mixture F-12) (1:1) + 1x B27 + 1% penicillin/streptomycin) and cells were incubated for 10 days at 37ºC and 5% CO2, replacing the medium every 5 days.

5.3.5 Immunohistochemistry

Cells were fixed in 4% paraformaldehyde (PFA). After fixation, they were washed with PBS, permeabilized in 0.3% Triton-X solution, and blocked in a 3% bovine serum albumin (BSA) solution prior to immunolabeling. Immunofluorescence was performed using the following primary antibodies: mouse anti-class III β-tubulin (MAB1637, Millipore), mouse anti-nestin (MAB5326, Chemicon). The following secondary antibodies were used: AlexaFluor 594 goat anti-mouse (A11032, Invitrogen). DAPI was used for nuclear staining. Images were acquired using a Leica TCS SP8 confocal microscope (Leica Microsystems, Wetzlar, Germany).

5.3.6 Inhibition of PHGDH protein using CBR5884

CBR5884 (ethyl 5-(furan-2-carboxamido)-3-methyl-4-thiocyanatothiophene-2-carboxylate; ToCris Bioscience, Cat. No. 5836) this molecule is capable of inhibiting the PHGDH protein. Thus, this molecule was added every two days to the culture medium of astrocytes and neurons for a period of 21 days of differentiation. This is a small, noncompetitive, cell-penetrating molecule that interrupts the oligomerization of the PHGDH protein, decreasing serine production by approximately 30%, at a recommended concentration of 33 $\pm$ 12 μM in immortalized cells for 24h and 7 μM in a chronic treatment.

5.3.7 MTT 3-(4,5-dimethylthiazol-2-yl)-2,5-diphenyltetrazolium bromide assay

Cell viability test using MTT (3-(4,5-dimethylthiazol-2-yl)-2,5-diphenyltetrazolium bromide) was carried out. Cells were seeded in 96-well plates at a density between 5000-7000 cells per well after cells had reached 70-80% confluence, approximately 3 days after

plating. Several concentrations of the CBR5884 inhibitor (8-30 μM) were added to the culture media of astrocytes and NSC. After 24h of exposure, the cells were washed with inhibitor-free medium before adding 90μL of fresh medium containing 10 μL of 12 mM MTT to each well before 4 hours of incubation at 37°C. After labeling, all but 25 μL of medium from the wells was removed and 50 μL of DMSO was added to each well followed by incubation for 10 minutes at 37°C. The absorbance was read at 540 nm in a Tecan Infinite 200 Pro (Life Science, Switzerland).

5.3.8 CellTiter-Glo® luminescent cell viability assay

The viability of neurons, astrocytes, and neurosphere derived from human neural stem cells was measured using the CellTiter-Glo® Luminescent Cell Viability Assay (Promega, Madison, USA). PHGDH inhibition was performed with 5 μM of CBR5884 over 21 days. Cells were washed with PBS, the CellTiter-Glo® was added to the cells following the manufacturer's instructions and the luminescent signals were analyzed using a FlexStation 3 (Molecular Devices, CA, USA).

5.3.9 Flow cytometry

PSD95, synaptophysin, and nestin expression was evaluated with FACS (fluorescence-activated cell sorting). Astrocytes and neurons were collected and stained with BD Horizon™ Fixable Viability Stain 510 for 20 min at 4°C. Primary antibodies were diluted in BD Perm/Wash™ buffer before being added to cells (1:500), which were then incubated for 1h at 4°C. The primary antibodies were: anti-synaptophysin (D35E4) XP® Rabbit mAb (Cell Signaling; cat. #5461); anti-nestin (EMD Millipore; cat. #ABD69); anti-PSD95, (Abcam, cat. #ab12093). Secondary antibodies were diluted in BD Perm/Wash™ buffer before being added to cells (1:250), which were then incubated for 30 min at 4°C. The secondary antibodies were: donkey anti-mouse IgG AlexaFluor 594 (Cell Signaling; cat. #8890S), donkey anti-rabbit IgG AlexaFluor 647 (Abcam; cat. #ab15006), and donkey anti-goat IgG AlexaFluor 488 (Abcam; cat. #ab150129). Cells were washed with BD Perm/Wash™ buffer and then transferred to polypropylene FACS tubes. The cells were analyzed on a FACSymphony cell analyzer (Becton & Dickinson Biosciences, San Diego, CA, USA). The viability of PHGDH-inhibited neurons and astrocytes derived from human neural stem cells (5μM of CBR5884 for 21 days) were analyzed with fixable viability stain (FVS510, BD Biosciences, #564406) and Apotracker™ Green (BioLegend, #427403). The percentages of live (Apotracker-/FVS510-), necrotic (Apotracker-/FVS510+), early apoptotic (Apotracker+/FVS510-), and late apoptotic (Apotracker+/FVS510+) cells were determined by flow cytometry (FACSymphony; Becton & Dickinson, San Diego, CA, USA). The experiments were performed in triplicate and are shown as mean ± SEM. P

values were determined by one-way ANOVA ($p \leqslant 0.05$) followed by Tukey's post-hoc test ($q \leqslant 0.05$).

5.3.10 RNA extraction and RT-PCR

TRI Reagent (Sigma, St Louis, USA) was used for total RNA extraction according to the manufacturer's instructions. RNA concentration was evaluated by a DeNovix spectrophotometer (DeNovix Inc.,Wilmington, USA) and RNA integrity was determined by visualizing 28S and 18S ribosomal RNA on a 1% agarose gel. Reverse transcription was performed with 0.5 μg of RNA using a GoScript Reverse Transcriptase Kit (Promega, Madison, WI, USA) according to the manufacturer's instructions. qPCR was performed using cDNA diluted 1:10 and the qPCR SybrGreen Supermix (Qiagen, Valencia, CA, USA) containing forward and reverse primers in RNAse-free water. All reactions were performed in a CFX384 Touch Real-Time PCR Detection System (Biorad, Hercules, CA, USA) and cycling conditions were set as follows: 50°C for 2 min; 95°C for 10 min; (95°C for 15s; 60°C for 1 min) x 40 cycles. To evaluate primer specificity, a melting curve analysis was performed by heating samples from 65°C to 99°C (1°C increment changes at 5s intervals). All sample measurements were performed in duplicate.

5.3.11 Proteomics HPLC-MS/MS sample preparation and processing

Neurons and astrocytes differentiated with PHGDH inhibitor (5 μM of CBR5884 for 21 and 30 days, respectively) were chemically lysed using Lysis Buffer: (100 mM Tris-HCl, 1 mM EDTA, 150 mM NaCl, 1% Triton-X, and protease and phosphatase inhibitors). The cells were then subjected to lysis with an ultrasonication probe: 3 cycles, 20s each, with 90% output. The total protein extract was quantified by BCA according to the manufacturer's instructions (Thermo Fisher Scientific, MA, USA). 40 μg of total protein extract from each sample was transferred to a Microcon-10kDa Centrifugal Filter for FASP protein digestion (Potriquet, 2017). Proteins were reduced (10 mM DTT), alkylated (50 mM IAA), and digested overnight by trypsin at 37°C. After 16 hours, peptides were recovered from the filter with 50 mM ammonium bicarbonate (AmBic), and trypsin activity was quenched by adding formic acid (FA) to a final concentration of 1% (v/v), whereupon the peptides were dried in in a SpeedVac and stored at -80°C until use. Peptides were injected into a liquid chromatography system nanoAcquity UPLC M-Class System (Waters Corporation, Milford, MA) coupled to Synapt G2-Si mass spectrometer (Waters Corporation) run in Resolution Mode. 5μg of peptides were separated using reverse-phase chromatography (M-Class BEH C18 Column; 130 Å, 5 μm, 300 μm X 50 mm, Waters Corporation). The MS analysis was performed using high-definition data-independent acquisition (DIA) enhanced with ion mobility separation (HDMSE). [Glu1]-Fibrinopeptide B (human) was used as the lock mass, which was sampled every 30 s. The mass spectrometer operated in resolution

mode with an m/z resolving power of at least 25,000 FWHM, using ion mobility with a cross-section resolving power of at least 40 $\Omega/\Delta\Omega$. The effective resolution obtained with the conjoined ion mobility was 1,800,000 FWHM. MS/MS analyses were performed by nano-electrospray ionization in positive ion mode nanoESI (+) using a NanoLock Spray (Waters, Manchester, UK). The raw data from each experiment were processed in Progenesis QI for Proteomics (version 3.0, Waters Corporation, Milford, MA), imported with a maximum charge of +8 and runs were aligned automatically. Tandem mass spectra were searched against the Homo sapiens proteome database (Uniprot, version 2021/05 reviewed - 20371 enters), using mass error tolerance parameters of 20 ppm for peptide. For peptide identification, cysteine carbamidomethylation was set as a fixed modification and methionine oxidation as a variable modification. Up to 2 missed cleavages were allowed, and the false discovery rate (FDR) was set to 1%, calculated on the fly with reverse sequences. Protein identification was performed using a minimum of 1 fragment ion matched per peptide, a minimum of 3 fragment ions per protein, and a minimum of 1 peptide per protein. Label-free quantitative analysis was carried out using the relative abundance intensity, normalized by all intensity peptide ions from identified proteins. The expression analysis was performed considering the technical replicates for each experimental condition, following the hypothesis that each group is independent. Proteins with ANOVA (p) $\leqslant 0.05$ between groups were considered differentially expressed. Raw data have been deposited in PRIDE (Proteomics Identifications Database) - Project accession:PXD029731.

5.3.12 Proteomic *in silico* analyses

Gene ontology and pathway enrichment analyses were performed in Enrichr (CHEN et al., 2013) and Metascape (ZHOU et al., 2019) using default settings and the following databases: KEGG Pathway, GO Biological Processes, and Reactome. Protein-protein interactions were applied to the networks to identify tightly connected clusters using the Molecular Complex Detection (MCODE) algorithm in Metascape.

5.3.13 Target proteomics data acquisition and processing

1 ug of peptides was injected into a NanoAcquity UPLC (Waters Corporation) coupled to a Xevo TQD mass spectrometer. Chromatography was performed in a Acquity UPLC Peptide HSS T3 100A, 1,8μM throughout 30 min of a binary gradient from 3 to 60%ACN in 6ul/min flow rate. MS analysis was carried out using selected reaction monitoring (SRM) acquisition, according to Skyline (PINO et al., 2020) workflow for method development and optimization. PHGDH (Accession: O43175) and ACTB (Accession: P60709) was evaluated using 3 unique peptides based on the Human uniprot database. For PHGDH, we targeted TLGILGLGR.2H+ (transitions: y7, y5,y4; CE 16V; Dwell-time 0.052s), GGIVDEGALLR.2H+ (transitions: y8, y7, y6; CE 19V; Dwell-time 0.052s), and

DLPLLLFR.2H+ (transitions: y6, y5, y4, y3; CE 17V ; Dwell-time 0.080s). To normalize PHGDH abundance, we choose ACTB as an endogenous protein targeting DSYVGDEAQSK.2H+ (transitions: y8, y7, y6; CE 21V; Dwell-time 0.034s), GYSFTTTAER.2H+ (transitions: y7, y6, y5; CE 20V; Dwell-time 0.034s), QEYDESGPSIVHR.3H+(transitions: y6, y5, y4 ;CE 17V; Dwell-time 0.034s). For statistical analysis we used MSStats (CHOI et al., 2014) in the R environment.

5.3.14 Metabolomics UPLC-MS/MS preparation, analysis, and data processing

PHGDH-inhibited neurons and astrocytes (5 μM of CBR5884 for 21 days) were washed twice with PBS and collected with 600 μL of methanol. Samples were dried using a SpeedVac and stored at -80 °C. For metabolite extraction, 2.24mL of water:methanol:chloroform (4:5:10) were added and then the tubes were shaken vigorously for 2 minutes. Samples were centrifuged for 5 minutes at 13,000 x g. The aqueous supernatant and the organic phase (lower phase) were collected and dried for 60 and 40 min (respectively) in a vacuum concentrator. All samples were stored at -80 °C until analysis by UPLC-MS/MS. The samples were resuspended in 100 μL of methanol:water (1:1) and for each analysis, 4 μL of the sample was injected. Sample separation was performed by hydrophobic interaction liquid chromatography (HILIC) using an Acquity UPLC® BEH amide column (1.7 μm, 2.1 mm x 100 mm). The mobile phases used for the separations were ACN:water (4:1) as mobile phase A and ACN:water (3:7) as mobile phase B; both phases also contained 10 mM ammonium formate and 0.1% ammonium hydroxide (v/v). The separation was then performed over a gradient from 99% to 1% buffer A over 7 min. The column was returned to 99% buffer A for 2 min for re-equilibration before the next injection for a total run time of 10 min. Data acquisition was performed in negative mode and the instrument was operated in MSE mode in the m/z range of 50–800 Da, with an acquisition time of 0.1 s per scan. The AUC (area under the curve) was performed manually in Progenies (version 3.0, Waters Corporation, Milford, MA). After the AUC data coleted was submitted a test t (univariate statistical analysis) with Welch's correction in GraphPad Prism 8.0.2 software.

5.3.15 Neurosphere migration assay

Neurospheres were embedded in 4% low melt agarose, then tissue sections of 75 μm were obtained using a vibratome (Leica VT1000S Vibratome, Leica Microsystems, Wetzlar, Germany). For immunofluorescence, sections were blocked and permeabilized in 0.3% Triton X-100 and 4% FBS in PBS for 2 hours at room temperature. Next, sections were then incubated with primary antibodies in 0.1% Triton X-100, 4% FBS at the following dilutions: Tubulin β-III (ab41489, 1:500), Glial Fibrillary Acidic Protein [GFAP] (Z0334DAKO, 1:500). After washing with PBS + 0.1% Tween-20 (PBS-T), secondary

antibodies used were goat Alexa Fluor 488 and 647 (Invitrogen, 1:500). Sections were washed three times with PBS-T and mounted on slides using Fluorescence Mounting Medium mounting medium (Dako). After 24 hours, cover slips were surrounded with nail polish and dried at 4°C, then stored in the dark at 4°C. Imaging was obtained using confocal microscopy.

5.3.16 Re-analysis of scRNA-seq Data

To analyze the expression of PHGDH throughout cortical development, we used the scRNA-seq data previously published by Nowakowski, 2017 (NOWAKOWSKI et al., 2017), avaiable on UCSC Browser. This data contains cells from primary cortical and medial ganglionic eminence, microdissected germinal zone and cortical plate; and cells from the prefrontal cortex and primary visual cortex, including 13 paired specimens. Seurat (v.4.0.2) workflow was used with default parameters to perform all subsequent analysis. Count data was log normalized and variable features were identified using the variance stabilizing transform (vst) method. Scaled z-scores for each gene were calculated using the ScaleData function and regressed against all genes. PCA was performed using scaled data based on variable genes. Clusters were identified using the shared nearest neighbor (SNN) algorithm, using the first 10 PCs with k = 20 and a resolution= 0.8. These PCs were used to generate TSNE projections. Differentially expressed genes among the clusters were identified using FDR < 0.05. These genes were used for over-representation analysis against the CellMaker database using Enrichr tool (CHEN et al., 2013). TOP5 enriched terms were manually curated to perform the cell type annotation in each cluster.

5.4 Results

5.4.1 Establishing *in vitro* neuronal cells models

Astrocyte cells at 4 weeks of differentiation (Figure 13A) were stained for intermediate filament proteins that are key astrocytic markers (HOL; PEKNY, 2015): glial fibrillary acidic protein (GFAP) vimentin (VIM) and SRY (sex determining region Y)-box 2 (SOX-2). Immature neurons at 21 days *in vitro* (21DIV) (Figure 13C) were stained for β3-tubulin (TUBB3), a marker of neuronal differentiation (Soltani et al. 2005); nestin, a marker for axonal growth in immature neurons (HUANG et al., 2018); and nuclei, with 4',6-diamidino-2-phenylindole (DAPI). Similarly, to confirm neural differentiation, the expression of classical differentiation markers was evaluated by flow cytometry and RT-qPCR. Differentiated astrocytes were stained of 96% GFAP+, 80% vimentin+, and 12% SOX2+ (Figure 13B). In addition, 87% of immature neurons expressed synaptophysin and 92% expressed PSD95 (Figure 13D). The RT-qPCR analyses indicated increased expression of neural cytoskeletal genes, such as TUBB3 and microtubule-associated protein

2 (MAP2), in addition to genes that indicate neuronal maturity, such as postsynaptic density protein 95 (PSD95), tyrosine 3-monooxygenase (TH), and RNA binding protein fox-1 homolog 3 (NeuN) (GUSEL'NIKOVA; KORZHEVSKIY, 2015) (Figure 13E).

5.4.2 PHGDH protein expression and D-serine production in different cell types

PHGDH is understood to be expressed exclusively in astrocytes across most brain regions regions (HORN; SILD; RUTHAZER, 2013; YAMASAKI et al., 2001; FURUYA et al., 2008). A single cell RNA-Seq analysis during development, using data for (NOWAKOWSKI et al., 2017) in R environment with Seurat workflow (HAO et al., 2021), showed that astrocytes mostly express the PHGDH gene (Figure 14A-B), in agreement with results observed in the literature. However, a specific population of neural progenitor cells (NPC) showed high levels of expression of this gene, similar to the expression level of astrocytes (Figure 14C). The PHGDH protein was found differentially expressed in the posterior cingulate cortex of patients with schizophrenia, using *shotgun* proteomics analysis (Figure 14D) (OLIVEIRA et al., 2020). Also, in a previous study by our group, PHGDH was found downregulated in neural progenitor cells (NPCs) and immature neurons derived from pluripotent stem cells from patients with schizophrenia (SCZ-iPSCs), but no difference in expression was observed in whole-tissue protein extracts from organoids derived from these same cells (Figure 14E). To confirm that the PHGDH protein is expressed in cell types other than astrocytes, we analyzed the expression of this protein in NSC, neurons and neuron/astrocytes co-culture. NSCs and neurons *in vitro* expressed PHGDH and NSCs had significantly higher levels when compared to neurons and a co-culture of neurons and astrocytes (Figure 14F). Since PHGDH protein is a fundamental enzyme in the production of D-Serine, we decided to measure the concentration of this molecule in astrocytes and neurons. Higher levels of free serine were additionally observed in the monoculture medium from astrocytes compared to neurons (Figure 14G); the culture media already contained equal starting levels of serine that could not be removed without a strong impairment of neuronal viability.

Based on the findings from SCZ-*postmortem* brain/iPS-derived neural cells, a molecule capable of partially inhibiting PHGDH was tested along with its effects on D-serine production. CBR5884 (ethyl 5-(furan-2-carboxamido)-3-methyl-4-thiocyanatothiophene-2-carboxylate) is molecule interrupts the oligomerization of the PHGDH protein, decreasing serine production by approximately 30%, at a recommended concentration of 33 ± 12 μM in immortalized cells for 24h and 7 μM in a chronic treatment (MULLARKY et al., 2016; SEN et al., 2018). Four concentrations were evaluated for each cell type after a 24-hour incubation period (Figures 15A and B). We also performed two different cytotoxicity assays by flow cytometry: fixable viability stain (FVS) and CellTiter-Glo® Luminescent Cell

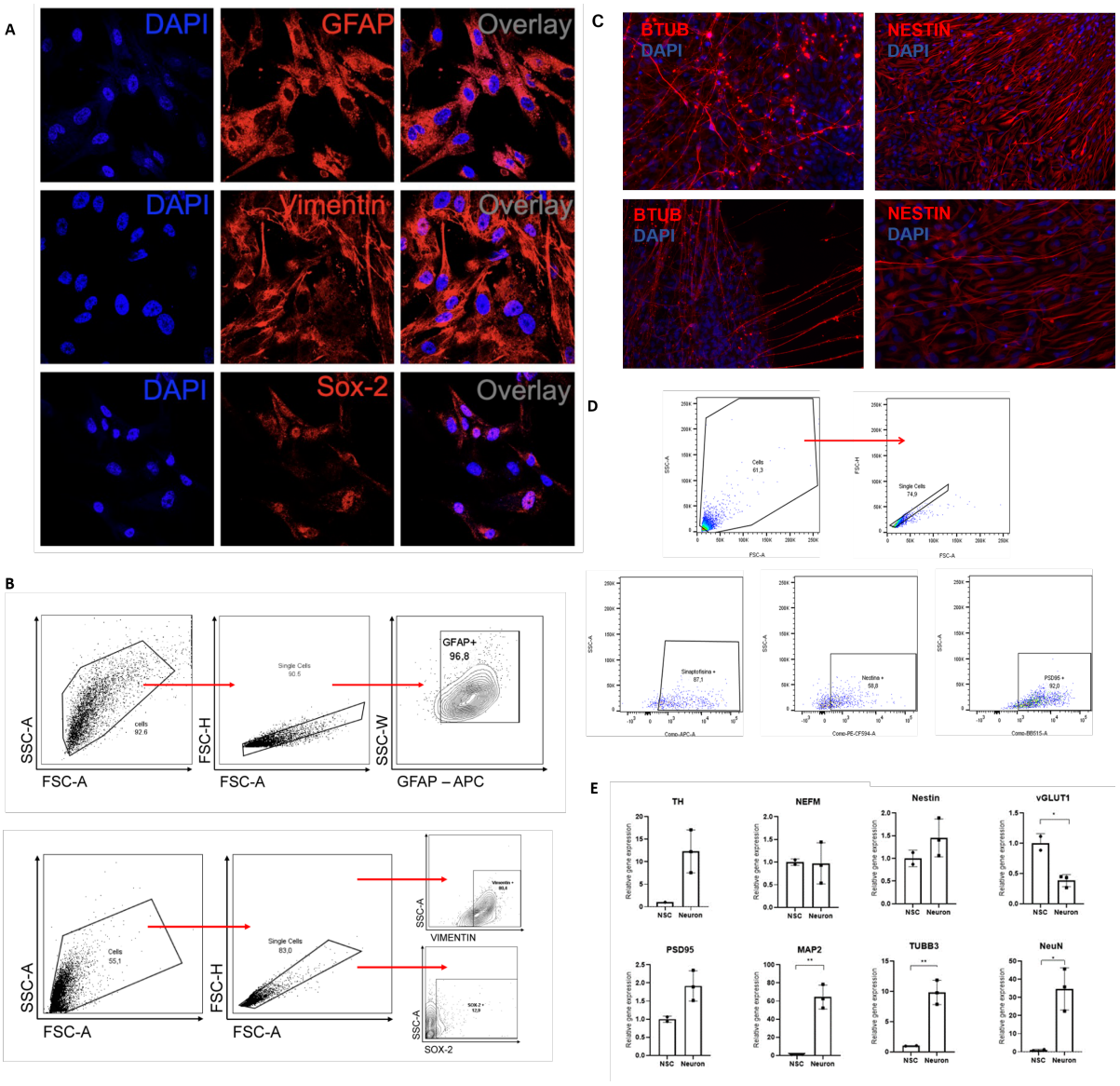

Figura 13 – Characterization of cellular models of embryonic stem cells. (A) Immunocytochemistry showing human astrocyte staining for vimentin, GFAP, and SOX2 (bars = 100 μm). (B) Cells positive for GFAP or SOX-2 and vimentin (astrocytic marker). The flow cytometry analysis was performed using astrocytes differentiated from human embryonic stem cells (hESC). (C) Immunocytochemistry showing human immature neurons (at 21 DIV) stained for TUBB3 (labeled BTUB) and nestin. (D) Flow cytometry analysis of immature neurons (21 DIV) positive for synaptophysin and PSD95 (neural maturation) and nestin (axon development). (E) RT-qPCR analysis of neural differentiation markers in immature neurons (21 DIV) differentiated from embryonic stem cells (hESC).

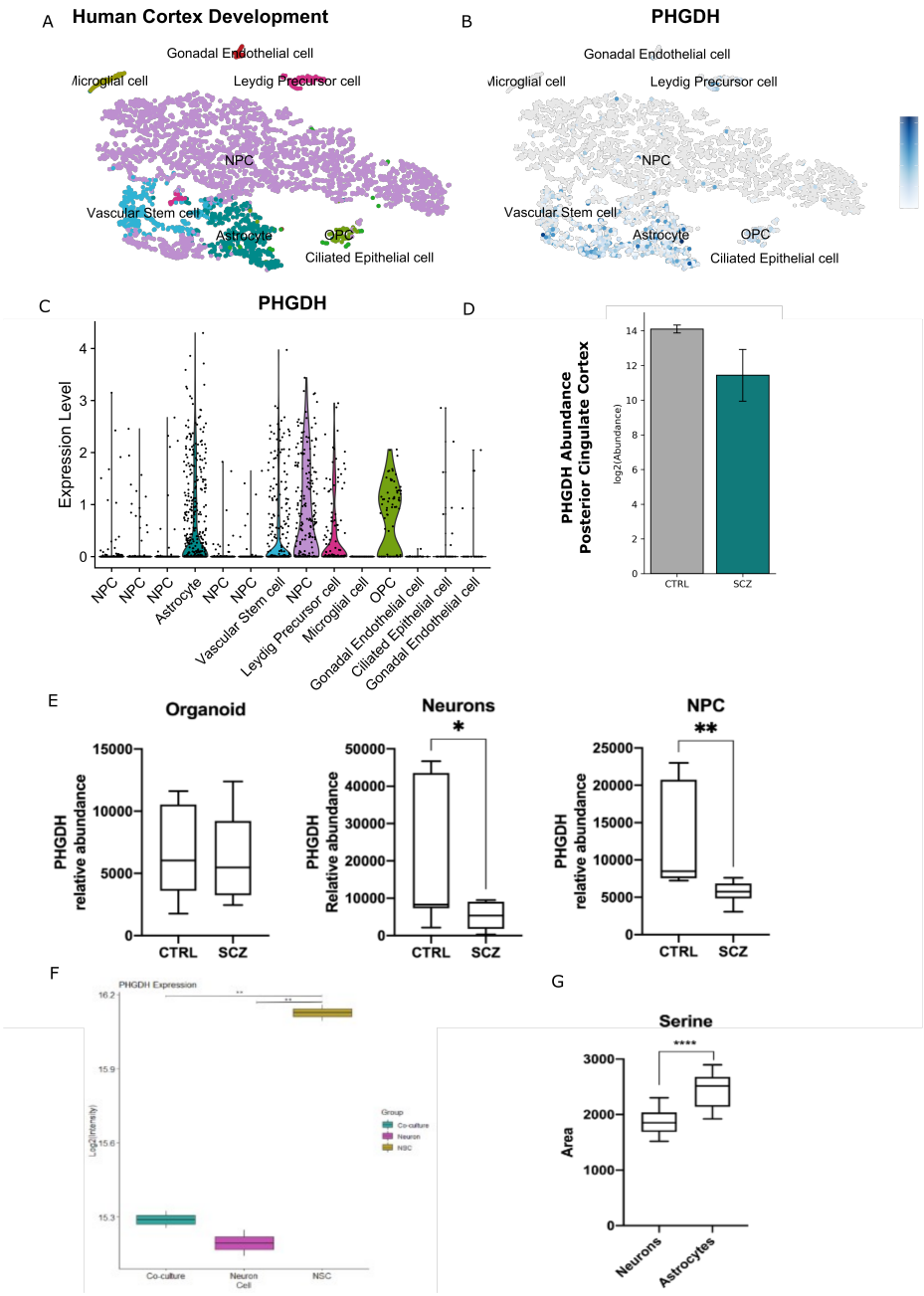

Figura 14 – Evaluation of PHGDH expression and serine production in different cell types of CNS. (A) Single-cell RNA-seq analysis - human cortex development. (B) Expression of PHGDH gene in several cells of the developing human cortex. (C) Violin plot of PHGDH gene in several cells of the developing human cortex, (D) Boxplots of PHGDH levels were calculated using label-free *shotgun* proteomics in posterior cingulate cortex (E) Boxplots of PHGDH levels were calculated using label-free *shotgun* proteomics: Organoids after 45 days of differentiation; Neural Progenitor Cells (NPCs); Immature neurons after 21 days of differentiation. (F) Targeted SRM (Selective Reaction Monitoring) analysis of PHGDH levels in a co-culture of astrocytes and neurons, immature neurons (21 DIV), and neural stem cells (NSCs). (G) Quantification by high-resolution mass spectrometry of free serine in the medium of astrocytes and neurons. An unpaired t-test was used for statistical comparison. *P<0.05, **P<0.01; ***P<0.001; compared to vehicle (DMSO).

Viability Assay. Cell viability remained above 85% in both astrocytes and neurons at 5μM CBR5884, concentration similar to previous chronic treatment in literature (MULLARKY et al., 2016; SEN et al., 2018) (Figures 15 C and D). Serine production was also estimated in each cell type with PHGDH inhibition. Astrocytes and neurons underwent differentiation over 21 days in a culture medium containing CBR5884 and serine levels were measured (Figure 15 E-G). Serine concentration in these CBR5884-exposed neurons was reduced, an effect that was observed both in the culture medium and intracellularly (Figure 15E and F); however, CBR5884-exposed astrocytes showed no significant differences in serine concentration in the culture medium (Figure 15G).

5.4.3 Molecular mechanisms of PHGDH inhibition

A decreased availability of functional PHGDH during neurodevelopment was expected to induce cellular response mechanisms. To investigate this, cells underwent proteomic analysis after being exposed to CBR5884 throughout a 21-day differentiation period from neural stem cells (NSCs) to immature neurons or a 30-day differentiation period from glial progenitor cells to astrocytes (Figure 16A). In neurons, a total of 1191 proteins were identified and quantified, 210 of which were deregulated (ANOVA, $p < 0.05$) by CBR5884. Of these differentially expressed proteins, 37 were down-regulated and 173 were up-regulated (Supplementary Table 1). In astrocytes, a total of 1003 proteins were identified and quantified, 175 of which were deregulated (ANOVA, $p < 0.05$). 149 proteins of these were found down-regulated and 26 up-regulated (Supplementary Table 2). Results of the comparison between these analyses can be seen in Figure 16. Then we performed analysis *in silico* of proteins differentially expressed in astrocytes and neurons treated with CBR5884 compared to vehicle. The first analysis was the over-representation analysis (ORA) against the Gene Ontology database, in order to verify which biological processes these proteins would be associated with. Only 36 proteins were similarly dysregulated between neurons and astrocytes (Figure 16B); however, as shown by the enrichment of canonical pathways and Gene Ontology (Figure 16C), there are several processes in common between the two analyses, such as axon guidance, RNA splicing, and carbon metabolism. Astrocytes presented dysregulation in actomyosin structure organization regulation, while neurons had a tendency for positive regulation of organelle organization (Figure 16D).

A metabolomic analysis using LC/MS was also carried out to evaluate any changes resulting from PHGDH inhibition. As inhibition of PHGDH causes a decrease in serine production, we evaluated some metabolites indirectly involved with this amino acid: lactate, glutamate, glutamine, GABA, acetate, and hexose (Figure 17A). Neurons differentiated in the presence of the PHGDH inhibitor (Figure 17B) showed significantly lower concentrations of intracellular glutamine and extracellular glutamate and lactate was found to be increased,

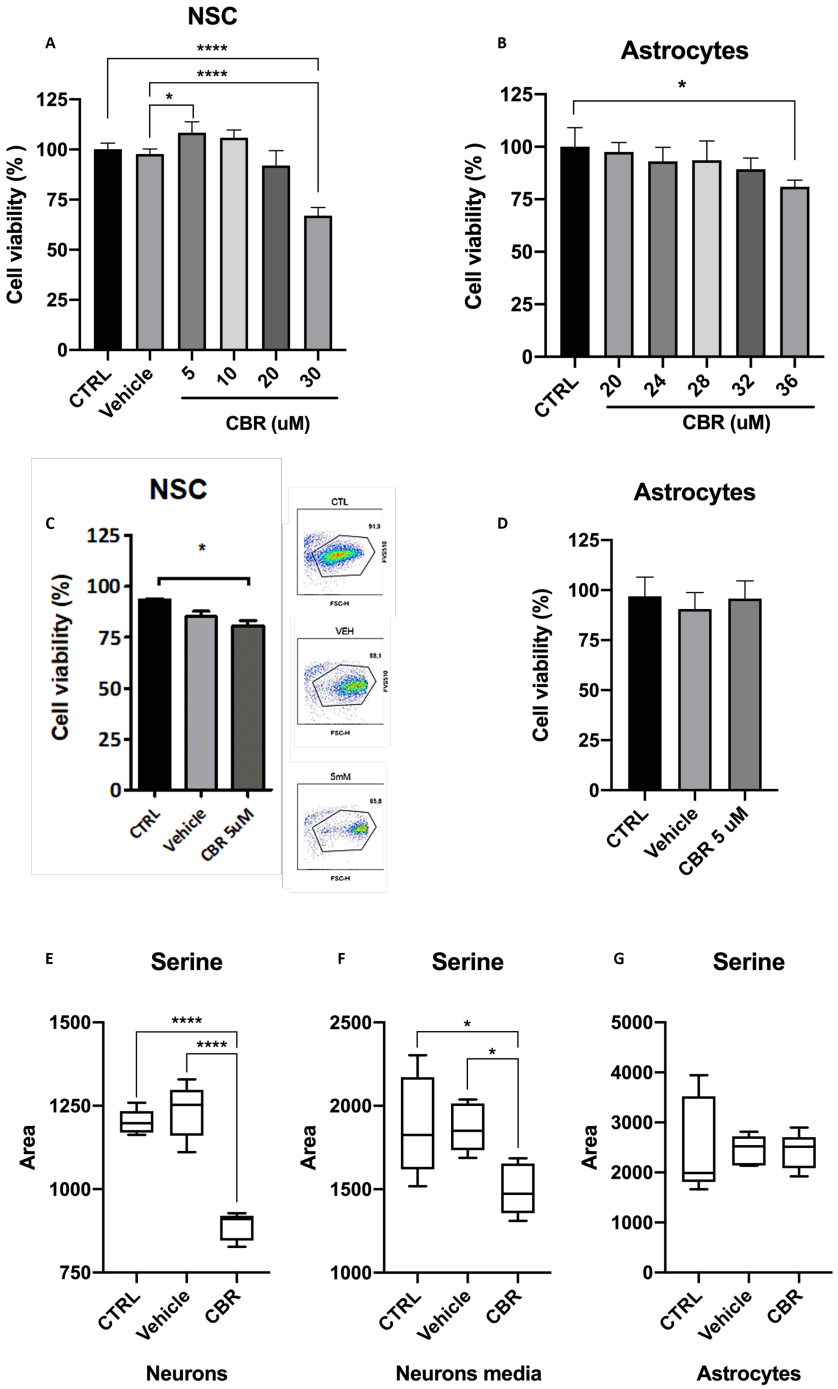

Figura 15 – Functionality of PHGDH inhibitor: (A) NSCs treated with 5 μM, 10 μM, 20 μM and 30 μM of the PHGDH protein inhibitor CBR5884 for 24 hours; (B) Astrocytes treated with 20 μM, 24 μM, 28 μM, 32 μM and 30 μM of the PHGDH protein inhibitor CBR5884 for 24 hours. Confirmation of cell viability with 5 μM CBR5884 after 24h in (C) NSCs, determined by flow cytometry (FVS) and (D) astrocytes, determined by CellTiter-Glo® Luminescent Cell Viability Assay. Quantification by high-resolution mass spectrometry of free serine in: (E) intracellular neurons, (F) neuron culture medium, and (G) astrocyte culture medium. An unpaired t-test followed by Tukey's test for post-hoc analysis was used for statistical comparison. *P<0.05, **P<0.01; ***P<0.001; compared to vehicle (DMSO). All differentiation processes were performed from embryonic stem cells (hESCs).

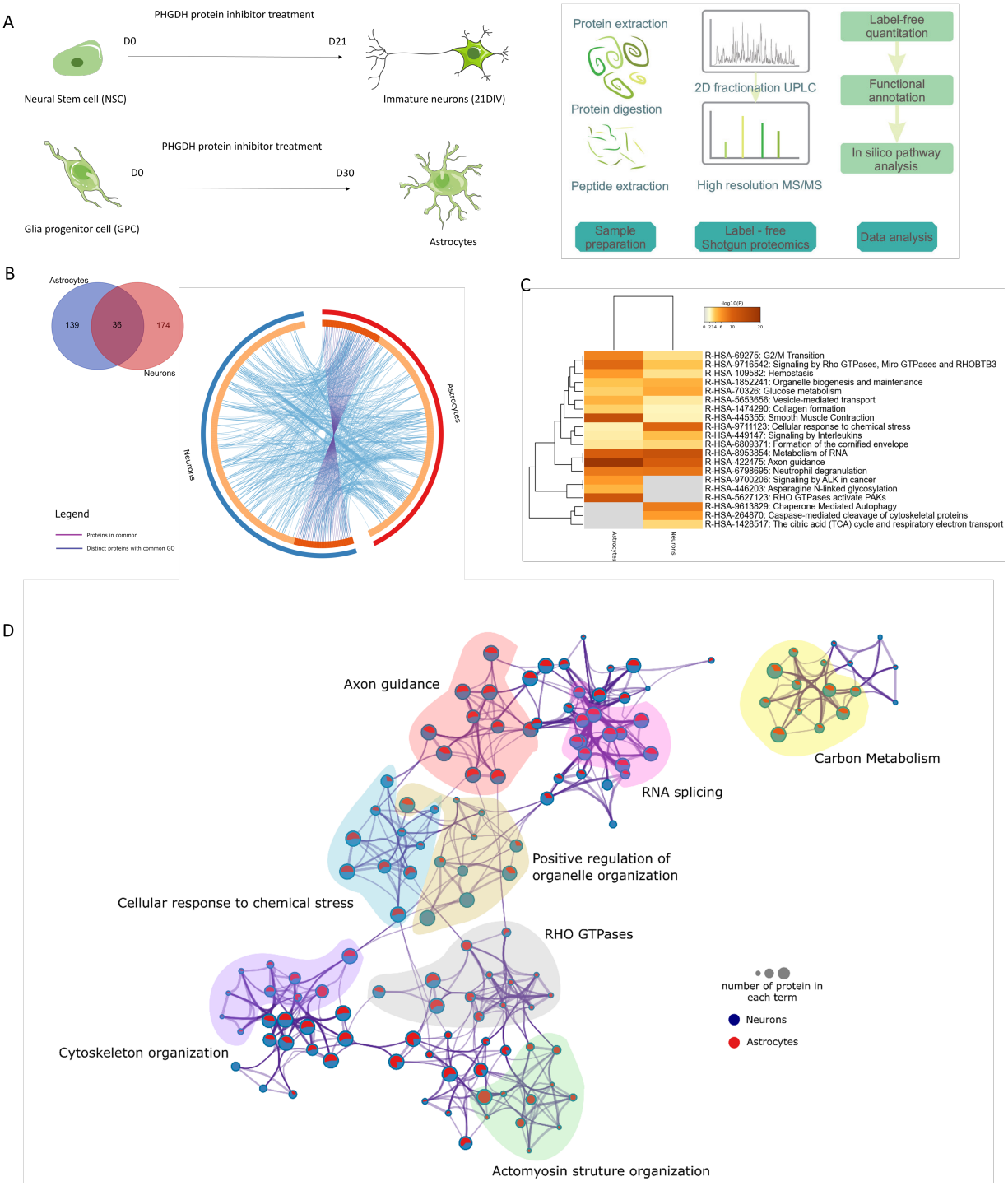

Figura 16 – Network representation of enriched pathways and processes in PHGDH-inhibited astrocytes and neurons. The terms were grouped by similarity metric (kappa scores) and the most statistically significant term within a cluster was defined to represent it. Analyses were performed in Metascape: (A) Diagram of treatments; (B) Circus plot of overlaps and Venn diagram comparing astrocytes and neurons; (C) Comparison enrichment of canonical pathways from Enricher, and (D) Enrichment of canonical pathways and Gene Ontology (GO) terms and their relationship tree for astrocytes and neurons. The enriched pathways were considered significant if they obtained the p-value less than 0.05.

indicating that the PHGDH inhibitor was indeed able to cause a bottleneck in serine production. In astrocytes, inhibition of PHGDH during differentiation caused a significant decrease in hexose and lactate levels in the culture medium, while glutamine and glutamate levels did not significantly change (Figure 17C).

5.4.4 Cell death caused by metabolic dysregulation is present in PHGDH protein inhibition

The proteomic data indicated that neurons with inhibited PHGDH during differentiation presented differentially expressed proteins linked to cell death, particularly apoptosis (p-value 5.710E-5) (Figure 18A and 19A). After 21 days of differentiation with the inhibitor, neuronal cell viability was assessed. Neuronal viability dropped to approximately 70% in response to the PHGDH inhibitor (Figure 19B). PHGDH inhibition over 21 days did not cause significant changes in astrocyte viability (Supplementary Figure 1). To better understand what type of cell death neurons were undergoing, an Apotracker/fixable viability stain (FVS) that indicates the different stages of cell death was used (Figure 19C). There was a predominance of late death both by apoptosis and necrosis, as was suggested by proteomic findings. In addition to apoptosis, amino acid metabolism was also affected (p-value 2.7 10E-6) (Figure 18A), likely due to a lack of certain amino acids downstream of serine (Figure 17) and may be one of the causes of energy metabolism impairment that is compromising cell viability.

5.4.5 Dysregulations caused by PHGDH inhibition decrease the ability of astrocytes to support neural functions

In response to PHGDH inhibition, both neurons and astrocytes exhibited dysregulations in axon guidance and Rho GTPase pathways (Figure 16D). The Rho GTPase family of proteins plays a role in regulating axon guidance (YUAN et al., 2003), and together with neurons, astrocytes play a key role in axonal outgrowth (REEMST et al., 2016). In addition, carbon metabolism was also found to be upregulated in both cells (Figure 16 D), specifically glycolysis (p-value 9.00E-07), pyruvate metabolism and citric acid (TCA) cycle (p-value 0.0016), and pentose production pathways (hexose monophosphate shunt) (p-value 0.0037) (Figure 18 A). These dysregulated pathways are indirectly linked to the production of D-serine (Figure 17A).

85 of the proteins were found to be downregulated in astrocytes, decreasing pathways involving neuronal support, such as Ephrin signaling (p-value 2.01E-05), Rho GTPases (p-value 1.58E-13), as well as metabolic processes to maintain the production of serine and not harm cell viability (Figure 16C).

Since axon outgrowth/guidance and energy metabolism, specifically, lactate production was

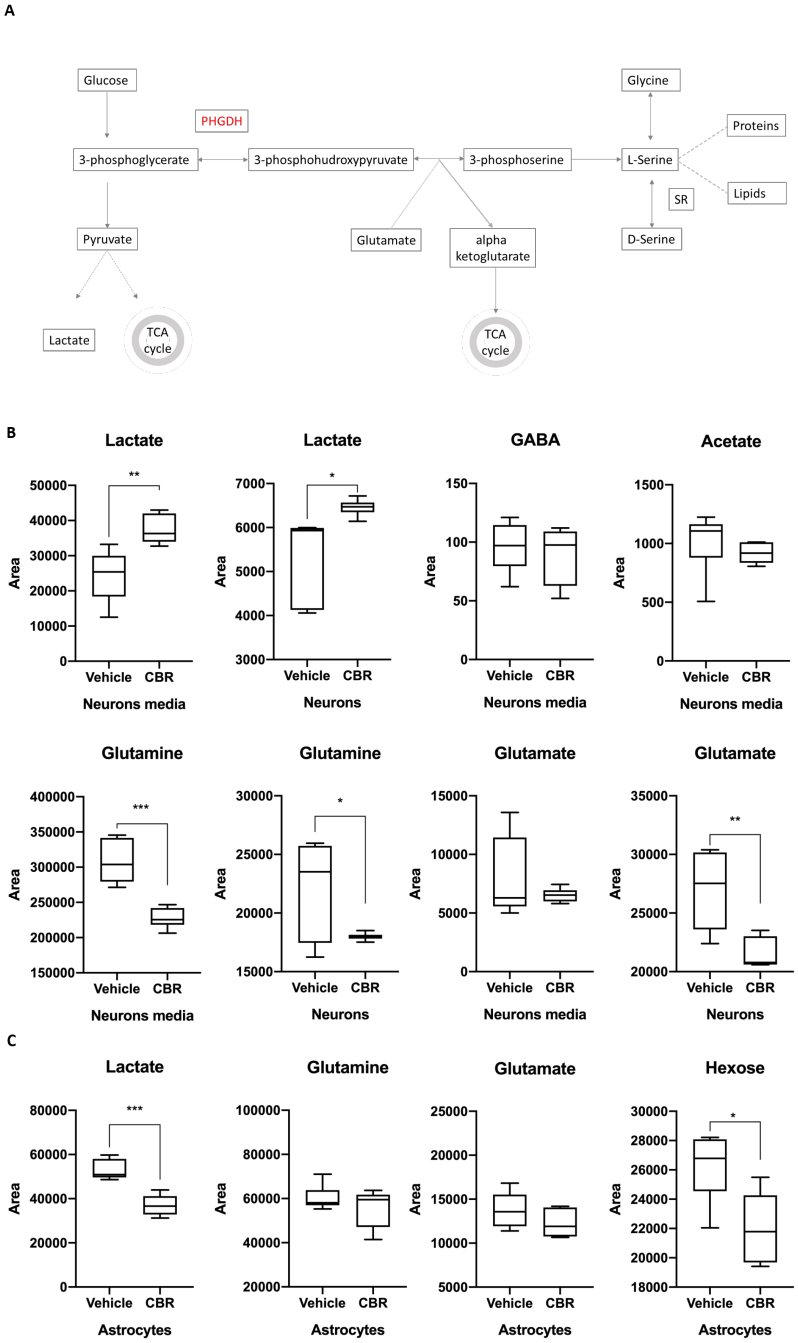

Figura 17 – Metabolic analysis of PHGDH-inhibited neurons and astrocytes derived from human neural stem cells. (A) Diagram of the metabolic pathway of D-serine production (modified from (KIM; PARK, 2018)). Quantification by high-resolution mass spectrometry of (B) lactate, glutamine, and glutamate in neurons subjected to PHGDH protein inhibition during differentiation and lactate, GABA, acetate, glutamine, and glutamate in neuronal media and (C) lactate, glutamine, glutamate, and hexose in astrocytes subjected to PHGDH protein inhibition during differentiation. The integration area of each peak (XIC; extracted ion chromatogram) was used to calculate the box plot graphs and an unpaired t-test followed by Tukey's test for post-hoc analysis was used for statistical comparison. *P<0.05, **P<0.01; ***P<0.001; compared to vehicle (DMSO).

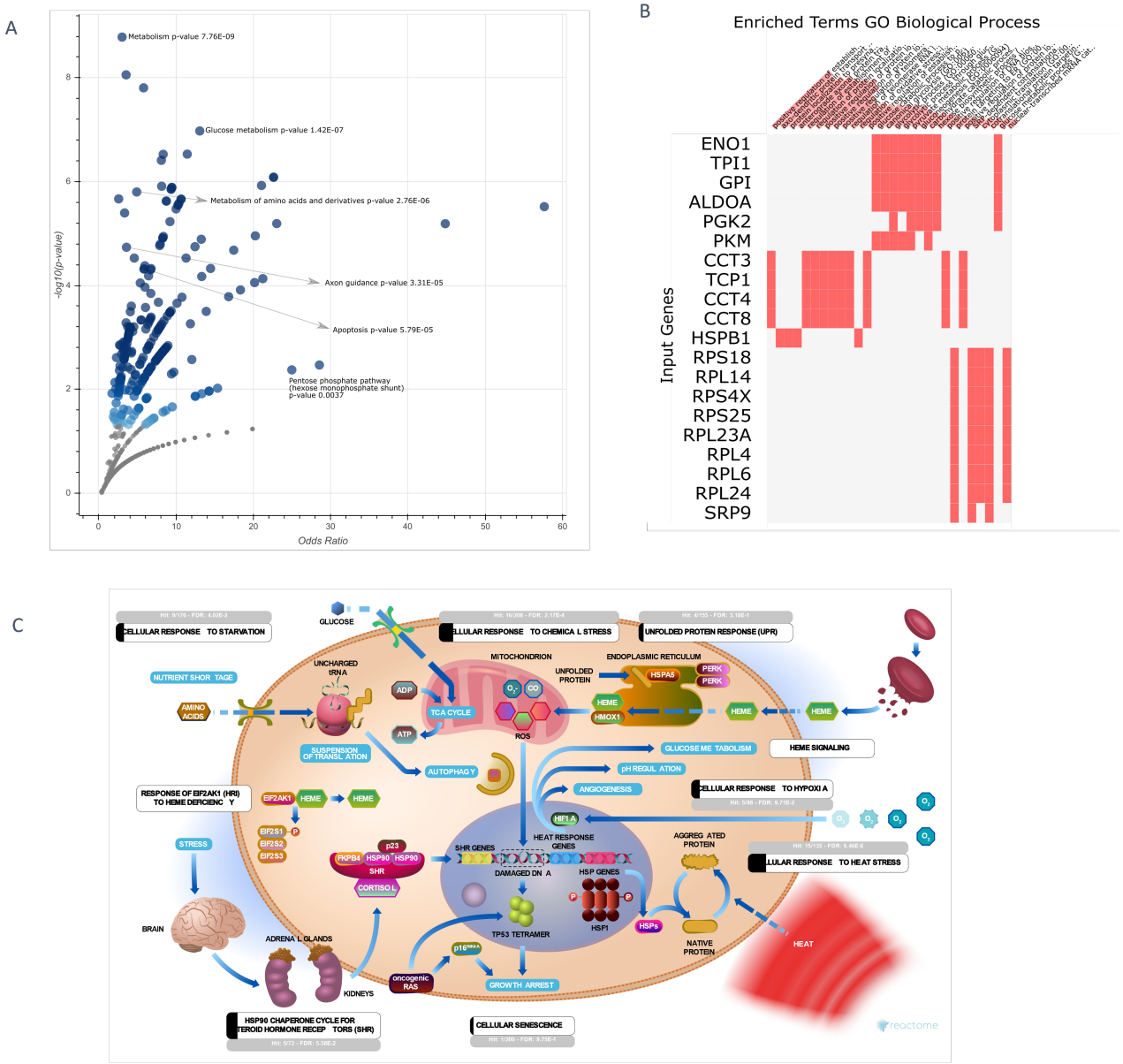

Figura 18 – *In silico* biology analysis of immature neurons (21 DIV) differentiated from embryonic stem cells (hESCs) with inhibited PHGDH (5 μM of CBR5884) during 21 days of differentiation: (A) Volcano plot of enriched pathways using the Reactome database (2016), created using Enricher. (B) Enriched Gene Ontology (GO) terms, using Enricher. (C) Pathway enrichment using proteomic data, using Reactome – Cellular response to stress (p-value 5.2E-4). P-value cutoff was 0.05 - CBR5884 (5μM) was compared to vehicle (DMSO). The enriched pathways were considered significant if they obtained the p-value less than 0.05.

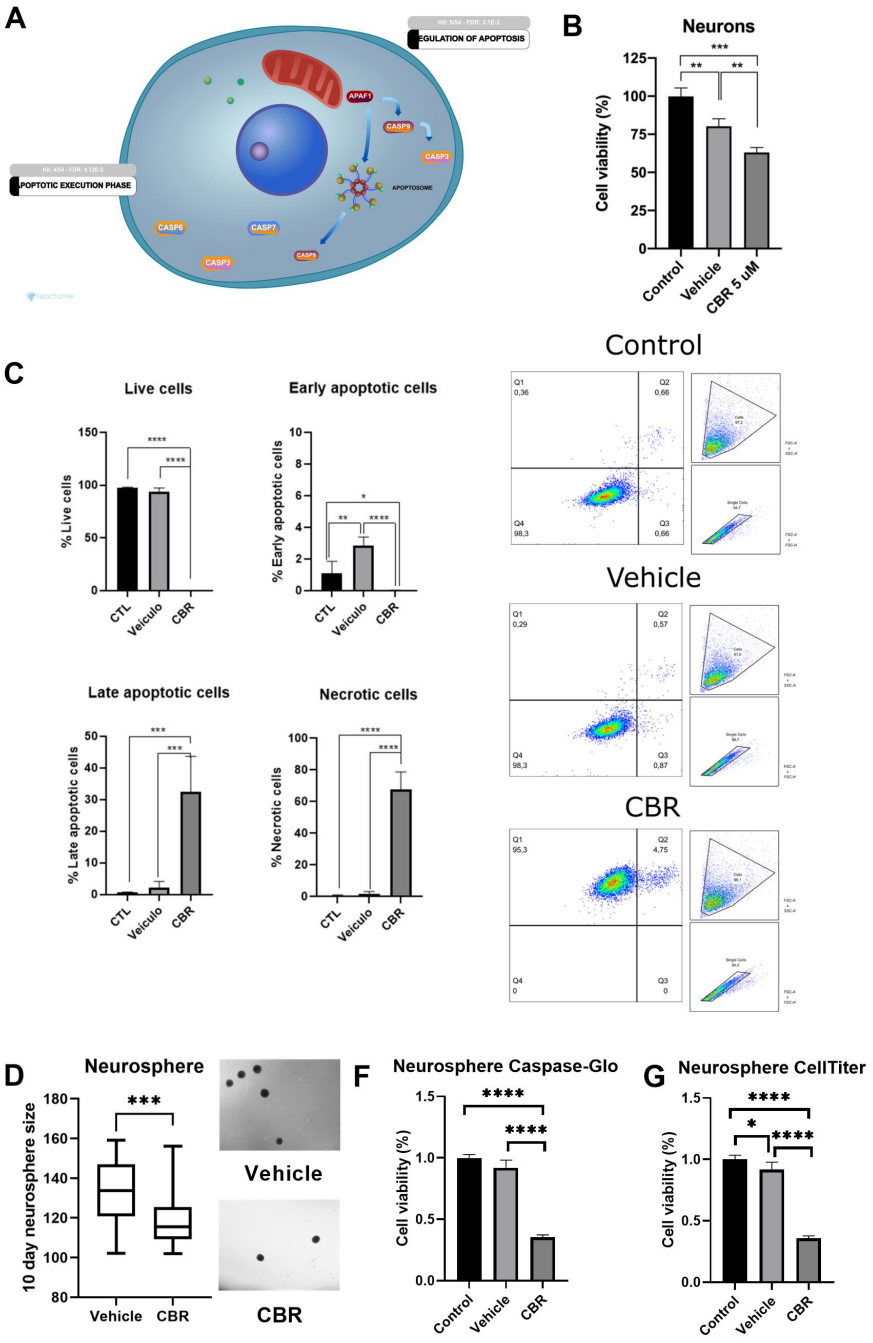

Figura 19 – (A) Pathway enrichment using proteomic data from PHGDH-inhibited immature neurons, generated using Reactome – Apoptosis (p-value 5.79E-5). (B) Viability assay of PHGDH-inhibited immature neurons, determined by luminescence using the CellTiter-Glo® Luminescent Cell Viability Assay kit (C) Cell viability of immature neurons measured by apotracker/fixable viability (FVS) staining, and representative dot-plots of neuronal viability. ; analyzed by flow cytometry; Cells were classified as living (double-negative), in early apoptosis (apotracker+/FVS-) in late apoptosis (double-positive) or necrotic (apotracker-/FVS+). (D) Size of differentiated neurospheres after 10 days of PHGDH inhibition (5 μM CBR5884). (F) Cell viability of neurospheres after 10 days of PHGDH inhibition measured by luminescence using the CellTiter-Glo® Luminescent Cell Viability Assay kit. P-values were determined by unpaired t-test followed by Tukey's post-hoc *P<0.05; **P<0.01; ***P<0.001; ****P<0.0001; compared to vehicle (DMSO). PHGDH-inhibited immature neurons were exposed to 5 μM CBR5884 during the 21-day differentiation

dysregulated by PHGDH inhibition, a neurosphere model was used to understand whether astrocytes were able to rescue or prevent neuronal cell death and axonal impairments. These 3D structures, after 10 days of differentiation, are known to generate immature neurons and young astrocytes (GARCEZ et al., 2016). To confirm that, neurospheres were stained for β3-tubulin (TUBB3) and glial fibrillary acidic protein (GFAP) (Supplementary Figure 3). After the 10-day differentiation period with 5μM of CBR5884, neurosphere size indicated that cell death is likely still occurring, despite the presence of those young astrocytes (Figure 19D). Cell death in neurospheres was confirmed in cell viability analysis by ATP assay (Figure 19F). To assess whether the number of neurons was decreased in relation to the amount of astrocytes since in monoculture neurons are more sensitive to treatment with a PHGDH protein inhibitor, an analysis of the TUBB3/GFAP ratio in neurospheres was performed by immunofluorescence. Supplemental Figure 4 indicates that there were no significant differences between these markers.
To analyze whether the astrocytes were in a state of reactivity: pan-reactive, A1 (neurotoxic) or A2 (neuroprotective); RT-qPCR analysis of reactive markers was performed according to the classification from Clarke el al (CLARKE et al., 2018) and Liddelow et al. (LIDDELOW et al., 2017). The analyses in the Supplementary Figure 5 indicate that these astrocytes are not reactive.

5.4.6 Neural maturation is unaffected by PHGDH inhibition and resulting lack of serine though axonal migration is impaired

Neural maturation markers were analyzed by RT-qPCR (Figure 20B) and flow cytometry (Figure 20C). Gene expression analysis did not show any significant changes in response to PHGDH inhibition except for TUBB3 (beta-tubulin 3). TUBB3 is part of the neuronal microtubule cytoskeleton and plays an important role in axon orientation and maintenance during neurodevelopment (HUANG et al., 2018). This is associated with proteomic upregulations in the canonical axon guidance pathway (p-value 3.31E-05) in PHGDH-inhibited neurons (Figure 18B and 20A). Expression of genes related to axon guidance were evaluated by RT-qPCR (Figure 20D). In neurons and astrocytes, the Roundabout guidance receptor 2 (ROBO2) gene was found with decreased expression under PHGDH inhibition when compared to vehicle. In astrocytes, the Roundabout guidance receptor 1 (ROBO1) gene expression was also decreased in the PHGDH inhibitor condition. The ROBO protein family plays a fundamental role in axon guidance and neurogenesis (cell proliferation and migration) (GONDA; NAMBA; HANASHIMA, 2020; THOMPSON et al., 2009). Neurospheres did not show any significant difference in gene expression of axon guidance genes (ROBO1, ROBO2 and SLIT1) (Figure 20D), by contrast, neurosphere model of axonal growth/migration assay shows reduced axonal outgrowth

when PHGDH was inhibited during the 10-day differentiation process (Figure 20E). Lastly, synaptophysin was upregulated in immature neurons (21DIV) with PHGDH inhibition, as indicated by flow cytometry (Figure 20C). Neural proliferation, another important aspect of early neuronal differentiation, showed no significant changes after PHGDH inhibition (Supplemental Figure 23).

5.5 Discussion

Neurons and astrocytes have complex metabolic interactions; energy metabolism must be properly functioning to ensure the survival of neurons and synaptic functionality (TURNER; ADAMSON, 2011). Neurons require lactate from astrocytes to meet high energy demands for proper synaptic functions via aerobic metabolism (IVANOV et al., 2011). As a result, a decrease in lactate production can be detrimental to astrocyte-neuron metabolic interactions. In addition, lactate has been recently shown to play an important role in axon guidance (XU et al., 2020) and a decrease in this molecule may have an inhibitory effect, confirmed by proteomic data in this study. We hypothesize that astrocytes are maintaining serine concentration in the medium by using a greater amount of hexose to maintain production since glucose is a precursor to serine. As a result, with more glucose being diverted to serine production, lactate production is slowed.

When energy demands spike, neurons increase their glycolytic rate, becoming net exporters of lactate (DÍAZ-GARCÍA; YELLEN, 2019), which explains the increase in lactate in neurons seen here. Furthermore, when glutamine consumption is increased, as in the case when there is a lack of serine, glucose oxidation decreases, while lactate production increases (DAMIANI et al., 2017). The observed decrease in serine and glutamine levels, both of which are NMDA receptor activation substrates, may lead to a hypofunction of this receptor, consequently affecting neuronal differentiation.

Two processes that are seen in schizophrenia are impairment in neural circuitry and long-term cognitive dysfunction, both of which can be attributed to cell death, as seen in patients with Alzheimer's and Huntington's disease (NIJHAWAN; HONARPOUR; WANG, 2000). Cell death via apoptosis is a natural process that occurs frequently during early neurodevelopment; however, when exacerbated, it can cause problems in brain development (JARSKOG et al., 2004). Pathological activation of apoptosis has been proposed as part of the etiology of neurodevelopmental diseases, such as schizophrenia, as it may also influence synaptic connection and neuronal complexity (GLANTZ et al., 2006). However, as most studies were carried out using *postmortem* brain tissue from patients, it is not possible to conclude whether apoptosis is a cause or merely a consequence of the disease (GLANTZ et al., 2006). Drastic metabolic changes during neurodevelopment have been suggested to be one of the main causes of cell death in neurons since, during cell differentiation, neurons become increasingly specialized and dependent on interactions with other cells to maintain

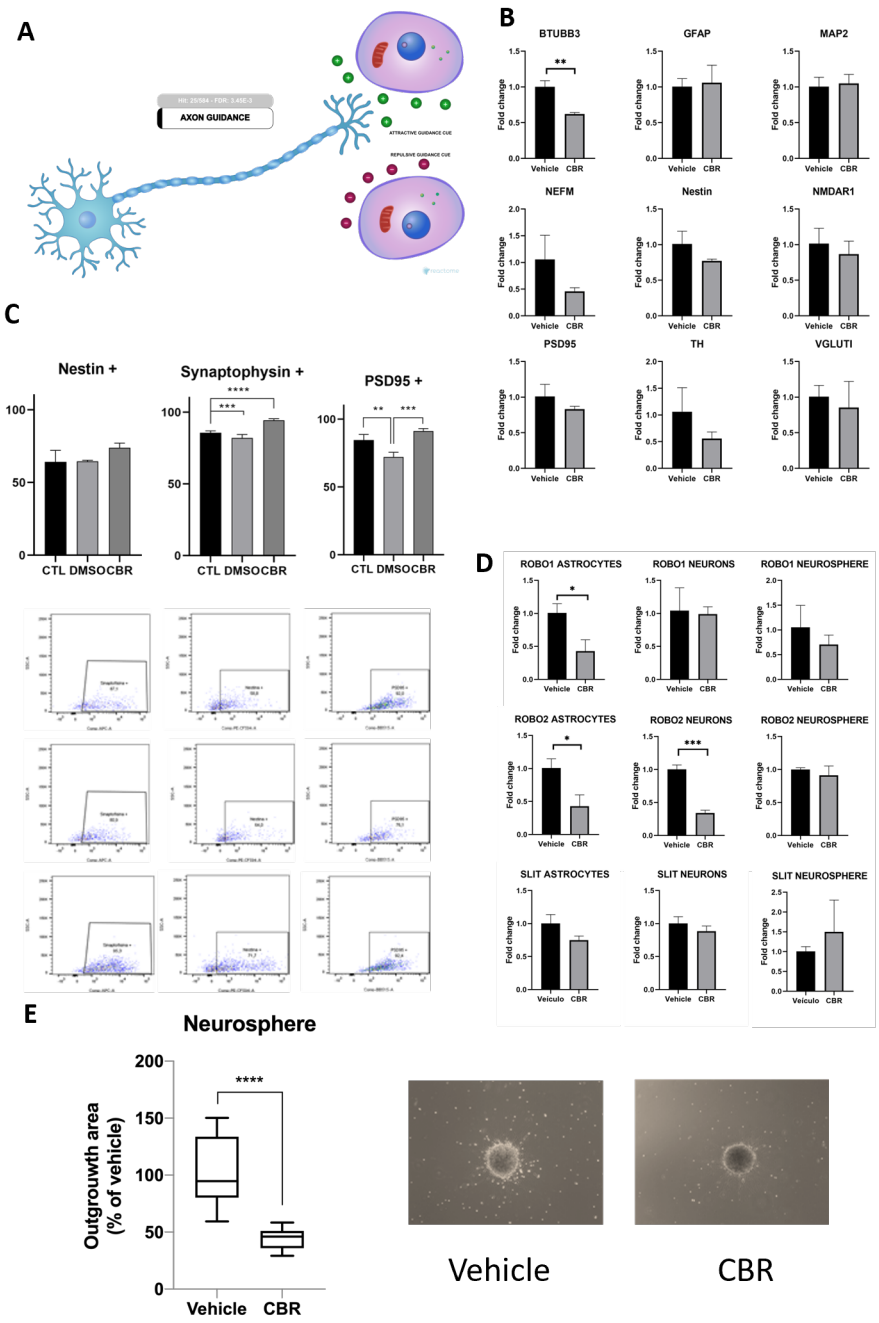

Figura 20 – (A) Pathway enrichment of PHGDH-inhibited immature neurons using proteomic data, generated with Reactome. (B) Quantitation of neural differentiation markers in immature neurons using RT-qPCR; (C) Analysis of immature neurons positive for nestin, synaptophysin, or PSD95, analyzed by flow cytometry; (D) Quantitation of axon guidance genes in immature neurons, astrocytes, and neurosphere using RT-qPCR; (E) Axonal migration assay in 10-day differentiated, PHGDH-inhibited (5 μM CBR5884) neurospheres. P values were determined by unpaired t-test followed by Tukey's post-hoc *P<0.05; **P<0.01; ***P<0.001; ****P<0.0001; compared to vehicle (DMSO). PHGDH-inhibited immature neurons were exposed to 5 μM CBR5884 during the 21-day differentiation process and were generated from embryonic stem cells (hESCs). The enriched pathways were considered significant if they obtained the p-value less than 0.05.

their metabolism. Therefore, apoptosis observed in neurons under these conditions can be tentatively attributed to dysfunctions in metabolism and a lack of interaction with astrocytes. This is in line with the increase in energy demands of these cells during the development of synapses (TURNER; ADAMSON, 2011).

Synaptic dysfunctions are extensively documented in patients with neurodegenerative and neurodevelopmental diseases, such as Alzheimer disease and schizophrenia (NASCIMENTO et al., 2019; BRENNAND et al., 2011; TOPOL et al., 2015; CHEN; FU; IP, 2019). After the advent of induced pluripotent stem cells, these findings were found in neural cells and brain organoids derived from cells from patients with schizophrenia, suggesting that this dysfunction occurs as early as during neurodevelopment (BRENNAND et al., 2011; TOPOL et al., 2015). Our results indicate that there is no decrease in neural maturation markers when PHGDH is inhibited, leading to a lack of serine; however, there is still a reduction in axonal migration, an important aspect in neural development. The elevated levels of this protein might be correlated to an attempt to strengthen neural maturation considering the dysregulations found in axonal migration.

In conclusion, the main phenotypic effect resulting from PHGDH inhibition during neural differentiation is cell death, possibly caused by the dysregulations in the energy metabolism of these cells. Furthermore, PHGDH inhibition does not alter the direct expression of markers of neural maturation but rather affects basic processes of neuronal differentiation such as energy metabolism and axonal migration. This preliminary study indicates that a co-culture of astrocytes and neurons does not seem to reverse the dysregulations caused by PHGDH inhibition in neurons during their differentiation. This is despite the expectation that astrocytes should maintain serine production and thus cell viability.

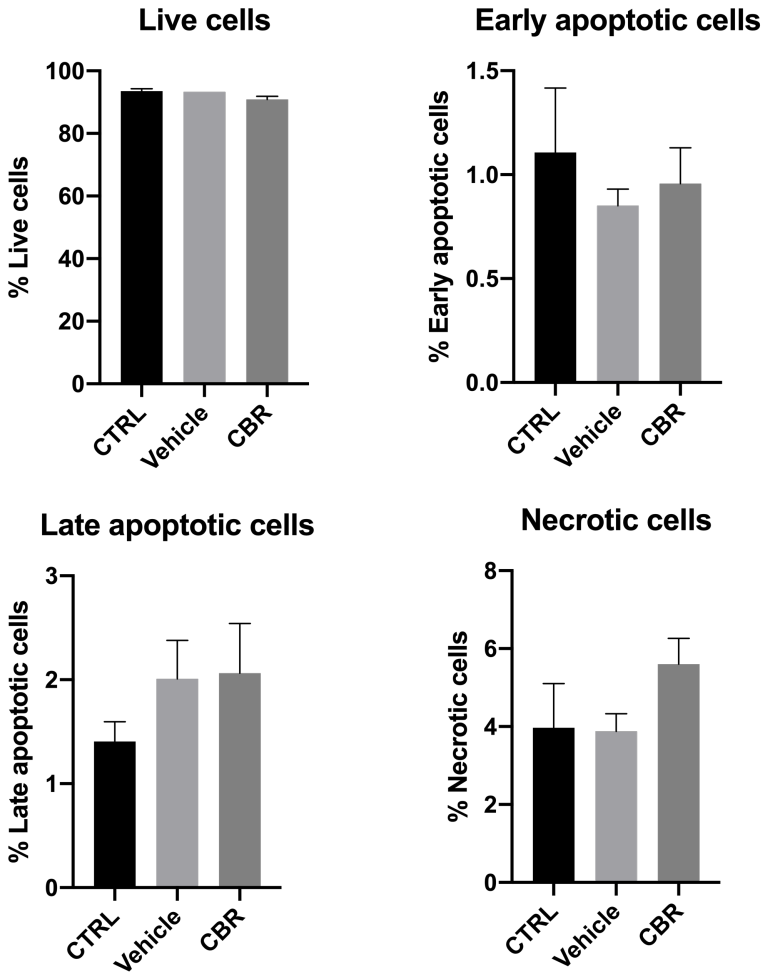

Figura 21 – Supplementary figure 1 - Cell viability of astrocytes measured by apotracker/-fixable viability (FVS) staining, analyzed by flow cytometry.

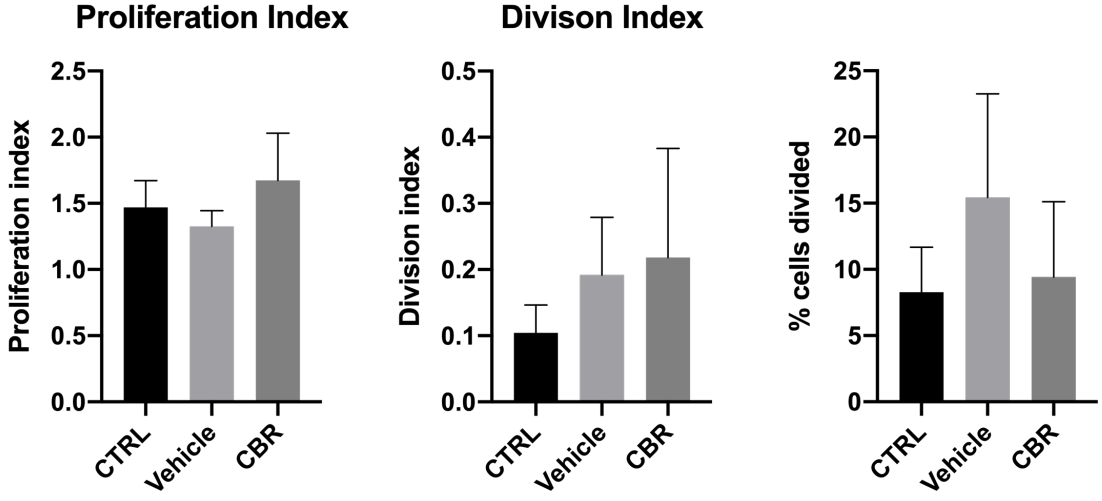

Figura 22 – Supplementary figure 2 - Cell proliferation of neural stem cell (NSC) measured by CellTrace™ CFSE Cell Proliferation Kit, analyzed by flow cytometry.

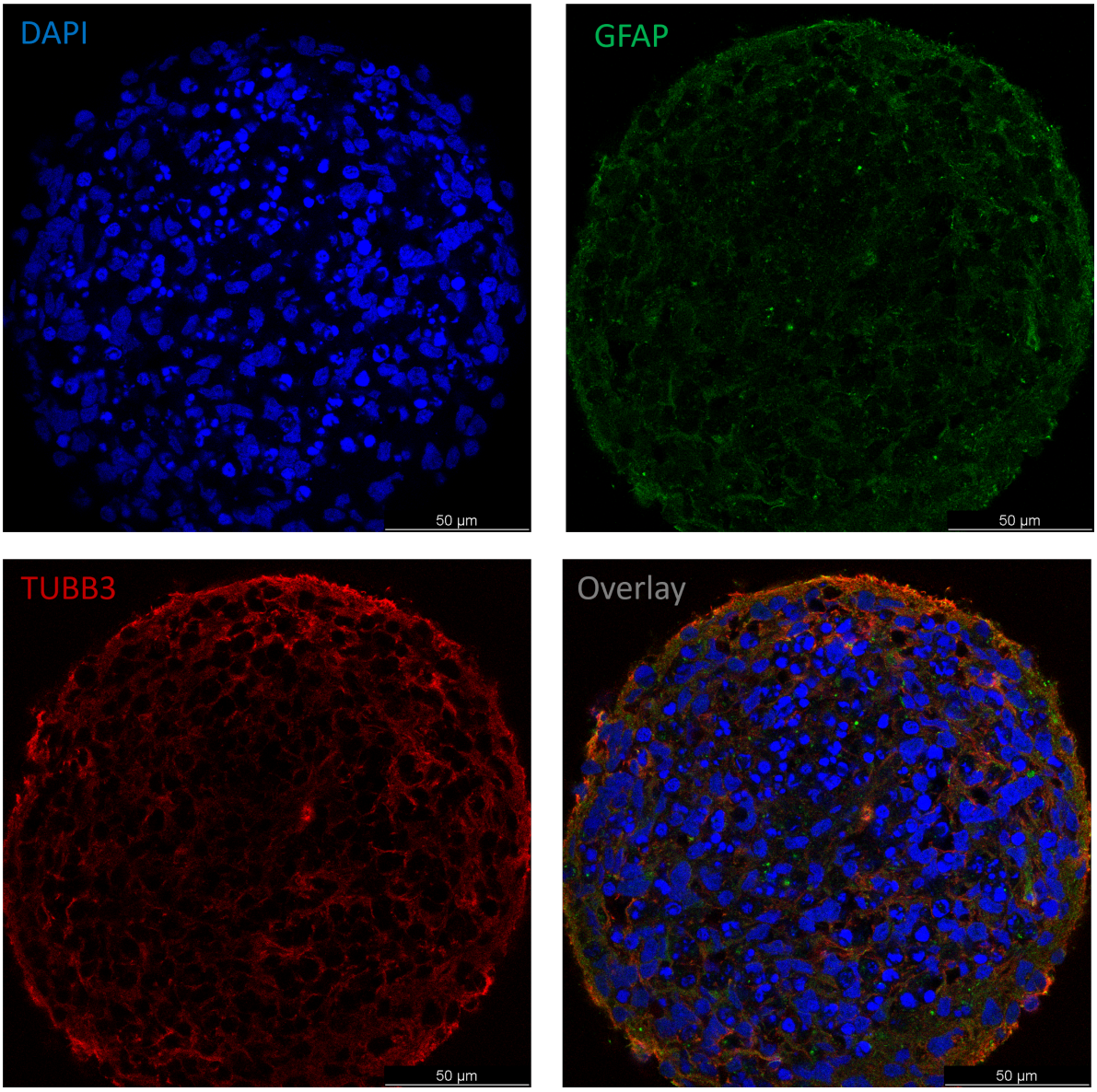

Figura 23 – Supplementary figure 3 - Characterization of cellular models of the neurosphere. Immunocytochemistry showing human young astrocyte staining for GFAP and human immature neurons (at 10 DIV) stained for TUBB3. bars = 50 μgm.

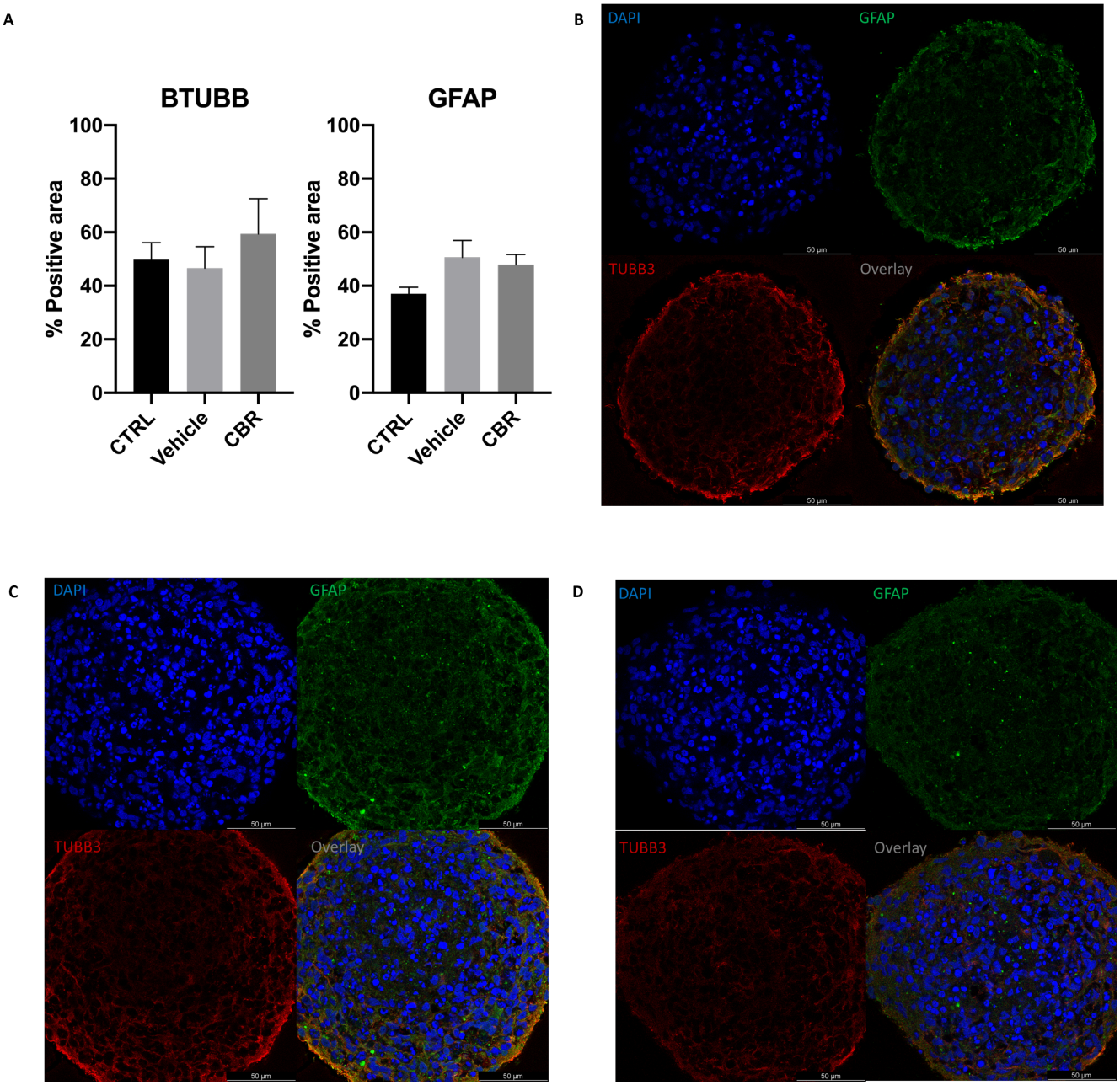

Figura 24 – Supplementary figure 4 - A) Percentage of neurons (TUBB3) and astrocytes (GFAP) in neurosphere. B) Immunocytochemistry showing human young astrocyte staining for GFAP and human immature neurons (at 10 DIV) stained for TUBB3. B) CBR5884, B) Vehicle (DMSO), and C) Control. bars = 50 μgm.

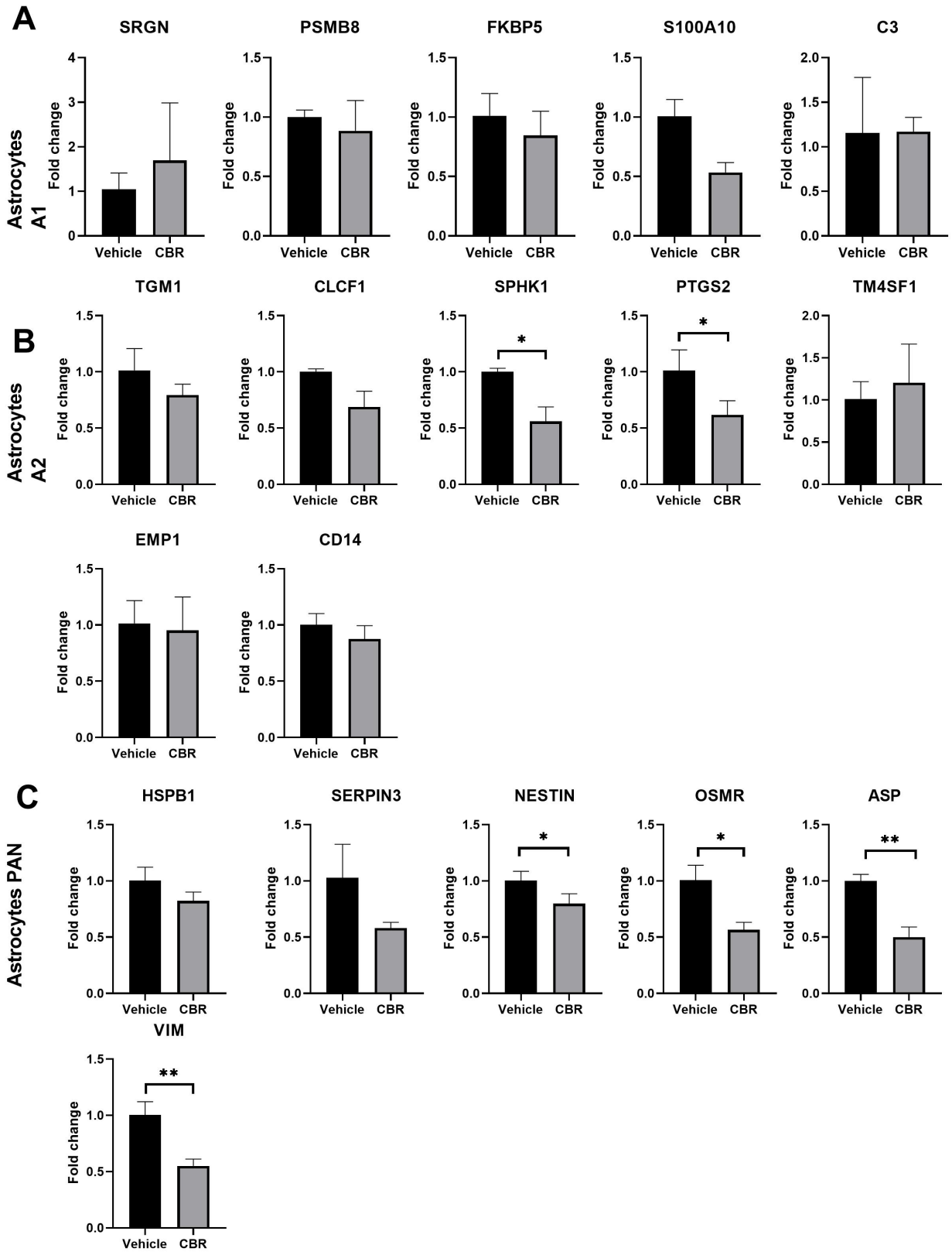

Figura 25 – Supplementary figure 5 - RT-qPCR analysis of genes related to the classification of reactive astrocyte types: (A) A1-specific (neurotoxic), (B) A2-specific (neuroprotective), and (C)pan-reactive.

6 Considerações Finais

A esquizofrenia é um transtorno multifatorial que tem como cerne a conjunção de características genéticas com fatores ambientais. Apesar de vários estudos terem mostrado diversas mutações gênicas com pequenos efeitos e níveis de expressão de proteínas que estão relacionados à fisiopatologia da esquizofrenia, ainda não há consenso quanto à etiologia da doença. Atualmente, tem-se estudado muito sobre o componente de neurodesenvolvimento (RAPOPORT; GIEDD; GOGTAY, 2012) e sua consequência nos sistemas neurotransmissores, principalmente dopaminérgicos e glutamatérgicos (HOWES; MCCUTCHEON; STONE, 2015). Aspectos do neurodesenvolvimento da esquizofrenia, principalmente relacionados a disfunção glutamatérgica, foram elucidados no capítulo 3.
Devido à incapacidade de estudar o desenvolvimento humano em embriões, a maioria dos estudos que testam a hipótese do neurodesenvolvimento são realizados em modelos animais, que possuem grandes diferenças se comparados ao desenvolvimento humano. Com o aparecimento de novas técnicas, como as células-tronco pluripotentes humanas induzidas (iPSCs), foi permitido o cultivo de células cerebrais humanas e a geração de modelos tridimensionais, como organóides e esferóides para estudos *in vitro*. Ainda, as iPSCs geradas a partir de pacientes carregam seus fatores genéticos.
O estudo do capítulo 4 realizado em células neurais derivadas de células tronco pluripotentes de pacientes com esquizofrenia nos mostrou múltiplas proteínas desreguladas relacionas à vias sinápticas, e, ainda, esses estudos estão em linha com os realizados em tecidos *post mortem* de pacientes. Organóides e neurônios imaturos exibem deficiências em vias ainda não encontradas em estudos de células-tronco pluripotentes induzidas derivadas de pacientes, como spliceossomos e metabolismo de aminoácidos.
Um aminoácido conhecidamente reduzido em pacientes com esquizofrenia é a D-serina, essa molécula é encontrada em abundância e co-localiza com os receptores NMDA durante o neurodesenvolvimento. Ainda, ela participa de funções como transmissão sináptica, migração neuronal e sinaptogênese. Uma das proteínas essenciais na produção da D-Serina é a proteína PHGDH, e ela foi encontrada desregulada no estudo do capítulo 4. Assim, utilizando o capítulo 4 como base teórica, no capítulo 5 realizamos a inibição da proteína PHGDH. Foi concluído que a inibição dsssa proteina não altera a expressão direta de marcadores de maturação neural, mas afeta processos básicos de diferenciação neuronal, como metabolismo energético e migração axonal. Além disso, o principal efeito fenotípico resultante da inibição da PHGDH durante a diferenciação neural é a morte celular, possivelmente causada pelas desregulações no metabolismo energético dessas células.
Por fim, esses estudos nos mostram uma visão geral de como o neurodesenvolvimento pode ser abordado em doenças relacionadas ao desenvolvimento humano, antes pouco

abordado devido à falta de modelos humanos. Ainda no estudo do capítulo 3, fornecemos dados abrangentes e em grande escala em nível de proteína que podem revelar mecanismos subjacentes das origens de desenvolvimento da esquizofrenia.

Por fim, acreditamos que nosso trabalho possibilitou uma visão geral dos aspectos do neurodesenvolvimento que são relacionados às desregulações moleculares da esquizofrenia, principalmente no que diz respeito a relação neurodesenvolvimento/sistema glutamatérgico. Porém, entendemos que, por se tratar de uma doença complexa, muito ainda se tem a desvendar sobre o papel do neurodesenvolvimento na patofisiologia desse transtorno

Referências

ABBRUZZESE, M.; BELLODI, L.; FERRI, S.; SCARONE, S. Frontal-lobe dysfunction in schizophrenia and obsessive-compulsive disorder-a neuropsychological study. *Brain and cognition*, Elsevier, v. 27, n. 2, p. 202–212, 1995. Citado na página 65.

ABDOLMALEKY, H. M.; SMITH, C. L.; FARAONE, S. V.; SHAFA, R.; STONE, W.; GLATT, S. J.; TSUANG, M. T. Methylomics in psychiatry: modulation of gene–environment interactions may be through dna methylation. *American Journal of Medical Genetics Part B: Neuropsychiatric Genetics*, Wiley Online Library, v. 127, n. 1, p. 51–59, 2004. Citado na página 62.

AKITA, T.; AOTO, K.; KATO, M.; SHIINA, M.; MUTOH, H.; NAKASHIMA, M.; KUKI, I.; OKAZAKI, S.; MAGARA, S.; SHIIHARA, T. et al. De novo variants in camk 2a and camk 2b cause neurodevelopmental disorders. *Annals of clinical and translational neurology*, Wiley Online Library, v. 5, n. 3, p. 280–296, 2018. Citado na página 46.

ANDREASEN, N.; NASRALLAH, H. A.; DUNN, V.; OLSON, S. C.; GROVE, W. M.; EHRHARDT, J. C.; COFFMAN, J. A.; CROSSETT, J. H. Structural abnormalities in the frontal system in schizophrenia: a magnetic resonance imaging study. *Archives of general psychiatry*, American Medical Association, v. 43, n. 2, p. 136–144, 1986. Citado na página 36.

ASHOK, A. H.; BAUGH, J.; YERAGANI, V. K. Paul eugen bleuler and the origin of the term schizophrenia (schizopreniegruppe). *Indian journal of psychiatry*, Wolters Kluwer–Medknow Publications, v. 54, n. 1, p. 95, 2012. Citado na página 35.

BAHARVAND, H.; MEHRJARDI, N.-Z.; HATAMI, M.; KIANI, S.; RAO, M.; HAGHIGHI, M.-M. Neural differentiation from human embryonic stem cells in a defined adherent culture condition. *International Journal of Developmental Biology*, UPV/EHU Press, v. 51, n. 5, p. 371–378, 2003. Citado na página 51.

BALAN, S.; YAMADA, K.; HATTORI, E.; IWAYAMA, Y.; TOYOTA, T.; OHNISHI, T.; MAEKAWA, M.; TOYOSHIMA, M.; IWATA, Y.; SUZUKI, K. et al. Population-specific haplotype association of the postsynaptic density gene dlg4 with schizophrenia, in family-based association studies. *PloS one*, Public Library of Science San Francisco, USA, v. 8, n. 7, p. e70302, 2013. Citado na página 45.

BALLON, J. S.; DEAN, K. A.; CADENHEAD, K. S. Obstetrical complications in people at risk for developing schizophrenia. *Schizophrenia research*, Elsevier, v. 98, n. 1-3, p. 307–311, 2008. Citado na página 36.

BALU, D. T.; LI, Y.; PUHL, M. D.; BENNEYWORTH, M. A.; BASU, A. C.; TAKAGI, S.; BOLSHAKOV, V. Y.; COYLE, J. T. Multiple risk pathways for schizophrenia converge in serine racemase knockout mice, a mouse model of nmda receptor hypofunction. *Proceedings of the National Academy of Sciences*, National Acad Sciences, v. 110, n. 26, p. E2400–E2409, 2013. Citado na página 65.

BARCH, D. M.; CEASER, A. Cognition in schizophrenia: core psychological and neural mechanisms. *Trends in cognitive sciences*, Elsevier, v. 16, n. 1, p. 27–34, 2012. Citado na página 25.

BELL, R.; MUNRO, J.; RUSS, C.; POWELL, J. F.; BRUINVELS, A.; KERWIN, R. W.; COLLIER, D. A. Systematic screening of the 14-3-3 eta (η) chain gene for polymorphic variants and case-control analysis in schizophrenia. *American journal of medical genetics*, Wiley Online Library, v. 96, n. 6, p. 736–743, 2000. Citado na página 63.

BENNETT, M. R. Synapse formation and regression in the cortex during adolescence and in schizophrenia. *Medical journal of Australia*, v. 190, n. S4, p. S14–S16, 2009. Citado na página 65.

BERARDIS, D. D.; FILIPPIS, S. D.; MASI, G.; VICARI, S.; ZUDDAS, A. A neurodevelopment approach for a transitional model of early onset schizophrenia. *Brain Sciences*, Multidisciplinary Digital Publishing Institute, v. 11, n. 2, p. 275, 2021. Citado na página 36.

BERGER, A. J.; DIEUDONNÉ, S.; ASCHER, P. Glycine uptake governs glycine site occupancy at nmda receptors of excitatory synapses. *Journal of neurophysiology*, American Physiological Society Bethesda, MD, v. 80, n. 6, p. 3336–3340, 1998. Citado 2 vezes nas páginas 10 e 39.

BERGMAN, O.; BEN-SHACHAR, D. Mitochondrial oxidative phosphorylation system (oxphos) deficits in schizophrenia: possible interactions with cellular processes. *The Canadian Journal of Psychiatry*, SAGE Publications Sage CA: Los Angeles, CA, v. 61, n. 8, p. 457–469, 2016. Citado na página 64.

BOPPART, M. D.; LISIO, M. D.; WITKOWSKI, S. Exercise and stem cells. *Progress in molecular biology and translational science*, Elsevier, v. 135, p. 423–456, 2015. Citado na página 27.

BRENNAND, K. J. Personalized medicine in a dish: the growing possibility of neuropsychiatric disease drug discovery tailored to patient genetic variants using stem cells. *Stem cell investigation*, AME Publications, v. 4, 2017. Citado na página 50.

BRENNAND, K. J.; SIMONE, A.; JOU, J.; GELBOIN-BURKHART, C.; TRAN, N.; SANGAR, S.; LI, Y.; MU, Y.; CHEN, G.; YU, D. et al. Modelling schizophrenia using human induced pluripotent stem cells. *Nature*, Nature Publishing Group, v. 473, n. 7346, p. 221–225, 2011. Citado 2 vezes nas páginas 41 e 89.

BROADBELT, K.; BYNE, W.; JONES, L. B. Evidence for a decrease in basilar dendrites of pyramidal cells in schizophrenic medial prefrontal cortex. *Schizophrenia research*, Elsevier, v. 58, n. 1, p. 75–81, 2002. Citado na página 45.

BROWN, A. S. Prenatal infection as a risk factor for schizophrenia. *Schizophrenia bulletin*, Oxford University Press, v. 32, n. 2, p. 200–202, 2006. Citado na página 36.

_____. The environment and susceptibility to schizophrenia. *Progress in neurobiology*, Elsevier, v. 93, n. 1, p. 23–58, 2011. Citado 2 vezes nas páginas 23 e 62.

BROWN, H. E.; ROFFMAN, J. L. Vitamin supplementation in the treatment of schizophrenia. *CNS drugs*, Springer, v. 28, n. 7, p. 611–622, 2014. Citado na página 24.

BYSTRON, I.; BLAKEMORE, C.; RAKIC, P. Development of the human cerebral cortex: Boulder committee revisited. *Nature Reviews Neuroscience*, Nature Publishing Group, v. 9, n. 2, p. 110–122, 2008. Citado 2 vezes nas páginas 47 e 68.

CAGNEY, G.; AMIRI, S.; PREMAWARADENA, T.; LINDO, M.; EMILI, A. In silico proteome analysis to facilitate proteomics experiments using mass spectrometry. *Proteome Science*, BioMed Central, v. 1, n. 1, p. 1–15, 2003. Citado na página 31.

CALVANO, S. E.; XIAO, W.; RICHARDS, D. R.; FELCIANO, R. M.; BAKER, H. V.; CHO, R. J.; CHEN, R. O.; BROWNSTEIN, B. H.; COBB, J. P.; TSCHOEKE, S. K. et al. A network-based analysis of systemic inflammation in humans. *Nature*, Nature Publishing Group, v. 437, n. 7061, p. 1032–1037, 2005. Citado na página 31.

CAMP, J. G.; BADSHA, F.; FLORIO, M.; KANTON, S.; GERBER, T.; WILSCH-BRÄUNINGER, M.; LEWITUS, E.; SYKES, A.; HEVERS, W.; LANCASTER, M. et al. Human cerebral organoids recapitulate gene expression programs of fetal neocortex development. *Proceedings of the National Academy of Sciences*, National Acad Sciences, v. 112, n. 51, p. 15672–15677, 2015. Citado na página 50.

CARDNO, A. G.; GOTTESMAN, I. I. Twin studies of schizophrenia: from bow-and-arrow concordances to star wars mx and functional genomics. *American journal of medical genetics*, Wiley Online Library, v. 97, n. 1, p. 12–17, 2000. Citado na página 35.

CASSOLI, J. S.; BRANDÃO-TELES, C.; SANTANA, A. G.; SOUZA, G. H.; SOUZA, D. Martins-de. Ion mobility-enhanced data-independent acquisitions enable a deep proteomic landscape of oligodendrocytes. *Proteomics*, Wiley Online Library, v. 17, n. 21, p. 1700209, 2017. Citado na página 54.

CASSOLI, J. S.; IWATA, K.; STEINER, J.; GUEST, P. C.; TURCK, C. W.; NASCIMENTO, J. M.; SOUZA, D. Martins-de. Effect of mk-801 and clozapine on the proteome of cultured human oligodendrocytes. *Frontiers in cellular neuroscience*, Frontiers, v. 10, p. 52, 2016. Citado na página 64.

CHÉDOTAL, A. Roles of axon guidance molecules in neuronal wiring in the developing spinal cord. *Nature Reviews Neuroscience*, Nature Publishing Group, v. 20, n. 7, p. 380–396, 2019. Citado na página 43.

CHEN, E. Y.; TAN, C. M.; KOU, Y.; DUAN, Q.; WANG, Z.; MEIRELLES, G. V.; CLARK, N. R.; MA'AYAN, A. Enrichr: interactive and collaborative html5 gene list enrichment analysis tool. *BMC bioinformatics*, BioMed Central, v. 14, n. 1, p. 1–14, 2013. Citado 2 vezes nas páginas 73 e 75.

CHEN, Y.; FU, A. K.; IP, N. Y. Synaptic dysfunction in alzheimer's disease: mechanisms and therapeutic strategies. *Pharmacology & therapeutics*, Elsevier, v. 195, p. 186–198, 2019. Citado na página 89.

CHOI, M.; CHANG, C.-Y.; CLOUGH, T.; BROUDY, D.; KILLEEN, T.; MACLEAN, B.; VITEK, O. Msstats: an r package for statistical analysis of quantitative mass spectrometry-based proteomic experiments. *Bioinformatics*, Oxford University Press, v. 30, n. 17, p. 2524–2526, 2014. Citado na página 74.

CLAIR, D. S.; XU, M.; WANG, P.; YU, Y.; FANG, Y.; ZHANG, F.; ZHENG, X.; GU, N.; FENG, G.; SHAM, P. et al. Rates of adult schizophrenia following prenatal exposure to the chinese famine of 1959-1961. *Jama*, American Medical Association, v. 294, n. 5, p. 557–562, 2005. Citado 2 vezes nas páginas 36 e 62.

CLANCY, B.; DARLINGTON, R. B.; FINLAY, B. L. Translating developmental time across mammalian species. *Neuroscience*, Elsevier, v. 105, n. 1, p. 7–17, 2001. Citado na página 46.

CLAPCOTE, S. J.; LIPINA, T. V.; MILLAR, J. K.; MACKIE, S.; CHRISTIE, S.; OGAWA, F.; LERCH, J. P.; TRIMBLE, K.; UCHIYAMA, M.; SAKURABA, Y. et al. Behavioral phenotypes of disc1 missense mutations in mice. *Neuron*, Elsevier, v. 54, n. 3, p. 387–402, 2007. Citado na página 63.

CLARKE, L. E.; LIDDELOW, S. A.; CHAKRABORTY, C.; MÜNCH, A. E.; HEIMAN, M.; BARRES, B. A. Normal aging induces a1-like astrocyte reactivity. *Proceedings of the National Academy of Sciences*, National Acad Sciences, v. 115, n. 8, p. E1896–E1905, 2018. Citado na página 86.

COLEY, A. A.; GAO, W.-J. Psd-95 deficiency disrupts pfc-associated function and behavior during neurodevelopment. *Scientific reports*, Nature Publishing Group, v. 9, n. 1, p. 1–13, 2019. Citado na página 45.

COLMAN, A.; DREESEN, O. Pluripotent stem cells and disease modeling. *Cell stem cell*, Elsevier, v. 5, n. 3, p. 244–247, 2009. Citado 2 vezes nas páginas 27 e 68.

CONESA, A.; GÖTZ, S.; GARCÍA-GÓMEZ, J. M.; TEROL, J.; TALÓN, M.; ROBLES, M. Blast2go: a universal tool for annotation, visualization and analysis in functional genomics research. *Bioinformatics*, Oxford University Press, v. 21, n. 18, p. 3674–3676, 2005. Citado na página 31.

CORNELL, B.; TOYO-OKA, K. 14-3-3 proteins in brain development: neurogenesis, neuronal migration and neuromorphogenesis. *Frontiers in molecular neuroscience*, Frontiers, v. 10, p. 318, 2017. Citado na página 63.

DAKIC, V.; NASCIMENTO, J. M.; SARTORE, R. C.; MACIEL, R. de M.; ARAUJO, D. B. de; RIBEIRO, S.; SOUZA, D. Martins-de; REHEN, S. K. Short term changes in the proteome of human cerebral organoids induced by 5-meo-dmt. *Scientific reports*, Nature Publishing Group, v. 7, n. 1, p. 1–13, 2017. Citado na página 52.

DAMIANI, C.; COLOMBO, R.; GAGLIO, D.; MASTROIANNI, F.; PESCINI, D.; WESTERHOFF, H. V.; MAURI, G.; VANONI, M.; ALBERGHINA, L. A metabolic core model elucidates how enhanced utilization of glucose and glutamine, with enhanced glutamine-dependent lactate production, promotes cancer cell growth: The warburq effect. *PLoS computational biology*, Public Library of Science San Francisco, CA USA, v. 13, n. 9, p. e1005758, 2017. Citado na página 87.

DÍAZ-GARCÍA, C. M.; YELLEN, G. Neurons rely on glucose rather than astrocytic lactate during stimulation. *Journal of neuroscience research*, Wiley Online Library, v. 97, n. 8, p. 883–889, 2019. Citado na página 87.

DIESET, I.; HOPE, S.; UELAND, T.; BJELLA, T.; AGARTZ, I.; MELLE, I.; AUKRUST, P.; RØSSBERG, J.-I.; ANDREASSEN, O. A. Cardiovascular risk factors during second generation antipsychotic treatment are associated with increased c-reactive protein. *Schizophrenia research*, Elsevier, v. 140, n. 1-3, p. 169–174, 2012. Citado 2 vezes nas páginas 24 e 35.

DJURIC, U.; RODRIGUES, D. C.; BATRUCH, I.; ELLIS, J.; SHANNON, P.; DIAMANDIS, P. Spatiotemporal proteomic profiling of human cerebral development. *Molecular & Cellular Proteomics*, ASBMB, v. 16, n. 9, p. 1548–1562, 2017. Citado na página 41.

DU, Y.; DREYFUS, C. F. Oligodendrocytes as providers of growth factors. *Journal of neuroscience research*, Wiley Online Library, v. 68, n. 6, p. 647–654, 2002. Citado na página 26.

DVASH, T.; BEN-YOSEF, D.; EIGES, R. Human embryonic stem cells as a powerful tool for studying human embryogenesis. *Pediatric research*, Nature Publishing Group, v. 60, n. 2, p. 111–117, 2006. Citado na página 27.

EACK, S. M.; HOGARTY, G. E.; GREENWALD, D. P.; HOGARTY, S. S.; KESHAVAN, M. S. Effects of cognitive enhancement therapy on employment outcomes in early schizophrenia: results from a 2-year randomized trial. *Research on social work practice*, Sage Publications Sage CA: Los Angeles, CA, v. 21, n. 1, p. 32–42, 2011. Citado na página 24.

EGERTON, A.; GRACE, A. A.; STONE, J.; BOSSONG, M. G.; SAND, M.; MCGUIRE, P. Glutamate in schizophrenia: neurodevelopmental perspectives and drug development. *Schizophrenia Research*, Elsevier, 2020. Citado 2 vezes nas páginas 38 e 39.

ENDELE, S.; ROSENBERGER, G.; GEIDER, K.; POPP, B.; TAMER, C.; STEFANOVA, I.; MILH, M.; KORTÜM, F.; FRITSCH, A.; PIENTKA, F. K. et al. Mutations in grin2a and grin2b encoding regulatory subunits of nmda receptors cause variable neurodevelopmental phenotypes. *Nature genetics*, Nature Publishing Group, v. 42, n. 11, p. 1021–1026, 2010. Citado na página 43.

ERP, T. G. V.; WALTON, E.; HIBAR, D. P.; SCHMAAL, L.; JIANG, W.; GLAHN, D. C.; PEARLSON, G. D.; YAO, N.; FUKUNAGA, M.; HASHIMOTO, R. et al. Cortical brain abnormalities in 4474 individuals with schizophrenia and 5098 control subjects via the enhancing neuro imaging genetics through meta analysis (enigma) consortium. *Biological psychiatry*, Elsevier, v. 84, n. 9, p. 644–654, 2018. Citado na página 36.

FALK, M. J. Neurodevelopmental manifestations of mitochondrial disease. *Journal of developmental and behavioral pediatrics: JDBP*, NIH Public Access, v. 31, n. 7, p. 610, 2010. Citado na página 64.

FATEMI, S. H.; FOLSOM, T. D. The neurodevelopmental hypothesis of schizophrenia, revisited. *Schizophrenia bulletin*, Oxford University Press, v. 35, n. 3, p. 528–548, 2009. Citado 2 vezes nas páginas 36 e 62.

FELDSTEIN, A.; HOAGLAND, H.; FREEMAN, H. On the relationship of serotonin to schizophrenia. *Science*, American Association for the Advancement of Science, v. 128, n. 3320, p. 358–358, 1958. Citado na página 25.

FÖCKING, M.; DICKER, P.; ENGLISH, J. A.; SCHUBERT, K. O.; DUNN, M. J.; COTTER, D. R. Common proteomic changes in the hippocampus in schizophrenia and bipolar disorder and particular evidence for involvement of cornu ammonis regions 2 and 3. *Archives of general psychiatry*, American Medical Association, v. 68, n. 5, p. 477–488, 2011. Citado na página 63.

FRAGA, A. M.; SUKOYAN, M.; RAJAN, P.; BRAGA, D. P. de A. F.; JR, A. I.; JR, J. G. F.; JR, E. B.; PEREIRA, L. V. Establishment of a brazilian line of human embryonic stem cells in defined medium: implications for cell therapy in an ethnically diverse population. *Cell transplantation*, SAGE Publications Sage CA: Los Angeles, CA, v. 20, n. 3, p. 431–440, 2011. Citado 2 vezes nas páginas 51 e 69.

FRANKLE, W. G.; LERMA, J.; LARUELLE, M. The synaptic hypothesis of schizophrenia. *Neuron*, Cell Press, v. 39, n. 2, p. 205–216, 2003. Citado 2 vezes nas páginas 25 e 38.

FREEMAN, M. R. Specification and morphogenesis of astrocytes. *Science*, American Association for the Advancement of Science, v. 330, n. 6005, p. 774–778, 2010. Citado na página 68.

FUJITA, Y.; ISHIMA, T.; HASHIMOTO, K. Supplementation with d-serine prevents the onset of cognitive deficits in adult offspring after maternal immune activation. *Scientific reports*, Nature Publishing Group, v. 6, n. 1, p. 1–10, 2016. Citado 2 vezes nas páginas 43 e 47.

FURUYA, S.; YOSHIDA, K.; KAWAKAMI, Y.; YANG, J. H.; SAYANO, T.; AZUMA, N.; TANAKA, H.; KUHARA, S.; HIRABAYASHI, Y. Inactivation of the 3-phosphoglycerate dehydrogenase gene in mice: changes in gene expression and associated regulatory networks resulting from serine deficiency. *Functional & integrative genomics*, Springer, v. 8, n. 3, p. 235–249, 2008. Citado na página 76.

FUSAR-POLI, P.; POLITI, P. Paul eugen bleuler and the birth of schizophrenia (1908). *American Journal of Psychiatry*, Am Psychiatric Assoc, v. 165, n. 11, p. 1407–1407, 2008. Citado na página 23.

GANGULY, P.; SOLIMAN, A.; MOUSTAFA, A. A. Holistic management of schizophrenia symptoms using pharmacological and non-pharmacological treatment. *Frontiers in public health*, Frontiers, v. 6, p. 166, 2018. Citado na página 24.

GARCEZ, P. P.; LOIOLA, E. C.; COSTA, R. M. D.; HIGA, L. M.; TRINDADE, P.; DELVECCHIO, R.; NASCIMENTO, J. M.; BRINDEIRO, R.; TANURI, A.; REHEN, S. K. Zika virus impairs growth in human neurospheres and brain organoids. *Science*, American Association for the Advancement of Science, v. 352, n. 6287, p. 816–818, 2016. Citado na página 86.

GAREY, L.; ONG, W.; PATEL, T.; KANANI, M.; DAVIS, A.; MORTIMER, A.; BARNES, T.; HIRSCH, S. Reduced dendritic spine density on cerebral cortical pyramidal neurons in schizophrenia. *Journal of Neurology, Neurosurgery & Psychiatry*, BMJ Publishing Group Ltd, v. 65, n. 4, p. 446–453, 1998. Citado na página 45.

GEJMAN, P. V.; SANDERS, A. R.; DUAN, J. The role of genetics in the etiology of schizophrenia. *Psychiatric Clinics*, Elsevier, v. 33, n. 1, p. 35–66, 2010. Citado na página 23.

GLANTZ, L. A.; GILMORE, J. H.; LIEBERMAN, J. A.; JARSKOG, L. F. Apoptotic mechanisms and the synaptic pathology of schizophrenia. *Schizophrenia research*, Elsevier, v. 81, n. 1, p. 47–63, 2006. Citado na página 87.

GLANTZ, L. A.; LEWIS, D. A. Decreased dendritic spine density on prefrontal cortical pyramidal neurons in schizophrenia. *Archives of general psychiatry*, American Medical Association, v. 57, n. 1, p. 65–73, 2000. Citado na página 45.

GLAUSIER, J. R.; LEWIS, D. A. Dendritic spine pathology in schizophrenia. *Neuroscience*, Elsevier, v. 251, p. 90–107, 2013. Citado na página 27.

GOLD, J. M.; ROBINSON, B.; LEONARD, C. J.; HAHN, B.; CHEN, S.; MCMAHON, R. P.; LUCK, S. J. Selective attention, working memory, and executive function as potential independent sources of cognitive dysfunction in schizophrenia. *Schizophrenia bulletin*, Oxford University Press US, v. 44, n. 6, p. 1227–1234, 2018. Citado na página 65.

GOMES, F. C. A.; TORTELLI, V. P.; DINIZ, L. Glia: dos velhos conceitos às novas funções de hoje e as que ainda virão. *estudos avançados*, SciELO Brasil, v. 27, p. 61–84, 2013. Citado na página 26.

GONDA, Y.; NAMBA, T.; HANASHIMA, C. Beyond axon guidance: Roles of slit-robo signaling in neocortical formation. *Frontiers in cell and developmental biology*, Frontiers, v. 8, p. 1691, 2020. Citado na página 86.

GONZALEZ-PINTO, A.; GUTIERREZ, M.; MOSQUERA, F.; BALLESTEROS, J.; LOPEZ, P.; EZCURRA, J.; FIGUERIDO, J. L.; LEON, J. de. First episode in bipolar disorder: misdiagnosis and psychotic symptoms. *Journal of affective disorders*, Elsevier, v. 50, n. 1, p. 41–44, 1998. Citado 2 vezes nas páginas 38 e 50.

GRAHAM, K.; KEEFE, R.; LIEBERMAN, J.; CALIKOGLU, A.; LANSING, K.; PERKINS, D. Relationship of low vitamin d status with positive, negative and cognitive symptom domains in people with first-episode schizophrenia. *Early intervention in psychiatry*, Wiley Online Library, v. 9, n. 5, p. 397–405, 2015. Citado na página 24.

GULCHINA, Y.; XU, S.-J.; SNYDER, M. A.; ELEFANT, F.; GAO, W.-J. Epigenetic mechanisms underlying nmda receptor hypofunction in the prefrontal cortex of juvenile animals in the mam model for schizophrenia. *Journal of neurochemistry*, Wiley Online Library, v. 143, n. 3, p. 320–333, 2017. Citado na página 38.

GULSUNER, S.; WALSH, T.; WATTS, A. C.; LEE, M. K.; THORNTON, A. M.; CASADEI, S.; RIPPEY, C.; SHAHIN, H.; BRAFF, D.; CADENHEAD, K. S. et al. Spatial and temporal mapping of de novo mutations in schizophrenia to a fetal prefrontal cortical network. *Cell*, Elsevier, v. 154, n. 3, p. 518–529, 2013. Citado na página 65.

GUPTA, S.; KULHARA, P. What is schizophrenia: A neurodevelopmental or neurodegenerative disorder or a combination of both? a critical analysis. *Indian journal of psychiatry*, Wolters Kluwer–Medknow Publications, v. 52, n. 1, p. 21, 2010. Citado 2 vezes nas páginas 36 e 37.

GUSEL'NIKOVA, V.; KORZHEVSKIY, D. Neun as a neuronal nuclear antigen and neuron differentiation marker. *Acta Naturae ( )*, -, v. 7, n. 2 (25), 2015. Citado na página 76.

HAO, Y.; HAO, S.; ANDERSEN-NISSEN, E.; III, W. M. M.; ZHENG, S.; BUTLER, A.; LEE, M. J.; WILK, A. J.; DARBY, C.; ZAGER, M. et al. Integrated analysis of multimodal single-cell data. *Cell*, Elsevier, 2021. Citado na página 76.

HASHIMOTO, A.; KUMASHIRO, S.; NISHIKAWA, T.; OKA, T.; TAKAHASHI, K.; MITO, T.; TAKASHIMA, S.; DOI, N.; MIZUTANI, Y.; YAMAZAKI, T. et al. Embryonic development and postnatal changes in free d-aspartate and d-serine in the human prefrontal cortex. *Journal of neurochemistry*, Wiley Online Library, v. 61, n. 1, p. 348–351, 1993. Citado 2 vezes nas páginas 39 e 68.

HASHIMOTO, A.; NISHIKAWA, T.; OKA, T.; TAKAHASHI, K. Endogenous d-serine in rat brain: N-methyl-d-aspartate receptor-related distribution and aging. *Journal of neurochemistry*, Wiley Online Library, v. 60, n. 2, p. 783–786, 1993. Citado na página 45.

HASHIMOTO, K.; ENGBERG, G.; SHIMIZU, E.; NORDIN, C.; LINDSTRÖM, L. H.; IYO, M. Reduced d-serine to total serine ratio in the cerebrospinal fluid of drug naive schizophrenic patients. *Progress in Neuro-Psychopharmacology and Biological Psychiatry*, Elsevier, v. 29, n. 5, p. 767–769, 2005. Citado na página 43.

HASHIMOTO, K.; FUKUSHIMA, T.; SHIMIZU, E.; KOMATSU, N.; WATANABE, H.; SHINODA, N.; NAKAZATO, M.; KUMAKIRI, C.; OKADA, S.-i.; HASEGAWA, H. et al. Decreased serum levels of d-serine in patients with schizophrenia: evidence in support of the n-methyl-d-aspartate receptor hypofunction hypothesis of schizophrenia. *Archives of general psychiatry*, American Medical Association, v. 60, n. 6, p. 572–576, 2003. Citado na página 39.

HENKEMEYER, M.; ITKIS, O. S.; NGO, M.; HICKMOTT, P. W.; ETHELL, I. M. Multiple ephb receptor tyrosine kinases shape dendritic spines in the hippocampus. *The Journal of cell biology*, Rockefeller University Press, v. 163, n. 6, p. 1313–1326, 2003. Citado na página 62.

HERESCO-LEVY, U.; ERMILOV, M.; SHIMONI, J.; SHAPIRA, B.; SILIPO, G.; JAVITT, D. C. Placebo-controlled trial of d-cycloserine added to conventional neuroleptics, olanzapine, or risperidone in schizophrenia. *American Journal of Psychiatry*, Am Psychiatric Assoc, v. 159, n. 3, p. 480–482, 2002. Citado na página 43.

HO, Y.-S. Removal of copper ions from aqueous solution by tree fern. *Water research*, Elsevier, v. 37, n. 10, p. 2323–2330, 2003. Citado na página 29.

HOFFMANN, E. D.; STROOBANT, V. *Mass spectrometry: principles and applications*. [S.l.]: John Wiley & Sons, 2007. Citado na página 29.

HOL, E. M.; PEKNY, M. Glial fibrillary acidic protein (gfap) and the astrocyte intermediate filament system in diseases of the central nervous system. *Current opinion in cell biology*, Elsevier, v. 32, p. 121–130, 2015. Citado na página 75.

HONG, S. J.; LI, H.; BECKER, K. G.; DAWSON, V. L.; DAWSON, T. M. Identification and analysis of plasticity-induced late-response genes. *Proceedings of the National Academy of Sciences*, National Acad Sciences, v. 101, n. 7, p. 2145–2150, 2004. Citado 2 vezes nas páginas 10 e 39.

HOR, K.; TAYLOR, M. Suicide and schizophrenia: a systematic review of rates and risk factors. *Journal of psychopharmacology*, Sage Publications Sage UK: London, England, v. 24, n. 4_suppl, p. 81–90, 2010. Citado 2 vezes nas páginas 24 e 35.

HORN, M. R. V.; SILD, M.; RUTHAZER, E. S. D-serine as a gliotransmitter and its roles in brain development and disease. *Frontiers in cellular neuroscience*, Frontiers, v. 7, p. 39, 2013. Citado 5 vezes nas páginas 39, 63, 65, 68 e 76.

HOWES, O.; MCCUTCHEON, R.; STONE, J. Glutamate and dopamine in schizophrenia: an update for the 21st century. *Journal of psychopharmacology*, Sage Publications Sage UK: London, England, v. 29, n. 2, p. 97–115, 2015. Citado 2 vezes nas páginas 35 e 94.

HUANG, D. W.; SHERMAN, B. T.; LEMPICKI, R. A. Bioinformatics enrichment tools: paths toward the comprehensive functional analysis of large gene lists. *Nucleic acids research*, Oxford University Press, v. 37, n. 1, p. 1–13, 2009. Citado na página 54.

_____. Systematic and integrative analysis of large gene lists using david bioinformatics resources. *Nature protocols*, Nature Publishing Group, v. 4, n. 1, p. 44–57, 2009. Citado na página 54.

HUANG, H.; YANG, T.; SHAO, Q.; MAJUMDER, T.; MELL, K.; LIU, G. Human tubb3 mutations disrupt netrin attractive signaling. *Neuroscience*, Elsevier, v. 374, p. 155–171, 2018. Citado 2 vezes nas páginas 75 e 86.

HUNTSMAN, M. M.; TRAN, B.-V.; POTKIN, S. G.; BUNNEY, W. E.; JONES, E. G. Altered ratios of alternatively spliced long and short $\gamma 2$ subunit mrnas of the γ-amino butyrate type a receptor in prefrontal cortex of schizophrenics. *Proceedings of the National Academy of Sciences*, National Acad Sciences, v. 95, n. 25, p. 15066–15071, 1998. Citado na página 64.

INCONTRO, S.; DÍAZ-ALONSO, J.; IAFRATI, J.; VIEIRA, M.; ASENSIO, C. S.; SOHAL, V. S.; ROCHE, K. W.; BENDER, K. J.; NICOLL, R. A. The camkii/nmda receptor complex controls hippocampal synaptic transmission by kinase-dependent and independent mechanisms. *Nature communications*, Nature Publishing Group, v. 9, n. 1, p. 1–21, 2018. Citado na página 45.

IRIE, F.; YAMAGUCHI, Y. Ephb receptors regulate dendritic spine development via intersectin, cdc42 and n-wasp. *Nature neuroscience*, Nature Publishing Group, v. 5, n. 11, p. 1117–1118, 2002. Citado na página 64.

IVANOV, A.; MUKHTAROV, M.; BREGESTOVSKI, P.; ZILBERTER, Y. Lactate effectively covers energy demands during neuronal network activity in neonatal hippocampal slices. *Frontiers in neuroenergetics*, Frontiers, v. 3, p. 2, 2011. Citado na página 87.

IWATA, K.; MATSUZAKI, H.; MANABE, T.; MORI, N. Altering the expression balance of hnrnp c1 and c2 changes the expression of myelination-related genes. *Psychiatry research*, Elsevier, v. 190, n. 2-3, p. 364–366, 2011. Citado na página 64.

JAARO-PELED, H.; AYHAN, Y.; PLETNIKOV, M. V.; SAWA, A. Review of pathological hallmarks of schizophrenia: comparison of genetic models with patients and nongenetic models. *Schizophrenia bulletin*, Oxford University Press, v. 36, n. 2, p. 301–313, 2010. Citado na página 25.

JAARO-PELED, H.; SAWA, A. Neurodevelopmental factors in schizophrenia. *Psychiatric Clinics*, Elsevier, v. 43, n. 2, p. 263–274, 2020. Citado 2 vezes nas páginas 36 e 37.

JARSKOG, L. F.; SELINGER, E. S.; LIEBERMAN, J. A.; GILMORE, J. H. Apoptotic proteins in the temporal cortex in schizophrenia: high bax/bcl-2 ratio without caspase-3 activation. *American Journal of Psychiatry*, Am Psychiatric Assoc, v. 161, n. 1, p. 109–115, 2004. Citado na página 87.

JASSAL, B.; MATTHEWS, L.; VITERI, G.; GONG, C.; LORENTE, P.; FABREGAT, A.; SIDIROPOULOS, K.; COOK, J.; GILLESPIE, M.; HAW, R. et al. The reactome pathway knowledgebase. *Nucleic acids research*, Oxford University Press, v. 48, n. D1, p. D498–D503, 2020. Citado na página 41.

JAVITT, D. C.; ZUKIN, S. R. Recent advances in the phencyclidine model of schizophrenia. *The American journal of psychiatry*, American Psychiatric Assn, 1991. Citado 3 vezes nas páginas 25, 63 e 68.

JENSEN, L. J.; KUHN, M.; STARK, M.; CHAFFRON, S.; CREEVEY, C.; MULLER, J.; DOERKS, T.; JULIEN, P.; ROTH, A.; SIMONOVIC, M. et al. String 8—a global view on proteins and their functional interactions in 630 organisms. *Nucleic acids research*, Oxford University Press, v. 37, n. suppl_1, p. D412–D416, 2009. Citado na página 31.

JESTE, S. S. Neurodevelopmental behavioral and cognitive disorders. *CONTINUUM: Lifelong Learning in Neurology*, LWW, v. 21, n. 3, p. 690–714, 2015. Citado na página 36.

JONGEN-RÊLO, A. L.; LENG, A.; LÜBER, M.; POTHUIZEN, H. H.; WEBER, L.; FELDON, J. The prenatal methylazoxymethanol acetate treatment: a neurodevelopmental animal model for schizophrenia? *Behavioural brain research*, Elsevier, v. 149, n. 2, p. 159–181, 2004. Citado na página 38.

KALAYDJIAN, A.; EATON, W.; CASCELLA, N.; FASANO, A. The gluten connection: the association between schizophrenia and celiac disease. *Acta Psychiatrica Scandinavica*, Wiley Online Library, v. 113, n. 2, p. 82–90, 2006. Citado na página 24.

KALUS, P.; MULLER, T. J.; ZUSCHRATTER, W.; SENITZ, D. The dendritic architecture of prefrontal pyramidal neurons in schizophrenic patients. *Neuroreport*, LWW, v. 11, n. 16, p. 3621–3625, 2000. Citado na página 45.

KANEHISA, M.; GOTO, S. Kegg: kyoto encyclopedia of genes and genomes. *Nucleic acids research*, Oxford University Press, v. 28, n. 1, p. 27–30, 2000. Citado 2 vezes nas páginas 31 e 41.

KANTROWITZ, J. T.; JAVITT, D. C. N-methyl-d-aspartate (nmda) receptor dysfunction or dysregulation: the final common pathway on the road to schizophrenia? *Brain research bulletin*, Elsevier, v. 83, n. 3-4, p. 108–121, 2010. Citado na página 25.

KAO, T.-J.; KANIA, A. Ephrin-mediated cis-attenuation of eph receptor signaling is essential for spinal motor axon guidance. *Neuron*, Elsevier, v. 71, n. 1, p. 76–91, 2011. Citado na página 62.

KARLSSON, H.; BACHMANN, S.; SCHRÖDER, J.; MCARTHUR, J.; TORREY, E. F.; YOLKEN, R. H. Retroviral rna identified in the cerebrospinal fluids and brains of individuals with schizophrenia. *Proceedings of the National Academy of Sciences*, National Acad Sciences, v. 98, n. 8, p. 4634–4639, 2001. Citado na página 36.

KATHURIA, A.; LOPEZ-LENGOWSKI, K.; JAGTAP, S. S.; MCPHIE, D.; PERLIS, R. H.; COHEN, B. M.; KARMACHARYA, R. Transcriptomic landscape and functional characterization of induced pluripotent stem cell–derived cerebral organoids in schizophrenia. *JAMA psychiatry*, American Medical Association, v. 77, n. 7, p. 745–754, 2020. Citado 2 vezes nas páginas 41 e 64.

KAYSER, M. S.; MCCLELLAND, A. C.; HUGHES, E. G.; DALVA, M. B. Intracellular and trans-synaptic regulation of glutamatergic synaptogenesis by ephb receptors. *Journal of Neuroscience*, Soc Neuroscience, v. 26, n. 47, p. 12152–12164, 2006. Citado 2 vezes nas páginas 62 e 63.

KELAVA, I.; LANCASTER, M. A. Stem cell models of human brain development. *Cell stem cell*, Elsevier, v. 18, n. 6, p. 736–748, 2016. Citado na página 50.

KETTENMANN, H. Chloride channels and carriers in cultured glial cells. In: *Chloride channels and carriers in nerve, muscle, and glial cells*. [S.l.]: Springer, 1990. p. 193–208. Citado na página 25.

KIM, H.; PARK, Y. J. Links between serine biosynthesis pathway and epigenetics in cancer metabolism. *Clinical nutrition research*, Korean Society of Clinical Nutrition, v. 7, n. 3, p. 153–160, 2018. Citado 2 vezes nas páginas 14 e 83.

KIROV, G.; O'DONOVAN, M. C.; OWEN, M. J. et al. Finding schizophrenia genes. *The Journal of clinical investigation*, Am Soc Clin Investig, v. 115, n. 6, p. 1440–1448, 2005. Citado na página 35.

KLEIN, R. Bidirectional modulation of synaptic functions by eph/ephrin signaling. *Nature neuroscience*, Nature Publishing Group, v. 12, n. 1, p. 15–20, 2009. Citado na página 62.

KOHANE, I. S.; MASYS, D. R.; ALTMAN, R. B. The incidentalome: a threat to genomic medicine. *Jama*, American Medical Association, v. 296, n. 2, p. 212–215, 2006. Citado na página 50.

KONIETZNY, A.; BÄR, J.; MIKHAYLOVA, M. Dendritic actin cytoskeleton: structure, functions, and regulations. *Frontiers in cellular neuroscience*, Frontiers, v. 11, p. 147, 2017. Citado na página 63.

KRYSTAL, J. H.; D'SOUZA, D. C.; MATHALON, D.; PERRY, E.; BELGER, A.; HOFFMAN, R. Nmda receptor antagonist effects, cortical glutamatergic function, and schizophrenia: toward a paradigm shift in medication development. *Psychopharmacology*, Springer, v. 169, n. 3, p. 215–233, 2003. Citado na página 38.

KRZYWINSKI, M.; SCHEIN, J.; BIROL, I.; CONNORS, J.; GASCOYNE, R.; HORSMAN, D.; JONES, S. J.; MARRA, M. A. Circos: an information aesthetic for comparative genomics. *Genome research*, Cold Spring Harbor Lab, v. 19, n. 9, p. 1639–1645, 2009. Citado na página 55.

KUHN, T. B.; MEBERG, P. J.; BROWN, M. D.; BERNSTEIN, B. W.; MINAMIDE, L. S.; JENSEN, J. R.; OKADA, K.; SODA, E. A.; BAMBURG, J. R. Regulating actin dynamics in neuronal growth cones by adf/cofilin and rho family gtpases. *Journal of neurobiology*, Wiley Online Library, v. 44, n. 2, p. 126–144, 2000. Citado na página 63.

LABRIE, V.; LIPINA, T.; RODER, J. C. Mice with reduced nmda receptor glycine affinity model some of the negative and cognitive symptoms of schizophrenia. *Psychopharmacology*, Springer, v. 200, n. 2, p. 217–230, 2008. Citado na página 65.

LAI, K.-O.; IP, N. Y. Synapse development and plasticity: roles of ephrin/eph receptor signaling. *Current opinion in neurobiology*, Elsevier, v. 19, n. 3, p. 275–283, 2009. Citado na página 62.

LALLI, P. M. et al. Mobilidade ionica acoplada a espectrometria de massas= interferencia de parametros do drift gas na resolução de anilinas substituidas e determinação da mobilidade intrinsica de agregados de liquidos ionicos. [sn], 2010. Citado na página 30.

LANCASTER, M. A.; KNOBLICH, J. A. Generation of cerebral organoids from human pluripotent stem cells. *Nature protocols*, Nature Publishing Group, v. 9, n. 10, p. 2329–2340, 2014. Citado na página 50.

LANCASTER, M. A.; RENNER, M.; MARTIN, C.-A.; WENZEL, D.; BICKNELL, L. S.; HURLES, M. E.; HOMFRAY, T.; PENNINGER, J. M.; JACKSON, A. P.; KNOBLICH, J. A. Cerebral organoids model human brain development and microcephaly. *Nature*, Nature Publishing Group, v. 501, n. 7467, p. 373–379, 2013. Citado na página 52.

LEGEAY, M.; DONCHEVA, N. T.; MORRIS, J. H.; JENSEN, L. J. Visualize omics data on networks with omics visualizer, a cytoscape app. *F1000Research*, Faculty of 1000 Ltd, v. 9, 2020. Citado na página 41.

LEVIN, Y.; HRADETZKY, E.; BAHN, S. Quantification of proteins using data-independent analysis (mse) in simple andcomplex samples: a systematic evaluation. *Proteomics*, Wiley Online Library, v. 11, n. 16, p. 3273–3287, 2011. Citado na página 30.

LEWIS, D. A.; GONZÁLEZ-BURGOS, G. Neuroplasticity of neocortical circuits in schizophrenia. *Neuropsychopharmacology*, Nature Publishing Group, v. 33, n. 1, p. 141–165, 2008. Citado 2 vezes nas páginas 38 e 47.

LEWIS, D. A.; LIEBERMAN, J. A. Catching up on schizophrenia: natural history and neurobiology. *Neuron*, Elsevier, v. 28, n. 2, p. 325–334, 2000. Citado 2 vezes nas páginas 23 e 26.

LI, J.; PELLETIER, M. R.; VELAZQUEZ, J.-L. P.; CARLEN, P. L. Reduced cortical synaptic plasticity and glur1 expression associated with fragile x mental retardation protein deficiency. *Molecular and Cellular Neuroscience*, Elsevier, v. 19, n. 2, p. 138–151, 2002. Citado na página 46.

LICHTENSTEIN, P.; YIP, B. H.; BJÖRK, C.; PAWITAN, Y.; CANNON, T. D.; SULLIVAN, P. F.; HULTMAN, C. M. Common genetic influences for schizophrenia and bipolar disorder: a population-based study of 2 million nuclear families. *Lancet*, NIH Public Access, v. 373, n. 9659, 2009. Citado na página 35.

LIDDELOW, S. A.; GUTTENPLAN, K. A.; CLARKE, L. E.; BENNETT, F. C.; BOHLEN, C. J.; SCHIRMER, L.; BENNETT, M. L.; MÜNCH, A. E.; CHUNG, W.-S.; PETERSON, T. C. et al. Neurotoxic reactive astrocytes are induced by activated microglia. *Nature*, Nature Publishing Group, v. 541, n. 7638, p. 481–487, 2017. Citado na página 86.

LIEBERMAN, J. A.; STROUP, T. S.; MCEVOY, J. P.; SWARTZ, M. S.; ROSENHECK, R. A.; PERKINS, D. O.; KEEFE, R. S.; DAVIS, S. M.; DAVIS, C. E.; LEBOWITZ, B. D. et al. Effectiveness of antipsychotic drugs in patients with chronic schizophrenia. *New England journal of medicine*, Mass Medical Soc, v. 353, n. 12, p. 1209–1223, 2005. Citado 2 vezes nas páginas 24 e 35.

LIN, C.-H.; LANE, H.-Y. Early identification and intervention of schizophrenia: insight from hypotheses of glutamate dysfunction and oxidative stress. *Frontiers in psychiatry*, Frontiers, v. 10, p. 93, 2019. Citado na página 43.

LUJÁN, R.; SHIGEMOTO, R.; LÓPEZ-BENDITO, G. Glutamate and gaba receptor signalling in the developing brain. *Neuroscience*, Elsevier, v. 130, n. 3, p. 567–580, 2005. Citado 2 vezes nas páginas 47 e 68.

MACKAY, M.-A. B.; KRAVTSENYUK, M.; THOMAS, R.; MITCHELL, N. D.; DURSUN, S. M.; BAKER, G. B. D-serine: potential therapeutic agent and/or biomarker in schizophrenia and depression? *Frontiers in psychiatry*, Frontiers, v. 10, p. 25, 2019. Citado na página 65.

MARCUS, S. C.; OLFSON, M. Outpatient antipsychotic treatment and inpatient costs of schizophrenia. *Schizophrenia bulletin*, Oxford University Press, v. 34, n. 1, p. 173–180, 2008. Citado na página 35.

MATOS, G.; GUARNIERO, F. B.; HALLAK, J. E.; BRESSAN, R. A. *Schizophrenia, the forgotten disorder: the scenario in Brazil*. [S.l.]: SciELO Brasil, 2015. Citado na página 35.

MAURER, I.; ZIERZ, S.; MÖLLER, H.-J. Evidence for a mitochondrial oxidative phosphorylation defect in brains from patients with schizophrenia. *Schizophrenia research*, Elsevier, v. 48, n. 1, p. 125–136, 2001. Citado 2 vezes nas páginas 64 e 65.

MAYNARD, T. M.; SIKICH, L.; LIEBERMAN, J. A.; LAMANTIA, A.-S. Neural development, cell-cell signaling, and the "two-hit" hypothesis of schizophrenia. *Schizophrenia bulletin*, Oxford University Press, v. 27, n. 3, p. 457–476, 2001. Citado na página 25.

MELDOLESI, J. Neurite outgrowth: this process, first discovered by santiago ramon y cajal, is sustained by the exocytosis of two distinct types of vesicles. *Brain research reviews*, Elsevier, v. 66, n. 1-2, p. 246–255, 2011. Citado na página 26.

MELDRUM, B. S. Glutamate as a neurotransmitter in the brain: review of physiology and pathology. *The Journal of nutrition*, Oxford University Press, v. 130, n. 4, p. 1007S–1015S, 2000. Citado na página 38.

MELTZER, H. Y.; STAHL, S. M. The dopamine hypothesis of schizophrenia: a review. *Schizophrenia bulletin*, National Institute of Mental Health, v. 2, n. 1, p. 19, 1976. Citado na página 25.

MIDDLETON, F. A.; PENG, L.; LEWIS, D. A.; LEVITT, P.; MIRNICS, K. Altered expression of 14-3-3 genes in the prefrontal cortex of subjects with schizophrenia. *Neuropsychopharmacology*, Nature Publishing Group, v. 30, n. 5, p. 974–983, 2005. Citado na página 63.

MIELNIK, C. A.; BINKO, M. A.; CHEN, Y.; FUNK, A. J.; JOHANSSON, E. M.; INTSON, K.; SIVANANTHAN, N.; ISLAM, R.; MILENKOVIC, M.; HORSFALL, W. et al. Consequences of nmda receptor deficiency can be rescued in the adult brain. *Molecular Psychiatry*, Nature Publishing Group, p. 1–14, 2020. Citado na página 43.

MOGHADDAM, B.; JAVITT, D. From revolution to evolution: the glutamate hypothesis of schizophrenia and its implication for treatment. *Neuropsychopharmacology*, Nature Publishing Group, v. 37, n. 1, p. 4–15, 2012. Citado 3 vezes nas páginas 25, 35 e 68.

MOLYNEAUX, B. J.; ARLOTTA, P.; MENEZES, J. R.; MACKLIS, J. D. Neuronal subtype specification in the cerebral cortex. *Nature reviews neuroscience*, Nature Publishing Group, v. 8, n. 6, p. 427–437, 2007. Citado 2 vezes nas páginas 37 e 68.

MORIKAWA, T.; MANABE, T. Aberrant regulation of alternative pre-mrna splicing in schizophrenia. *Neurochemistry international*, Elsevier, v. 57, n. 7, p. 691–704, 2010. Citado na página 64.

MORRISON, A. K. Cognitive behavior therapy for people with schizophrenia. *Psychiatry (Edgmont)*, Matrix Medical Communications, v. 6, n. 12, p. 32, 2009. Citado na página 24.

MOYER, C. E.; SHELTON, M. A.; SWEET, R. A. Dendritic spine alterations in schizophrenia. *Neuroscience letters*, Elsevier, v. 601, p. 46–53, 2015. Citado na página 62.

MULLARKY, E.; LUCKI, N. C.; ZAVAREH, R. B.; ANGLIN, J. L.; GOMES, A. P.; NICOLAY, B. N.; WONG, J. C.; CHRISTEN, S.; TAKAHASHI, H.; SINGH, P. K. et al. Identification of a small molecule inhibitor of 3-phosphoglycerate dehydrogenase to target serine biosynthesis in cancers. *Proceedings of the National Academy of Sciences*, National Acad Sciences, v. 113, n. 7, p. 1778–1783, 2016. Citado 2 vezes nas páginas 76 e 79.

MURATAKE, T.; HAYASHI, S.; ICHIKAWA, T.; KUMANISHI, T.; ICHIMURA, Y.; KUWANO, R.; ISOBE, T.; WANG, Y.; MINOSHIMA, S.; SHIMIZU, N. et al. Structural organization and chromosomal assignment of the human 14-3-3 η chain gene (ywhah). *Genomics*, Elsevier, v. 36, n. 1, p. 63–69, 1996. Citado na página 63.

MURRAY, R. M.; BHAVSAR, V.; TRIPOLI, G.; HOWES, O. 30 years on: how the neurodevelopmental hypothesis of schizophrenia morphed into the developmental risk factor model of psychosis. *Schizophrenia bulletin*, Oxford University Press, v. 43, n. 6, p. 1190–1196, 2017. Citado na página 35.

NASCIMENTO, J. M.; SAIA-CEREDA, V. M.; SARTORE, R. C.; COSTA, R. M. da; SCHITINE, C. S.; FREITAS, H. R.; MURGU, M.; REIS, R. A. de M.; REHEN, S. K.; SOUZA, D. Martins-de. Human cerebral organoids and fetal brain tissue share proteomic similarities. *Frontiers in cell and developmental biology*, Frontiers, v. 7, p. 303, 2019. Citado 3 vezes nas páginas 51, 56 e 89.

NEWCOMER, J. W.; FARBER, N. B.; JEVTOVIC-TODOROVIC, V.; SELKE, G.; MELSON, A. K.; HERSHEY, T.; CRAFT, S.; OLNEY, J. W. Ketamine-induced nmda receptor hypofunction as a model of memory impairment and psychosis. *Neuropsychopharmacology*, Elsevier, v. 20, n. 2, p. 106–118, 1999. Citado na página 38.

NIJHAWAN, D.; HONARPOUR, N.; WANG, X. Apoptosis in neural development and disease. *Annual review of neuroscience*, Annual Reviews 4139 El Camino Way, PO Box 10139, Palo Alto, CA 94303-0139, USA, v. 23, n. 1, p. 73–87, 2000. Citado na página 87.

NOWAKOWSKI, T. J.; BHADURI, A.; POLLEN, A. A.; ALVARADO, B.; MOSTAJO-RADJI, M. A.; LULLO, E. D.; HAEUSSLER, M.; SANDOVAL-ESPINOSA, C.; LIU, S. J.; VELMESHEV, D. et al. Spatiotemporal gene expression trajectories reveal developmental hierarchies of the human cortex. *Science*, American Association for the Advancement of Science, v. 358, n. 6368, p. 1318–1323, 2017. Citado 2 vezes nas páginas 75 e 76.

O'CONNELL, P.; WOODRUFF, P.; WRIGHT, I.; JONES, P.; MURRAY, R. Developmental insanity or dementia praecox: was the wrong concept adopted? *Schizophrenia research*, Elsevier, v. 23, n. 2, p. 97–106, 1997. Citado na página 36.

OLIVEIRA, G. Reis-de; ZUCCOLI, G.; FIORAMONTE, M.; SCHIMITT, A.; FALKAI, P.; ALMEIDA, V.; SOUZA, D. Martins-de. Digging deeper in the proteome of different regions from schizophrenia brains. *Journal of proteomics*, Elsevier, v. 223, p. 103814, 2020. Citado 3 vezes nas páginas 40, 68 e 76.

OWEN, M. J.; O'DONOVAN, M. C. Schizophrenia and the neurodevelopmental continuum: evidence from genomics. *World Psychiatry*, Wiley Online Library, v. 16, n. 3, p. 227–235, 2017. Citado na página 26.

OWEN, M. J.; O'DONOVAN, M. C.; THAPAR, A.; CRADDOCK, N. Neurodevelopmental hypothesis of schizophrenia. *The British journal of psychiatry*, Cambridge University Press, v. 198, n. 3, p. 173–175, 2011. Citado 3 vezes nas páginas 26, 36 e 62.

PARK, E.; IACCARINO, C.; LEE, J.; KWON, I.; BAIK, S. M.; KIM, M.; SEONG, J. Y.; SON, G. H.; BORRELLI, E.; KIM, K. Regulatory roles of heterogeneous nuclear ribonucleoprotein m and nova-1 protein in alternative splicing of dopamine d2 receptor pre-mrna. *Journal of Biological Chemistry*, ASBMB, v. 286, n. 28, p. 25301–25308, 2011. Citado na página 64.

PAULSON, L.; MARTIN, P.; PERSSON, A.; NILSSON, C. L.; LJUNG, E.; WESTMAN-BRINKMALM, A.; ERIKSSON, P. S.; BLENNOW, K.; DAVIDSSON, P. Comparative genome-and proteome analysis of cerebral cortex from mk-801-treated rats. *Journal of neuroscience research*, Wiley Online Library, v. 71, n. 4, p. 526–533, 2003. Citado na página 46.

PEDROSA, E.; SANDLER, V.; SHAH, A.; CARROLL, R.; CHANG, C.; ROCKOWITZ, S.; GUO, X.; ZHENG, D.; LACHMAN, H. M. Development of patient-specific neurons in schizophrenia using induced pluripotent stem cells. *Journal of neurogenetics*, Taylor & Francis, v. 25, n. 3, p. 88–103, 2011. Citado na página 50.

PERA, M. F.; REUBINOFF, B.; TROUNSON, A. Human embryonic stem cells. *Journal of cell science*, Company of Biologists The Company of Biologists, Bidder Building, 140 Cowley ..., v. 113, n. 1, p. 5–10, 2000. Citado na página 27.

PERI, L. D.; CRESCINI, A.; DESTE, G.; FUSAR-POLI, P.; SACCHETTI, E.; VITA, A. Brain structural abnormalities at the onset of schizophrenia and bipolar disorder: a meta-analysis of controlled magnetic resonance imaging studies. *Current pharmaceutical design*, Bentham Science Publishers, v. 18, n. 4, p. 486–494, 2012. Citado na página 36.

PINO, L. K.; SEARLE, B. C.; BOLLINGER, J. G.; NUNN, B.; MACLEAN, B.; MACCOSS, M. J. The skyline ecosystem: Informatics for quantitative mass spectrometry proteomics. *Mass spectrometry reviews*, Wiley Online Library, v. 39, n. 3, p. 229–244, 2020. Citado na página 73.

PITTENGER, C.; BLOCH, M. H.; WILLIAMS, K. Glutamate abnormalities in obsessive compulsive disorder: neurobiology, pathophysiology, and treatment. *Pharmacology & therapeutics*, Elsevier, v. 132, n. 3, p. 314–332, 2011. Citado na página 39.

POLAK, M.; HAYMAKER, W.; JOHNSON, J.; D'AMELIO, F. Neuroglia and their reactions. *Histology and histopathology of the nervous system*, Charles C. Thomas Publishing, v. 1, p. 363–480, 1982. Citado na página 26.

PRABAKARAN, S.; SWATTON, J.; RYAN, M.; HUFFAKER, S.; HUANG, J.-J.; GRIFFIN, J.; WAYLAND, M.; FREEMAN, T.; DUDBRIDGE, F.; LILLEY, K. et al. Mitochondrial dysfunction in schizophrenia: evidence for compromised brain metabolism and oxidative stress. *Molecular psychiatry*, Nature Publishing Group, v. 9, n. 7, p. 684–697, 2004. Citado na página 65.

QIAN, X.; NGUYEN, H. N.; SONG, M. M.; HADIONO, C.; OGDEN, S. C.; HAMMACK, C.; YAO, B.; HAMERSKY, G. R.; JACOB, F.; ZHONG, C. et al. Brain-region-specific organoids using mini-bioreactors for modeling zikv exposure. *Cell*, Elsevier, v. 165, n. 5, p. 1238–1254, 2016. Citado na página 50.

QUADRATO, G.; BROWN, J.; ARLOTTA, P. The promises and challenges of human brain organoids as models of neuropsychiatric disease. *Nature medicine*, Nature Publishing Group, v. 22, n. 11, p. 1220–1228, 2016. Citado na página 62.

RAPOPORT, J.; GIEDD, J.; GOGTAY, N. Neurodevelopmental model of schizophrenia: update 2012. *Molecular psychiatry*, Nature Publishing Group, v. 17, n. 12, p. 1228–1238, 2012. Citado 2 vezes nas páginas 35 e 94.

REEMST, K.; NOCTOR, S. C.; LUCASSEN, P. J.; HOL, E. M. The indispensable roles of microglia and astrocytes during brain development. *Frontiers in human neuroscience*, Frontiers, v. 10, p. 566, 2016. Citado na página 82.

RICE, M. W.; SMITH, K. L.; ROBERTS, R. C.; PEREZ-COSTAS, E.; MELENDEZ-FERRO, M. Assessment of cytochrome c oxidase dysfunction in the substantia nigra/ventral tegmental area in schizophrenia. *PLoS One*, Public Library of Science San Francisco, USA, v. 9, n. 6, p. e100054, 2014. Citado na página 65.

RIPKE, S.; NEALE, B. M.; CORVIN, A.; WALTERS, J. T.; FARH, K.-H.; HOLMANS, P. A.; LEE, P.; BULIK-SULLIVAN, B.; COLLIER, D. A.; HUANG, H. et al. Biological insights from 108 schizophrenia-associated genetic loci. *Nature*, Europe PMC Funders, v. 511, n. 7510, p. 421, 2014. Citado na página 37.

ROMANIELLO, R.; TONELLI, A.; ARRIGONI, F.; BASCHIROTTO, C.; TRIULZI, F.; BRESOLIN, N.; BASSI, M. T.; BORGATTI, R. A novel mutation in the β-tubulin gene tubb2b associated with complex malformation of cortical development and deficits in axonal guidance. *Developmental Medicine & Child Neurology*, Wiley Online Library, v. 54, n. 8, p. 765–769, 2012. Citado na página 45.

ROSENBERG, D.; ARTOUL, S.; SEGAL, A. C.; KOLODNEY, G.; RADZISHEVSKY, I.; DIKOPOLTSEV, E.; FOLTYN, V. N.; INOUE, R.; MORI, H.; BILLARD, J.-M. et al. Neuronal d-serine and glycine release via the asc-1 transporter regulates nmda receptor-dependent synaptic activity. *Journal of Neuroscience*, Soc Neuroscience, v. 33, n. 8, p. 3533–3544, 2013. Citado na página 38.

ROUACH, N.; KOULAKOFF, A.; ABUDARA, V.; WILLECKE, K.; GIAUME, C. Astroglial metabolic networks sustain hippocampal synaptic transmission. *science*, American Association for the Advancement of Science, v. 322, n. 5907, p. 1551–1555, 2008. Citado na página 26.

RUIZ, S.; BIRBAUMER, N.; SITARAM, R. Abnormal neural connectivity in schizophrenia and fmri-brain-computer interface as a potential therapeutic approach. *Frontiers in psychiatry*, Frontiers, v. 4, p. 17, 2013. Citado na página 27.

SADOCK, B. J.; SADOCK, V. A.; LEVIN, Z. *Kaplan and Sadock's study guide and self-examination review in psychiatry*. [S.l.]: Lippincott Williams & Wilkins, 2007. Citado na página 23.

SAIA-CEREDA, V. M.; CASSOLI, J. S.; SCHMITT, A.; FALKAI, P.; NASCIMENTO, J. M.; SOUZA, D. Martins-de. Proteomics of the corpus callosum unravel pivotal players in the dysfunction of cell signaling, structure, and myelination in schizophrenia brains. *European archives of psychiatry and clinical neuroscience*, Springer, v. 265, n. 7, p. 601–612, 2015. Citado 2 vezes nas páginas 45 e 63.

SAIA-CEREDA, V. M.; CASSOLI, J. S.; SCHMITT, A.; FALKAI, P.; SOUZA, D. Martins-de. Differential proteome and phosphoproteome may impact cell signaling in the corpus callosum of schizophrenia patients. *Schizophrenia research*, Elsevier, v. 177, n. 1-3, p. 70–77, 2016. Citado 2 vezes nas páginas 25 e 43.

SAIA-CEREDA, V. M.; CASSOLI, J. S.; SOUZA, D. Martins-de; NASCIMENTO, J. M. Psychiatric disorders biochemical pathways unraveled by human brain proteomics. *European archives of psychiatry and clinical neuroscience*, Springer, v. 267, n. 1, p. 3–17, 2017. Citado 4 vezes nas páginas 40, 41, 62 e 63.

SAIA-CEREDA, V. M.; SANTANA, A. G.; SCHMITT, A.; FALKAI, P.; SOUZA, D. Martins-de. The nuclear proteome of white and gray matter from schizophrenia postmortem brains. *Molecular neuropsychiatry*, Karger Publishers, v. 3, n. 1, p. 37–52, 2017. Citado na página 64.

SALEEM, S.; SHAUKAT, F.; GUL, A.; AROOJ, M.; MALIK, A. Potential role of amino acids in pathogenesis of schizophrenia. *International journal of health sciences*, Qassim University, v. 11, n. 3, p. 63, 2017. Citado na página 65.

SARTORE, R. C.; CARDOSO, S. C.; LAGES, Y. V.; PARAGUASSU, J. M.; STELLING, M. P.; COSTA, R. F. M. da; GUIMARAES, M. Z.; PEREZ, C. A.; REHEN, S. K. Trace elements during primordial plexiform network formation in human cerebral organoids. *PeerJ*, PeerJ Inc., v. 5, p. e2927, 2017. Citado 2 vezes nas páginas 52 e 56.

SCHAFER, D. P.; LEHRMAN, E. K.; STEVENS, B. The "quad-partite" synapse: Microglia-synapse interactions in the developing and mature cns. *Glia*, Wiley Online Library, v. 61, n. 1, p. 24–36, 2013. Citado na página 25.

SCHMIDT, M. J.; MIRNICS, K. Neurodevelopment, gaba system dysfunction, and schizophrenia. *Neuropsychopharmacology*, Nature Publishing Group, v. 40, n. 1, p. 190–206, 2015. Citado na página 50.

SEN, N.; CROSS, A. M.; LORENZI, P. L.; KHAN, J.; GRYDER, B. E.; KIM, S.; CAPLEN, N. J. Ews-fli1 reprograms the metabolism of ewing sarcoma cells via positive regulation of glutamine import and serine-glycine biosynthesis. *Molecular carcinogenesis*, Wiley Online Library, v. 57, n. 10, p. 1342–1357, 2018. Citado 2 vezes nas páginas 76 e 79.

SENSKY, T.; TURKINGTON, D.; KINGDON, D.; SCOTT, J. L.; SCOTT, J.; SIDDLE, R.; O'CARROLL, M.; BARNES, T. R. A randomized controlled trial of cognitive-behavioral therapy for persistent symptoms in schizophrenia resistant to medication. *Archives of general psychiatry*, American Medical Association, v. 57, n. 2, p. 165–172, 2000. Citado na página 24.

SILVA, J. C.; GORENSTEIN, M. V.; LI, G.-Z.; VISSERS, J. P.; GEROMANOS, S. J. Absolute quantification of proteins by lcmse: A virtue of parallel ms acquisition* s. *Molecular & Cellular Proteomics*, ASBMB, v. 5, n. 1, p. 144–156, 2006. Citado na página 30.

SINGH, S.; MURPHY, B.; O'REILLY, R. Involvement of gene–diet/drug interaction in dna methylation and its contribution to complex diseases: from cancer to schizophrenia. *Clinical genetics*, Wiley Online Library, v. 64, n. 6, p. 451–460, 2003. Citado na página 62.

SNYDER, M. A.; ADELMAN, A. E.; GAO, W.-J. Gestational methylazoxymethanol exposure leads to nmdar dysfunction in hippocampus during early development and lasting deficits in learning. *Neuropsychopharmacology*, Nature Publishing Group, v. 38, n. 2, p. 328–340, 2013. Citado na página 38.

SOCHACKI, J.; DEVALLE, S.; REIS, M.; MACIEL, R. de M.; PAULSEN, B. da S.; BRENTANI, H.; ABREU, P. S. Belmonte-de; REHEN, S. Generation of ips cell lines from schizophrenia patients using a non-integrative method. *Stem cell research*, Elsevier, v. 17, n. 1, p. 97–101, 2016. Citado na página 51.

SØRENSEN, H. J.; MORTENSEN, E. L.; SCHIFFMAN, J.; REINISCH, J. M.; MAEDA, J.; MEDNICK, S. A. Early developmental milestones and risk of schizophrenia: a 45-year follow-up of the copenhagen perinatal cohort. *Schizophrenia research*, Elsevier, v. 118, n. 1-3, p. 41–47, 2010. Citado na página 62.

SOUZA, D. Martins-de; GATTAZ, W. F.; SCHMITT, A.; MACCARRONE, G.; HUNYADI-GULYÁS, E.; EBERLIN, M. N.; SOUZA, G. H.; MARANGONI, S.; NOVELLO, J. C.; TURCK, C. W. et al. Proteomic analysis of dorsolateral prefrontal cortex indicates the involvement of cytoskeleton, oligodendrocyte, energy metabolism and new potential markers in schizophrenia. *Journal of psychiatric research*, Elsevier, v. 43, n. 11, p. 978–986, 2009. Citado na página 63.

STAHL, S. M. Beyond the dopamine hypothesis of schizophrenia to three neural networks of psychosis: dopamine, serotonin, and glutamate. *CNS spectrums*, Cambridge University Press, v. 23, n. 3, p. 187–191, 2018. Citado na página 47.

STARK, K. L.; XU, B.; BAGCHI, A.; LAI, W.-S.; LIU, H.; HSU, R.; WAN, X.; PAVLIDIS, P.; MILLS, A. A.; KARAYIORGOU, M. et al. Altered brain microrna biogenesis contributes to phenotypic deficits in a 22q11-deletion mouse model. *Nature genetics*, Nature Publishing Group, v. 40, n. 6, p. 751–760, 2008. Citado na página 63.

STEVENS, E. R.; ESGUERRA, M.; KIM, P. M.; NEWMAN, E. A.; SNYDER, S. H.; ZAHS, K. R.; MILLER, R. F. D-serine and serine racemase are present in the vertebrate retina and contribute to the physiological activation of nmda receptors. *Proceedings of the National Academy of Sciences*, National Acad Sciences, v. 100, n. 11, p. 6789–6794, 2003. Citado na página 43.

STIPURSKY, J.; SOUSA, V. O.; GOMES, F. C. A. et al. Neuron–astroglial interactions in cell-fate commitment and maturation in the central nervous system. *Neurochemical research*, Springer, v. 37, n. 11, p. 2402–2418, 2012. Citado na página 26.

SUBRAMANIAM, K.; LUKS, T. L.; FISHER, M.; SIMPSON, G. V.; NAGARAJAN, S.; VINOGRADOV, S. Computerized cognitive training restores neural activity within the reality monitoring network in schizophrenia. *Neuron*, Elsevier, v. 73, n. 4, p. 842–853, 2012. Citado na página 24.

SULLIVAN, P. F.; KENDLER, K. S.; NEALE, M. C. Schizophrenia as a complex trait: evidence from a meta-analysis of twin studies. *Archives of general psychiatry*, American Medical Association, v. 60, n. 12, p. 1187–1192, 2003. Citado na página 35.

TAI, S.; TURKINGTON, D. The evolution of cognitive behavior therapy for schizophrenia: current practice and recent developments. *Schizophrenia bulletin*, Oxford University Press, v. 35, n. 5, p. 865–873, 2009. Citado na página 24.

TAKEUCHI, S.; KATOH, H.; NEGISHI, M. Eph/ephrin reverse signalling induces axonal retraction through rhoa/rock pathway. *The Journal of Biochemistry*, Oxford University Press, v. 158, n. 3, p. 245–252, 2015. Citado na página 62.

TALAMINI, L.; KOCH, T.; HORST, G. T.; KORF, J. Methylazoxymethanol acetate-induced abnormalities in the entorhinal cortex of the rat; parallels with morphological findings in schizophrenia. *Brain research*, Elsevier, v. 789, n. 2, p. 293–306, 1998. Citado na página 38.

TANDON, R.; KESHAVAN, M. S.; NASRALLAH, H. A. Schizophrenia,"just the facts" what we know in 2008. 2. epidemiology and etiology. *Schizophrenia research*, Elsevier, v. 102, n. 1-3, p. 1–18, 2008. Citado na página 35.

TANDON, R.; NASRALLAH, H. A.; KESHAVAN, M. S. Schizophrenia,"just the facts" 5. treatment and prevention past, present, and future. *Schizophrenia research*, Elsevier, v. 122, n. 1-3, p. 1–23, 2010. Citado 2 vezes nas páginas 23 e 24.

TARABEUX, J.; KEBIR, O.; GAUTHIER, J.; HAMDAN, F.; XIONG, L.; PITON, A.; SPIEGELMAN, D.; HENRION, É.; MILLET, B.; FATHALLI, F. et al. Rare mutations in n-methyl-d-aspartate glutamate receptors in autism spectrum disorders and schizophrenia. *Translational psychiatry*, Nature Publishing Group, v. 1, n. 11, p. e55–e55, 2011. Citado na página 43.

THOMASON, M. E.; HECT, J. L.; WALLER, R.; CURTIN, P. Interactive relations between maternal prenatal stress, fetal brain connectivity, and gestational age at delivery. *Neuropsychopharmacology*, Nature Publishing Group, v. 46, n. 10, p. 1839–1847, 2021. Citado 2 vezes nas páginas 28 e 37.

THOMPSON, H.; ANDREWS, W.; PARNAVELAS, J. G.; ERSKINE, L. Robo2 is required for slit-mediated intraretinal axon guidance. *Developmental biology*, Elsevier, v. 335, n. 2, p. 418–426, 2009. Citado na página 86.

THOMSON, J. A.; ITSKOVITZ-ELDOR, J.; SHAPIRO, S. S.; WAKNITZ, M. A.; SWIERGIEL, J. J.; MARSHALL, V. S.; JONES, J. M. Embryonic stem cell lines derived from human blastocysts. *science*, American Association for the Advancement of Science, v. 282, n. 5391, p. 1145–1147, 1998. Citado na página 27.

TOPOL, A.; ZHU, S.; TRAN, N.; SIMONE, A.; FANG, G.; BRENNAND, K. J. Altered wnt signaling in human induced pluripotent stem cell neural progenitor cells derived from four schizophrenia patients. *Biological psychiatry*, Elsevier, v. 78, n. 6, p. e29–e34, 2015. Citado 6 vezes nas páginas 41, 43, 50, 51, 64 e 89.

TORREY, E. F. Epidemiological comparison of schizophrenia and bipolar disorder. *Schizophrenia Research*, Elsevier, v. 39, n. 2, p. 101–106, 1999. Citado na página 35.

TOYOOKA, K.; ASAMA, K.; WATANABE, Y.; MURATAKE, T.; TAKAHASHI, M.; SOMEYA, T.; NAWA, H. Decreased levels of brain-derived neurotrophic factor in serum of chronic schizophrenic patients. *Psychiatry research*, Elsevier, v. 110, n. 3, p. 249–257, 2002. Citado na página 63.

TRINDADE, P.; LOIOLA, E. C.; GASPAROTTO, J.; RIBEIRO, C. T.; CARDOZO, P. L.; DEVALLE, S.; SALERNO, J. A.; ORNELAS, I. M.; LEDUR, P. F.; RIBEIRO, F. M. et al. Short and long tnf-alpha exposure recapitulates canonical astrogliosis events in human-induced pluripotent stem cells-derived astrocytes. *Glia*, Wiley Online Library, v. 68, n. 7, p. 1396–1409, 2020. Citado na página 69.

TSAI, G.; YANG, P.; CHUNG, L.-C.; LANGE, N.; COYLE, J. T. D-serine added to antipsychotics for the treatment of schizophrenia. *Biological psychiatry*, Elsevier, v. 44, n. 11, p. 1081–1089, 1998. Citado na página 43.

TURNER, D. A.; ADAMSON, D. C. Neuronal-astrocyte metabolic interactions: understanding the transition into abnormal astrocytoma metabolism. *Journal of Neuropathology & Experimental Neurology*, American Association of Neuropathologists, Inc., v. 70, n. 3, p. 167–176, 2011. Citado 2 vezes nas páginas 87 e 89.

VANCAMPFORT, D.; FIRTH, J.; CORRELL, C. U.; SOLMI, M.; SISKIND, D.; HERT, M. D.; CARNEY, R.; KOYANAGI, A.; CARVALHO, A. F.; GAUGHRAN, F. et al. The impact of pharmacological and non-pharmacological interventions to improve physical health outcomes in people with schizophrenia: a meta-review of meta-analyses of randomized controlled trials. *World Psychiatry*, Wiley Online Library, v. 18, n. 1, p. 53–66, 2019. Citado na página 24.

VAWTER, M. P.; BARRETT, T.; CHEADLE, C.; SOKOLOV, B. P.; III, W. H. W.; DONOVAN, D. M.; WEBSTER, M.; FREED, W. J.; BECKER, K. G. Application of cdna microarrays to examine gene expression differences in schizophrenia. *Brain research bulletin*, Elsevier, v. 55, n. 5, p. 641–650, 2001. Citado na página 63.

VIBERG, H. Neonatal ontogeny and neurotoxic effect of decabrominated diphenyl ether (pbde 209) on levels of synaptophysin and tau. *International Journal of Developmental Neuroscience*, Elsevier, v. 27, n. 5, p. 423–429, 2009. Citado na página 45.

WALKER, E. F.; SAVOIE, T.; DAVIS, D. Neuromotor precursors of schizophrenia. *Schizophrenia bulletin*, Oxford University Press, v. 20, n. 3, p. 441–451, 1994. Citado na página 36.

WARD, A. J.; COOPER, T. A. The pathobiology of splicing. *The Journal of Pathology: A Journal of the Pathological Society of Great Britain and Ireland*, Wiley Online Library, v. 220, n. 2, p. 152–163, 2010. Citado na página 64.

WEICKERT, T. W.; GOLDBERG, T. E.; GOLD, J. M.; BIGELOW, L. B.; EGAN, M. F.; WEINBERGER, D. R. Cognitive impairments in patients with schizophrenia displaying preserved and compromised intellect. *Archives of general psychiatry*, American Medical Association, v. 57, n. 9, p. 907–913, 2000. Citado na página 35.

WIBLE, C. G.; ANDERSON, J.; SHENTON, M. E.; KRICUN, A.; HIRAYASU, Y.; TANAKA, S.; LEVITT, J. J.; O'DONNELL, B. F.; KIKINIS, R.; JOLESZ, F. A. et al. Prefrontal cortex, negative symptoms, and schizophrenia: an mri study. *Psychiatry Research: Neuroimaging*, Elsevier, v. 108, n. 2, p. 65–78, 2001. Citado na página 65.

WILKINS, M. R.; SANCHEZ, J.-C.; GOOLEY, A. A.; APPEL, R. D.; HUMPHERY-SMITH, I.; HOCHSTRASSER, D. F.; WILLIAMS, K. L. Progress with proteome projects: why all proteins expressed by a genome should be identified and how to do it. *Biotechnology and genetic engineering reviews*, Taylor & Francis, v. 13, n. 1, p. 19–50, 1996. Citado na página 28.

WILLARD, S. S.; KOOCHEKPOUR, S. Glutamate, glutamate receptors, and downstream signaling pathways. *International journal of biological sciences*, Ivyspring International Publisher, v. 9, n. 9, p. 948, 2013. Citado na página 39.

WOO, T.-U. W.; WALSH, J. P.; BENES, F. M. Density of glutamic acid decarboxylase 67 messenger rna–containingneurons that express the n-methyl-d-aspartatereceptor subunit nr2a in the anterior cingulate cortex in schizophreniaand bipolar disorder. *Archives of general psychiatry*, American Medical Association, v. 61, n. 7, p. 649–657, 2004. Citado na página 46.

WU, T.; HU, E.; XU, S.; CHEN, M.; GUO, P.; DAI, Z.; FENG, T.; ZHOU, L.; TANG, W.; ZHAN, L. et al. clusterprofiler 4.0: A universal enrichment tool for interpreting omics data. *The Innovation*, Elsevier, v. 2, n. 3, p. 100141, 2021. Citado na página 40.

XU, J.; ZHENG, Y.; LV, S.; KANG, J.; YU, Y.; HOU, K.; LI, Y.; CHI, G. Lactate promotes reactive astrogliosis and confers axon guidance potential to astrocytes under oxygen-glucose deprivation. *Neuroscience*, Elsevier, v. 442, p. 54–68, 2020. Citado na página 87.

XU, Y.; YUE, W.; SHUGART, Y. Y.; LI, S.; CAI, L.; LI, Q.; CHENG, Z.; WANG, G.; ZHOU, Z.; JIN, C. et al. Exploring transcription factors-micrornas co-regulation networks in schizophrenia. *Schizophrenia bulletin*, Oxford University Press US, v. 42, n. 4, p. 1037–1045, 2016. Citado na página 63.

YAMANAKA, S. Patient-specific pluripotent stem cells become even more accessible. *Cell Stem Cell*, Elsevier, v. 7, n. 1, p. 1–2, 2010. Citado na página 27.

YAMASAKI, M.; YAMADA, K.; FURUYA, S.; MITOMA, J.; HIRABAYASHI, Y.; WATANABE, M. 3-phosphoglycerate dehydrogenase, a key enzyme forl-serine biosynthesis, is preferentially expressed in the radial glia/astrocyte lineage and olfactory ensheathing glia in the mouse brain. *Journal of Neuroscience*, Soc Neuroscience, v. 21, n. 19, p. 7691–7704, 2001. Citado na página 76.

YAN, Y.; SHIN, S.; JHA, B. S.; LIU, Q.; SHENG, J.; LI, F.; ZHAN, M.; DAVIS, J.; BHARTI, K.; ZENG, X. et al. Efficient and rapid derivation of primitive neural stem cells and generation of brain subtype neurons from human pluripotent stem cells. *Stem cells translational medicine*, Wiley Online Library, v. 2, n. 11, p. 862–870, 2013. Citado na página 69.

YU, G.; HE, Q.-Y. Reactomepa: an r/bioconductor package for reactome pathway analysis and visualization. *Molecular BioSystems*, Royal Society of Chemistry, v. 12, n. 2, p. 477–479, 2016. Citado na página 40.

YU, G.; WANG, L.-G.; HAN, Y.; HE, Q.-Y. clusterprofiler: an r package for comparing biological themes among gene clusters. *Omics: a journal of integrative biology*, Mary Ann Liebert, Inc. 140 Huguenot Street, 3rd Floor New Rochelle, NY 10801 USA, v. 16, n. 5, p. 284–287, 2012. Citado na página 55.

YU, J.; THOMSON, J. A. Pluripotent stem cell lines. *Genes & development*, Cold Spring Harbor Lab, v. 22, n. 15, p. 1987–1997, 2008. Citado na página 27.

YUAN, X.-b.; JIN, M.; XU, X.; SONG, Y.-q.; WU, C.-p.; POO, M.-m.; DUAN, S. Signalling and crosstalk of rho gtpases in mediating axon guidance. *Nature cell biology*, Nature Publishing Group, v. 5, n. 1, p. 38–45, 2003. Citado na página 82.

ZHANG, B.; GUAN, F.; CHEN, G.; LIN, H.; ZHANG, T.; FENG, J.; LI, L.; FU, D. Common variants in slc1a2 and schizophrenia: Association and cognitive function in patients with schizophrenia and healthy individuals. *Schizophrenia Research*, Elsevier, v. 169, n. 1-3, p. 128–134, 2015. Citado na página 45.

ZHANG, J.; ZHOU, Y. 14-3-3 proteins in glutamatergic synapses. *Neural plasticity*, Hindawi, v. 2018, 2018. Citado na página 63.

ZHOU, Y.; DANBOLT, N. C. Glutamate as a neurotransmitter in the healthy brain. *Journal of neural transmission*, Springer, v. 121, n. 8, p. 799–817, 2014. Citado na página 38.

ZHOU, Y.; ZHOU, B.; PACHE, L.; CHANG, M.; KHODABAKHSHI, A. H.; TANASEICHUK, O.; BENNER, C.; CHANDA, S. K. Metascape provides a biologist-oriented resource for the analysis of systems-level datasets. *Nature communications*, Nature Publishing Group, v. 10, n. 1, p. 1–10, 2019. Citado 2 vezes nas páginas 55 e 73.

ZUCCOLI, G. S.; OLIVEIRA, G. Reis-de; GARBES, B.; FALKAI, P.; SCHMITT, A.; NAKAYA, H. I.; SOUZA, D. Martins-de. Linking proteomic alterations in schizophrenia hippocampus to nmdar hypofunction in human neurons and oligodendrocytes. *European Archives of Psychiatry and Clinical Neuroscience*, Springer, p. 1–8, 2021. Citado 2 vezes nas páginas 25 e 40.

Anexos

ANEXO A – Tabelas suplementares

Supplementary Table 1

Accession	gene name	brain region	Proteome reference (doi)
P31946	YWHAB	PCC ACC CC	10.1016/j.jprot.2020.103814 10.1016/j.jpsychires.2010.03.003 10.1007/s00406-015-0621-1
P62258	YWHAE	CN DLPC CC	10.1016/j.jprot.2020.103814 10.1002/pmic.200900015 10.1007/s00406-015-0621-1
Q04917	YWHAH	PCC CC ATL	10.1016/j.jprot.2020.103814 10.1007/s00406-015-0621-1 10.1007/s00702-008-0156-y
P61981	YWHAG	PCC CC ATL ACC	10.1016/j.jprot.2020.103814 10.1007/s00406-015-0621- 1 10.1002/prca.200700230 10.1007/s00702-008-0156-y 10.1016/j.jpsychires.2010.03.003
P63104	YWHAZ	PCC CC ATL ACC DFPC MDT IC	10.1016/j.jprot.2020.103814 10.1007/s00406-015-0621-1 10.1007/s00702-008-0156-y 10.1016/j.jpsychires.2010.03.003 10.1002/pmic.200900015 10.1002/prca.200700230 10.1016/j.jpsychires.2010.04.014 10.1002/pmic.200800416
P27348	YWHAQ	IC	10.1002/pmic.200800415
P48426	PIP4K2A	PCC ACC	10.1016/j.jprot.2020.103814 10.1038/mp.2014.63
P09543	CNP	PCC CN DLPC CC ATL	10.1016/j.jprot.2020.103814 10.1038/sj.mp.4001532 10.1007/s00406-015-0621-1 10.1007/s00702-008-0156-y
O95861	BPNT1	IC	10.1002/pmic.200800415
P46783	RPS10	PCC ATL	10.1016/j.jprot.2020.103814 10.1007/s00702-008-0156-y

Supplementary Table 1

Accession	**gene name**	**brain region**	**Proteome reference (doi)**
P62701	RPS4X	PCC CC	10.1016/j.jprot.2020.103814
			10.1007/s00406-015-0621-1
P10809	HSPD1	MDT	10.1016/j.jpsychires.2010.04.014
P05387	RPLP2	ACC	10.1038/mp.2014.63
P26373	RPL13	CER ATL	10.1016/j.jprot.2020.103814
			10.1007/s00702-008-0156-y
P84098	RPL19	ACC	10.1038/mp.2014.63
P62888	RPL30	PCC ACC	10.1016/j.jprot.2020.103814
			10.1038/mp.2014.63
O95336	PGLS	PCC CN DLPC	10.1016/j.jprot.2020.103814
			10.1038/sj.mp.4002098
Q9NYB9	ABI2	ACC	10.1038/mp.2014.63
P24752	ACAT1	PCC ACC	10.1016/j.jprot.2020.103814
			10.1038/mp.2014.63
Q9BWD1	ACAT2	ACC ACC	10.1038/sj.mp.4001806
			10.1038/mp.2014.63
P05386	RPLP1	ACC	10.1038/mp.2014.63
Q99798	ACO2	PCC DLPC DLPC	10.1016/j.jprot.2020.103814
		WA ACC	10.1016/j.jpsychires.2008.11.006
			10.1038/sj.mp.4001532
			10.1186/1471-244X-9-17
			10.1002/pmic.200500069
P02568	ACTA1	DLPC	10.1038/sj.mp.4001532
P03996	ACTA2	DLPC	10.1038/sj.mp.4001532
P04270	ACTC1	DLPC	10.1038/sj.mp.4001532
P02570	ACTB	DLPC CC	10.1038/sj.mp.4001532
			10.1002/prca.200700230
P60709	ACTB	IC ACC	10.1002/pmic.200800422
			10.1016/j.jpsychires.2010.03.003
P63261	ACTG1	ACC CC	10.1016/j.jpsychires.2010.03.003
			10.1002/prca.200700230
P02571	ACTG1	DLPC	10.1038/sj.mp.4001532
			10.1016/j.jpsychires.2008.11.006
O43707	ACTN4	PCC CER DLPC	10.1016/j.jprot.2020.103814
			10.1038/sj.mp.4001532
Q562P0	ACT	MDT	10.1016/j.jpsychires.2010.04.014

Supplementary Table 1

Accession	**gene name**	**brain region**	**Proteome reference (doi)**
P61158	ACTR3	ACC IC	10.1038/sj.mp.4001806 10.1002/p-mic.200800415
Q92747	ARPC1A	DLPC	10.1038/sj.mp.4001532
P61160	ACTR2	ACC	10.1038/mp.2014.63
O15143	ARPC1B	DLPC	10.1038/sj.mp.4001532
Q12979	ABR	ACC	10.1038/mp.2014.63
Q10567	AP1B1	PCC ACC	10.1016/j.jprot.2020.103814 10.1038/mp.2014.63
P63010	AP2B1	PCC ACC	10.1016/j.jprot.2020.103814 10.1038/mp.2014.63
P63010	AP2B1	PCC ACC	10.1016/j.jprot.2020.103814 10.1038/mp.2014.63
Q96CW1	AP2M1	PCC CN ACC	10.1016/j.jprot.2020.103814 10.1038/mp.2014.63
Q5JWF2	GNAS	PCC ACC	10.1016/j.jprot.2020.103814 10.1038/mp.2014.63
P00568	AK1	DLPC	10.1007/s00406-008-0847-2
Q01518	CAP1	PCC MDT	10.1016/j.jprot.2020.103814 10.1016/j.jpsychires.2010.04.014
P40123	CAP2	PCC ACC	10.1016/j.jprot.2020.103814 10.1038/mp.2014.63
P84077	ARF1	ACC	10.1038/sj.mp.4001806
P84085	ARF5	PCC ACC	10.1016/j.jprot.2020.103814 10.1038/mp.2014.63
P62330	ARF6	PCC ACC	10.1016/j.jprot.2020.103814 10.1038/mp.2014.63
Q8N6T3	ARFGAP1	ACC	10.1038/mp.2014.63
P16112	ACAN	ATL	10.1007/s00702-008-0156-y
O43572	AKAP10	CC	10.1007/s00406-015-0621-1
P30838	ALDH3A1	IC	10.1002/pmic.200800415
P00352	ALDH1A1	DLPC	10.1038/sj.mp.4001532
P05091	ALDH2	PCC ACC	10.1016/j.jprot.2020.103814 10.1016/j.jpsychires.2010.03.003
P04075	ALDOA	DLPC ACC CC	10.1038/sj.mp.4001532 10.1002/pmic.200500069 10.1007/s00406-015-0621-1 10.1016/j.jpsychires.2010.03.003

Supplementary Table 1

Accession	**gene name**	**brain region**	**Proteome reference (doi)**
P09972	ALDOC	DLPC ACC WA IC ATL	10.1016/j.jpsychires.2008.11.006 10.1038/sj.mp.4001532 10.1038/sj.mp.4001806 10.1002/pmic.200900015 10.1002/pmic.200800415 10.1007/s00702-008-0156-y 10.1186/1471-244X-9-17
P01011	SERPINA3	DLPC	10.1007/s00406-008-0847-2
P02511	CRYAB	PCC ACC CC	10.1016/j.jprot.2020.103814 10.1016/j.jpsychires.2010.03.003 10.1007/s00406-015-0621-1
P06733	ENO1	CC	10.1007/s00406-015-0621-1
P06733	ENO1	DLPC	10.1038/sj.mp.4001532
Q16352	INA	PCC CN IC CC ACC	10.1016/j.jprot.2020.103814 10.1002/pmic.200800415 10.1007/s00406-015-0621-1 10.1038/mp.2014.63
P54920	NAPA	ACC	10.1038/mp.2014.63
P37840	SNCA	ACC	10.1016/j.jpsychires.2010.03.003
P37840	SNCA	IC	10.1002/pmic.200800415
P49418	AMPH	ACC	10.1038/mp.2014.63
P49418	AMPH	DLPC	10.1002/pmic.200900015
Q01484	ANK2	PCC MDT	10.1016/j.jprot.2020.103814 10.1016/j.jpsychires.2010.04.014
P04083	ANXA1	ACC	10.1038/sj.mp.4001806
P08758	ANXA5	PCC ACC ACC	10.1016/j.jprot.2020.103814 10.1038/mp.2014.63 10.1038/sj.mp.4001806
P08758	ANXA5	PCC ACC ACC	10.1016/j.jprot.2020.103814 10.1038/mp.2014.63 10.1038/sj.mp.4001806
P08758	ANXA5	PCC CC	10.1016/j.jprot.2020.103814 10.1002/prca.200700230
P08758	ANXA5	PCC CC	10.1016/j.jprot.2020.103814 10.1002/prca.200700230
P20073	ANXA7	PCC ACC	10.1016/j.jprot.2020.103814 10.1038/mp.2014.63

Supplementary Table 1

Accession	**gene name**	**brain region**	**Proteome reference (doi)**
P02647	APOA1	PCC IC	10.1016/j.jprot.2020.103814
			10.1002/pmic.200800415
P02649	APOE	DLPC	10.1007/s00406-008-0847-2
P14868	DARS1	PCC ACC	10.1016/j.jprot.2020.103814
			10.1038/mp.2014.63
Q5VUB5	FAM171A1	ACC	10.1038/mp.2014.63
P25705	ATP5F1A	WA	10.1186/1471-244X-9-17
P25705	ATP5F1A	CC	10.1007/s00406-015-0621-1
P25705	ATP5F1A	DLPC	10.1016/j.jpsychires.2008.11.006
P06576	ATP5F1B	PCC ACC	10.1016/j.jprot.2020.103814
			10.1002/pmic.200500069
P06576	ATP5F1B	PCC CC	10.1016/j.jprot.2020.103814
			10.1002/prca.200700230
P36542	ATP5F1C	PCC IC	10.1016/j.jprot.2020.103814
			10.1002/pmic.200800415
P36542	ATP5F1C	PCC IC	10.1016/j.jprot.2020.103814
			10.1002/pmic.200800415
O75947	ATP5PD	PCC DLPC	10.1016/j.jprot.2020.103814
			10.1016/j.jpsychires.2008.11.006
Q4G1C1	ATP8A1	ACC	10.1038/mp.2014.63
P36543	ATP6V1E1	PCC DLPC	10.1016/j.jprot.2020.103814
			10.1038/sj.mp.4001532
P36543	ATP6V1E1	PCC DLPC	10.1016/j.jprot.2020.103814
			10.1038/sj.mp.4001532
Q93050	ATP6V0A1	CN ACC	10.1016/j.jprot.2020.103814
			10.1038/mp.2014.63
O00571	DDX3X	PCC ACC	10.1016/j.jprot.2020.103814
			10.1038/mp.2014.63
P17677	GAP43	ACC	10.1038/mp.2014.63
Q9H4G0	EPB41L1	PCC MDT	10.1016/j.jprot.2020.103814
			10.1016/j.jpsychires.2010.04.014
P25098	GRK2	ACC	10.1038/mp.2014.63
Q6ZP65	BICDL1	ACC	10.1038/mp.2014.63
P30043	BLVRB	PCC ACC	10.1016/j.jprot.2020.103814
			10.1038/sj.mp.4001806
P80723	BASP1	PCC DLPC	10.1016/j.jprot.2020.103814
			10.1038/sj.mp.4001532

Supplementary Table 1

Accession	**gene name**	**brain region**	**Proteome reference (doi)**
P80723	BASP1	PCC DLPC	10.1016/j.jprot.2020.103814 10.1038/sj.mp.4001532
Q9UQB8	BAIAP2	PCC ACC	10.1016/j.jprot.2020.103814 10.1038/mp.2014.63
Q9HCU9	BRMS1	WA	10.1186/1471-244X-9-17
Q16143	SNCB	CN IC	10.1016/j.jprot.2020.103814 10.1002/pmic.200800415
Q86YS7	C2CD5	ACC	10.1038/mp.2014.63
Q08209	PPP3CA	PCC ATL	10.1016/j.jprot.2020.103814 10.1007/s00702-008-0156-y
Q13554	CAMK2B	PCC ACC	10.1016/j.jprot.2020.103814 10.1038/mp.2014.63
Q13554	CAMK2B	PCC ACC	10.1016/j.jprot.2020.103814 10.1038/mp.2014.63
Q4G1A8	CAMK2D	ACC	10.1038/mp.2014.63
Q8WU40	CAMK2G	ACC	10.1038/mp.2014.63
P06703	S100A6	ACC	10.1038/mp.2014.63
P62158	CALM1	CC ATL ACC	10.1007/s00406-015-0621-1 10.1007/s00702-008-0156-y 10.1038/mp.2014.63
Q8NCB2	CAMKV	PCC ACC	10.1016/j.jprot.2020.103814 10.1038/mp.2014.63
P00915	CA1	PCC ACC	10.1016/j.jprot.2020.103814 10.1038/sj.mp.4001806 10.1002/pmic.200500069
P00918	CA2	ATL	10.1007/s00702-008-0156-y
P16152	CBR1	PCC MDT DLPC	10.1016/j.jprot.2020.103814 10.1016/j.jpsychires.2010.04.014 10.1038/sj.mp.4001532
O75828	CBR3	PCC DLPC	10.1016/j.jprot.2020.103814 10.1038/sj.mp.4001532
P21964	COMT	ACC	10.1038/mp.2014.63
Q9UQB3	CTNND2	ACC	10.1038/mp.2014.63
P07339	CTSD	CC	10.1002/prca.200700230
Q86WG3	ATCAY	DLPC	10.1007/s00406-008-0847-2
O95674	CDS2	ACC	10.1038/mp.2014.63
Q8N126	CADM3	DLPC	10.1007/s00406-008-0847-2

Supplementary Table 1

Accession	**gene name**	**brain region**	**Proteome reference (doi)**
Q00535	CDK5	PCC ACC	10.1016/j.jprot.2020.103814 10.1038/mp.2014.63
P61163	ACTR1A	CC	10.1002/prca.200700230
A0A024R702	CGI-38	DLPC	10.1007/s00406-008-0847-2
P49368	CCT3	PCC DLPC IC	10.1016/j.jprot.2020.103814 10.1007/s00406-008-0847-2 10.1002/pmic.200800415
A0A024RDL1	CCT6A	ACC	10.1038/mp.2014.63
Q96F85	CNRIP1	PCC ACC DLPC	10.1016/j.jprot.2020.103814 10.1038/sj.mp.4001808 10.1038/sj.mp.4002098
Q96F85	CNRIP1	PCC ACC DLPC	10.1016/j.jprot.2020.103814 10.1038/sj.mp.4001808 10.1038/sj.mp.4002098
O75390	CS	ACC	10.1038/sj.mp.4001806
Q00610	CLTC	PCC CC	10.1016/j.jprot.2020.103814 10.1007/s00406-015-0621-1
P09497	CLTB	ATL	10.1007/s00702-008-0156-y
Q14019	COTL1	CC	10.1002/prca.200700230
P23528	CFL1	CER DLPC MDT	10.1016/j.jprot.2020.103814 10.1016/j.jpsychires.2008.11.006 10.1016/j.jpsychires.2010.04.014
A4D1N4	CHCHD3	ACC	10.1038/mp.2014.63
Q14194	CRMP1	PCC DLPC ACC	10.1016/j.jprot.2020.103814 10.1038/sj.mp.4001532 10.1038/sj.mp.4001806 10.1002/pmic.200500069
Q14194	CRMP1	PCC DLPC ACC	10.1016/j.jprot.2020.103814 10.1038/sj.mp.4001532 10.1038/sj.mp.4001806 10.1002/pmic.200500069
Q12860	CNTN1	PCC ACC	10.1016/j.jprot.2020.103814 10.1038/mp.2014.63
Q9BT78	COPS4	IC	10.1002/pmic.200800415
P31146	CORO1A	IC	10.1002/pmic.200800415

Supplementary Table 1

Accession	**gene name**	**brain region**	**Proteome reference (doi)**
P12277	CKB	PCC ACC DLPC CC WA	10.1016/j.jprot.2020.103814 10.1038/sj.mp.4001806 10.1002/pmic.200500069 10.1007/s00406-008-0847-2 10.1002/prca.200700230 10.1186/1471-244X-9-17 10.1038/sj.mp.4001532
P12532	CKMT1A	PCC ACC	10.1016/j.jprot.2020.103814 10.1038/sj.mp.4001806
Q13363	CTBP1	PCC IC	10.1016/j.jprot.2020.103814 10.1002/pmic.200800415
Q5T2Q4	CCNYL2	ACC	10.1038/mp.2014.63
P30085	CMPK1	PCC ACC	10.1016/j.jprot.2020.103814 10.1038/mp.2014.63
P00403	MT-CO2	PCC ACC MDT	10.1016/j.jprot.2020.103814 10.1038/mp.2014.63 10.1016/j.jpsychires.2010.04.014
Q14204	DYNC1H1	ACC	10.1038/mp.2014.63
Q96F07	CYFIP2	ACC	10.1038/mp.2014.63
P30038	ALDH4A1	PCC CC	10.1016/j.jprot.2020.103814 10.1007/s00406-015-0621-1
Q08495	DMTN	ACC	10.1038/mp.2014.63
P60981	DSTN	ACC	10.1038/mp.2014.63
P09622	DLD	PCC WA	10.1016/j.jprot.2020.103814 10.1186/1471-244X-9-17
P09622	DLD	PCC WA	10.1016/j.jprot.2020.103814 10.1186/1471-244X-9-17
P09417	QDPR	PCC WA MDT DLPC	10.1016/j.jprot.2020.103814 10.1186/1471-244X-9-17 10.1016/j.jpsychires.2010.04.014 10.1038/sj.mp.4001532
P09417	QDPR	PCC WA MDT DLPC	10.1016/j.jprot.2020.103814 10.1186/1471-244X-9-17 10.1016/j.jpsychires.2010.04.014 10.1038/sj.mp.4001532

Supplementary Table 1

Accession	**gene name**	**brain region**	**Proteome reference (doi)**
Q16555	DPYSL2	PCC ACC WA DLPC CC FC ACC IC	10.1016/j.jprot.2020.103814 10.1038/sj.mp.4001806 10.1186/1471-244X-9-17 10.1038/sj.mp.4001532 10.1016/j.jpsychires.2008.11.006 10.1002/prca.200700230 10.1038/sj.mp.4000696 10.1016/j.jpsychires.2010.03.003 10.1038/mp.2014.63 10.1002/pmic.200800418
O14531	DPYSL4	PCC DLPC	10.1016/j.jprot.2020.103814 10.1038/sj.mp.4001532
Q9BPU6	DPYSL5	PCC DLPC	10.1016/j.jprot.2020.103814 10.1002/pmic.200900015 10.1038/sj.mp.4001532
O94760	DDAH1	ACC CC	10.1038/sj.mp.4001806 10.1016/j.jpsychires.2010.03.003 10.1002/prca.200700230
Q99497	PARK7	CC	10.1002/prca.200700230
Q9UBZ4	APEX2	PCC DLPC	10.1016/j.jprot.2020.103814 10.1007/s00406-008-0847-2
L0N9S0	DNAJC6	DLPC	10.1007/s00406-008-0847-2
Q13561	DCTN2	ACC	10.1038/mp.2014.63 10.1038/sj.mp.4001806
Q05193	DNM1	PCC DLPC ACC	10.1016/j.jprot.2020.103814 10.1016/j.jpsychires.2008.11.006 10.1038/sj.mp.4002098 10.1038/sj.mp.4001532 10.1038/sj.mp.4001806 10.1038/mp.2014.63
P50570	DNM2	CN DLPC	10.1016/j.jprot.2020.103814 10.1038/sj.mp.4001532
Q6UWR7	ENPP6	PCC CC	10.1016/j.jprot.2020.103814 10.1007/s00406-015-0621-1
Q6UWR7	ENPP6	PCC CC	10.1016/j.jprot.2020.103814 10.1007/s00406-015-0621-1

Supplementary Table 1

Accession	**gene name**	**brain region**	**Proteome reference (doi)**
Q96C19	EFHD2	MDT DLPC	10.1016/j.jpsychires.2010.04.014
			10.1007/s00406-008-0847-2
Q9NZN4	EHD2	PCC DLPC	10.1016/j.jprot.2020.103814
			10.1038/sj.mp.4001532
Q9NZN3	EHD3	CER ACC	10.1016/j.jprot.2020.103814
			10.1038/sj.mp.4001806
Q9NZN3	EHD3	PCC ACC	10.1016/j.jprot.2020.103814
			10.1038/sj.mp.4001806
P30040	ERP29	DLPC	10.1038/sj.mp.4002098
P09104	ENO2	DLPC WA CC	10.1038/sj.mp.4001532
			10.1002/prca.200700230
			10.1038/sj.mp.4002098
			10.1186/1471-244X-9-17
			10.1007/s00406-015-0621-1
Q9BTI6	FLOT2	ACC	10.1038/mp.2014.63
O75477	ERLIN1	MDT	10.1016/j.jpsychires.2010.04.014
Q8TAM6	ERMN	DLPC ATL	10.1007/s00406-008-0847-2
			10.1007/s00702-008-0156-y
P10768	ESD	PCC DLPC	10.1016/j.jprot.2020.103814
			10.1038/sj.mp.4001532
Q14240	EIF4A2	ACC ATL	10.1038/mp.2014.63
			10.1007/s00702-008-0156-y
Q05639	EEF1A2	PCC CER ACC	10.1016/j.jprot.2020.103814
			10.1038/mp.2014.63
O00303	EIF3F	PCC IC	10.1016/j.jprot.2020.103814
			10.1002/pmic.200800415
Q6PKD5	RPH3A	ACC	10.1038/mp.2014.63
Q9BSJ8	ESYT1	ACC	10.1038/mp.2014.63
A0FGR8	ESYT2	ACC	10.1038/mp.2014.63
O14745	SLC9A3R1	PCC ATL	10.1016/j.jprot.2020.103814
			10.1007/s00702-008-0156-y
Q96AE4	FUBP1	DLPC	10.1007/s00406-008-0847-2
Q16658	FSCN1	DLPC CC	10.1038/sj.mp.4001532
			10.1007/s00406-015-0621-1
P05413	FABP3	CC	10.1002/prca.200700230
P02794	FTH1	PCC CC	10.1016/j.jprot.2020.103814
			10.1002/prca.200700230

Supplementary Table 1

Accession	**gene name**	**brain region**	**Proteome reference (doi)**
P02792	FTL	PCC MDT ACC CC	10.1016/j.jprot.2020.103814 10.1016/j.jpsychires.2010.04.014 10.1016/j.jpsychires.2010.03.003 10.1007/s00406-015-0621-1
P02792	FTL	PCC MDT ACC CC	10.1016/j.jprot.2020.103814 10.1016/j.jpsychires.2010.04.014 10.1016/j.jpsychires.2010.03.003 10.1007/s00406-015-0621-1
Q02790	FKBP4	PCC IC	10.1016/j.jprot.2020.103814 10.1002/pmic.200800415
Q13642	FHL1	ACC	10.1038/mp.2014.63
P09382	LGALS1	PCC DLPC	10.1016/j.jprot.2020.103814 10.1002/pmic.200900015
Q9BXF6	RAB11FIP5	ACC	10.1038/mp.2014.63
P17302	GJA1	ACC	10.1038/mp.2014.63
P06396	GSN	PCC CC DLPC	10.1016/j.jprot.2020.103814 10.1007/s00406-015-0621-1 10.1038/sj.mp.4001532
P06396	GSN	PCC CC DLPC	10.1016/j.jprot.2020.103814 10.1007/s00406-015-0621-1 10.1038/sj.mp.4001532
P14136	GFAP	PCC MDT DLPC CC ACC IC FC WA DLPC ATL	10.1016/j.jprot.2020.103814 10.1016/j.jpsychires.2010.04.014 10.1016/j.jpsychires.2008.11.006 10.1002/prca.200700230 10.1038/sj.mp.4001806 10.1002/pmic.200800415 10.1038/sj.mp.4000698 10.1186/1471-244X-9-17 10.1038/sj.mp.4002098 10.1007/s00702-008-0156-y
P30101	PDIA3	PCC DLPC	10.1016/j.jprot.2020.103814 10.1038/sj.mp.4001532
P00367	GLUD1	PCC ACC CC	10.1016/j.jprot.2020.103814 10.1002/pmic.200500069 10.1007/s00406-015-0621-1

Supplementary Table 1

Accession	**gene name**	**brain region**	**Proteome reference (doi)**
P00367	GLUD1	PCC ACC CC	10.1016/j.jprot.2020.103814 10.1002/pmic.200500069 10.1007/s00406-015-0621-1
P42262	GRIA2	ACC	10.1038/mp.2014.63
P15104	GLUL	PCC DLPC MDT ACC	10.1016/j.jprot.2020.103814 10.1038/sj.mp.4001532 10.1016/j.jpsychires.2010.04.014 10.1002/pmic.200500069
P15104	GLUL	PCC DLPC MDT ACC	10.1016/j.jprot.2020.103814 10.1038/sj.mp.4001532 10.1016/j.jpsychires.2010.04.014 10.1002/pmic.200500069
P09211	GSTP1	CC MDT	10.1002/prca.200700230 10.1016/j.jpsychires.2010.04.014
P78417	GSTO1	PCC DLPC	10.1016/j.jprot.2020.103814 10.1038/sj.mp.4001532
P21266	GSTM3	PCC DLPC	10.1016/j.jprot.2020.103814 10.1038/sj.mp.4001532
P04406	GAPDH	PCC MDT CC WA DLPC	10.1016/j.jprot.2020.103814 10.1016/j.jpsychires.2010.04.014 10.1007/s00406-015-0621-1 10.1186/1471-244X-9-17 10.1038/sj.mp.4001532
P11216	PYGB	PCC MDT CC	10.1016/j.jprot.2020.103814 10.1016/j.jpsychires.2010.04.014 10.1007/s00406-015-0621-1
P11217	PYGM	PCC CC	10.1016/j.jprot.2020.103814 10.1007/s00406-015-0621-1
Q9NZD2	GLTP	DLPC	10.1038/sj.mp.4001532
O76070	SNCG	IC	10.1002/pmic.200800415
Q9Y2T3	GDA	PCC MDT DLPC IC	10.1016/j.jprot.2020.103814 10.1016/j.jpsychires.2010.04.014 10.1038/sj.mp.4002098 10.1002/pmic.200800415

Supplementary Table 1

Accession	**gene name**	**brain region**	**Proteome reference (doi)**
P62873	GNB1	DLPC ACC CC	10.1016/j.jpsychires.2008.11.006
			10.1038/sj.mp.4001806
			10.1002/pmic.200500069
			10.1007/s00406-015-0621-1
			10.1016/j.jpsychires.2010.03.003
P62879	GNB2	ACC	10.1016/j.jpsychires.2010.03.003
P0DMV8	HSPA1A	DLPC MDT	10.1007/s00406-008-0847-2
			10.1016/j.jpsychires.2010.04.014
P11021	HSPA5	PCC ACC CC DLPC	10.1016/j.jprot.2020.103814
			10.1038/mp.2014.63
			10.1002/prca.200700230
			10.1038/sj.mp.4001532,10.1007/s00406-008-0847-2
P17066	HSPA6	PCC CC ACC	10.1016/j.jprot.2020.103814
			10.1007/s00406-015-0621-1
			10.1038/mp.2014.63
P17066	HSPA6	PCC CC ACC	10.1016/j.jprot.2020.103814
			10.1007/s00406-015-0621-1
			10.1038/mp.2014.63
P11142	HSPA8	DLPC CC MDT IC ACC	10.1016/j.jpsychires.2008.11.006
			10.1038/sj.mp.4001532
			10.1002/prca.200700230
			10.1016/j.jpsychires.2010.04.014
			10.1002/p-mic.200800415,10.1038/mp.2014.63
P34931	HSPA1L	CER DLPC CC	10.1016/j.jprot.2020.103814
			10.1038/sj.mp.4001532
			10.1002/prca.200700230
P08107	HSPA1A	DLPC ACC	10.1038/sj.mp.4001532
			10.1038/sj.mp.4001806
P07900	HSP90AA1	DLPC	10.1016/j.jpsychires.2008.11.006
P04792	HSPB1	PCC ACC	10.1016/j.jprot.2020.103814
			10.1038/mp.2014.63
P54652	HSPA2	PCC DLPC	10.1016/j.jprot.2020.103814
			10.1038/sj.mp.4001532
P54652	HSPA2	PCC DLPC	10.1016/j.jprot.2020.103814
			10.1038/sj.mp.4001532

Supplementary Table 1

Accession	**gene name**	**brain region**	**Proteome reference (doi)**
Q9NRV9	HEBP1	PCC CC	10.1016/j.jprot.2020.103814
			10.1002/prca.200700230
P68871	HBB	PCC DLPC CC ATL	10.1016/j.jprot.2020.103814
			10.1007/s00406-008-0847-2
			10.1007/s00406-015-0621-1
			10.1007/s00702-008-0156-y
P02042	HBD	CC	10.1007/s00406-015-0621-1
Q14CZ8	HEPACAM	ACC	10.1038/mp.2014.63
Q5SSJ5	HP1BP3	PCC DLPC	10.1016/j.jprot.2020.103814
			10.1007/s00406-008-0847-2
Q13151	HNRNPA0	DLPC	10.1007/s00406-008-0847-2
P51991	HNRNPA3	PCC ACC	10.1016/j.jprot.2020.103814
			10.1038/mp.2014.63
P61978	HNRNPK	ACC DLPC IC	10.1038/mp.2014.63
			10.1007/s00406-008-0847-2
			10.1002/pmic.200800415
Q00839	HNRNPU	PCC DLPC ACC	10.1016/j.jprot.2020.103814
			10.1007/s00406-008-0847-2
			10.1038/mp.2014.63
Q00839	HNRNPU	PCC DLPC ACC	10.1016/j.jprot.2020.103814
			10.1007/s00406-008-0847-2
			10.1038/mp.2014.63
P22626	HNRNPA2B1	PCC MDT	10.1016/j.jprot.2020.103814
			10.1016/j.jpsychires.2010.04.014
P07910	HNRNPC	WA ACC	10.1186/1471-244X-9-17
			10.1038/mp.2014.63
P19367	HK1	PCC ACC DLPC ATL	10.1016/j.jprot.2020.103814
			10.1038/mp.2014.63
			10.1038/sj.mp.4001532
			10.1007/s00702-008-0156-y
P49773	HINT1	CC	10.1007/s00406-015-0621-1
Q4VB24	HIST1H1E	ACC	10.1038/mp.2014.63
K7EK07	H3-3B	ACC	10.1038/mp.2014.63
P68431	H3C1	PCC ATL	10.1016/j.jprot.2020.103814
			10.1007/s00702-008-0156-y
Q6NXT2	H3-5	CC	10.1007/s00406-015-0621-1

Supplementary Table 1

Accession	**gene name**	**brain region**	**Proteome reference (doi)**
P62805	H4-16	PCC CC	10.1016/j.jprot.2020.103814
			10.1007/s00406-015-0621-1
Q5T3J1	HAPLN2	CC ATL	10.1007/s00406-015-0621-1
			10.1007/s00702-008-0156-y
Q16775	HAGH	ACC	10.1038/sj.mp.4001806
A2N192	IGH@	MDT	10.1016/j.jpsychires.2010.04.014
Q969P0	IGSF8	PCC DLPC	10.1016/j.jprot.2020.103814
			10.1002/pmic.200900015
P12268	IMPDH2	DLPC	10.1002/pmic.200900015
P29218	IMPA1	PCC DLPC	10.1016/j.jprot.2020.103814
			10.1002/pmic.200900015
Q96PE3	INPP4A	ACC	10.1038/mp.2014.63
P50213	IDH3A	ACC	10.1038/sj.mp.4001806
P48735	IDH2	PCC ACC	10.1016/j.jprot.2020.103814
			10.1038/mp.2014.63
P41252	IARS1	ACC	10.1038/mp.2014.63
Q14894	CRYM	PCC DLPC CC	10.1016/j.jprot.2020.103814
		MDT	10.1007/s00406-008-0847-2
			10.1016/j.jpsychires.2008.11.006
			10.1002/prca.200700230
			10.1016/j.jpsychires.2010.04.014
Q7Z2J9	L1CAM	DLPC	10.1007/s00406-008-0847-2
Q9Y2S2	CRYL1	CC	10.1007/s00406-015-0621-1
Q68FQ9	Lancl2	DLPC	10.1007/s00406-008-0847-2
P28838	LAP3	PCC DLPC	10.1016/j.jprot.2020.103814
			10.1038/sj.mp.4001532
P42704	LRPPRC	ACC	10.1038/mp.2014.63
P07195	LDHB	PCC CC	10.1016/j.jprot.2020.103814
			10.1002/prca.200700230
P36776	LONP1	PCC ACC	10.1016/j.jprot.2020.103814
			10.1038/mp.2014.63
P36776	LONP1	PCC ACC	10.1016/j.jprot.2020.103814
			10.1038/mp.2014.63
O95573	ACSL3	ACC	10.1038/mp.2014.63
P14174	MIF	CER CC	10.1016/j.jprot.2020.103814
			10.1007/s00406-015-0621-1

Supplementary Table 1

Accession	**gene name**	**brain region**	**Proteome reference (doi)**
P40925	MDH1	PCC DLPC CC	10.1016/j.jprot.2020.103814
			10.1016/j.jpsychires.2008.11.006
			10.1038/sj.mp.4001532
			10.1007/s00406-015-0621-1
P40926	MDH2	PCC ACC	10.1016/j.jprot.2020.103814
			10.1002/pmic.200500069
Q16798	ME3	MDT	10.1016/j.jpsychires.2010.04.014
O14910	LIN7A	ACC	10.1038/mp.2014.63
A0A024R652	MTHFD1	ACC	10.1038/mp.2014.63
Q9H8H3	METTL7A	ACC	10.1038/mp.2014.63
Q96PK2	MACF1	WA	10.1186/1471-244X-9-17
P78559	MAP1A	MDT	10.1016/j.jpsychires.2010.04.014
P11137	MAP2	PCC ACC	10.1016/j.jprot.2020.103814
			10.1038/mp.2014.63
Q15555	MAPRE2	PCC ACC	10.1016/j.jprot.2020.103814
			10.1038/mp.2014.63
Q9UPY8	MAPRE3	ACC	10.1038/mp.2014.63
P10636	MAPT	MDT	10.1016/j.jpsychires.2010.04.014
Q9Y6C9	MTCH2	PCC ACC	10.1016/j.jprot.2020.103814
			10.1038/mp.2014.63
Q16891	IMMT	ACC	10.1038/sj.mp.4001807
			10.1038/mp.2014.63
P27361	MAPK3	ACC	10.1038/mp.2014.63
P26038	MSN	PCC DLPC	10.1016/j.jprot.2020.103814
			10.1038/sj.mp.4001532
Q9UPW8	UNC13A	ACC	10.1038/mp.2014.63
P02686	MBP	PCC MDT DLPC	10.1016/j.jprot.2020.103814
		CC ATL	10.1016/j.jpsychires.2010.04.014
			10.1016/j.jpsychires.2008.11.006
			10.1007/s00406-015-0621-1
			10.1007/s00702-008-0156-y
Q16653	MOG	PCC MDT DLPC	10.1016/j.jprot.2020.103814
		ATL CC	10.1016/j.jpsychires.2010.04.014
			10.1007/s00406-008-0847-2
			10.1007/s00702-008-0156-y
			10.1007/s00406-015-0621-1
P60201	PLP1	DLPC	10.1002/pmic.200900015

Supplementary Table 1

Accession	**gene name**	**brain region**	**Proteome reference (doi)**
Q4G140	MYH11	ACC	10.1038/mp.2014.63
P60660	MYL6	ACC	10.1038/mp.2014.63
P46459	NSF	PCC DLPC ACC	10.1016/j.jprot.2020.103814
			10.1038/sj.mp.4001532
			10.1038/sj.mp.4001806
Q8N1C4	NDUFS1	DLPC	10.1038/sj.mp.4001532
Q6IB76	NDUFV2	ATL	10.1007/s00702-008-0156-y
Q6IBA0	NDUFS5	ACC	10.1038/mp.2014.63
Q9Y6M9	NDUFB9	MDT	10.1016/j.jpsychires.2010.04.014
Q16718	NDUFA5	PCC ACC	10.1016/j.jprot.2020.103814
			10.1038/sj.mp.4001806
O75380	NDUFS6	ATL	10.1007/s00702-008-0156-y
O75489	NDUFS3	ATL	10.1007/s00702-008-0156-y
Q16795	NDUFA9	PCC ACC	10.1016/j.jprot.2020.103814
			10.1038/mp.2014.63
P28331	NDUFS1	WA	10.1186/1471-244X-9-17
O43674	NDUFB5	ATL	10.1007/s00702-008-0156-y
Q9NZQ3	NCKIPSD	ACC	10.1038/mp.2014.63
P12036	NEFH	CER CC	10.1016/j.jprot.2020.103814
			10.1007/s00406-015-0621-1
P12036	NEFH	PCC CC	10.1016/j.jprot.2020.103814
			10.1007/s00406-015-0621-1
P07196	NEFL	PCC ACC ACC CC	10.1016/j.jprot.2020.103814
		DLPC ATL	10.1038/mp.2014.63
			10.1016/j.jpsychires.2010.03.003
			10.1007/s00702-008-0156-
			y 10.1002/prca.200700230
			10.1038/sj.mp.4002098
			10.1016/j.jpsychires.2008.11.006
			10.1007/s00406-015-0621-1
P07197	NEFM	PCC DLPC MDT	10.1016/j.jprot.2020.103814
		CC ACC ATL	10.1002/pmic.200900015
			10.1007/s00702-008-0156-y
			10.1016/j.jpsychires.2010.04.014
			10.1007/s00406-015-0621-1
			10.1016/j.jpsychires.2010.03.003
			10.1002/prca.200700230

Supplementary Table 1

Accession	**gene name**	**brain region**	**Proteome reference (doi)**
P07197	NEFM	PCC DLPC MDT CC ACC ATL	10.1016/j.jprot.2020.103814 10.1002/pmic.200900015 10.1007/s00702-008-0156-y 10.1016/j.jpsychires.2010.04.014 10.1007/s00406-015-0621-1 10.1016/j.jpsychires.2010.03.003 10.1002/prca.200700230
Q15818	NPTX1	CN IC	10.1016/j.jprot.2020.103814 10.1002/pmic.200800415
Q9NZR1	TMOD2	PCC IC	10.1016/j.jprot.2020.103814 10.1002/pmic.200800415
P84074	HPCA	ACC	10.1038/mp.2014.63
P43630	KIR3DL2	DLPC	10.1007/s00406-008-0847-2
Q15233	NONO	PCC CN DLPC	10.1016/j.jprot.2020.103814 10.1007/s00406-008-0847-2
Q5T0D9	TPRG1L	PCC ACC	10.1016/j.jprot.2020.103814 10.1038/sj.mp.4001808
Q9UI15	TAGLN3	PCC ACC	10.1016/j.jprot.2020.103814 10.1002/pmic.200500069
Q9H1E3	NUCKS1	DLPC	10.1007/s00406-008-0847-2
P06748	NPM1	PCC CN IC	10.1016/j.jprot.2020.103814 10.1002/pmic.200800415
Q02218	OGDH	PCC ACC	10.1016/j.jprot.2020.103814 10.1038/mp.2014.63
P50897	PPT1	DLPC	10.1007/s00406-008-0847-2
P62937	PPIA	PCC ACC MDT	10.1016/j.jprot.2020.103814 10.1038/sj.mp.4001806 10.1016/j.jpsychires.2010.04.014
Q06830	PRDX1	PCC ACC CC DLPC	10.1016/j.jprot.2020.103814 10.1016/j.jpsychires.2010.03.003 10.1038/mp.2014.63 10.1007/s00406-015-0621-1 10.1038/sj.mp.4001532
P32119	PRDX2	PCC CC DLPC ACC	10.1016/j.jprot.2020.103814 10.1002/prca.200700230 10.1038/sj.mp.4001532 10.1038/mp.2014.63

Supplementary Table 1

Accession	**gene name**	**brain region**	**Proteome reference (doi)**
P32119	PRDX2	PCC CC DLPC ACC	10.1016/j.jprot.2020.103814 10.1002/prca.200700230 10.1038/sj.mp.4001532 10.1038/mp.2014.63
Q13162	PRDX4	DLPC	10.1002/pmic.200900015
P30041	PRDX6	PCC CER DLPC WA	10.1016/j.jprot.2020.103814 10.1007/s00406-008-0847-2 10.1186/1471-244X-9-17
Q9Y285	FARSA	ACC	10.1038/mp.2014.63
Q6IBR2	FARSLA	DLPC	10.1007/s00406-008-0847-2
Q00325	SLC25A3	PCC WA ACC	10.1016/j.jprot.2020.103814 10.1186/1471-244X-9-17 10.1038/mp.2014.63
P30086	PEBP1	WA ACC CC ATL	10.1186/1471-244X-9-17 10.1038/sj.mp.4001806 10.1007/s00406-015-0621-1 10.1007/s00702-008-0156-y
Q00169	PITPNA	MDT	10.1016/j.jpsychires.2010.04.014
O95263	PDE8B	DLPC	10.1002/pmic.200900015
P17858	PFKL	ACC	10.1038/mp.2014.63
P36871	PGM1	PCC IC	10.1016/j.jprot.2020.103814 10.1002/pmic.200800415
O43175	PHGDH	PCC DLPC	10.1016/j.jprot.2020.103814 10.1038/sj.mp.4001532
P18669	PGAM1	DLPC WA MDT	10.1016/j.jpsychires.2008.11.006 10.1186/1471-244X-9-17 10.1016/j.jpsychires.2010.04.014 10.1038/sj.mp.4001532
P15259	PGAM2	DLPC	10.1038/sj.mp.4001532
Q9H008	LHPP	DLPC	10.1038/sj.mp.4001532
P60891	PRPS1	ACC	10.1038/mp.2014.63
Q92561	PHYHIP	ACC	10.1038/mp.2014.63
P23634	ATP2B4	PCC ATL	10.1016/j.jprot.2020.103814 10.1007/s00702-008-0156-y
P23634	ATP2B4	PCC ATL	10.1016/j.jprot.2020.103814 10.1007/s00702-008-0156-y

Supplementary Table 1

Accession	**gene name**	**brain region**	**Proteome reference (doi)**
Q15149	PLEC	PCC MDT DLPC	10.1016/j.jprot.2020.103814
			10.1016/j.jpsychires.2010.04.014
			10.1007/s00406-008-0847-2
O60925	PFDN1	IC	10.1002/pmic.200800415
P35080	PFN2	PCC ACC	10.1016/j.jprot.2020.103814
			10.1038/mp.2014.63
P35232	PHB	ACC ATL	10.1038/sj.mp.4001806
			10.1007/s00702-008-0156-y
P07237	P4HB	CN IC	10.1016/j.jprot.2020.103814
			10.1002/pmic.200800415
Q9BY11	PACSIN1	DLPC CC	10.1038/sj.mp.4002098
			10.1007/s00406-015-0621-1
P05129	PRKCG	PCC MDT	10.1016/j.jprot.2020.103814
			10.1016/j.jpsychires.2010.04.014
P05129	PRKCG	PCC MDT	10.1016/j.jprot.2020.103814
			10.1016/j.jpsychires.2010.04.014
Q9BPW8	NIPSNAP1	PCC ACC	10.1016/j.jprot.2020.103814
			10.1038/mp.2014.63
Q15435	PPP1R7	CC	10.1007/s00406-015-0621-1
P22061	PCMT1	MDT DLPC DLPC	10.1016/j.jpsychires.2010.04.014
			10.1016/j.jpsychires.2008.11.006
			10.1002/pmic.200900015
A8K9L3	PLP1	ACC	10.1038/mp.2014.63
Q2NLD4	PURA	DLPC	10.1007/s00406-008-0847-2
Q9UPE4	hTIM44	MDT	10.1016/j.jpsychires.2010.04.014
Q96GD0	PDXP	DLPC	10.1002/pmic.200900015
P08559	PDHA1	PCC DLPC	10.1016/j.jprot.2020.103814
			10.1038/sj.mp.4001532
P14618	PKM	PCC CC DLPC	10.1016/j.jprot.2020.103814
			10.1007/s00406-015-0621-1
			10.1038/sj.mp.4001532
P31150	GDI1	DLPC ACC	10.1002/pmic.200900015
			10.1016/j.jpsychires.2010.03.003
O14827	RASGRF2	ACC	10.1038/mp.2014.63
Q15907	RAB11B	PCC CC	10.1016/j.jprot.2020.103814
			10.1007/s00406-015-0621-1

Supplementary Table 1

Accession	**gene name**	**brain region**	**Proteome reference (doi)**
P20336	RAB3A	PCC ACC	10.1016/j.jprot.2020.103814
			10.1038/mp.2014.63
P20337	RAB3B	ACC	10.1038/mp.2014.63
P62834	RAP1A	ACC	10.1038/mp.2014.63
P61225	RAP2B	MDT	10.1016/j.jpsychires.2010.04.014
Q9NQC3	RTN4	PCC DLPC	10.1016/j.jprot.2020.103814
			10.1007/s00406-008-0847-2
P12271	RLBP1	DLPC	10.1007/s00406-008-0847-2
P52565	ARHGDIA	PCC CC ACC	10.1016/j.jprot.2020.103814
			10.1002/prca.200700230
			10.1016/j.jpsychires.2010.03.003
P13489	RNH1	PCC ATL	10.1016/j.jprot.2020.103814
			10.1007/s00702-008-0156-y
P13489	RNH1	PCC ATL	10.1016/j.jprot.2020.103814
			10.1007/s00702-008-0156-y
Q12765	SCRN1	PCC ACC	10.1016/j.jprot.2020.103814
			10.1016/j.jpsychires.2010.03.003
Q15019	SEPTIN2	PCC CER MDT	10.1016/j.jprot.2020.103814
			10.1016/j.jpsychires.2010.04.014
Q15019	SEPTIN2	PCC CER MDT	10.1016/j.jprot.2020.103814
			10.1016/j.jpsychires.2010.04.014
Q9UH03	SEPTIN3	IC DLPC	10.1002/pmic.200800415
			10.1038/sj.mp.4001532
O43236	SEPTIN4	PCC DLPC	10.1016/j.jprot.2020.103814
			10.1007/s00406-008-0847-2
Q9UHD8	SEPTIN9	PCC ACC	10.1016/j.jprot.2020.103814
			10.1038/mp.2014.63
Q16181	SEPTIN7	DLPC ACC	10.1038/sj.mp.4001532
			10.1038/mp.2014.63
Q9Y3F4	STRAP	IC	10.1002/pmic.200800415
P30153	PPP2R1A	PCC IC	10.1016/j.jprot.2020.103814
			10.1002/pmic.200800415
P62136	PPP1CA	ACC	10.1038/sj.mp.4001806
Q9UEW8	STK39	ACC	10.1038/mp.2014.63
P49591	SARS1	CC	10.1007/s00406-015-0621-1

Supplementary Table 1

Accession	**gene name**	**brain region**	**Proteome reference (doi)**
P02787	TF	PCC ACC DLPC	10.1016/j.jprot.2020.103814
			10.1038/sj.mp.4001806
			10.1016/j.jpsychires.2008.11.006
			10.1038/sj.mp.4001532
P02768	ALB	PCC ACC DLPC	10.1016/j.jprot.2020.103814
		MDT	10.1002/pmic.200500069
			10.1038/sj.mp.4001532
			10.1016/j.jpsychires.2010.04.014
			10.1016/j.jpsychires.2010.03.003
Q9BYB0	SHANK3	ACC	10.1038/mp.2014.63
Q9H299	SH3BGRL3	CC	10.1007/s00406-015-0621-1
Q99962	SH3GL2	PCC DLPC	10.1016/j.jprot.2020.103814
			10.1038/sj.mp.4001532
P37108	SRP14	CN ACC	10.1016/j.jprot.2020.103814
			10.1038/mp.2014.63
Q9Y5M8	SRPRB	ACC	10.1038/mp.2014.63
O00241	SIRPB1	PCC ATL	10.1016/j.jprot.2020.103814
			10.1007/s00702-008-0156-y
Q96E39	RBMXL1	DLPC	10.1007/s00406-008-0847-2
Q04837	SSBP1	ACC	10.1038/mp.2014.63
P43004	SLC1A2	PCC ACC	10.1016/j.jprot.2020.103814
			10.1038/mp.2014.63
P43004	SLC1A2	PCC ACC	10.1016/j.jprot.2020.103814
			10.1038/mp.2014.63
Q9H2X9	SLC12A5	ACC	10.1038/mp.2014.63
Q02978	SLC25A11	ACC	10.1038/mp.2014.63
P30626	SRI	PCC ACC	10.1016/j.jprot.2020.103814
			10.1002/pmic.200500069
Q9Y512	SAMM50	ACC	10.1038/mp.2014.63
Q13813	SPTAN1	PCC ACC ATL	10.1016/j.jprot.2020.103814
		DLPC	10.1016/j.jpsychires.2010.03.003
			10.1007/s00702-008-0156-y
			10.1038/sj.mp.4001532
Q13813	SPTAN1	PCC ACC ATL	10.1016/j.jprot.2020.103814
		DLPC	10.1016/j.jpsychires.2010.03.003
			10.1007/s00702-008-0156-y
			10.1038/sj.mp.4001532

Supplementary Table 1

Accession	**gene name**	**brain region**	**Proteome reference (doi)**
Q01082	SPTBN1	ACC	10.1038/mp.2014.63
O94905	ERLIN2	PCC IC	10.1016/j.jprot.2020.103814 10.1002/pmic.200800415
Q13247	SRSF6	DLPC	10.1007/s00406-008-0847-2
Q16629	SRSF7	DLPC	10.1007/s00406-008-0847-2
P16949	STMN1	CC CC ACC DLPC	10.1007/s00406-015-0621-1 10.1002/prca.200700230 10.1038/sj.mp.4001806 10.1002/pmic.200900015
P55809	OXCT1	PCC ACC ACC	10.1016/j.jprot.2020.103814 10.1002/pmic.200500069 10.1016/j.jpsychires.2010.03.003
P55809	OXCT1	PCC ACC ACC	10.1016/j.jprot.2020.103814 10.1002/pmic.200500069 10.1016/j.jpsychires.2010.03.003
P00441	SOD1	PCC CC ACC	10.1016/j.jprot.2020.103814 10.1002/prca.200700230 10.1038/sj.mp.4001806 10.1007/s00406-015-0621-1
P00441	SOD1	PCC CC ACC	10.1016/j.jprot.2020.103814 10.1002/prca.200700230 10.1038/sj.mp.4001806 10.1007/s00406-015-0621-1
P17600	SYN1	PCC ACC	10.1016/j.jprot.2020.103814 10.1038/mp.2014.63
P17600	SYN1	PCC ACC	10.1016/j.jprot.2020.103814 10.1038/mp.2014.63
O14994	SYN3	MDT	10.1016/j.jpsychires.2010.04.014
Q8N3V7	SYNPO	CN ACC	10.1016/j.jprot.2020.103814 10.1038/mp.2014.63
P60880	SNAP25	PCC ACC	10.1016/j.jprot.2020.103814 10.1038/sj.mp.4001806
P60880	SNAP25	PCC ACC	10.1016/j.jprot.2020.103814 10.1038/sj.mp.4001806
O00445	SYT5	MDT	10.1016/j.jpsychires.2010.04.014
Q7Z5K3	STX1A	MDT	10.1016/j.jpsychires.2010.04.014

Supplementary Table 1

Accession	**gene name**	**brain region**	**Proteome reference (doi)**
P61764	STXBP1	PCC CN MDT IC	10.1016/j.jprot.2020.103814 10.1016/j.jpsychires.2010.04.014 10.1002/pmic.200800415
P48643	CCT5	ACC	10.1038/mp.2014.63
Q8N5M4	TTC9C	DLPC	10.1007/s00406-008-0847-2
P29401	TKT	MDT DLPC	10.1016/j.jpsychires.2010.04.014 10.1016/j.jpsychires.2008.11.006
P60174	TPI1	CC WA DLPC IC MDT	10.1007/s00406-015-0621-1 10.1186/1471-244X-9-17 10.1002/pmic.200900015 10.1002/pmic.200800415 10.1016/j.jpsychires.2010.04.014
P00938	TPI1	DLPC	10.1038/sj.mp.4001532
P09493	TPM1	ACC	10.1016/j.jpsychires.2010.03.003
P06753	TPM3	ACC WA	10.1016/j.jpsychires.2010.03.003 10.1186/1471-244X-9-17
P67936	TPM4	PCC ACC CC	10.1016/j.jprot.2020.103814 10.1016/j.jpsychires.2010.03.003 10.1007/s00406-015-0621-1
P67936	TPM4	PCC ACC CC	10.1016/j.jprot.2020.103814 10.1016/j.jpsychires.2010.03.003 10.1007/s00406-015-0621-1
P07951	TPM2	ACC	10.1016/j.jpsychires.2010.03.003
P35030	PRSS3	ACC	10.1002/pmic.200500069
P49411	TUFM	PCC DLPC	10.1016/j.jprot.2020.103814 10.1038/sj.mp.4001532
Q71U36	TUBA1A	CC	10.1007/s00406-015-0621-1
Q13748	TUBA3C	DLPC	10.1038/sj.mp.4001532
P68366	TUBA4A	WA ACC CC	10.1186/1471-244X-9-17 10.1038/mp.2014.63 10.1007/s00406-015-0621-1
Q9BQE3	TUBA1C	PCC ACC DLPC	10.1016/j.jprot.2020.103814 10.1038/sj.mp.4001806 10.1038/sj.mp.4001532
A6NHL2	TUBAL3	CC	10.1007/s00406-015-0621-1

Supplementary Table 1

Accession	**gene name**	**brain region**	**Proteome reference (doi)**
P68363	TUBA1B	DLPC ACC WA	10.1038/sj.mp.4001532
			10.1002/pmic.200500069
			10.1186/1471-244X-9-17
			10.1016/j.jpsychires.2010.03.003
P04350	TUBB4A	CC	10.1002/prca.200700230
			10.1007/s00406-015-0621-1
Q13885	TUBB2A	ACC	10.1016/j.jpsychires.2010.03.003
Q9BVA1	TUBB2B	CC ATL	10.1007/s00406-015-0621-1
			10.1007/s00702-008-0156-y
Q13509	TUBB3	PCC CC WA	10.1016/j.jprot.2020.103814
			10.1007/s00406-015-0621-1
			10.1186/1471-244X-9-17
P68371	TUBB4B	PCC CC	10.1016/j.jprot.2020.103814
			10.1007/s00406-015-0621-1
P05218	TUBB	DLPC	10.1038/sj.mp.4001532
Q9BUF5	TUBB6	CC	10.1007/s00406-015-0621-1
Q3ZCM7	TUBB8	PCC ACC	10.1016/j.jprot.2020.103814
			10.1038/mp.2014.63
P07437	TUBB	ACC WA DLPC	10.1002/pmic.200500069
			10.1186/1471-244X-9-17
			10.1002/pmic.200900015
P54577	YARS1	PCC DLPC	10.1016/j.jprot.2020.103814
			10.1038/sj.mp.4001532
P31930	UQCRC1	DLPC DLPC	10.1016/j.jpsychires.2008.11.006
			10.1038/sj.mp.4001532
P09936	UCHL1	DLPC CC ACC	10.1038/sj.mp.4001532
			10.1002/prca.200700230
			10.1016/j.jpsychires.2010.03.003
P61088	UBE2N	CN DLPC CC ATL	10.1016/j.jprot.2020.103814
			10.1007/s00406-008-0847-2
			10.1007/s00406-015-0621-1
			10.1007/s00702-008-0156-y
P45974	USP5	PCC ACC	10.1016/j.jprot.2020.103814
			10.1038/mp.2014.63
Q5SNV9	C1orf167	ACC	10.1038/mp.2014.63
Q9Y4I1	MYO5A	PCC ACC	10.1016/j.jprot.2020.103814
			10.1038/mp.2014.63

Supplementary Table 1

Accession	**gene name**	**brain region**	**Proteome reference (doi)**
Q86W61	VCAN	CC	10.1007/s00406-015-0621-1
P63027	VAMP2	CN MDT	10.1016/j.jprot.2020.103814
			10.1016/j.jpsychires.2010.04.014
O95292	VAPB	PCC DLPC ACC	10.1016/j.jprot.2020.103814
			10.1007/s00406-008-0847-2
			10.1038/mp.2014.63
O75396	SEC22B	ACC	10.1038/mp.2014.63
P08670	VIM	MDT CC DLPC	10.1016/j.jpsychires.2010.04.014
			10.1007/s00406-015-0621-1
			10.1002/pmic.200900015
P62763	VSNL1	ATL	10.1007/s00702-008-0156-y
Q60932	Vdac1	ACC	10.1038/mp.2014.63
P45880	VDAC2	ACC	10.1038/mp.2014.63
P38606	ATP6V1A	PCC DLPC	10.1016/j.jprot.2020.103814
			10.1016/j.jpsychires.2008.11.006
P38606	ATP6V1A	PCC DLPC	10.1016/j.jprot.2020.103814
			10.1016/j.jpsychires.2008.11.006
P21281	ATP6V1B2	PCC CC ACC	10.1016/j.jprot.2020.103814
			10.1007/s00406-015-0621-1
			10.1016/j.jpsychires.2010.03.003
			10.1002/pmic.200500069
P61421	ATP6V0D1	PCC DLPC	10.1016/j.jprot.2020.103814
			10.1007/s00406-008-0847-2
O75083	WDR1	DLPC	10.1007/s00406-008-0847-2
Q9UPA5	BSN	DLPC	10.1007/s00406-008-0847-2
Q07157	TJP1	CER	10.1016/j.jprot.2020.103814
P00505	GOT2	PCC CER	10.1016/j.jprot.2020.103814
O43633	CHMP2A	CER	10.1016/j.jprot.2020.103814
O43633	CHMP2A	CER	10.1016/j.jprot.2020.103814
Q05682	CALD1	CER	10.1016/j.jprot.2020.103814
Q9GZV7	HAPLN2	PCC CER	10.1016/j.jprot.2020.103814
Q96GW7	BCAN	CER	10.1016/j.jprot.2020.103814
O46584	COX4I1	CER	10.1016/j.jprot.2020.103814
P27105	STOM	CER	10.1016/j.jprot.2020.103814
P56134	ATP5MF	PCC CER	10.1016/j.jprot.2020.103814
O94826	TOMM70	CER	10.1016/j.jprot.2020.103814
C9JRZ8	AKR1B15	CER	10.1016/j.jprot.2020.103814

Supplementary Table 1

Accession	**gene name**	**brain region**	**Proteome reference (doi)**
P43034	PAFAH1B1	CER	10.1016/j.jprot.2020.103814
Q13057	COASY	CER	10.1016/j.jprot.2020.103814
Q16695	H3-4	PCC CER	10.1016/j.jprot.2020.103814
Q9UBL6	CPNE7	CER	10.1016/j.jprot.2020.103814
Q9JI55	PLEC	CER	10.1016/j.jprot.2020.103814
P55008	AIF1	CER	10.1016/j.jprot.2020.103814
Q9R269	Ppl	CER	10.1016/j.jprot.2020.103814
P40227	CCT6A	CER	10.1016/j.jprot.2020.103814
P05230	FGF1	PCC CER	10.1016/j.jprot.2020.103814
O00139	KIF2A	CER	10.1016/j.jprot.2020.103814
P68402	PAFAH1B2	CER	10.1016/j.jprot.2020.103814
P20338	RAB4A	PCC CER	10.1016/j.jprot.2020.103814
P53999	SUB1	CER	10.1016/j.jprot.2020.103814
P23526	AHCY	PCC CER	10.1016/j.jprot.2020.103814
Q9BUP0	EFHD1	PCC CER	10.1016/j.jprot.2020.103814
Q14517	FAT1	CER	10.1016/j.jprot.2020.103814
Q13557	CAMK2D	PCC CER	10.1016/j.jprot.2020.103814
P0DP24	CALM2	CER	10.1016/j.jprot.2020.103814
P22314	UBA1	CER	10.1016/j.jprot.2020.103814
O00442	RTCA	CER	10.1016/j.jprot.2020.103814
Q13825	AUH	CER	10.1016/j.jprot.2020.103814
P11177	PDHB	CER	10.1016/j.jprot.2020.103814
Q8N568	DCLK2	PCC CER	10.1016/j.jprot.2020.103814
Q8IVB5	LIX1L	CER	10.1016/j.jprot.2020.103814
P15531	NME1	PCC CER	10.1016/j.jprot.2020.103814
Q9Y2A7	NCKAP1	PCC CER	10.1016/j.jprot.2020.103814
P36915	GNL1	CER	10.1016/j.jprot.2020.103814
Q9H0B6	KLC2	CER	10.1016/j.jprot.2020.103814
P50402	EMD	CER	10.1016/j.jprot.2020.103814
Q03113	GNA12	PCC CER	10.1016/j.jprot.2020.103814
Q03113	GNA12	PCC CER	10.1016/j.jprot.2020.103814
Q9UQ80	PA2G4	CER	10.1016/j.jprot.2020.103814
P52564	MAP2K6	CER	10.1016/j.jprot.2020.103814
Q58FG1	HSP90AA4P	PCC CER	10.1016/j.jprot.2020.103814
Q14344	GNA13	PCC CER	10.1016/j.jprot.2020.103814
Q14344	GNA13	PCC CER	10.1016/j.jprot.2020.103814
Q9Y265	RUVBL1	CER	10.1016/j.jprot.2020.103814

Supplementary Table 1

Accession	**gene name**	**brain region**	**Proteome reference (doi)**
P62249	RPS16	PCC CER	10.1016/j.jprot.2020.103814
P62249	RPS16	PCC CER	10.1016/j.jprot.2020.103814
P49589	CARS1	CER	10.1016/j.jprot.2020.103814
P28907	CD38	CER	10.1016/j.jprot.2020.103814
P30048	PRDX3	CER	10.1016/j.jprot.2020.103814
P35579	MYH9	CER	10.1016/j.jprot.2020.103814
Q765P7	MTSS2	CER	10.1016/j.jprot.2020.103814
P30154	PPP2R1B	PCC CER	10.1016/j.jprot.2020.103814
P35968	KDR	PCC CER	10.1016/j.jprot.2020.103814
Q96QK1	VPS35	CER CN	10.1016/j.jprot.2020.103814
Q8N9I0	SYT2	CER	10.1016/j.jprot.2020.103814
P01834	IGKC	CER	10.1016/j.jprot.2020.103814
P46782	RPS5	CER	10.1016/j.jprot.2020.103814
Q14568	HSP90AA2P	CER	10.1016/j.jprot.2020.103814
Q8WUM4	PDCD6IP	CER	10.1016/j.jprot.2020.103814
Q16566	CAMK4	CER	10.1016/j.jprot.2020.103814
Q07866	KLC1	CER	10.1016/j.jprot.2020.103814
O43426	SYNJ1	CER	10.1016/j.jprot.2020.103814
P13796	LCP1	PCC CER	10.1016/j.jprot.2020.103814
Q8NCW5	NAXE	PCC CER	10.1016/j.jprot.2020.103814
Q9UIW2	PLXNA1	CER	10.1016/j.jprot.2020.103814
P27635	RPL10	CER	10.1016/j.jprot.2020.103814
Q9H425	C1orf198	CER	10.1016/j.jprot.2020.103814
Q9BUR5	APOO	CER	10.1016/j.jprot.2020.103814
P60983	GMFB	CER	10.1016/j.jprot.2020.103814
Q9H0Q0	CYRIA	CER	10.1016/j.jprot.2020.103814
P02533	KRT14	CER	10.1016/j.jprot.2020.103814
O43741	PRKAB2	CER	10.1016/j.jprot.2020.103814
Q9C0I1	MTMR12	CER	10.1016/j.jprot.2020.103814
P43250	GRK6	CER	10.1016/j.jprot.2020.103814
P46664	Adss2	CER	10.1016/j.jprot.2020.103814
O75347	TBCA	CER	10.1016/j.jprot.2020.103814
P47297	deoA	CER	10.1016/j.jprot.2020.103814
Q7L1I2	SV2B	CER	10.1016/j.jprot.2020.103814
Q8TE73	DNAH5	CER	10.1016/j.jprot.2020.103814
Q99614	TTC1	CER	10.1016/j.jprot.2020.103814
P42041	ALTA10	CER	10.1016/j.jprot.2020.103814

Supplementary Table 1

Accession	**gene name**	**brain region**	**Proteome reference (doi)**
Q9UBC5	MYO1A	CER	10.1016/j.jprot.2020.103814
Q96G28	CFAP36	CER	10.1016/j.jprot.2020.103814
P0DME0	SETSIP	CER	10.1016/j.jprot.2020.103814
P35612	ADD2	CER	10.1016/j.jprot.2020.103814
O75306	NDUFS2	CER	10.1016/j.jprot.2020.103814
O75306	NDUFS2	PCC	10.1016/j.jprot.2020.103814
O75306	NDUFS2	PCC	10.1016/j.jprot.2020.103814
P51153	RAB13	CER	10.1016/j.jprot.2020.103814
P51153	RAB13	PCC	10.1016/j.jprot.2020.103814
P44017	HI_0577	CER	10.1016/j.jprot.2020.103814
Q8N3J6	CADM2	PCC CER	10.1016/j.jprot.2020.103814
Q9H8Y8	GORASP2	CER	10.1016/j.jprot.2020.103814
Q9UBW7	ZMYM2	PCC CER	10.1016/j.jprot.2020.103814
P43347	TPT1	CER	10.1016/j.jprot.2020.103814
P24844	MYL9	CER	10.1016/j.jprot.2020.103814
Q9UL26	RAB22A	CER	10.1016/j.jprot.2020.103814
Q9BS26	ERP44	CER	10.1016/j.jprot.2020.103814
Q8N715	CCDC185	CER	10.1016/j.jprot.2020.103814
P01876	IGHA1	CER	10.1016/j.jprot.2020.103814
Q9NX63	CHCHD3	PCC CER	10.1016/j.jprot.2020.103814
Q8NFZ8	CADM4	PCC CER	10.1016/j.jprot.2020.103814
Q8NFZ8	CADM4	PCC CER	10.1016/j.jprot.2020.103814
Q9BY44	EIF2A	CER	10.1016/j.jprot.2020.103814
Q9UL15	BAG5	CER	10.1016/j.jprot.2020.103814
Q14BN4	SLMAP	CER	10.1016/j.jprot.2020.103814
P54619	PRKAG1	CER	10.1016/j.jprot.2020.103814
Q9UHQ9	CYB5R1	CER	10.1016/j.jprot.2020.103814
P08729	KRT7	CER	10.1016/j.jprot.2020.103814
P08729	KRT7	PCC	10.1016/j.jprot.2020.103814
P15508	Sptb	CER	10.1016/j.jprot.2020.103814
P11019	ATP6V1E1	CER	10.1016/j.jprot.2020.103814
Q9ULC4	MCTS1	CER	10.1016/j.jprot.2020.103814
P35222	CTNNB1	CER	10.1016/j.jprot.2020.103814
P35222	CTNNB1	PCC	10.1016/j.jprot.2020.103814
P38919	EIF4A3	CER	10.1016/j.jprot.2020.103814
Q9Y5X3	SNX5	CER	10.1016/j.jprot.2020.103814
P42224	STAT1	CER	10.1016/j.jprot.2020.103814

Supplementary Table 1

Accession	**gene name**	**brain region**	**Proteome reference (doi)**
Q9H444	CHMP4B	CER	10.1016/j.jprot.2020.103814
Q62812	Myh9	CER	10.1016/j.jprot.2020.103814
Q15738	NSDHL	CER	10.1016/j.jprot.2020.103814
Q9BW85	YJU2	CER	10.1016/j.jprot.2020.103814
P09455	RBP1	PCC CER	10.1016/j.jprot.2020.103814
P53396	ACLY	CER	10.1016/j.jprot.2020.103814
Q13303	KCNAB2	CER	10.1016/j.jprot.2020.103814
Q96RU3	FNBP1	CER	10.1016/j.jprot.2020.103814
P48454	PPP3CC	PCC CN	10.1016/j.jprot.2020.103814
Q02878	RPL6	CN	10.1016/j.jprot.2020.103814
P01860	IGHG3	CN	10.1016/j.jprot.2020.103814
P15559	NQO1	CN	10.1016/j.jprot.2020.103814
P54750	PDE1A	CN	10.1016/j.jprot.2020.103814
P18206	VCL	CN	10.1016/j.jprot.2020.103814
P05062	ALDOB	CN	10.1016/j.jprot.2020.103814
P05388	RPLP0	CN	10.1016/j.jprot.2020.103814
P38117	ETFB	CN	10.1016/j.jprot.2020.103814
Q53FP2	TMEM35A	CN	10.1016/j.jprot.2020.103814
Q08257	CRYZ	PCC CN	10.1016/j.jprot.2020.103814
A6NGU5	GGT3P	CN	10.1016/j.jprot.2020.103814
P62277	RPS13	CN	10.1016/j.jprot.2020.103814
Q16836	HADH	PCC CN	10.1016/j.jprot.2020.103814
P10515	DLAT	CN	10.1016/j.jprot.2020.103814
Q9Y4L1	HYOU1	PCC CN	10.1016/j.jprot.2020.103814
Q58FF6	HSP90AB4P	PCC CN	10.1016/j.jprot.2020.103814
P13521	SCG2	CN	10.1016/j.jprot.2020.103814
Q9BVC3	DSCC1	CN	10.1016/j.jprot.2020.103814
Q9UD71	PPP1R1B	CN	10.1016/j.jprot.2020.103814
O00330	PDHX	PCC CN	10.1016/j.jprot.2020.103814
Q14203	DCTN1	PCC CN	10.1016/j.jprot.2020.103814
O15020	SPTBN2	CN	10.1016/j.jprot.2020.103814
P35916	FLT4	CN	10.1016/j.jprot.2020.103814
P20674	COX5A	PCC CN	10.1016/j.jprot.2020.103814
Q9H6W3	RIOX1	CN	10.1016/j.jprot.2020.103814
P29992	GNA11	CN	10.1016/j.jprot.2020.103814
O43681	GET3	PCC CN	10.1016/j.jprot.2020.103814
Q9NY97	B3GNT2	CN	10.1016/j.jprot.2020.103814

Supplementary Table 1

Accession	**gene name**	**brain region**	**Proteome reference (doi)**
Q9Y6R1	SLC4A4	CN	10.1016/j.jprot.2020.103814
Q9HBJ7	USP29	CN	10.1016/j.jprot.2020.103814
Q9UJZ1	STOML2	PCC CN	10.1016/j.jprot.2020.103814
Q9UJZ1	STOML2	PCC CN	10.1016/j.jprot.2020.103814
P29966	MARCKS	CN	10.1016/j.jprot.2020.103814
O95741	CPNE6	PCC CN	10.1016/j.jprot.2020.103814
Q96S97	MYADM	CN	10.1016/j.jprot.2020.103814
Q16543	CDC37	CN	10.1016/j.jprot.2020.103814
A6NHG4	DDTL	CN	10.1016/j.jprot.2020.103814
Q02750	MAP2K1	PCC CN	10.1016/j.jprot.2020.103814
Q8IYJ1	CPNE9	PCC CN	10.1016/j.jprot.2020.103814
O00264	PGRMC1	CN	10.1016/j.jprot.2020.103814
Q13424	SNTA1	PCC CN	10.1016/j.jprot.2020.103814
P55011	SLC12A2	CN	10.1016/j.jprot.2020.103814
Q8IXS6	PALM2	CN	10.1016/j.jprot.2020.103814
Q96JE9	MAP6	CN	10.1016/j.jprot.2020.103814
Q00577	PURA	CN	10.1016/j.jprot.2020.103814
Q9Y6I3	EPN1	CN	10.1016/j.jprot.2020.103814
P62736	ACTA2	CN	10.1016/j.jprot.2020.103814
Q96FE5	LINGO1	CN	10.1016/j.jprot.2020.103814
O75891	ALDH1L1	PCC CN	10.1016/j.jprot.2020.103814
Q92823	NRCAM	PCC CN	10.1016/j.jprot.2020.103814
P41217	CD200	PCC CN	10.1016/j.jprot.2020.103814
P49448	GLUD2	PCC CN	10.1016/j.jprot.2020.103814
P99999	CYCS	CN	10.1016/j.jprot.2020.103814
O43169	CYB5B	CN	10.1016/j.jprot.2020.103814
O15264	MAPK13	CN	10.1016/j.jprot.2020.103814
Q9BSD7	NTPCR	CN	10.1016/j.jprot.2020.103814
P0CG47	UBB	PCC CN	10.1016/j.jprot.2020.103814
P10114	RAP2A	PCC CN	10.1016/j.jprot.2020.103814
Q13233	MAP3K1	CN	10.1016/j.jprot.2020.103814
O43776	NARS1	CN	10.1016/j.jprot.2020.103814
Q96FN4	CPNE2	PCC CN	10.1016/j.jprot.2020.103814
Q13510	ASAH1	CN	10.1016/j.jprot.2020.103814
P0CG39	POTEJ	CN	10.1016/j.jprot.2020.103814
Q9UN37	VPS4A	CN	10.1016/j.jprot.2020.103814
Q9HAV0	GNB4	CN	10.1016/j.jprot.2020.103814

Supplementary Table 1

Accession	**gene name**	**brain region**	**Proteome reference (doi)**
Q6ZU15	SEPTIN14	PCC CN	10.1016/j.jprot.2020.103814
Q96HN2	AHCYL2	CN	10.1016/j.jprot.2020.103814
Q9NQR4	NIT2	CN	10.1016/j.jprot.2020.103814
P62195	PSMC5	CN	10.1016/j.jprot.2020.103814
P62081	RPS7	PCC CN	10.1016/j.jprot.2020.103814
Q9NSD9	FARSB	PCC CN	10.1016/j.jprot.2020.103814
O60884	DNAJA2	CN	10.1016/j.jprot.2020.103814
Q9ULP0	NDRG4	CN	10.1016/j.jprot.2020.103814
Q5VTE0	EEF1A1P5	PCC CN	10.1016/j.jprot.2020.103814
Q9BRX8	PRXL2A	CN	10.1016/j.jprot.2020.103814
Q8WWZ4	ABCA10	CN	10.1016/j.jprot.2020.103814
Q9Y230	RUVBL2	CN	10.1016/j.jprot.2020.103814
Q07955	SRSF1	CN	10.1016/j.jprot.2020.103814
P07205	PGK2	CN	10.1016/j.jprot.2020.103814
P78356	PIP4K2B	CN	10.1016/j.jprot.2020.103814
O00217	NDUFS8	PCC CN	10.1016/j.jprot.2020.103814
O60664	PLIN3	PCC CN	10.1016/j.jprot.2020.103814
Q9Y385	UBE2J1	CN	10.1016/j.jprot.2020.103814
Q9H0E2	TOLLIP	CN	10.1016/j.jprot.2020.103814
Q02224	CENPE	PCC CN	10.1016/j.jprot.2020.103814
Q16623	STX1A	CN	10.1016/j.jprot.2020.103814
Q96MM6	HSPA12B	CN	10.1016/j.jprot.2020.103814
Q8IUQ0	CLVS1	CN	10.1016/j.jprot.2020.103814
Q3ZCQ8	TIMM50	PCC	10.1016/j.jprot.2020.103814
Q14254	FLOT2	PCC	10.1016/j.jprot.2020.103814
Q96E17	RAB3C	PCC	10.1016/j.jprot.2020.103814
O14561	NDUFAB1	PCC	10.1016/j.jprot.2020.103814
P14854	COX6B1	PCC	10.1016/j.jprot.2020.103814
P14854	COX6B1	PCC	10.1016/j.jprot.2020.103814
P12235	SLC25A4	PCC	10.1016/j.jprot.2020.103814
P12235	SLC25A4	PCC	10.1016/j.jprot.2020.103814
P21912	SDHB	PCC	10.1016/j.jprot.2020.103814
Q14914	PTGR1	PCC	10.1016/j.jprot.2020.103814
P05141	SLC25A5	PCC	10.1016/j.jprot.2020.103814
P49721	PSMB2	PCC	10.1016/j.jprot.2020.103814
P24539	ATP5PB	PCC	10.1016/j.jprot.2020.103814
P24539	ATP5PB	PCC	10.1016/j.jprot.2020.103814

Supplementary Table 1

Accession	**gene name**	**brain region**	**Proteome reference (doi)**
P12236	SLC25A6	PCC	10.1016/j.jprot.2020.103814
Q58FF7	HSP90AB3P	PCC	10.1016/j.jprot.2020.103814
Q8WUD1	RAB2B	PCC	10.1016/j.jprot.2020.103814
P32004	L1CAM	PCC	10.1016/j.jprot.2020.103814
P43003	SLC1A3	PCC	10.1016/j.jprot.2020.103814
Q15126	PMVK	PCC	10.1016/j.jprot.2020.103814
P68133	ACTA1	PCC	10.1016/j.jprot.2020.103814
P51970	NDUFA8	PCC	10.1016/j.jprot.2020.103814
P14406	COX7A2	PCC	10.1016/j.jprot.2020.103814
P23763	VAMP1	PCC	10.1016/j.jprot.2020.103814
Q02539	H1-1	PCC	10.1016/j.jprot.2020.103814
Q13492	PICALM	PCC	10.1016/j.jprot.2020.103814
Q15120	PDK3	PCC	10.1016/j.jprot.2020.103814
P16615	ATP2A2	PCC	10.1016/j.jprot.2020.103814
O60313	OPA1	PCC	10.1016/j.jprot.2020.103814
Q12840	KIF5A	PCC	10.1016/j.jprot.2020.103814
P61201	COPS2	PCC	10.1016/j.jprot.2020.103814
P25325	MPST	PCC	10.1016/j.jprot.2020.103814
P21926	CD9	PCC	10.1016/j.jprot.2020.103814
P13929	ENO3	PCC	10.1016/j.jprot.2020.103814
P15880	RPS2	PCC	10.1016/j.jprot.2020.103814
P13010	XRCC5	PCC	10.1016/j.jprot.2020.103814
Q9BV57	ADI1	PCC	10.1016/j.jprot.2020.103814
Q9H2J1	ARRDC1-AS1	PCC	10.1016/j.jprot.2020.103814
Q99714	HSD17B10	PCC	10.1016/j.jprot.2020.103814
P09874	PARP1	PCC	10.1016/j.jprot.2020.103814
O75880	SCO1	PCC	10.1016/j.jprot.2020.103814
P55060	CSE1L	PCC	10.1016/j.jprot.2020.103814
Q99623	PHB2	PCC	10.1016/j.jprot.2020.103814
Q99623	PHB2	PCC	10.1016/j.jprot.2020.103814
P19404	NDUFV2	PCC	10.1016/j.jprot.2020.103814
Q13367	AP3B2	PCC	10.1016/j.jprot.2020.103814
Q2TB90	HKDC1	PCC	10.1016/j.jprot.2020.103814
Q9P0J0	NDUFA13	PCC	10.1016/j.jprot.2020.103814
O94973	AP2A2	PCC	10.1016/j.jprot.2020.103814
Q13491	GPM6B	PCC	10.1016/j.jprot.2020.103814

Supplementary Table 1

Accession	**gene name**	**brain region**	**Proteome reference (doi)**
O94925	GLS	PCC	10.1016/j.jprot.2020.103814
O94925	GLS	PCC	10.1016/j.jprot.2020.103814
Q9H061	TMEM126A	PCC	10.1016/j.jprot.2020.103814
P23515	OMG	PCC	10.1016/j.jprot.2020.103814
P13611	VCAN	PCC	10.1016/j.jprot.2020.103814
Q9BQ69	MACROD1	PCC	10.1016/j.jprot.2020.103814
P80404	ABAT	PCC	10.1016/j.jprot.2020.103814
P00390	GSR	PCC	10.1016/j.jprot.2020.103814
Q8NHW5	RPLP0P6	PCC	10.1016/j.jprot.2020.103814
Q9GZT8	NIF3L1	PCC	10.1016/j.jprot.2020.103814
O95299	NDUFA10	PCC	10.1016/j.jprot.2020.103814
O75569	PRKRA	PCC	10.1016/j.jprot.2020.103814
P12814	ACTN1	PCC	10.1016/j.jprot.2020.103814
Q16864	ATP6V1F	PCC	10.1016/j.jprot.2020.103814
P10721	KIT	PCC	10.1016/j.jprot.2020.103814
P07954	FH	PCC	10.1016/j.jprot.2020.103814
Q96QR8	PURB	PCC	10.1016/j.jprot.2020.103814
P11498	PC	PCC	10.1016/j.jprot.2020.103814
P31040	SDHA	PCC	10.1016/j.jprot.2020.103814
O75874	IDH1	PCC	10.1016/j.jprot.2020.103814
P42658	DPP6	PCC	10.1016/j.jprot.2020.103814
P42658	DPP6	PCC	10.1016/j.jprot.2020.103814
Q13733	ATP1A4	PCC	10.1016/j.jprot.2020.103814
P01019	AGT	PCC	10.1016/j.jprot.2020.103814
Q99685	MGLL	PCC	10.1016/j.jprot.2020.103814
O95782	AP2A1	PCC	10.1016/j.jprot.2020.103814
Q99961	SH3GL1	PCC	10.1016/j.jprot.2020.103814
O96000	NDUFB10	PCC	10.1016/j.jprot.2020.103814
O96000	NDUFB10	PCC	10.1016/j.jprot.2020.103814
P59768	GNG2	PCC	10.1016/j.jprot.2020.103814
P37837	TALDO1	PCC	10.1016/j.jprot.2020.103814
Q16720	ATP2B3	PCC	10.1016/j.jprot.2020.103814
Q16720	ATP2B3	PCC	10.1016/j.jprot.2020.103814
Q8IYI6	EXOC8	PCC	10.1016/j.jprot.2020.103814
O14880	MGST3	PCC	10.1016/j.jprot.2020.103814
Q9HCJ6	VAT1L	PCC	10.1016/j.jprot.2020.103814
P38405	GNAL	PCC	10.1016/j.jprot.2020.103814

Supplementary Table 1

Accession	**gene name**	**brain region**	**Proteome reference (doi)**
P13473	LAMP2	PCC	10.1016/j.jprot.2020.103814
Q15506	SPA17	PCC	10.1016/j.jprot.2020.103814
P84095	RHOG	PCC	10.1016/j.jprot.2020.103814
P39210	MPV17	PCC	10.1016/j.jprot.2020.103814
O75363	BCAS1	PCC	10.1016/j.jprot.2020.103814
P04899	GNAI2	PCC	10.1016/j.jprot.2020.103814
Q9BW72	HIGD2A	PCC	10.1016/j.jprot.2020.103814
Q99719	SEPTIN5	PCC	10.1016/j.jprot.2020.103814
Q8WXF7	ATL1	PCC	10.1016/j.jprot.2020.103814
P20618	PSMB1	PCC	10.1016/j.jprot.2020.103814
Q14195	DPYSL3	PCC	10.1016/j.jprot.2020.103814
Q14195	DPYSL3	PCC	10.1016/j.jprot.2020.103814
Q13449	LSAMP	PCC	10.1016/j.jprot.2020.103814
Q96A00	PPP1R14A	PCC	10.1016/j.jprot.2020.103814
Q96MZ0	GDAP1L1	PCC	10.1016/j.jprot.2020.103814
P43243	MATR3	PCC	10.1016/j.jprot.2020.103814
Q9UHG3	PCYOX1	PCC	10.1016/j.jprot.2020.103814
P51553	IDH3G	PCC	10.1016/j.jprot.2020.103814
P51553	IDH3G	PCC	10.1016/j.jprot.2020.103814
P07864	LDHC	PCC	10.1016/j.jprot.2020.103814
Q00013	MPP1	PCC	10.1016/j.jprot.2020.103814
Q13555	CAMK2G	PCC	10.1016/j.jprot.2020.103814
P10644	PRKAR1A	PCC	10.1016/j.jprot.2020.103814
Q9NS69	TOMM22	PCC	10.1016/j.jprot.2020.103814
P17948	FLT1	PCC	10.1016/j.jprot.2020.103814
P02689	PMP2	PCC	10.1016/j.jprot.2020.103814
O75955	FLOT1	PCC	10.1016/j.jprot.2020.103814
O75955	FLOT1	PCC	10.1016/j.jprot.2020.103814
P46821	MAP1B	PCC	10.1016/j.jprot.2020.103814
P56385	ATP5ME	PCC	10.1016/j.jprot.2020.103814
P12074	COX6A1	PCC	10.1016/j.jprot.2020.103814
Q9BUX1	CHAC1	PCC	10.1016/j.jprot.2020.103814
Q14964	RAB39A	PCC	10.1016/j.jprot.2020.103814
Q92597	NDRG1	PCC	10.1016/j.jprot.2020.103814
P01111	NRAS	PCC	10.1016/j.jprot.2020.103814
P61313	RPL15	PCC	10.1016/j.jprot.2020.103814
O75746	SLC25A12	PCC	10.1016/j.jprot.2020.103814

Supplementary Table 1

Accession	**gene name**	**brain region**	**Proteome reference (doi)**
Q8N5S9	CAMKK1	PCC	10.1016/j.jprot.2020.103814
P01009	SERPINA1	PCC	10.1016/j.jprot.2020.103814
Q9H0W9	C11orf54	PCC	10.1016/j.jprot.2020.103814
Q9UJQ1	LAMP5	PCC	10.1016/j.jprot.2020.103814
O95847	SLC25A27	PCC	10.1016/j.jprot.2020.103814
P16403	H1-2	PCC	10.1016/j.jprot.2020.103814
Q86X76	NIT1	PCC	10.1016/j.jprot.2020.103814
Q9UBQ7	GRHPR	PCC	10.1016/j.jprot.2020.103814
Q9BX67	JAM3	PCC	10.1016/j.jprot.2020.103814
Q5XKP0	MICOS13	PCC	10.1016/j.jprot.2020.103814
P62760	VSNL1	PCC	10.1016/j.jprot.2020.103814
Q86YQ8	CPNE8	PCC	10.1016/j.jprot.2020.103814
A6NJ78	METTL15	PCC	10.1016/j.jprot.2020.103814
Q14764	MVP	PCC	10.1016/j.jprot.2020.103814
Q9UM22	EPDR1	PCC	10.1016/j.jprot.2020.103814
Q8TBX8	PIP4K2C	PCC	10.1016/j.jprot.2020.103814
Q16762	TST	PCC	10.1016/j.jprot.2020.103814
Q08380	LGALS3BP	PCC	10.1016/j.jprot.2020.103814
O60282	KIF5C	PCC	10.1016/j.jprot.2020.103814
P04259	KRT6B	PCC	10.1016/j.jprot.2020.103814
Q9H0Q3	FXYD6	PCC	10.1016/j.jprot.2020.103814
Q9H0Q3	FXYD6	PCC	10.1016/j.jprot.2020.103814
Q02246	CNTN2	PCC	10.1016/j.jprot.2020.103814
P19087	GNAT2	PCC	10.1016/j.jprot.2020.103814
P07384	CAPN1	PCC	10.1016/j.jprot.2020.103814
Q9Y617	PSAT1	PCC	10.1016/j.jprot.2020.103814
P30044	PRDX5	PCC	10.1016/j.jprot.2020.103814
P30044	PRDX5	PCC	10.1016/j.jprot.2020.103814
P62820	RAB1A	PCC	10.1016/j.jprot.2020.103814
Q96HU8	DIRAS2	PCC	10.1016/j.jprot.2020.103814
Q9Y697	NFS1	PCC	10.1016/j.jprot.2020.103814
P27338	MAOB	PCC	10.1016/j.jprot.2020.103814
P27338	MAOB	PCC	10.1016/j.jprot.2020.103814
P13716	ALAD	PCC	10.1016/j.jprot.2020.103814
Q15041	ARL6IP1	PCC	10.1016/j.jprot.2020.103814
P61018	RAB4B	PCC	10.1016/j.jprot.2020.103814
Q15388	TOMM20	PCC	10.1016/j.jprot.2020.103814

Supplementary Table 1

Accession	**gene name**	**brain region**	**Proteome reference (doi)**
Q9UDW1	UQCR10	PCC	10.1016/j.jprot.2020.103814
Q9Y281	CFL2	PCC	10.1016/j.jprot.2020.103814
O14508	SOCS2	PCC	10.1016/j.jprot.2020.103814
O14672	ADAM10	PCC	10.1016/j.jprot.2020.103814
Q86T65	DAAM2	PCC	10.1016/j.jprot.2020.103814
P63215	GNG3	PCC	10.1016/j.jprot.2020.103814
Q9UQM7	CAMK2A	PCC	10.1016/j.jprot.2020.103814
P16402	H1-3	PCC	10.1016/j.jprot.2020.103814
O95219	SNX4	PCC	10.1016/j.jprot.2020.103814
Q9NQW7	XPNPEP1	PCC	10.1016/j.jprot.2020.103814
P18124	RPL7	PCC	10.1016/j.jprot.2020.103814
P35609	ACTN2	PCC	10.1016/j.jprot.2020.103814
P35609	ACTN2	PCC	10.1016/j.jprot.2020.103814
P49354	FNTA	PCC	10.1016/j.jprot.2020.103814
Q9NRG7	SDR39U1	PCC	10.1016/j.jprot.2020.103814
Q9UPV7	PHF24	PCC	10.1016/j.jprot.2020.103814
P05166	PCCB	PCC	10.1016/j.jprot.2020.103814
P21579	SYT1	PCC	10.1016/j.jprot.2020.103814
Q9UJC5	SH3BGRL2	PCC	10.1016/j.jprot.2020.103814
P40616	ARL1	PCC	10.1016/j.jprot.2020.103814
O75190	DNAJB6	PCC	10.1016/j.jprot.2020.103814
Q92752	TNR	PCC	10.1016/j.jprot.2020.103814
O00408	PDE2A	PCC	10.1016/j.jprot.2020.103814
O75323	NIPSNAP2	PCC	10.1016/j.jprot.2020.103814
O75323	NIPSNAP2	PCC	10.1016/j.jprot.2020.103814
Q9H4G4	GLIPR2	PCC	10.1016/j.jprot.2020.103814
Q9H4G4	GLIPR2	PCC	10.1016/j.jprot.2020.103814
O95182	NDUFA7	PCC	10.1016/j.jprot.2020.103814
P36222	CHI3L1	PCC	10.1016/j.jprot.2020.103814
Q14353	GAMT	PCC	10.1016/j.jprot.2020.103814
Q9Y2X7	GIT1	PCC	10.1016/j.jprot.2020.103814
Q9UQ16	DNM3	PCC	10.1016/j.jprot.2020.103814
Q5TBA9	FRY	PCC	10.1016/j.jprot.2020.103814
P13987	CD59	PCC	10.1016/j.jprot.2020.103814
P49419	ALDH7A1	PCC	10.1016/j.jprot.2020.103814
O95865	DDAH2	PCC	10.1016/j.jprot.2020.103814
Q9BY67	CADM1	PCC	10.1016/j.jprot.2020.103814

Supplementary Table 1

Accession	**gene name**	**brain region**	**Proteome reference (doi)**
O60361	NME2P1	PCC	10.1016/j.jprot.2020.103814
Q9C040	TRIM2	PCC	10.1016/j.jprot.2020.103814
Q9C040	TRIM2	PCC	10.1016/j.jprot.2020.103814
P41222	PTGDS	PCC	10.1016/j.jprot.2020.103814
P41222	PTGDS	PCC	10.1016/j.jprot.2020.103814
O75663	TIPRL	PCC	10.1016/j.jprot.2020.103814
Q9BYZ2	LDHAL6B	PCC	10.1016/j.jprot.2020.103814
P37235	HPCAL1	PCC	10.1016/j.jprot.2020.103814
O00629	KPNA4	PCC	10.1016/j.jprot.2020.103814
P61019	RAB2A	PCC	10.1016/j.jprot.2020.103814
P61019	RAB2A	PCC	10.1016/j.jprot.2020.103814
Q9NQX3	GPHN	PCC	10.1016/j.jprot.2020.103814
P49189	ALDH9A1	PCC	10.1016/j.jprot.2020.103814
P55084	HADHB	PCC	10.1016/j.jprot.2020.103814
P29803	PDHA2	PCC	10.1016/j.jprot.2020.103814
O43809	NUDT21	PCC	10.1016/j.jprot.2020.103814
Q9H7Z7	PTGES2	PCC	10.1016/j.jprot.2020.103814
O75431	MTX2	PCC	10.1016/j.jprot.2020.103814
O14548	COX7A2L	PCC	10.1016/j.jprot.2020.103814
O43813	LANCL1	PCC	10.1016/j.jprot.2020.103814
O43813	LANCL1	PCC	10.1016/j.jprot.2020.103814
Q92599	SEPTIN8	PCC	10.1016/j.jprot.2020.103814
Q02338	BDH1	PCC	10.1016/j.jprot.2020.103814
P28161	GSTM2	PCC	10.1016/j.jprot.2020.103814
Q86Y82	STX12	PCC	10.1016/j.jprot.2020.103814
P35241	RDX	PCC	10.1016/j.jprot.2020.103814
Q9H479	FN3K	PCC	10.1016/j.jprot.2020.103814
P11586	MTHFD1	PCC	10.1016/j.jprot.2020.103814
Q16537	PPP2R5E	PCC	10.1016/j.jprot.2020.103814
O00764	PDXK	PCC	10.1016/j.jprot.2020.103814
O00764	PDXK	PCC	10.1016/j.jprot.2020.103814
Q9UI12	ATP6V1H	PCC	10.1016/j.jprot.2020.103814
Q9UI12	ATP6V1H	PCC	10.1016/j.jprot.2020.103814
Q8N145	LGI3	PCC	10.1016/j.jprot.2020.103814
P62244	RPS15A	PCC	10.1016/j.jprot.2020.103814
P51649	ALDH5A1	PCC	10.1016/j.jprot.2020.103814
P51649	ALDH5A1	PCC	10.1016/j.jprot.2020.103814

Supplementary Table 1

Accession	**gene name**	**brain region**	**Proteome reference (doi)**
Q14108	SCARB2	PCC	10.1016/j.jprot.2020.103814
P60510	PPP4C	PCC	10.1016/j.jprot.2020.103814
P13804	ETFA	PCC	10.1016/j.jprot.2020.103814
P13804	ETFA	PCC	10.1016/j.jprot.2020.103814
P23246	SFPQ	PCC	10.1016/j.jprot.2020.103814
P62318	SNRPD3	PCC	10.1016/j.jprot.2020.103814
Q2M2I8	AAK1	PCC	10.1016/j.jprot.2020.103814
Q6PEY2	TUBA3E	PCC	10.1016/j.jprot.2020.103814
P61006	RAB8A	PCC	10.1016/j.jprot.2020.103814
O00483	NDUFA4	PCC	10.1016/j.jprot.2020.103814
P07741	APRT	PCC	10.1016/j.jprot.2020.103814
P23396	RPS3	PCC	10.1016/j.jprot.2020.103814
P14550	AKR1A1	PCC	10.1016/j.jprot.2020.103814
P14550	AKR1A1	PCC	10.1016/j.jprot.2020.103814
Q9NPJ3	ACOT13	PCC	10.1016/j.jprot.2020.103814
Q07960	ARHGAP1	PCC	10.1016/j.jprot.2020.103814
Q9NQ66	PLCB1	PCC	10.1016/j.jprot.2020.103814
Q9NQ66	PLCB1	PCC	10.1016/j.jprot.2020.103814
P46926	GNPDA1	PCC	10.1016/j.jprot.2020.103814
P25686	DNAJB2	PCC	10.1016/j.jprot.2020.103814
P20916	MAG	PCC	10.1016/j.jprot.2020.103814
P15954	COX7C	PCC	10.1016/j.jprot.2020.103814
Q6BCY4	CYB5R2	PCC	10.1016/j.jprot.2020.103814
Q96AB3	ISOC2	PCC	10.1016/j.jprot.2020.103814
Q96AB3	ISOC2	PCC	10.1016/j.jprot.2020.103814
P55290	CDH13	PCC	10.1016/j.jprot.2020.103814
P08574	CYC1	PCC	10.1016/j.jprot.2020.103814
P63244	RACK1	PCC	10.1016/j.jprot.2020.103814
P49441	INPP1	PCC	10.1016/j.jprot.2020.103814
P04179	SOD2	PCC	10.1016/j.jprot.2020.103814
P56556	NDUFA6	PCC	10.1016/j.jprot.2020.103814
P56556	NDUFA6	PCC	10.1016/j.jprot.2020.103814
P56556	NDUFA6	PCC	10.1016/j.jprot.2020.103814
P62841	RPS15	PCC	10.1016/j.jprot.2020.103814
Q9H3N1	TMX1	PCC	10.1016/j.jprot.2020.103814
Q96AX2	RAB37	PCC	10.1016/j.jprot.2020.103814
Q96GK7	FAHD2A	PCC	10.1016/j.jprot.2020.103814

Supplementary Table 1

Accession	**gene name**	**brain region**	**Proteome reference (doi)**
P50990	CCT8	PCC	10.1016/j.jprot.2020.103814
P12694	BCKDHA	PCC	10.1016/j.jprot.2020.103814
P27797	CALR	PCC	10.1016/j.jprot.2020.103814
P27797	CALR	PCC	10.1016/j.jprot.2020.103814
P62942	FKBP1A	PCC	10.1016/j.jprot.2020.103814
O60331	PIP5K1C	PCC	10.1016/j.jprot.2020.103814
P49720	PSMB3	PCC	10.1016/j.jprot.2020.103814
Q969G6	RFK	PCC	10.1016/j.jprot.2020.103814
Q9UNM6	PSMD13	PCC	10.1016/j.jprot.2020.103814
P69905	HBA1	PCC	10.1016/j.jprot.2020.103814
P05771	PRKCB	PCC	10.1016/j.jprot.2020.103814
Q9Y2Z0	SUGT1	PCC	10.1016/j.jprot.2020.103814
P61026	RAB10	PCC	10.1016/j.jprot.2020.103814
O75915	ARL6IP5	PCC	10.1016/j.jprot.2020.103814
P59190	RAB15	PCC	10.1016/j.jprot.2020.103814
P24666	ACP1	PCC	10.1016/j.jprot.2020.103814
Q07021	C1QBP	PCC	10.1016/j.jprot.2020.103814
Q07021	C1QBP	PCC	10.1016/j.jprot.2020.103814
P49821	NDUFV1	PCC	10.1016/j.jprot.2020.103814
P39687	ANP32A	PCC	10.1016/j.jprot.2020.103814
Q12905	ILF2	PCC	10.1016/j.jprot.2020.103814
O94856	NFASC	PCC	10.1016/j.jprot.2020.103814
P11413	G6PD	PCC	10.1016/j.jprot.2020.103814
P61106	RAB14	PCC	10.1016/j.jprot.2020.103814
P00491	PNP	PCC	10.1016/j.jprot.2020.103814
Q6KB66	KRT80	PCC	10.1016/j.jprot.2020.103814
Q8N573	OXR1	PCC	10.1016/j.jprot.2020.103814
P13797	PLS3	PCC	10.1016/j.jprot.2020.103814
O43678	NDUFA2	PCC	10.1016/j.jprot.2020.103814
P49753	ACOT2	PCC	10.1016/j.jprot.2020.103814
Q9NY65	TUBA8	PCC	10.1016/j.jprot.2020.103814
Q8TBF2	PRXL2B	PCC	10.1016/j.jprot.2020.103814
Q86UW8	HAPLN4	PCC	10.1016/j.jprot.2020.103814
O00499	BIN1	PCC	10.1016/j.jprot.2020.103814
O00499	BIN1	PCC	10.1016/j.jprot.2020.103814
Q15102	PAFAH1B3	PCC	10.1016/j.jprot.2020.103814
P40939	HADHA	PCC	10.1016/j.jprot.2020.103814

Supplementary Table 1

Accession	**gene name**	**brain region**	**Proteome reference (doi)**
P04435	TRBV7-9	PCC	10.1016/j.jprot.2020.103814
P52790	HK3	PCC	10.1016/j.jprot.2020.103814
P52790	HK3	PCC	10.1016/j.jprot.2020.103814
Q9NRX4	PHPT1	PCC	10.1016/j.jprot.2020.103814
Q9NRX4	PHPT1	PCC	10.1016/j.jprot.2020.103814
P47756	CAPZB	PCC	10.1016/j.jprot.2020.103814
P48163	ME1	PCC	10.1016/j.jprot.2020.103814
Q8WXF1	PSPC1	PCC	10.1016/j.jprot.2020.103814
O14773	TPP1	PCC	10.1016/j.jprot.2020.103814
P78352	DLG4	PCC	10.1016/j.jprot.2020.103814
P78352	DLG4	PCC	10.1016/j.jprot.2020.103814
P25787	PSMA2	PCC	10.1016/j.jprot.2020.103814
P52789	HK2	PCC	10.1016/j.jprot.2020.103814
P0CG38	POTEI	PCC	10.1016/j.jprot.2020.103814
P67775	PPP2CA	PCC	10.1016/j.jprot.2020.103814
P67775	PPP2CA	PCC	10.1016/j.jprot.2020.103814
A6NDG6	PGP	PCC	10.1016/j.jprot.2020.103814
P45381	ASPA	PCC	10.1016/j.jprot.2020.103814
Q9UM19	HPCAL4	PCC	10.1016/j.jprot.2020.103814
Q9Y5K8	ATP6V1D	PCC	10.1016/j.jprot.2020.103814
Q7L576	CYFIP1	PCC	10.1016/j.jprot.2020.103814
P13861	PRKAR2A	PCC	10.1016/j.jprot.2020.103814
P36507	MAP2K2	PCC	10.1016/j.jprot.2020.103814
P06737	PYGL	PCC	10.1016/j.jprot.2020.103814
Q8IVF7	FMNL3	PCC	10.1016/j.jprot.2020.103814
Q99426	TBCB	PCC	10.1016/j.jprot.2020.103814
Q9NQE9	HINT3	PCC	10.1016/j.jprot.2020.103814
P17661	DES	PCC	10.1016/j.jprot.2020.103814
P04156	PRNP	PCC	10.1016/j.jprot.2020.103814
P42765	ACAA2	PCC	10.1016/j.jprot.2020.103814
P42765	ACAA2	PCC	10.1016/j.jprot.2020.103814
P11279	LAMP1	PCC	10.1016/j.jprot.2020.103814
P10915	HAPLN1	PCC	10.1016/j.jprot.2020.103814
P10915	HAPLN1	PCC	10.1016/j.jprot.2020.103814
Q9BR01	SULT4A1	PCC	10.1016/j.jprot.2020.103814
P02545	LMNA	PCC	10.1016/j.jprot.2020.103814
O00154	ACOT7	PCC	10.1016/j.jprot.2020.103814

Supplementary Table 1

Accession	**gene name**	**brain region**	**Proteome reference (doi)**
Q8N335	GPD1L	PCC	10.1016/j.jprot.2020.103814
Q6S8J3	POTEE	PCC	10.1016/j.jprot.2020.103814
Q6S8J3	POTEE	PCC	10.1016/j.jprot.2020.103814
P51149	RAB7A	PCC	10.1016/j.jprot.2020.103814
Q68DU8	KCTD16	PCC	10.1016/j.jprot.2020.103814
P62333	PSMC6	PCC	10.1016/j.jprot.2020.103814
Q96AG4	LRRC59	PCC	10.1016/j.jprot.2020.103814
Q9UIJ7	AK3	PCC	10.1016/j.jprot.2020.103814
P62424	RPL7A	PCC	10.1016/j.jprot.2020.103814
P20340	RAB6A	PCC	10.1016/j.jprot.2020.103814
O94819	KBTBD11	PCC	10.1016/j.jprot.2020.103814
Q96A23	CPNE4	PCC	10.1016/j.jprot.2020.103814
Q8IXJ6	SIRT2	PCC	10.1016/j.jprot.2020.103814
Q9UF11	PLEKHB1	PCC	10.1016/j.jprot.2020.103814
Q9UF11	PLEKHB1	PCC	10.1016/j.jprot.2020.103814
Q9UBW8	COPS7A	PCC	10.1016/j.jprot.2020.103814
Q08043	ACTN3	PCC	10.1016/j.jprot.2020.103814
P27695	APEX1	PCC	10.1016/j.jprot.2020.103814
P51665	PSMD7	PCC	10.1016/j.jprot.2020.103814
P52943	CRIP2	PCC	10.1016/j.jprot.2020.103814
Q16799	RTN1	PCC	10.1016/j.jprot.2020.103814
P63000	RAC1	PCC	10.1016/j.jprot.2020.103814
P63000	RAC1	PCC	10.1016/j.jprot.2020.103814
O00625	PIR	PCC	10.1016/j.jprot.2020.103814
Q7Z3B1	NEGR1	PCC	10.1016/j.jprot.2020.103814
P35270	SPR	PCC	10.1016/j.jprot.2020.103814
Q9NZG7	NINJ2	PCC	10.1016/j.jprot.2020.103814
Q92499	DDX1	PCC	10.1016/j.jprot.2020.103814
P04040	CAT	PCC	10.1016/j.jprot.2020.103814
Q8ND76	CCNY	PCC	10.1016/j.jprot.2020.103814
Q9Y5U8	MPC1	PCC	10.1016/j.jprot.2020.103814
O95670	ATP6V1G2	PCC	10.1016/j.jprot.2020.103814
Q562R1	ACTBL2	PCC	10.1016/j.jprot.2020.103814
Q562R1	ACTBL2	PCC	10.1016/j.jprot.2020.103814
Q9H4B7	TUBB1	PCC	10.1016/j.jprot.2020.103814
P36873	PPP1CC	PCC	10.1016/j.jprot.2020.103814
Q9BW30	TPPP3	PCC	10.1016/j.jprot.2020.103814

Supplementary Table 1

Accession	**gene name**	**brain region**	**Proteome reference (doi)**
Q14103	HNRNPD	PCC	10.1016/j.jprot.2020.103814
Q14103	HNRNPD	PCC	10.1016/j.jprot.2020.103814
Q9HCH3	CPNE5	PCC	10.1016/j.jprot.2020.103814
P43304	GPD2	PCC	10.1016/j.jprot.2020.103814
Q96MZ4	FAM218A	PCC	10.1016/j.jprot.2020.103814
P62714	PPP2CB	PCC	10.1016/j.jprot.2020.103814
P42126	ECI1	PCC	10.1016/j.jprot.2020.103814
P19338	NCL	PCC	10.1016/j.jprot.2020.103814
P60900	PSMA6	PCC	10.1016/j.jprot.2020.103814
P49802	RGS7	PCC	10.1016/j.jprot.2020.103814
Q05329	GAD2	PCC	10.1016/j.jprot.2020.103814
Q13362	PPP2R5C	PCC	10.1016/j.jprot.2020.103814
P27824	CANX	PCC	10.1016/j.jprot.2020.103814
Q13228	SELENBP1	PCC	10.1016/j.jprot.2020.103814
Q6IQ22	RAB12	PCC	10.1016/j.jprot.2020.103814
P26641	EEF1G	PCC	10.1016/j.jprot.2020.103814
O75638	CTAG2	PCC	10.1016/j.jprot.2020.103814
P08237	PFKM	PCC	10.1016/j.jprot.2020.103814
Q12931	TRAP1	PCC	10.1016/j.jprot.2020.103814
O95202	LETM1	PCC	10.1016/j.jprot.2020.103814
Q99878	H2AC14	PCC	10.1016/j.jprot.2020.103814
Q99878	H2AC14	PCC	10.1016/j.jprot.2020.103814
Q7Z4W1	DCXR	PCC	10.1016/j.jprot.2020.103814
P31947	SFN	PCC	10.1016/j.jprot.2020.103814
P22694	PRKACB	PCC	10.1016/j.jprot.2020.103814
P01236	PRL	PCC	10.1016/j.jprot.2020.103814
Q9H0R4	HDHD2	PCC	10.1016/j.jprot.2020.103814
P63208	SKP1	PCC	10.1016/j.jprot.2020.103814
P62140	PPP1CB	PCC	10.1016/j.jprot.2020.103814
P35237	SERPINB6	PCC	10.1016/j.jprot.2020.103814
P43897	TSFM	PCC	10.1016/j.jprot.2020.103814
Q6P587	FAHD1	PCC	10.1016/j.jprot.2020.103814
P06744	GPI	PCC	10.1016/j.jprot.2020.103814
P52758	RIDA	PCC	10.1016/j.jprot.2020.103814
Q8TD08	MAPK15	PCC	10.1016/j.jprot.2020.103814
P61586	RHOA	PCC	10.1016/j.jprot.2020.103814
O43491	EPB41L2	PCC	10.1016/j.jprot.2020.103814

Supplementary Table 1

Accession	**gene name**	**brain region**	**Proteome reference (doi)**
O15173	PGRMC2	PCC	10.1016/j.jprot.2020.103814
P35908	KRT2	PCC	10.1016/j.jprot.2020.103814
P26196	DDX6	PCC	10.1016/j.jprot.2020.103814
O75251	NDUFS7	PCC	10.1016/j.jprot.2020.103814
O75251	NDUFS7	PCC	10.1016/j.jprot.2020.103814
P24863	CCNC	PCC	10.1016/j.jprot.2020.103814
P35613	BSG	PCC	10.1016/j.jprot.2020.103814
Q9HBH0	RHOF	PCC	10.1016/j.jprot.2020.103814
P35611	ADD1	PCC	10.1016/j.jprot.2020.103814
P35611	ADD1	PCC	10.1016/j.jprot.2020.103814
B4DX44	ZNF736	PCC	10.1016/j.jprot.2020.103814
Q53H12	AGK	PCC	10.1016/j.jprot.2020.103814
Q53H12	AGK	PCC	10.1016/j.jprot.2020.103814
Q8N0Y7	PGAM4	PCC	10.1016/j.jprot.2020.103814
Q8TCD5	NT5C	PCC	10.1016/j.jprot.2020.103814
P15121	AKR1B1	PCC	10.1016/j.jprot.2020.103814
P08238	HSP90AB1	PCC	10.1016/j.jprot.2020.103814
Q6UXQ4	C2orf66	PCC	10.1016/j.jprot.2020.103814
Q96A26	FAM162A	PCC	10.1016/j.jprot.2020.103814
Q9Y6N7	ROBO1	PCC	10.1016/j.jprot.2020.103814
P27449	ATP6V0C	PCC	10.1016/j.jprot.2020.103814
Q9H4L5	OSBPL3	PCC	10.1016/j.jprot.2020.103814
Q96ND0	FAM210A	PCC	10.1016/j.jprot.2020.103814
O60493	SNX3	PCC	10.1016/j.jprot.2020.103814
Q9Y3D6	FIS1	PCC	10.1016/j.jprot.2020.103814
Q8NBX0	SCCPDH	PCC	10.1016/j.jprot.2020.103814
Q9HD67	MYO10	PCC	10.1016/j.jprot.2020.103814
Q08170	SRSF4	PCC	10.1016/j.jprot.2020.103814
O00429	DNM1L	PCC	10.1016/j.jprot.2020.103814
O00487	PSMD14	PCC	10.1016/j.jprot.2020.103814
Q9UHY7	ENOPH1	PCC	10.1016/j.jprot.2020.103814
Q8WXW3	PIBF1	PCC	10.1016/j.jprot.2020.103814
Q9Y5F7	PCDHGC4	PCC	10.1016/j.jprot.2020.103814
Q96CB9	NSUN4	PCC	10.1016/j.jprot.2020.103814
P36578	RPL4	PCC	10.1016/j.jprot.2020.103814
P29692	EEF1D	PCC	10.1016/j.jprot.2020.103814
Q13423	NNT	PCC	10.1016/j.jprot.2020.103814

Supplementary Table 1

Accession	**gene name**	**brain region**	**Proteome reference (doi)**
O15145	ARPC3	PCC	10.1016/j.jprot.2020.103814
Q53GQ0	HSD17B12	PCC	10.1016/j.jprot.2020.103814
Q9UN36	NDRG2	PCC	10.1016/j.jprot.2020.103814
O00170	AIP	PCC	10.1016/j.jprot.2020.103814
O60506	SYNCRIP	PCC	10.1016/j.jprot.2020.103814
O15455	TLR3	PCC	10.1016/j.jprot.2020.103814
Q13740	ALCAM	PCC	10.1016/j.jprot.2020.103814
Q6PUV4	CPLX2	PCC	10.1016/j.jprot.2020.103814
Q96M86	DNHD1	PCC	10.1016/j.jprot.2020.103814
P47985	UQCRFS1	PCC	10.1016/j.jprot.2020.103814
Q9UKL3	CASP8AP2	PCC	10.1016/j.jprot.2020.103814
Q9NV96	TMEM30A	PCC	10.1016/j.jprot.2020.103814
Q9C0I4	THSD7B	PCC	10.1016/j.jprot.2020.103814
P30050	RPL12	PCC	10.1016/j.jprot.2020.103814
Q9ULD0	OGDHL	PCC	10.1016/j.jprot.2020.103814
P46109	CRKL	PCC	10.1016/j.jprot.2020.103814
P31943	HNRNPH1	PCC	10.1016/j.jprot.2020.103814
P05090	APOD	PCC	10.1016/j.jprot.2020.103814
Q8IVL1	NAV2	PCC	10.1016/j.jprot.2020.103814
Q96CX2	KCTD12	PCC	10.1016/j.jprot.2020.103814
Q96BM9	ARL8A	PCC	10.1016/j.jprot.2020.103814
Q08722	CD47	PCC	10.1016/j.jprot.2020.103814
P46939	UTRN	PCC	10.1016/j.jprot.2020.103814
Q9Y2J8	PADI2	PCC	10.1016/j.jprot.2020.103814
P05026	ATP1B1	PCC	10.1016/j.jprot.2020.103814
O43390	HNRNPR	PCC	10.1016/j.jprot.2020.103814
P23677	ITPKA	PCC	10.1016/j.jprot.2020.103814
P61266	STX1B	PCC	10.1016/j.jprot.2020.103814
O43920	NDUFS5	PCC	10.1016/j.jprot.2020.103814
Q8TB36	GDAP1	PCC	10.1016/j.jprot.2020.103814
O95298	NDUFC2	PCC	10.1016/j.jprot.2020.103814
P51888	PRELP	PCC	10.1016/j.jprot.2020.103814
Q9H361	PABPC3	PCC	10.1016/j.jprot.2020.103814
P36969	GPX4	PCC	10.1016/j.jprot.2020.103814
Q8IVF5	TIAM2	PCC	10.1016/j.jprot.2020.103814
O75787	ATP6AP2	PCC	10.1016/j.jprot.2020.103814
Q96IX5	ATP5MD	PCC	10.1016/j.jprot.2020.103814

Supplementary Table 1

Accession	**gene name**	**brain region**	**Proteome reference (doi)**
A6NHQ2	FBLL1	PCC	10.1016/j.jprot.2020.103814
P51452	DUSP3	PCC	10.1016/j.jprot.2020.103814
P51571	SSR4	PCC	10.1016/j.jprot.2020.103814
O94927	HAUS5	PCC	10.1016/j.jprot.2020.103814
P19784	CSNK2A2	PCC	10.1016/j.jprot.2020.103814
P09651	HNRNPA1	PCC	10.1016/j.jprot.2020.103814
P78371	CCT2	PCC	10.1016/j.jprot.2020.103814
Q8NHH9	ATL2	PCC	10.1016/j.jprot.2020.103814
P04114	APOB	PCC	10.1016/j.jprot.2020.103814
A1KZ92	PXDNL	PCC	10.1016/j.jprot.2020.103814
P07602	PSAP	PCC	10.1016/j.jprot.2020.103814
Q14257	RCN2	PCC	10.1016/j.jprot.2020.103814
P30613	PKLR	PCC	10.1016/j.jprot.2020.103814
Q9H0C2	SLC25A31	PCC	10.1016/j.jprot.2020.103814
P19086	GNAZ	PCC	10.1016/j.jprot.2020.103814
P07919	UQCRH	PCC	10.1016/j.jprot.2020.103814
P42336	PIK3CA	PCC	10.1016/j.jprot.2020.103814
P84103	SRSF3	PCC	10.1016/j.jprot.2020.103814
Q99726	SLC30A3	PCC	10.1016/j.jprot.2020.103814
P50993	ATP1A2	PCC	10.1016/j.jprot.2020.103814
Q8WWF6	DNAJB3	PCC	10.1016/j.jprot.2020.103814
Q9UBB6	NCDN	PCC	10.1016/j.jprot.2020.103814
Q8N1G4	LRRC47	PCC	10.1016/j.jprot.2020.103814
O75367	MACROH2A1	PCC	10.1016/j.jprot.2020.103814
Q8TBG9	SYNPR	PCC	10.1016/j.jprot.2020.103814
P62266	RPS23	PCC	10.1016/j.jprot.2020.103814
Q00059	TFAM	PCC	10.1016/j.jprot.2020.103814
Q99418	CYTH2	PCC	10.1016/j.jprot.2020.103814
O15078	CEP290	PCC	10.1016/j.jprot.2020.103814
P36957	DLST	PCC	10.1016/j.jprot.2020.103814
P13645	KRT10	PCC	10.1016/j.jprot.2020.103814
P17174	GOT1	PCC	10.1016/j.jprot.2020.103814
P31939	ATIC	PCC	10.1016/j.jprot.2020.103814
P08247	SYP	PCC	10.1016/j.jprot.2020.103814
P62191	PSMC1	PCC	10.1016/j.jprot.2020.103814
P55327	TPD52	PCC	10.1016/j.jprot.2020.103814
P49454	CENPF	PCC	10.1016/j.jprot.2020.103814

Supplementary Table 1

Accession	**gene name**	**brain region**	**Proteome reference (doi)**
P25398	RPS12	PCC	10.1016/j.jprot.2020.103814
Q8WVM7	STAG1	PCC	10.1016/j.jprot.2020.103814
Q15691	MAPRE1	PCC	10.1016/j.jprot.2020.103814
O15144	ARPC2	PCC	10.1016/j.jprot.2020.103814
P08123	COL1A2	PCC	10.1016/j.jprot.2020.103814
Q13409	DYNC1I2	PCC	10.1016/j.jprot.2020.103814
P53597	SUCLG1	PCC	10.1016/j.jprot.2020.103814
Q9ULC5	ACSL5	PCC	10.1016/j.jprot.2020.103814
P54707	ATP12A	PCC	10.1016/j.jprot.2020.103814
Q02252	ALDH6A1	PCC	10.1016/j.jprot.2020.103814
Q9Y2H0	DLGAP4	PCC	10.1016/j.jprot.2020.103814
P17540	CKMT2	PCC	10.1016/j.jprot.2020.103814

Supplementary Table 2

Organoids		
Accession	Anova (p)	logFC
Q8NFV4	0.013796673	-1.176756129
Q13085	0.001152796	0.831513569
P49748	0.012264623	0.758985712
P68133	0.030434012	-2.374187896
O43707	0.013790518	0.632686129
P61160	0.029315868	-2.914165672
P55265	0.01956046	-0.508310487
P35612	0.010157094	-1.376581929
O00116	0.0136324	1.474861275
Q96HN2	0.007351876	-3.652761254
Q13155	0.039996206	-0.783619539
O00170	0.018397783	0.772119306
C9JRZ8	0.007425784	0.569341359
P30837	0.017138627	-1.067913946
P51648	0.035586479	-0.479665614
Q02252	0.03721775	0.905687722
P04075	0.047273361	0.464190942
P49418	0.010217737	-4.099455937
Q86XL3	0.002758396	0.829734108
Q92688	0.001324797	0.851675372
P09525	0.043508485	-1.092383607

P08133	0.023145482	0.430983728
P27695	0.029432055	1.048246572
Q9BZZ5	0.046708764	-0.725624654
Q9HDC9	0.014849641	-0.756635853
Q9BUR5	0.028674286	-0.936186236
Q9Y6D6	0.012166886	-0.97333952
Q9NR48	0.000840221	-4.414958184
O43681	0.006501696	-1.37361612
Q12797	0.012014637	1.474671436
Q5SQI0	0.043654055	-0.943913005
Q13315	0.030973519	1.460243928
P23634	0.003450608	-1.256491831
Q9Y487	0.049909903	-0.604123676
P61421	0.007527325	2.238725824
Q9UBB4	0.024667705	-1.347973725
O75531	0.019196087	-2.053852592
P51572	0.000171627	0.8521064
P12694	0.041580644	0.603411488
Q9BXK5	0.031065647	-1.575109767
Q5T5X7	0.030710913	0.871978776
P38398	0.001644705	-2.265133726
Q15059	0.000762136	0.807588169
O43683	0.007778504	-0.450628405
Q7L1Q6	0.003540412	1.202581645
Q5U649	0.000350596	-1.299138276
Q07021	0.003754229	0.871901871
P54289	0.040344939	0.703964611
Q9HB71	0.039024021	-0.508245438
P22676	0.000226705	-2.874174837
Q9UQM7	0.032070723	-1.02463114
Q13554	0.004666503	-2.715019
P27824	0.000801408	1.339365056
P47755	0.041472357	-1.849844205
P47756	0.004275513	-0.931885488
P49589	0.013475705	0.653133547
Q8WXD9	0.004530308	0.749016875
Q4VC31	0.028743373	-4.700872509
A6NC98	0.002137088	-1.478601669

P50990	0.024608684	0.311151205
P41217	0.015033532	-1.064513221
Q9H251	0.020419541	-1.447844948
P21127	0.000679723	1.366943129
Q92879	0.033055209	-0.536716022
P49454	0.004143477	-0.617429728
Q7Z7K6	0.015382463	1.465250703
A0A0M3HER2	0.005575348	1.620251822
Q6ZU80	0.00016008	-1.025418517
Q9BV73	0.002507177	-2.669252741
Q0VF96	0.015020791	-1.753520223
Q8IWX8	0.020743314	-1.294321449
Q9NZZ3	0.002904658	-2.455903682
P06732	0.028717307	-1.618286335
Q9Y696	0.016328883	0.722012025
Q96NY7	0.001824698	-2.310729195
Q96JQ2	0.017164211	-3.494855655
P53675	0.002154881	-2.13969112
Q96KP4	0.022037211	-0.550050673
Q16281	0.020769147	-0.773654842
Q15417	0.030808721	-1.828212102
Q9NXG0	0.003686821	-0.764184243
Q9H9E3	0.002642203	-2.524989612
P12109	0.018311122	-3.233483471
P21964	0.00261439	2.073871711
Q9BT78	0.019953169	0.580053375
Q99829	0.007010662	-2.152861726
Q8N684	0.002693226	0.881865658
P29762	0.026773552	1.384250689
P46108	0.003269457	-2.173008437
Q68DQ2	0.045912501	2.635470653
Q08257	0.008989036	1.806506129
Q9H0L4	0.001516578	-0.968622327
P56545	0.015475939	-1.222342253
P35222	0.002450948	-10.65115063
P53634	0.027096646	-1.269020782
Q13618	0.039300996	1.075944132
Q13619	0.04114603	-4.426602686

P14868	0.000371251	-1.280586658
Q96EP5	0.044577744	-1.036282119
Q14203	0.016236487	0.499321375
Q13561	0.013799949	-0.902546996
Q9BTE1	0.003399284	-0.944101987
O94760	0.037868042	-1.267428423
Q92841	0.021286004	1.08359773
Q9BUQ8	0.014804573	0.725919707
P35659	0.002379026	-3.63809239
P10515	0.003539054	-1.960742411
P29803	4.36E-06	-6.806770485
P09622	0.026694508	-0.844309901
Q8TDM6	0.004900192	1.122962023
Q9UGM3	0.001895998	-2.355946468
P11532	0.031668375	0.598448312
Q9UFH2	0.036718538	-2.424962118
Q9UBS4	0.048024645	-0.901570174
Q9H3Z4	0.001615961	-1.072340565
Q96M86	0.013100407	0.348144506
Q05193	0.000142599	-5.457380724
O00429	0.014535599	-2.916433611
O14531	0.024988568	0.888627023
A0A0U1RQJ2	0.026523772	-1.079216003
O43237	0.008288091	-0.966799443
Q8NCM8	0.040638291	1.734470095
Q9NTX5	0.040025168	-1.702687768
O75521	0.030814234	0.773589461
Q05639	0.002346082	-2.065489785
Q14152	0.00857868	1.653415428
Q99613	0.040379695	0.963646337
O15371	0.000306962	0.983300895
P60228	0.049652274	-2.410899563
O15372	0.008478654	-4.010741258
Q9UBQ5	0.004966611	-1.847186831
P78344	0.002195466	1.659660185
O43432	0.009437026	3.187871056
Q9GZV4	0.015791286	1.190131707
O60841	0.01122768	-1.133800806

P56537	0.003115669	-2.14006318
Q14576	0.031388286	-1.730487392
P09104	0.018598581	-0.61344064
P11171	0.002447569	1.065422917
Q9H4G0	0.004637877	-2.775981436
Q9Y2J2	0.029024041	-1.49715841
Q969X5	0.015722902	0.720601955
P38117	0.026128782	0.524005255
Q01844	0.001553706	1.178363934
Q01469	0.031090997	-0.358662756
O15540	9.03E-07	-0.754302619
Q6P587	0.001769926	-0.944326086
Q5VWN6	0.018001599	-3.989539414
Q9BRX8	0.037780818	0.691945351
A6NHR8	0.000289758	2.7612434
P22087	0.011557415	-1.135502142
P23142	0.004213807	-0.87437281
Q9UK22	0.038568881	-5.167305058
P37268	0.027461814	-0.65885689
P22570	0.00096312	1.077056662
B1AJZ9	0.000283864	-1.107413035
Q00688	0.000986324	0.768121728
Q14318	0.047650146	1.246430645
Q9H479	0.005008395	-2.102189018
Q9BXM9	0.049454958	-1.265873542
Q9H0Q3	0.002972541	-1.314720325
Q9BQS8	0.002173553	-3.549599885
P11413	0.001797149	-1.208699309
P54803	0.009524205	-2.007484353
Q14697	0.047070047	-0.523378954
Q92538	0.011242502	-0.623907805
P50395	0.003628563	3.191090083
Q9HC38	0.003134862	0.679655625
O76003	0.00499363	0.58983899
P00367	0.017430576	1.546406055
P60983	0.003580308	-0.575709153
P08754	0.003749088	0.776496941
P50148	0.025813853	-1.272513331

P62873	0.04500309	-1.965841365
P62879	0.005638682	-0.982202179
P59768	0.000602013	-1.05737775
P15586	0.049899675	-0.977474451
P35052	0.010151628	0.651424946
P43304	0.041714394	-0.67505218
P62993	0.01562985	-1.229729353
Q9UBQ7	0.01117385	-0.843799598
P06396	0.021503988	1.280728252
P28161	0.024510812	-0.824300972
P21266	0.00061077	-2.714886928
Q00403	0.000293479	1.183403375
Q6EKJ0	0.006988264	-0.927147935
Q92522	0.017960382	0.612742104
Q16775	0.015593863	-1.729160191
P51858	0.045436416	0.669798175
Q9Y3E1	0.021245307	-1.182890705
Q6NVY1	0.018486802	-1.409975065
P16401	0.01326465	0.783538902
P16403	0.007114924	0.962672792
P16402	0.011246023	0.77026095
P10412	0.012888139	0.395874131
Q8IUE6	0.049126952	0.340093095
Q8NDA2	0.011004949	-0.480941599
B2RPK0	0.001341483	0.528439958
H0YH80	0.03098668	1.481581382
P51991	0.012138518	0.494134356
P52597	0.038579761	0.68969584
P55795	0.029616906	-1.669237379
P14866	0.028430443	0.458395557
P52272	0.048790638	0.256290159
O43390	0.01185689	0.780316769
Q00839	0.048167191	0.579538434
Q9BUJ2	0.011656603	-3.536675469
Q5SSJ5	0.017953214	0.805589897
Q9NWY4	0.005759019	-1.198827543
P01112	0.000827348	-2.15039224
Q58FF7	0.017601579	-2.595243553

P14625	0.046566387	0.3932165
O95757	0.002015267	0.752343304
P17066	0.047362419	0.243613239
P04792	0.00055524	-5.038980026
Q92598	0.009634876	0.258181549
Q9NZI8	0.00206773	0.97999255
O00425	0.038878832	0.552042702
Q9UPX0	0.01301963	-0.648566915
Q12906	0.000174041	1.156504706
Q16891	0.017373333	-0.887740767
O15357	5.21E-05	3.300585699
Q96CN7	0.021353267	-1.787254629
P53990	0.001265686	-1.563387851
P05556	0.035282141	-0.583568251
P26012	0.001986505	0.84828227
Q9Y287	0.006830895	1.667006453
A8CTZ0	3.21E-06	-3.40881136
P57087	0.002476721	1.229434229
Q6NY19	0.021122108	-0.639027948
Q8IYT4	0.038058783	-1.053419323
Q07666	0.00319563	1.805319068
Q92945	0.04724304	-0.38494116
Q9NQT8	0.006322832	0.678563672
Q86VH2	0.009781288	-3.010100998
O00139	0.038696156	2.154075084
Q07866	0.033974298	-0.718195552
P52294	0.001903856	-1.675402966
P04264	0.003593413	1.687897496
P13645	0.017088869	1.503537778
P02533	0.009005863	0.871303219
P35900	0.003115309	-3.48163561
P08729	0.049543759	-1.777868974
P35527	0.010056486	0.94604983
Q86UP2	0.015858004	0.698258607
P32004	0.003878372	1.809616905
Q53H82	0.037300671	0.595261361
P11047	0.030087885	-1.616644705
P07864	0.013776724	1.212829568

O95202	0.043683011	-0.905125951
P49257	0.000862145	0.844260083
Q8WWI1	0.009885809	-0.882298558
M0QZD8	0.00150994	1.067582165
Q6ZRR7	0.016739734	-0.384093512
Q9Y608	0.008522354	-0.679585445
Q9BX40	0.047487573	-1.584602906
Q9NQ29	0.049619416	-1.337272948
Q9Y383	0.0003455	-1.174802532
E9PNZ4	0.017227258	1.107250617
P20916	0.041958753	-1.731697148
H0YKM7	0.003298344	0.994709295
O00754	0.041018479	-1.708862436
Q9H492	0.03415104	-0.584310058
P11137	0.041605838	0.923647472
Q02750	0.00060066	-1.974627747
Q6ZN16	0.007939031	2.92480709
P31152	0.024844447	0.768405152
Q9UPY8	0.00690259	-1.406881392
I3L170	0.002497042	-1.615220598
P10636	0.011651399	0.37543353
P31153	0.043775556	0.362947761
P43243	0.00241113	0.593850931
Q7Z434	0.018426963	1.633950373
Q14703	0.035628907	-2.21934341
P33991	0.00383212	-0.85507898
O60502	0.006228328	0.712031237
Q5JRA6	0.025274529	1.110067261
Q7L9L4	0.00205056	0.765210923
P34949	0.002815801	-6.759753166
Q6WCQ1	0.012429405	0.854047798
P00403	0.007102544	1.146540588
P11586	0.005997753	-2.607381944
Q9NR99	0.000139401	-1.491058891
Q14324	0.00925111	-0.668632444
P35580	0.036058951	-1.474168099
A7E2Y1	0.020778509	0.892143549
P35579	0.030703076	2.330977589

P05976	0.016532419	-1.81440288
Q9Y6X6	0.024272283	-1.868093283
Q9NQX4	0.006785688	2.272671877
P49321	0.039166664	0.555317942
A0A0D9SF30	0.031392443	-1.070552881
P16333	0.046356297	0.599709909
P19338	0.002274516	0.726768209
Q9HCD5	0.048189931	-3.253869763
O75306	0.049638527	0.449404409
H0Y786	0.01378663	0.888567334
P12036	0.003039867	0.913327602
P07197	0.000830401	0.559754337
Q6P3R8	0.009147131	-7.969602929
O00221	0.034520694	-0.578510339
O75323	0.001298348	-3.611114868
Q9BS92	0.001366865	-2.115902244
Q86X76	0.004898302	-1.581570633
Q9Y2X3	0.026594558	0.704178705
Q9UNW9	0.003470869	-2.405932681
P55786	0.041272103	-1.947161219
Q9BXI3	0.049998119	-0.903240358
Q9UKK9	0.000754823	-2.056192577
Q14980	0.011173821	-0.520050542
P57740	0.029900103	0.30594059
P52948	0.030071701	0.796876039
Q9ULD0	0.004814805	-1.617638941
Q13438	0.04595861	-0.9054898
Q96FW1	0.00180134	-1.625555794
Q9UQ80	0.006289967	0.915815612
Q13310	0.004322191	-0.922214723
Q13153	0.018026559	-0.912666935
O75781	0.032274904	-4.892546135
Q99497	0.027662402	-0.546236002
P09874	0.002324889	1.059128601
P40425	0.039675112	0.884155494
Q96AQ6	0.000139424	-1.556483698
P05165	0.034731365	-0.825800777
Q8WW12	0.029622286	-0.94817437

Q9H2J4	0.000981129	-9.66816715
P11177	0.028232551	0.497562782
O00764	0.001415175	-7.343147636
Q01813	0.006735197	-1.702465038
G5E9Q6	0.004746977	-2.214929354
P52209	0.016860453	0.785506311
O00264	0.031492452	0.598269713
Q8WXW3	0.005297791	-1.49195178
A2A3N6	0.048518182	-1.730365853
P30613	0.031696424	0.403137765
P51178	0.031476266	0.618152975
Q9P212	0.019697235	-2.95612888
Q15149	0.041287482	0.550349495
Q9UIW2	0.002316243	0.719605488
O60486	0.009978601	-2.836074638
Q9H307	0.029268562	0.745276451
O14802	0.004685316	-2.034390613
Q15063	0.000572637	-3.969317192
P0CG39	0.048790752	-0.615762172
Q9H2U2	0.013813541	-2.182832339
P62937	0.00822779	1.041642228
O75688	0.012906451	-1.553742932
P62136	0.042254397	-1.634210312
P62140	0.032967563	1.857860269
O14974	0.000735633	-1.226601395
Q96C90	0.046174884	-3.975288807
P30153	0.043913893	-0.566592609
P42785	0.041127027	1.353736579
P31323	3.51E-05	-1.48636791
O14744	0.003254045	-2.130886298
O75475	0.024828054	0.643078478
P25786	0.03777743	0.347364279
P25789	0.006002801	-0.67461085
P60900	0.004691027	-2.196042354
P49720	0.010827682	-0.724948291
O00233	0.000856394	-2.874216972
Q14997	0.047853884	-0.602009731
P26599	0.033811019	-0.699693002

Q9P2B2	0.013824317	-4.804927638
Q8N8N7	0.010237095	-3.252562642
Q05397	5.98E-05	-3.402260886
Q13308	0.014171409	0.770360849
Q9UMZ3	0.041276723	-1.110525583
Q13332	0.005514623	-10.52509519
P09417	0.005863344	-1.167992615
Q15274	0.048689387	1.042802116
P62491	0.021209328	-1.322689299
Q6WKZ4	0.031970677	-6.038769932
P61106	0.040160209	-2.891257223
Q9NP72	0.026367697	-1.119580451
P61019	0.012792414	-0.047644233
P51148	0.045713438	0.744172138
Q9NRW1	0.041677048	-0.707415381
P51149	0.000320588	-1.275727844
Q5HYI8	0.035323573	-0.876460537
P63244	0.024800882	-0.778839614
Q92878	0.005665303	-0.787679438
Q9P0K7	0.028068241	-0.412037438
P62826	0.048647887	-0.59164713
Q9H6Z4	0.027115565	-4.70114397
Q96S59	0.01048699	-4.318591031
P62834	0.030874153	-0.759677522
Q5T8P6	0.001648416	-1.687904775
Q9BWF3	0.01005314	0.766770401
P52756	0.044020719	-0.421463461
P38159	0.015177334	0.366440686
Q14257	0.038762163	-1.403694625
P35241	0.02461723	0.44988308
P61586	0.023879061	-0.838189888
Q8IUC4	0.012236817	-8.846456624
Q5UIP0	0.002536326	-1.108058161
Q9Y4F9	0.043406997	1.012956386
Q96TC7	0.014606422	0.727821901
Q15287	0.002959989	-0.766527232
Q13464	0.016300768	-2.842722064
Q68CZ1	0.003326876	-2.738572521

P27635	0.048508035	0.550531567
P62906	0.005030878	0.843543935
P30050	0.02986567	0.482731061
P26373	0.000462462	1.015971666
P50914	0.031859865	0.850508088
P84098	0.037552017	0.60389514
P61353	0.027433352	0.639610412
P62910	0.04365418	-2.157520173
P49207	0.008109617	1.253935325
Q969Q0	0.005000185	1.028780375
Q92901	0.002297797	-2.473875151
P46777	0.025130384	0.755726759
P62424	0.036458597	0.71883507
P62917	0.011233444	0.66870727
P04844	0.001251182	0.689010753
P62244	0.012090656	0.77603795
P62701	0.037787216	0.544308977
P46782	0.001873807	1.131285793
P62753	0.038308228	0.33914504
Q9P2E9	0.038070345	-0.311874434
Q15050	0.028360327	0.49084267
Q9Y3I0	0.012463359	0.483095837
F8W914	0.000110006	2.805958698
Q8WXA3	0.042996706	-0.919374933
Q15424	0.011024782	0.73394253
Q14151	0.01665107	0.687223639
Q9Y6B6	0.017980889	-0.748899993
P49591	0.010744168	1.357778817
Q15020	0.012668238	-0.817084055
Q8NBX0	0.011718345	0.892141311
P55735	0.040814165	-2.763272458
O75396	0.017649549	-0.990084133
O94979	0.024170949	-2.068824166
P60468	0.043537584	-0.727489642
Q9NVA2	0.004932425	-0.730498257
Q99719	0.016924816	-1.119894312
Q8NC51	0.004246305	0.790313879
P50454	0.044467429	-1.093126136

Q9BYW2	0.004837376	-0.863466998
Q7Z333	0.000204202	-1.909449456
Q15393	0.020306971	1.092523382
Q9H9B4	0.021363753	-0.346119794
P34897	0.008852826	1.167458232
O60292	0.04045421	-1.120141777
Q9UJS0	0.018811192	-1.427034539
O14745	0.000555166	0.646260807
Q14BN4	0.001951472	2.97165303
Q9NWH9	0.047330477	-1.933332293
O95391	0.001604652	-2.06732415
Q92922	0.044242582	0.474568095
Q8TAQ2	0.001652154	0.707531487
Q14683	0.018618341	0.543079796
P60880	0.002322799	-1.365754454
Q7KZF4	0.035429503	-0.431544422
P08621	0.021625108	0.542108171
P62314	0.001423333	1.306196618
P62316	0.012053494	0.592248434
O60504	0.027050824	1.04717485
P61009	0.005620111	1.41509095
O15020	0.030830356	-1.429830827
O43295	0.033790093	-0.897840503
P19623	0.036424225	-4.038178059
Q9UHB9	0.009427924	0.685885024
O76094	0.014268783	-1.952039097
Q9BXP5	0.003658564	1.40503987
Q13247	0.003234496	0.382224644
Q13242	0.019620862	0.346919322
Q04837	0.011306945	-0.745651153
Q13043	0.032570455	-3.64311475
O43815	0.005149202	-2.548979271
Q86Y82	0.02524379	-0.883877717
O43752	0.008675616	-0.889651962
P53999	0.001225589	-0.777396224
Q7KZ85	0.022278434	-4.022475321
B7Z645	0.006705484	0.66752129
O60506	0.006705526	0.66752129

A0A0C4DGK3	0.01118536	-0.947518397
O15061	0.001760784	-0.822649872
Q5T011	0.002848249	2.354868271
Q15750	0.044943546	-0.918909419
Q13148	0.041169129	-0.862226538
Q66K14	0.001744921	-1.142962291
Q99426	0.034121864	0.918211923
O14776	0.008182309	2.317890937
Q6N021	0.029123064	-2.23748966
P04216	0.002308407	-1.18535694
Q8IVF5	0.00017819	-0.595951224
Q7Z2Z1	0.015457846	-0.46808708
P29401	0.00051609	-0.770637152
Q04724	0.013122501	-0.32230197
Q9NYL9	0.033106445	-0.843923654
P24821	0.023651975	-1.664178952
Q9C0C2	0.023763652	-0.621825757
P11387	0.007731149	0.914595717
B7Z596	0.005088623	0.658912544
Q15643	0.000532716	-1.800067574
Q15650	0.028644318	-5.397849617
Q7L0Y3	0.006209571	0.983390986
G3V435	0.013025535	-0.51314661
P68363	0.029437481	-0.664796594
Q9BQE3	0.032536853	-4.271242126
Q3ZCM7	0.012717145	-1.182663588
Q6IBS0	0.023257019	-1.548607359
O15042	0.010089442	1.382575218
A0AVT1	0.003038592	-1.731800377
Q14157	0.010038026	-10.40567461
P63279	0.032663781	-1.14142584
P61088	0.020274767	-2.023734993
Q5JXB2	0.025668429	-1.142341268
P09936	0.000865848	-1.145594841
O94874	0.03319254	1.100868444
P47985	0.022685324	2.410497962
P0C7P4	0.034715278	-1.066385763
O14949	0.00275064	-2.369421174

Q96K76	0.027737583	-3.634231622
Q9ULK5	0.029074052	0.711994587
Q5ST30	0.00302282	-1.43516347
Q9HCJ6	0.027405994	-1.738303453
P45880	4.87E-08	-1.285848738
Q9Y277	0.030282783	-0.363700152
Q7Z7G8	0.003894305	0.93652369
P04275	0.001298963	2.483268513
Q9BQA1	0.005549894	-1.858005259
O14980	0.037877579	1.358188056
P12956	0.008807694	-1.130712434
P46937	0.02754372	-3.273292364
P67809	0.00247379	-1.983767741
Q04917	0.003665582	-0.692994897
Q8WU90	0.001991526	0.491347966
Q9UGR2	0.027965025	-0.926112199
Q7Z2W4	0.004860844	-5.132171821
Q9UQR1	0.000922233	-2.193636764
Q96ME7	0.029367161	-2.217972941
Q5TYW1	0.03613008	0.645628604
	NPC	
Accession	Anova (p)	logFC
Q9NUT2	0.030368818	0.528690356
Q15027	0.005034636	-2.969115598
P61160	3.52E-05	-1.133908244
Q76LX8	0.000705045	1.674770062
O60503	0.002520638	2.948032627
Q719I0	0.020358581	-0.862204693
Q92667	0.003310305	-5.506779375
Q02952	0.018244587	-0.919299456
O43488	0.028496286	-1.750940462
P31749	6.59E-06	-1.542373132
P02768	0.013940768	-0.906341799
P00352	0.032470999	2.302710709
O75891	6.17E-05	-3.649743841
P49189	0.031112576	-1.511434519
Q96QP1	0.004213475	-3.108655297
Q6UB99	0.000380876	-2.013823784

Q96NW4	0.015491474	1.662951208
Q5JPF3	0.009063796	-1.94810438
P04083	0.032658683	-1.316110332
P08133	0.046428688	-0.658207491
E9PFW3	0.000106094	-3.943692121
Q13367	0.001252827	-2.274031968
Q9HDC9	0.049149232	-0.441228667
P84085	0.032807832	2.240578328
Q8N1W1	0.008313191	2.490266389
E7EV07	0.049318568	3.969085094
Q8N3C0	0.005413363	-2.619300021
Q12797	0.003243072	-0.820592409
Q9BZE9	0.00515789	-2.434940218
Q13315	2.13E-05	-2.407041568
P05023	0.025920947	-0.712635711
O14983	0.000323607	-6.140418429
Q93084	0.011678463	-2.005907022
P20020	0.033142012	-0.796405878
P25705	0.028760477	-0.766650544
P06576	0.017991738	-0.507044845
P80723	0.036703174	-0.734618835
P54687	0.006325575	-2.455644216
Q86UU0	0.002406211	-1.92644591
A6H8Y1	0.006571083	3.613773355
Q13867	0.001491127	-4.302432009
P38398	0.005742461	-0.59131186
Q9NPI1	0.044308543	0.978864212
Q9UPA5	0.002868645	-1.609072778
Q9NP86	0.013998998	2.427327064
P27797	0.046526192	-0.958463961
Q01518	0.005053681	-1.020648006
P07384	0.016512028	-0.595653823
Q96MW1	6.02E-08	-2.371758042
P50990	0.021337962	-1.587322856
Q9ULB4	0.006089468	-3.687358982
Q00537	0.013328775	1.542513976
K7EJ83	0.045995352	-0.451195377
Q8WUJ3	0.02046159	-1.193726496

Q9UPV0	0.006647843	-1.320632453
A0A0A0MTQ1	0.012948532	-2.992415449
A5D8W1	0.005321042	-3.263330857
P23528	0.042814612	1.285938038
P05060	0.006181045	-2.213332233
I3L2J0	0.033828799	-1.056118308
Q07065	0.000190324	-1.233491933
Q96S66	0.03559247	-3.053503862
F8WF69	0.00239593	2.474180755
Q15417	0.033518426	-1.182364321
A5YKK6	0.003876046	-0.696918495
Q07092	0.03708638	-1.335449947
P02462	0.013529665	-0.676750174
P12110	0.029036916	-0.773448259
P53618	0.029785538	-0.647587482
P35606	0.005790549	-0.712122988
Q9BR76	0.025813385	-0.849440487
Q14194	0.044694996	0.509985127
A0A087WW81	0.005258707	-0.863584283
H7BZ55	0.001921771	-0.835265417
Q1MSJ5	0.049968525	-0.800321965
P26232	0.02237701	-0.2310671
P07858	0.007269887	-1.085075423
P17844	0.044833271	3.552895325
Q9BQ39	0.038196816	1.168168059
P26196	0.033940824	-0.772593359
Q16698	0.00641901	-1.455312798
Q9UPY3	0.003098111	-1.693818842
F8VR31	0.026444235	-0.9421545
Q6ZR08	0.027782441	-0.64926676
Q0VDD8	0.042628536	-0.886845883
Q8TD57	0.02415887	-0.705038034
Q8IXB1	0.039535144	-0.488651523
Q96M86	0.002531535	2.050585918
Q8IZD9	0.021143249	-1.672871129
Q8TEK3	0.023051921	-1.462768021
Q14195	2.11E-05	-0.907390185
Q14204	0.039725261	-0.697823724

Q6P2E9	0.008353702	-1.07709478
P68104	0.002437874	1.33522189
P24534	0.02107656	-0.69457988
Q9NZN3	0.030361133	-1.287337543
P20042	0.00272274	-1.418313543
P41091	0.002928821	-1.013326119
P38919	0.049328727	-1.987983391
Q9Y6C2	0.018848176	-0.860966987
Q6ZMW3	0.03539205	-0.7370222
P22413	0.03208018	-5.228378192
Q96L91	0.034700773	-1.094874477
Q9Y6I3	0.002914563	-1.664595514
Q5T890	0.031386285	-0.442844517
Q96HE7	0.010715016	-3.017053123
Q9BS26	0.035060109	-1.087181919
P38117	0.00848362	-0.722938455
Q01844	0.009775466	-1.010796845
Q49AJ0	0.003221196	-1.243561563
B1AHL2	2.19E-06	-5.037204522
P35555	3.05E-06	-2.366811466
P35556	0.037453189	-2.651286771
P11362	0.013450949	2.798293069
O95302	0.003916314	-1.438143658
P21333	0.022100729	-1.408580779
O75369	0.006373184	-0.977338893
P02751	0.004342398	-1.553123901
P11413	0.013001851	-1.754516966
P10253	0.013671847	-0.692382056
P41250	0.008364572	-0.612388054
Q8IWJ2	0.04512732	-0.455015939
Q06210	0.000166464	-0.717429565
P00367	0.036014411	-0.598885296
Q14344	0.002783619	1.192985902
Q9UBI6	0.03228084	-0.683023095
Q08379	0.012193773	1.116159512
Q13439	0.009947017	-1.854725173
Q9Y625	0.001742863	-1.283320901
H0YDB0	0.041627861	15.5266491

P78417	0.01555302	-1.28556358
P09211	0.035317503	-0.622030028
P31937	0.010204042	-2.551357209
P68431	0.010699737	5.826954782
P50747	0.043905192	2.155707942
O60812	0.002727835	1.648811196
P31943	0.012911507	-1.49491087
Q00839	0.025972665	-1.631004603
Q86VS8	0.038117878	-1.909845768
Q53GQ0	0.020464174	3.662669742
Q14568	0.030745507	-0.714206575
Q58FF7	0.025644483	-1.773027402
P14625	0.029364577	-0.629262559
Q58FF3	0.01924594	-0.726595836
P11021	0.010487282	-1.001720403
P04792	0.003348845	-1.092150445
P10809	0.002836846	-1.633353692
Q9UG01	0.029645697	-3.305453664
Q16270	0.045530186	-1.181486432
A6XGL2	0.041843699	-1.902450098
Q8N201	0.004369088	-2.937760687
P18084	0.013954825	-2.387947807
Q15811	0.001984243	-1.088523373
Q9P2N6	0.005118787	-3.682244955
Q8WZ19	0.024781699	-1.675996046
Q9UGL1	0.048232925	-1.333818268
Q2LD37	0.032918712	-1.06973746
Q5T5P2	0.016723372	-1.338957688
Q86VH2	0.036046161	-11.19829297
O60282	0.013589447	-1.557894331
Q9BW19	0.03078137	-0.834005536
Q9NSK0	0.014858937	-2.901852196
Q8NEZ4	0.014178235	-4.176558427
P19012	0.000527576	-1.279958708
P05783	0.01677973	-1.131481566
Q7Z3Y8	0.000871057	-1.579414518
Q14532	4.84E-05	-0.867078167
Q01546	0.022339987	-1.116811573

P05787	0.001909325	-1.147061624
Q16787	0.010879924	-1.600932267
P11047	0.036654624	-0.59570364
P07195	0.037700384	-0.651004289
P09382	0.009769527	-1.193459487
Q08380	0.029034946	0.851716937
P49257	0.003540585	-1.682191589
P02545	0.00013683	-0.731430076
P20700	0.037914124	-0.909314058
P50851	0.024467964	-2.003337933
A0A1B0GU45	0.014581921	-2.155988751
P42704	0.012971775	-0.899973487
Q96AG4	0.010675509	-0.737739016
Q5S007	0.020643268	-0.879986021
Q9UFC0	0.013346332	5.473336334
Q9BS40	0.022136907	-2.331699026
P46821	0.038400963	-2.124281508
P27816	0.01924234	-0.641378114
P29966	0.012608423	-1.428278847
P31153	0.047121307	-1.043406189
P33993	0.000161768	2.778786691
K7EKS6	0.003955358	6.045837089
P55001	0.028455533	0.95423188
P14174	0.038829531	-1.218195139
P50281	0.000194488	-0.64667778
Q9UBG0	0.03745693	-0.739108419
P26038	0.009241746	-0.337069945
P20592	0.036117854	1.21015322
Q9NR99	0.002047783	-2.386597195
Q96S97	4.89E-05	-3.083010982
Q9UKX3	0.012656696	-1.107834225
P13533	0.009565508	-1.194820316
P35579	0.000738718	-0.581073519
P60660	0.041263754	-1.252912813
Q6PIF6	0.009009327	2.296825762
Q86TC9	0.043195568	-1.404416527
O00370	0.00039256	-1.059240524
E9PAV3	0.005739979	-2.739569362

A0A087WUL8	0.000363194	-3.4656289
O75376	0.014700489	-0.960298066
O76041	0.01634248	1.47151682
P07196	0.025970824	1.341839824
O00567	0.000744009	-0.736573551
Q7Z494	0.029544568	-1.706600276
Q96L73	1.61E-06	-3.407825099
O15381	0.017005213	-3.464266815
E9PLN3	0.040549541	-1.153139065
P13674	0.012191851	-0.497683894
O15460	0.000687433	-0.770539425
Q9H361	0.002589128	-2.505997805
Q13310	0.033545343	-1.076015496
P43034	0.032392579	-7.51799785
P09874	0.026121139	-0.69300306
Q8NI35	0.026560817	-4.087205663
P12004	0.00253582	1.188973704
A6NKB5	0.002757404	-2.450776147
Q15113	0.015137851	-1.051257307
Q07343	0.043775951	-0.866613359
P09619	0.009682778	-1.963752585
H7BZJ3	0.00141762	-1.116446949
P30101	0.026238243	-0.838752022
Q14554	0.001065037	-0.554318641
O00151	0.002313528	-0.874119858
P50479	0.018194312	-0.994804927
Q96HC4	0.013131693	0.839394606
Q29RF7	0.043187673	-1.296673687
P12955	0.025456865	-1.504876553
P18669	0.012612349	-0.643607474
P00558	0.031412932	-0.654793816
Q92576	0.04883784	-0.619669968
O43175	0.002041176	-1.136937881
Q8N3E9	0.002344674	-7.615284235
P13797	0.048529973	0.981321175
Q9H488	0.006802201	-6.148338148
Q7Z3K3	0.001863189	11.15418422
X6R2I3	0.023454807	-4.1668576

P16435	0.025118149	-3.710185396
A5A3E0	0.001770124	-1.758669901
P0CG38	0.002525352	-3.194795
Q15181	0.008553847	-1.41625437
Q9H2U2	0.047546702	0.80748025
Q86W92	0.022104954	-3.187316229
P23284	0.007449159	-0.995559538
P63151	0.009682108	-5.100294602
P30048	0.031619791	-0.899325627
P30041	0.010545424	-0.838314783
P13861	0.019315179	-6.946113709
P78527	0.048345602	-1.35779736
O75569	0.018068743	-0.69942567
P60891	0.011376561	-0.977327048
P28072	0.036355113	-0.559314919
P62191	0.018690504	-0.773171142
Q05209	0.022196379	1.018747675
Q92626	0.018314025	-0.889791894
Q15907	0.029270449	1.720034968
P61106	0.029167419	-0.617518221
Q92928	0.049812404	-0.727032869
P20339	0.012857132	3.328410356
D6RF23	0.034066437	-0.574088529
P04049	0.009560608	5.575028256
Q86X27	0.021117654	-1.800109756
P49756	0.006787865	-3.664547299
P98179	0.016639502	-3.408715483
Q9HBD1	0.029451551	4.958914314
Q15293	0.001297231	-1.680261912
Q9P2K3	0.003455237	-1.801219093
Q96D71	0.020061384	-0.950486938
O60673	0.004500197	-0.782026125
P61586	0.02200717	-0.534573337
Q6R327	0.014743454	-3.30727551
P18621	0.04221489	3.69215223
P83731	0.001339347	4.993417983
Q02878	0.034242059	-0.458315764
P18124	0.011953485	-0.573090698

P04844	0.027281356	-0.697119773
P25398	0.042973363	-0.440345647
P62244	0.003528502	0.985648456
P62979	0.019995329	-2.231535296
P62857	0.019516553	-0.603713905
P62273	0.030215389	-0.673159529
Q9P2E9	0.018538541	-1.204859478
Q86VV8	0.013171825	-1.058891716
P60903	0.001173538	-4.125439049
P31949	0.002070631	-1.257570216
Q99584	0.017764928	-1.36723993
Q86WG5	0.002633185	-1.325753216
Q15437	0.000736072	-1.879825338
O94855	0.046791963	-2.134698076
P60468	0.006024376	-1.779566951
P07093	0.034768736	-4.447114729
Q15393	0.00325987	-0.550445299
Q8N5H7	0.016958949	6.518640075
F8VVM2	0.01907275	-0.527182581
Q00325	0.000378706	-0.998246044
Q14BN4	0.015722385	-1.481970336
Q92922	0.028682793	0.12507663
P53814	0.022390618	6.597978441
Q7KZF4	0.027867079	-0.97395602
Q9H3E2	0.020602843	-0.676624325
P09486	0.001550432	-4.271570737
Q9C093	0.020046968	-0.866346384
Q13813	0.001512638	-2.730507451
O15020	0.014930718	-0.739652082
Q9UQ35	0.043622173	-1.508182492
Q9BRL6	0.018936995	-1.859306389
P53999	0.016386558	-1.414888573
A0A0C4DGK3	0.018699042	-0.901612139
Q92804	0.007156393	-6.765024639
Q01995	0.036123202	1.01551691
Q13148	0.035950222	-1.390671801
Q86TI0	0.039130902	-1.258756496
Q9NUY8	0.005454592	-3.623437826

Q969E4	0.042875699	-1.418032044
Q9UGU0	0.000644131	-4.712621955
Q6ZMP0	0.044360344	-1.264468036
Q9Y4G6	0.034718337	-0.759901121
Q12767	0.046395734	-2.277795769
Q9NYL9	0.039210869	-1.255806643
P62328	0.04876917	-0.773167546
Q9H3N1	0.001786216	-10.5553078
H0YGZ3	0.001117227	-2.551979995
P11388	0.04529267	-1.247207079
O95985	0.035791269	4.019905862
Q6ZN40	0.014752188	-1.250586142
B7Z596	0.036295622	-0.965924282
Q9C040	0.021965073	-1.474162598
Q13263	0.005924459	-0.74546951
Q8TD43	0.000217219	2.203137709
Q9UHF7	0.023745548	-0.767152602
Q5W5X9	0.000188864	-1.967969675
Q14679	0.02096421	0.799328419
Q9BVA1	0.004935553	0.927664713
P68371	0.000606081	-2.027197723
Q8NBS9	0.037550429	-1.000143142
P26368	0.012187079	-8.738363545
A0AVT1	0.001760691	-3.090392637
Q5T4S7	0.000976132	-1.954271133
P31930	0.032506051	-2.063421811
O60763	0.01030869	-1.805869142
Q96RU2	0.010964144	-2.146200819
Q9HBJ7	0.04594632	-7.940281999
Q9P0L0	0.049689243	-1.184147048
O95292	0.037933509	0.953323929
P18206	0.020583506	-1.22479866
P21796	0.002944787	-0.895959974
A4UGR9	0.012434579	-2.61171249
Q9H0D6	0.038738019	-2.991423957
Q9ULM3	0.033254451	-0.729714479
Q04917	8.06E-05	-3.887914344
Q7Z3T8	0.004244156	-6.153499009

Q96SE7	0.000309348	-2.741435627
Q96LW1	0.038408243	-1.753828864
Q92618	0.001026632	-3.774312654
Q86YE8	0.019922583	-1.018366839
O15015	0.000561343	-1.47328717
O43149	0.018525006	-0.477187903
	Neurons	
Accession	Anova (p)	logFC
O00763	0.044516067	1.909040332
Q15057	0.018199449	-1.991829866
P24752	0.010301114	-0.989062281
P68133	0.047347625	1.216216559
Q562R1	0.003766445	-4.457245492
Q9P2N4	0.033893088	-1.233047595
P23526	0.046164975	-1.032835018
Q719I0	0.023451297	-2.717973877
Q5TCS8	0.044311466	0.30051978
Q3SY69	0.029344594	-1.498550687
Q9H1A4	0.038829293	-2.542513579
Q01484	0.038300487	-1.953143614
Q9P2R3	0.008060853	2.86399095
Q5JPF3	0.015899419	-2.411596813
P07355	0.045386368	-1.560029215
P25054	0.005053327	-1.787995734
O95996	0.021608611	-4.578351964
Q5T5U3	0.027531693	-2.659004381
F5H1R4	0.00022202	2.268620112
E7EV07	0.019098301	1.744044744
O15144	0.020526265	1.627786587
P05023	0.005306316	-2.222968045
Q13733	0.007811392	-1.697248557
P23634	0.044735337	4.164428834
P25705	0.027059459	-1.003410044
P24539	0.006520416	3.009077262
O43861	0.015765432	-2.306298484
Q86UU0	0.005586691	-1.743943818
Q13867	0.020533149	-3.148855734
Q9BX63	0.001032875	2.429728505

Q9UPA5	0.035784344	-3.501240508
P27797	0.023507476	-1.26680223
O43852	0.004004005	-1.677039464
P07384	0.041805211	-2.325110097
P52907	0.042654623	-0.998515714
Q8N163	0.001783929	-3.050676831
Q9P1Z9	0.000155661	3.701950397
Q92526	0.005472896	4.468460227
Q9Y5S2	0.002140846	-2.540556477
K7EJ83	0.031213041	-1.142067586
Q9UPV0	0.024427902	-3.227966279
A0A0A0MTQ1	0.009932113	3.422421807
I3L2J0	0.000555706	-3.438735273
Q07065	0.006834916	-1.561278101
A5YKK6	0.029567251	-1.143503758
Q7Z7A1	0.014492043	-2.650206467
P08123	0.000332771	-3.269028505
P12109	0.014500057	3.458862273
P12110	0.014828751	-2.008334167
P53618	0.038181311	2.512838423
Q9UBF2	0.047647586	-0.525625107
Q9UKF6	0.030138302	2.341517022
Q16630	0.02018665	6.265574658
P53673	0.006547497	-4.024276516
P53674	0.038644207	-3.959983273
P43320	0.010600286	-3.212355912
P07858	0.027191426	-1.13203327
Q13619	0.035196327	11.41620124
Q16678	0.010414644	3.965108704
P51398	0.007491855	-2.535664529
O15075	0.047841445	-0.901993045
O95865	0.029113868	-4.651261421
Q9NR30	0.007472147	2.547983254
Q9BQ39	0.001241116	3.952895176
P26196	0.031121684	-1.150362024
Q16698	0.023604724	-2.948095447
Q8TDJ6	0.003554549	-2.662146067
E9PG32	0.015355029	-1.884313533

Q0VDD8	0.005562245	-4.737268322
O75165	0.019946082	-2.98407145
Q96N67	0.012320565	-3.474892245
A0A140TA28	0.020247634	4.721769222
Q9BPU6	0.00027109	2.817080907
Q8WVE0	0.041767095	-5.193780261
P38919	0.016841201	-2.987200604
Q15717	0.021951048	-1.626020572
Q92556	0.006281444	-1.326482471
Q9Y6C2	0.039073471	-1.521336016
Q6ZMW3	0.046686673	-1.718563467
O43491	0.001273799	4.968789606
Q9Y2J2	0.044338098	1.239423595
Q01844	0.028532662	-2.629617496
Q9P2D6	0.022612627	-1.463997904
Q14517	0.000339839	-3.832465812
P98095	0.012054602	-2.008967549
F6U495	0.002664507	-2.016446841
P35555	0.019611556	-1.867753946
P35556	0.042287208	-4.326520586
P21333	0.049114439	-1.619942609
Q14315	0.016594466	-1.204845457
P35916	0.0428875	-2.117557286
P02751	0.002577492	-2.708280473
Q13283	0.042047244	-3.252019038
P10253	0.015483867	-1.774220364
O14556	0.025328949	4.287910303

Supplementary Table 3

Neurons PHGDH inhibition

Accession	Anova (p)	LogFC	Peptide count	Unique peptides
P08670	0.006372528	-0.55370966	77	52
Q15149	0.015683054	0.161269705	131	33
Q01082	0.013207408	0.180637754	88	29
P14618	0.047129529	0.147590283	37	29
Q13813	0.048095977	0.205495464	80	24
P49327	0.037810353	0.113244545	51	20
P48681	0.000314575	-0.208535595	41	17
P08238	0.017042883	0.144282259	52	17

P06733	0.012143813	0.085712479	21	16
P02768	0.001665478	0.592039717	30	15
P12277	0.020677956	-0.245612525	23	14
P07237	0.018545634	0.245166821	29	13
P29401	0.0005932	0.292095928	25	12
P14136	0.002786549	0.251052852	26	12
Q06830	0.001294416	0.351485161	20	11
P25705	0.005106968	0.451406393	23	11
Q01995	0.020490932	0.321858376	19	11
P04083	0.036413014	0.157049774	21	11
P52209	0.037075774	0.151417524	20	11
P50990	0.001360371	0.279533597	25	10
Q9Y4L1	0.020897707	0.242626493	29	10
Q08211	0.027426064	0.15843881	30	10
Q14697	0.032217304	0.108053844	23	10
P04075	0.049070261	0.125186206	21	10
P04792	0.000509198	0.339773339	11	9
P12814	0.002662917	0.430746814	43	9
P60174	0.017930026	0.200940417	22	9
Q15417	0.033755343	0.127518779	14	9
Q8NB66	7.53478E-06	-0.240200678	19	8
P09936	0.001050883	0.313725498	22	8
P50454	0.001885165	-0.283482001	16	8
P29966	0.002874551	0.309352832	8	8
P63104	0.01518189	0.135843023	18	8
P07195	0.020662854	-0.124800598	15	8
P09874	0.043973	0.159164199	25	8
Q9BPU6	0.045945321	0.122793981	16	8
Q15185	0.000523467	0.631365076	11	7
Q15233	0.001083968	0.442956588	20	7
P11216	0.002032192	0.300873325	17	7
Q99798	0.002517883	0.37527604	17	7
P22234	0.007308536	0.238777888	15	7
Q99497	0.008393535	0.328938223	9	7
Q16658	0.010521292	0.19404377	16	7
E9PAV3	0.00022777	0.137990444	27	6
O43707	0.019183863	0.09132482	41	6
P16949	0.023880983	0.190149514	12	6

P12236	0.000195636	0.40031522	15	5
P23284	0.000214671	0.576632238	15	5
P36578	0.000643613	0.349863752	14	5
Q92841	0.002885909	0.856544489	17	5
Q13867	0.003478859	0.622856098	9	5
P55209	0.003514334	0.175147204	9	5
P06396	0.011012671	0.261002449	13	5
P49411	0.01114019	0.510587596	13	5
Q02952	0.011660149	0.326949581	7	5
P49368	0.025936678	0.224982559	16	5
P45880	0.030831988	0.076787928	8	5
Q14240	0.03380502	0.184246259	18	5
Q01518	0.043600709	0.269175575	16	5
P29692	0.000207848	0.3669576	8	4
Q12906	0.000661352	0.232568344	21	4
O60506	0.00220192	0.539271323	14	4
P35637	0.002297326	-0.340470136	12	4
P62826	0.003995517	0.238265387	10	4
P26196	0.005529581	0.406654829	9	4
O75874	0.008096342	-0.28279444	9	4
P41219	0.009380434	-0.207081355	15	4
Q58FG1	0.011415838	-0.191087675	14	4
P30044	0.011657631	0.242991476	7	4
O60282	0.012552648	0.349459057	14	4
P59998	0.018463074	0.536281948	8	4
Q9HDC9	0.02162548	-0.282759413	8	4
P10155	0.028711673	0.215164684	8	4
P55786	0.030886861	0.173377895	26	4
P23246	0.031604142	0.445613423	9	4
O43852	0.038626223	0.285317889	5	4
P17987	0.045124588	0.309715324	15	4
O60664	1.25773E-05	0.777621974	7	3
P07355	0.000813595	0.293275048	38	3
P78559	0.000938725	0.369344843	17	3
P53675	0.001276013	0.402953002	24	3
P17980	0.002030891	-0.269671928	4	3
Q8IUD2	0.002502456	0.375886581	16	3
P14314	0.006404496	0.267044969	15	3

P13473	0.008867485	0.228485663	8	3
Q16352	0.015308711	0.122538754	22	3
P50991	0.016661968	0.282973407	10	3
Q96FW1	0.016842216	0.798638653	8	3
O14983	0.01987943	0.524184413	8	3
Q13557	0.029703175	0.415795126	7	3
O00264	0.031211042	-0.204073491	4	3
Q9Y383	0.035018699	0.633122767	3	3
P11387	0.03561087	0.492178637	4	3
P30048	0.036608091	0.200464096	8	3
P61970	0.037086111	0.243030659	3	3
O95251	0.037668868	0.31828053	6	3
O43765	0.038248476	0.277972591	5	3
P83731	0.038574715	0.223352267	8	3
Q96KP4	0.045504538	0.333098204	3	3
Q13247	0.049996575	0.280224739	7	3
Q14108	0.000119011	0.626166484	4	2
Q8IV08	0.000677655	0.238465665	12	2
P53396	0.000841349	-0.372489506	7	2
Q15691	0.001196763	0.275379163	6	2
Q9UNZ2	0.001239951	0.230146566	6	2
P98160	0.001804078	0.617204813	8	2
P18440	0.001826774	1.073937369	3	2
P06744	0.002896406	0.221707507	11	2
Q6N021	0.004218816	0.415482436	5	2
P49458	0.004285122	-0.131472165	3	2
Q9Y2G9	0.004448056	0.439123369	6	2
Q16527	0.00578922	0.756814888	4	2
Q14344	0.006373577	0.533567565	6	2
P25789	0.007810778	0.367844308	6	2
P62701	0.008144033	0.166588738	5	2
P13637	0.009283252	0.281247566	10	2
P0DMV8	0.011665035	-0.428099936	16	2
Q04760	0.013030621	-0.329030566	3	2
P30086	0.015788067	0.143285573	6	2
P20648	0.016164235	0.995441101	9	2
P11488	0.017276332	0.419127241	10	2
O76011	0.017959397	0.474446505	7	2

O95741	0.019278144	-0.191468615	3	2
P07949	0.019708651	0.431093492	5	2
P35613	0.019995686	0.38808106	8	2
P48637	0.02012242	0.394891751	5	2
Q9UBB9	0.020577885	0.632665584	4	2
Q53SF7	0.021917043	-0.20214275	9	2
O00567	0.023148326	0.534169267	3	2
Q9HBT8	0.029354095	0.198973965	3	2
P51991	0.030246807	0.162563896	8	2
Q01469	0.030861351	0.211883015	3	2
Q99961	0.039923265	0.45237212	5	2
P63208	0.041403011	0.378403684	3	2
Q6TFL3	0.041525007	0.379406139	7	2
Q02878	0.0425487	0.315386433	8	2
Q00688	0.044763268	0.232922397	6	2
P15735	0.000126925	0.546254058	5	1
Q9BRA2	0.000442835	0.752335346	2	1
O14773	0.000792175	-0.503973712	1	1
Q04837	0.001069619	0.255967511	3	1
O60231	0.001192545	0.65307289	2	1
P00403	0.001598704	-0.451991486	1	1
P62491	0.001636927	0.5922448	5	1
P12004	0.001684444	0.337428453	2	1
O43681	0.001757169	0.549286033	5	1
P18859	0.00186399	0.620993663	2	1
P62191	0.001896683	0.536047563	2	1
P12883	0.00206806	0.586603622	4	1
Q99733	0.002446754	0.309408569	6	1
P49321	0.002935501	0.480503141	12	1
P00441	0.003407304	0.304639371	2	1
Q7Z406	0.003533656	0.274017278	13	1
O43396	0.003818954	0.533697735	2	1
P11586	0.003963262	0.331732128	19	1
Q8IWG1	0.005038425	0.273938836	5	1
Q96DN5	0.005127235	-0.591472582	5	1
O94905	0.005719604	0.327748927	4	1
P36405	0.005828186	0.344520923	5	1
Q8NEK8	0.005841955	-0.483571756	4	1

Q15345	0.006295164	0.528943318	2	1
Q14194	0.006443382	-0.210347688	19	1
O76009	0.00798671	0.302111944	6	1
Q5T2N8	0.008313815	-0.319095935	4	1
O15347	0.008612683	0.303750092	6	1
P31942	0.008639781	-0.563554637	3	1
Q9UBX5	0.008893819	0.248357747	3	1
P17066	0.009454386	0.142336841	8	1
Q2M2I5	0.009839241	-0.58987657	5	1
Q9UQB9	0.010245485	-0.350580847	2	1
Q9NVP1	0.010668227	-0.320978686	3	1
Q9P2E9	0.010720685	0.706394442	5	1
Q9GZQ4	0.011009844	0.251566473	2	1
P62750	0.011141781	0.238701716	3	1
P07951	0.011801197	-0.160991186	17	1
Q14258	0.012467695	0.136099979	9	1
O43790	0.013098404	1.179286049	8	1
Q14533	0.013132016	1.179473189	8	1
Q32P51	0.013754791	-0.148700857	11	1
Q15102	0.01407099	0.493538797	3	1
P56211	0.015075243	0.264793223	2	1
Q8TCG1	0.01516819	0.411555892	4	1
Q15717	0.015605968	-0.279504086	4	1
Q16629	0.017158624	0.252711811	7	1
P50914	0.017897198	0.28852107	7	1
Q8TCT9	0.020011974	0.471592867	3	1
P62269	0.02039889	0.433921808	3	1
Q9UI15	0.020747714	0.329393598	6	1
Q9C0C9	0.022987788	0.226593249	4	1
Q8NCM8	0.024485258	0.219144541	7	1
Q8IXQ9	0.024504629	-0.270917263	2	1
Q8ND61	0.027796118	0.417747027	2	1
P62851	0.030492414	0.335668724	1	1
P26368	0.03053669	-0.510424105	1	1
P04259	0.030577991	0.191510657	19	1
Q68D10	0.03097683	0.579657989	2	1
Q14444	0.031669081	0.153818685	3	1
P07205	0.03259511	0.416480387	8	1

Q8NA58	0.034413756	-0.287264751	1	1
P35241	0.036736138	0.169965564	20	1
P28074	0.037997485	0.395675368	2	1
Q9BRP8	0.039154436	0.638316194	5	1
Q14566	0.040777671	0.339587712	4	1
P15502	0.041567113	0.273008149	2	1
P43487	0.043399126	0.198901471	4	1
P53621	0.043419542	-0.275727287	15	1
Q9NSD9	0.044353744	-0.256848964	2	1
P17174	0.04546576	0.18112559	2	1
P24903	0.047231901	0.247325454	2	1
Q93050	0.050020178	0.181773043	4	1

Supplementary Table 4

Neurons PHGDH inhibition

Accession	Anova (p)	LogFC	Peptide count	Unique peptides
P08670	0.006372528	-0.55370966	77	52
Q15149	0.015683054	0.161269705	131	33
Q01082	0.013207408	0.180637754	88	29
P14618	0.047129529	0.147590283	37	29
Q13813	0.048095977	0.205495464	80	24
P49327	0.037810353	0.113244545	51	20
P48681	0.000314575	-0.208535595	41	17
P08238	0.017042883	0.144282259	52	17
P06733	0.012143813	0.085712479	21	16
P02768	0.001665478	0.592039717	30	15
P12277	0.020677956	-0.245612525	23	14
P07237	0.018545634	0.245166821	29	13
P29401	0.0005932	0.292095928	25	12
P14136	0.002786549	0.251052852	26	12
Q06830	0.001294416	0.351485161	20	11
P25705	0.005106968	0.451406393	23	11
Q01995	0.020490932	0.321858376	19	11
P04083	0.036413014	0.157049774	21	11
P52209	0.037075774	0.151417524	20	11
P50990	0.001360371	0.279533597	25	10
Q9Y4L1	0.020897707	0.242626493	29	10
Q08211	0.027426064	0.15843881	30	10
Q14697	0.032217304	0.108053844	23	10

P04075	0.049070261	0.125186206	21	10
P04792	0.000509198	0.339773339	11	9
P12814	0.002662917	0.430746814	43	9
P60174	0.017930026	0.200940417	22	9
Q15417	0.033755343	0.127518779	14	9
Q8NB66	7.53478E-06	-0.240200678	19	8
P09936	0.001050883	0.313725498	22	8
P50454	0.001885165	-0.283482001	16	8
P29966	0.002874551	0.309352832	8	8
P63104	0.01518189	0.135843023	18	8
P07195	0.020662854	-0.124800598	15	8
P09874	0.043973	0.159164199	25	8
Q9BPU6	0.045945321	0.122793981	16	8
Q15185	0.000523467	0.631365076	11	7
Q15233	0.001083968	0.442956588	20	7
P11216	0.002032192	0.300873325	17	7
Q99798	0.002517883	0.37527604	17	7
P22234	0.007308536	0.238777888	15	7
Q99497	0.008393535	0.328938223	9	7
Q16658	0.010521292	0.19404377	16	7
E9PAV3	0.00022777	0.137990444	27	6
O43707	0.019183863	0.09132482	41	6
P16949	0.023880983	0.190149514	12	6
P12236	0.000195636	0.40031522	15	5
P23284	0.000214671	0.576632238	15	5
P36578	0.000643613	0.349863752	14	5
Q92841	0.002885909	0.856544489	17	5
Q13867	0.003478859	0.622856098	9	5
P55209	0.003514334	0.175147204	9	5
P06396	0.011012671	0.261002449	13	5
P49411	0.01114019	0.510587596	13	5
Q02952	0.011660149	0.326949581	7	5
P49368	0.025936678	0.224982559	16	5
P45880	0.030831988	0.076787928	8	5
Q14240	0.03380502	0.184246259	18	5
Q01518	0.043600709	0.269175575	16	5
P29692	0.000207848	0.3669576	8	4
Q12906	0.000661352	0.232568344	21	4

O60506	0.00220192	0.539271323	14	4
P35637	0.002297326	-0.340470136	12	4
P62826	0.003995517	0.238265387	10	4
P26196	0.005529581	0.406654829	9	4
O75874	0.008096342	-0.28279444	9	4
P41219	0.009380434	-0.207081355	15	4
Q58FG1	0.011415838	-0.191087675	14	4
P30044	0.011657631	0.242991476	7	4
O60282	0.012552648	0.349459057	14	4
P59998	0.018463074	0.536281948	8	4
Q9HDC9	0.02162548	-0.282759413	8	4
P10155	0.028711673	0.215164684	8	4
P55786	0.030886861	0.173377895	26	4
P23246	0.031604142	0.445613423	9	4
O43852	0.038626223	0.285317889	5	4
P17987	0.045124588	0.309715324	15	4
O60664	1.25773E-05	0.777621974	7	3
P07355	0.000813595	0.293275048	38	3
P78559	0.000938725	0.369344843	17	3
P53675	0.001276013	0.402953002	24	3
P17980	0.002030891	-0.269671928	4	3
Q8IUD2	0.002502456	0.375886581	16	3
P14314	0.006404496	0.267044969	15	3
P13473	0.008867485	0.228485663	8	3
Q16352	0.015308711	0.122538754	22	3
P50991	0.016661968	0.282973407	10	3
Q96FW1	0.016842216	0.798638653	8	3
O14983	0.01987943	0.524184413	8	3
Q13557	0.029703175	0.415795126	7	3
O00264	0.031211042	-0.204073491	4	3
Q9Y383	0.035018699	0.633122767	3	3
P11387	0.03561087	0.492178637	4	3
P30048	0.036608091	0.200464096	8	3
P61970	0.037086111	0.243030659	3	3
O95251	0.037668868	0.31828053	6	3
O43765	0.038248476	0.277972591	5	3
P83731	0.038574715	0.223352267	8	3
Q96KP4	0.045504538	0.333098204	3	3

Q13247	0.049996575	0.280224739	7	3
Q14108	0.000119011	0.626166484	4	2
Q8IV08	0.000677655	0.238465665	12	2
P53396	0.000841349	-0.372489506	7	2
Q15691	0.001196763	0.275379163	6	2
Q9UNZ2	0.001239951	0.230146566	6	2
P98160	0.001804078	0.617204813	8	2
P18440	0.001826774	1.073937369	3	2
P06744	0.002896406	0.221707507	11	2
Q6N021	0.004218816	0.415482436	5	2
P49458	0.004285122	-0.131472165	3	2
Q9Y2G9	0.004448056	0.439123369	6	2
Q16527	0.00578922	0.756814888	4	2
Q14344	0.006373577	0.533567565	6	2
P25789	0.007810778	0.367844308	6	2
P62701	0.008144033	0.166588738	5	2
P13637	0.009283252	0.281247566	10	2
P0DMV8	0.011665035	-0.428099936	16	2
Q04760	0.013030621	-0.329030566	3	2
P30086	0.015788067	0.143285573	6	2
P20648	0.016164235	0.995441101	9	2
P11488	0.017276332	0.419127241	10	2
O76011	0.017959397	0.474446505	7	2
O95741	0.019278144	-0.191468615	3	2
P07949	0.019708651	0.431093492	5	2
P35613	0.019995686	0.38808106	8	2
P48637	0.02012242	0.394891751	5	2
Q9UBB9	0.020577885	0.632665584	4	2
Q53SF7	0.021917043	-0.20214275	9	2
O00567	0.023148326	0.534169267	3	2
Q9HBT8	0.029354095	0.198973965	3	2
P51991	0.030246807	0.162563896	8	2
Q01469	0.030861351	0.211883015	3	2
Q99961	0.039923265	0.45237212	5	2
P63208	0.041403011	0.378403684	3	2
Q6TFL3	0.041525007	0.379406139	7	2
Q02878	0.0425487	0.315386433	8	2
Q00688	0.044763268	0.232922397	6	2

P15735	0.000126925	0.546254058	5	1
Q9BRA2	0.000442835	0.752335346	2	1
O14773	0.000792175	-0.503973712	1	1
Q04837	0.001069619	0.255967511	3	1
O60231	0.001192545	0.65307289	2	1
P00403	0.001598704	-0.451991486	1	1
P62491	0.001636927	0.5922448	5	1
P12004	0.001684444	0.337428453	2	1
O43681	0.001757169	0.549286033	5	1
P18859	0.00186399	0.620993663	2	1
P62191	0.001896683	0.536047563	2	1
P12883	0.00206806	0.586603622	4	1
Q99733	0.002446754	0.309408569	6	1
P49321	0.002935501	0.480503141	12	1
P00441	0.003407304	0.304639371	2	1
Q7Z406	0.003533656	0.274017278	13	1
O43396	0.003818954	0.533697735	2	1
P11586	0.003963262	0.331732128	19	1
Q8IWG1	0.005038425	0.273938836	5	1
Q96DN5	0.005127235	-0.591472582	5	1
O94905	0.005719604	0.327748927	4	1
P36405	0.005828186	0.344520923	5	1
Q8NEK8	0.005841955	-0.483571756	4	1
Q15345	0.006295164	0.528943318	2	1
Q14194	0.006443382	-0.210347688	19	1
O76009	0.00798671	0.302111944	6	1
Q5T2N8	0.008313815	-0.319095935	4	1
O15347	0.008612683	0.303750092	6	1
P31942	0.008639781	-0.563554637	3	1
Q9UBX5	0.008893819	0.248357747	3	1
P17066	0.009454386	0.142336841	8	1
Q2M2I5	0.009839241	-0.58987657	5	1
Q9UQB9	0.010245485	-0.350580847	2	1
Q9NVP1	0.010668227	-0.320978686	3	1
Q9P2E9	0.010720685	0.706394442	5	1
Q9GZQ4	0.011009844	0.251566473	2	1
P62750	0.011141781	0.238701716	3	1
P07951	0.011801197	-0.160991186	17	1

Q14258	0.012467695	0.136099979	9	1
O43790	0.013098404	1.179286049	8	1
Q14533	0.013132016	1.179473189	8	1
Q32P51	0.013754791	-0.148700857	11	1
Q15102	0.01407099	0.493538797	3	1
P56211	0.015075243	0.264793223	2	1
Q8TCG1	0.01516819	0.411555892	4	1
Q15717	0.015605968	-0.279504086	4	1
Q16629	0.017158624	0.252711811	7	1
P50914	0.017897198	0.28852107	7	1
Q8TCT9	0.020011974	0.471592867	3	1
P62269	0.02039889	0.433921808	3	1
Q9UI15	0.020747714	0.329393598	6	1
Q9C0C9	0.022987788	0.226593249	4	1
Q8NCM8	0.024485258	0.219144541	7	1
Q8IXQ9	0.024504629	-0.270917263	2	1
Q8ND61	0.027796118	0.417747027	2	1
P62851	0.030492414	0.335668724	1	1
P26368	0.03053669	-0.510424105	1	1
P04259	0.030577991	0.191510657	19	1
Q68D10	0.03097683	0.579657989	2	1
Q14444	0.031669081	0.153818685	3	1
P07205	0.03259511	0.416480387	8	1
Q8NA58	0.034413756	-0.287264751	1	1
P35241	0.036736138	0.169965564	20	1
P28074	0.037997485	0.395675368	2	1
Q9BRP8	0.039154436	0.638316194	5	1
Q14566	0.040777671	0.339587712	4	1
P15502	0.041567113	0.273008149	2	1
P43487	0.043399126	0.198901471	4	1
P53621	0.043419542	-0.275727287	15	1
Q9NSD9	0.044353744	-0.256848964	2	1
P17174	0.04546576	0.18112559	2	1
P24903	0.047231901	0.247325454	2	1
Q93050	0.050020178	0.181773043	4	1

ANEXO B – Bioética Biossegurança e Declaração de Direitos Autorais

COORDENADORIA DE PÓS-GRADUAÇÃO
INSTITUTO DE BIOLOGIA
Universidade Estadual de Campinas
Caixa Postal 6109. 13083-970, Campinas, SP, Brasil
Fone (19) 3521-6378. email: cpgib@unicamp.br

DECLARAÇÃO

Em observância ao **§5º do Artigo 1º da Informação CCPG-UNICAMP/001/15**, referente a Bioética e Biossegurança, declaro que o conteúdo de minha Tese de Doutorado, intitulada "***Células tronco pluripotentes na compreensão dos aspectos do neurodesenvolvimento na esquizofrenia***", desenvolvida no Programa de Pós-Graduação em Biologia Funcional e Molecular do Instituto de Biologia da Unicamp, não versa sobre pesquisa envolvendo seres humanos, animais ou temas afetos a Biossegurança.

Assinatura: _____
Nome do(a) aluno(a): VERONICA APARECIDA MONTEIRO SAIA CEREDA

Assinatura: _____
Nome do(a) orientador(a): DANIEL MARTINS DE SOUZA

Data: 26/11/2021

Declaração

As cópias de artigos de minha autoria ou de minha co-autoria, já publicados ou submetidos para publicação em revistas científicas ou anais de congressos sujeitos a arbitragem, que constam da minha Dissertação/Tese de Mestrado/Doutorado, intitulada **Células tronco pluripotentes na compreensão dos aspectos do neurodesenvolvimento na esquizofrenia**, não infringem os dispositivos da Lei n.° 9.610/98, nem o direito autoral de qualquer editora.

Campinas, 26/11/2021

Assinatura : _____
Nome do(a) autor(a): **VERONICA APARECIDA MONTEIRO SAIA CEREDA**
RG n.° 320360234

Assinatura : _____
Nome do(a) orientador(a): **DANIEL MARTINS DE SOUZA**
RG n.° 324313792